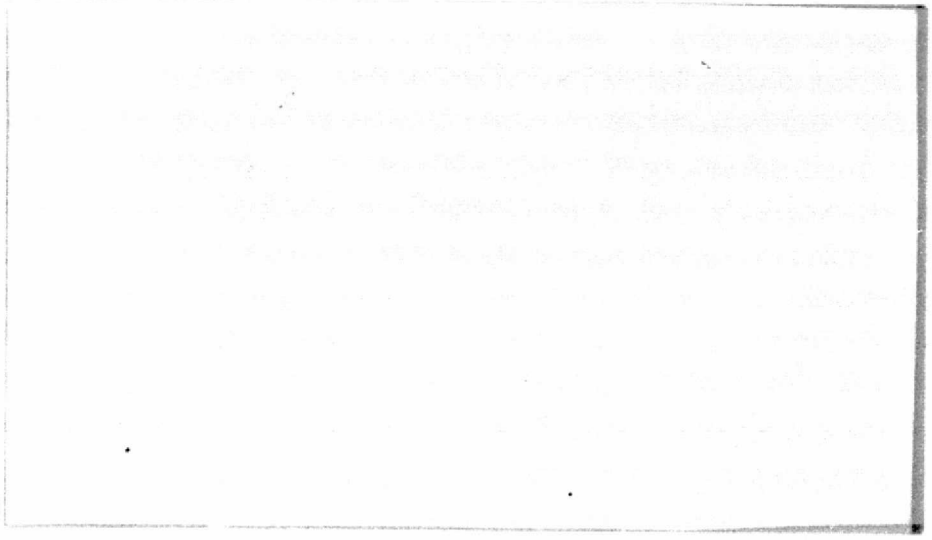

Department of

ELECTRICAL ENGINEERING

UNIVERSITY OF NOTRE DAME, NOTRE DAME, INDIANA

Final Technical Report

to the

National Aeronautics and Space Administration

on

NASA Grant NSG-3048, Supplement No. 2

ALTERNATIVES FOR JET ENGINE CONTROL

(March 1, 1977 - February 28, 1978)

Under the Direction of

Dr. R.J. Leake
Dr. M.K. Sain

Department of Electrical Engineering
University of Notre Dame
Notre Dame, Indiana 46556

ALTERNATIVES FOR JET ENGINE CONTROL

NASA Grant NSG-3048

Supplement No. 2

ABSTRACT

This report deals with progress made on the Grant NSG-3048 during the calendar year beginning March 1, 1977 and ending February 28, 1978. This year coincides with Supplement No. 2 of the award, which originated on March 1, 1975. The NASA Technical Officer for this period was Dr. Bruce Lehtinen of Lewis Research Center. The directors of the research at the University of Notre Dame were Dr. R. Jeffrey Leake and Dr. Michael K. Sain.

General goals of the research have been classified into two categories. The first category involves the use of modern multivariable frequency domain methods for control of engine models in the neighborhood of a quiescent point. The second category involves the use of nonlinear modelling and optimization techniques for control of engine models over a more extensive part of the flight envelope.

Substantial progress has been made in both categories.

In the frequency domain category, works have been published in the areas of low-interaction design, polynomial design, the CARDIAD* method, and multiple setpoint studies. A number of these ideas have progressed to the point at which they are starting to attract practical interest. Further effort is yet required, however, to carry the ideas to maturity

*The acronym stands for Complex Acceptability Region for DIAgonal Dominance. See report for details.

and to ensure their adequate dissemination. A highlight of the year was the incorporation of realistic jet engine data as a theme problem into the International Forum on Alternatives for Linear Multivariable Control. Dr. Sain was Program Chairman for this meeting, which attracted nearly two hundred persons from industry, laboratories, and universities to hear thirty papers focused in the general subject area of this grant.

In the nonlinear category, advances have been made both in engine modelling and in the details associated with software for determination of time optimal controls. Nonlinear models for a two spool turbofan engine have been expanded and refined; and a promising new approach to automatic model generation has been placed under study. A two time scale scheme has been developed to do two-dimensional dynamic programming, and an outward spiral sweep technique has greatly speeded convergence times in time optimal calculations.

The details of these and other aspects of the year's investigations may be found in the body of the report, which covers the most active grant period to date.

TABLE OF CONTENTS

I. INTRODUCTION

The purpose of this section is to provide some of the broad background which underlies and clarifies the general nature of the Research Highlights, which are stated in the section following.

Initiation of Grant NSG-3048 in March 1975 was timed with developments in the engine industry, which was beginning to experience some limitations in the application of classical hydromechanical control technique as the primary base technology for modern engines with ever increasing sophistication. At the same time, milestone developments in digital hardware began to open realistic possibilities for onboard computation to an extent not heretofore possible. This confluence of events led directly to the concept of increasing the role of electronics in engine control. In turn, the availability of digital electronics itself created a wide variety of opportunity for application of new control design philosophy and technique. Among the earliest of such studies is the F100 Multivariable Control Synthesis Program [1] sponsored by the National Aeronautics and Space Administration, Lewis Research Center and the Air Force Aero-Propulsion Laboratory, Wright-Patterson Air Force Base. This program is currently in the test phase.

The advent of digital technology on the engine scene offers not only the opportunity to control more engine variables but also the possibility of integrating engine and airframe control. Studies of this type have also begun.

Primary tools in the F100 Multivariable Control Synthesis Program

were linear quadratic regulator (LQR) theory in the linear case. For the global control, nonlinear optimal methods were not directly applied.

The purpose of Grant NSG-3048 is to evaluate alternatives to LQR in the linear case and to examine nonlinear modelling and optimization approaches for global control.

Context for the studies is set by the DYNGEN digital simulator [2]. Based upon earlier computer codes GENENG [3] and GENENG II [4], DYNGEN has the combined capabilities of [3] and [4], for calculating steady-state performance, together with the further capability for calculating transient performance. DYNGEN uses a modified Euler method to solve the differential equations which model the dynamics of the engine. This modified Euler method permits the user to specify large time steps, for example a tenth of a second; and this can result in considerable savings of execution time. On the other hand, convergence problems are sometimes encountered with DYNGEN wher small time steps are used.

The DYNGEN digital simulation is particularized to a given situation by a process of loading data for the various maps associated with a given engine. The maps for the Grant NSG-3048 have been provided by engineering personnel at Lewis Research Center. These maps correspond to a paper engine, which is not closely identified with any current engine. But the data do correspond in a broad, general sense to realistic two spool turbofan engines. The simulation provides for two essential controls, main burner fuel flow and jet exhaust area. Portions of the envelope which can be used for linear or nonlinear experimentation are limited by the convergence capabilities of the available engine data on DYNGEN.

With respect to multivariable frequency domain work, the basic approaches may be classified into two groups. These two groups are often called "direct" and "indirect".

The direct approach can usually be recognized by its attention to achieving a completely specified dynamic performance. Such ideas have been discussed from the early days of organized control study. See, for example, [5] and [6]. In fact, some of the earliest attempts to expand the direct approach to the multi-input, multi-output case involved work with jet engines [7,8]. Direct approaches in multivariable applications typically involve matrices of transfer functions. In the 1950's, there were some nontrivial difficulties with such methods in cases of more than one input and output. Among these difficulties may be mentioned

(1) the meaning and extent of cancellations of various types in the transfer functions,

(2) the question of loop stability,

(3) the problem of specification, and

(4) numerical computations.

Advances in the last two decades have resolved (1) and (2); in industry, a reservoir of expertise has built up relative to (3); and progress in the numerical sciences is rapidly achieving an interface with control theory in such a way as to resolve (4). It is believed that work on this grant is continuing to stimulate rapid developments in areas (3) and (4).

Indirect approaches are usually recognizable by their affinities

to the classic works of Nyquist or Evans, involving, respectively, frequency response plots in the complex plane or versions of the root locus. It is a relatively easy matter to describe the focus of generalized Nyquist methods. The key constituent ideas are related to three polynomials:

(1) $p_c(s)$ - the closed loop characteristic polynomial (CLCP),

(2) $p_o(s)$ - the open loop characteristic polynomial (OLCP), and

(3) $|M(s)|$ - the determinant of return difference.

The CLCP is a polynomial whose zeros characterize the exponential impulse response of the closed loop control system; the OLCP serves the same purpose for the open loop system. M(s) is a matrix of transfer functions associated with the following experiment. Break the control loops at a convenient point and inject impulses. The difference between the transform of the signal injected and that which returns at the other end of the loop is established by the columns of M(s). The quantities $p_c(s)$, $p_o(s)$ and M(s) derive their importance from the fact that they are related to each other by the equation

$$p_c(s) = |M(s)|\, p_o(s).$$

Typically, $p_o(s)$ is known; and M(s) is partly given and partly designed, in such a way that $p_c(s)$ becomes desirable.

Generally speaking, a Nyquist plot of $|M(s)|$ tends to contain the same types of information which proved so successful in classical designs. A great deal of the design effort centers upon the way in which dynamical compensation affects the determinant which acts on M(s). There are three well recognized ways to study this effect. These are

(1) direct construction of $|M(s)|$ by any of the known methods for determinant calculation,

(2) construction of the eigenvalues of $|M(s)|$ as a function of s, and use of the idea that the determinant is equal to the product of its eigenvalues [9], and

(3) design of compensation so that M(s) is approximately diagonal, and establishment of a relation between the plot of $|M(s)|$ and plots of the diagonal elements of M(s) [10].

It is believed that work on this grant has advanced the application of all these methods to jet engine design, but particularly method (3), where a special technique has been developed to design compensation so that M(s) is approximately diagonal. This technique is called the CARDIAD Plot, where the acronym stands for Complex Acceptability Region for DIAgonal Dominance, the latter term referring to a specific definition of "approximately diagonal."

With respect to nonlinear modelling and optimization, the emphasis has been twofold: to develop good analytical nonlinear models of the jet engine and to use these models in conjunction with techniques of mathematical programming in order to develop advances in global control over significant reaches of the flight envelope.

In general, there are several aspects to this part of the investigation. First, it is possible to conceive the basic differential equations from fundamental principles. In this case, there are usually about sixteen nonlinear differential equations, as well as a large number of nonlinear static functions which serve as part of the coupling between

the equations. These functions often have more than one argument. If the equations arise in this fashion, then there is a significant need to identify the parameters. This must normally be done from the DYNGEN digital simulation. Second, it is possible to assume a general form for the nonlinear differential equations in such a way that fundamental principles are not ignored but that added emphasis is placed upon general mathematical form. If this general form is chosen according to a scheme designed to make maximum use of the type of data which is directly available from the digital simulation, then a type of "automatic" nonlinear model generation becomes possible. Third, whether the first or second modelling procedure is employed, there is almost always a need to consider the problem of reducing the order of the models. Though order reduction can often be highly mathematical in nature, it is almost always the case that the reduced order model depends upon the scaling of the equations. As a result, the final reduced models often depend in a nontrivial way upon physical insight, as well as mathematical method.

Work on this grant has focused especially upon the first and second aspects of the modelling problem, with a gradual specialization toward automatic model generation.

Insofar as optimization is concerned, the stress has been placed upon time optimal control, and considerable effort has been invested in specialized programming methodology designed to take maximum advantage of the particular features of jet engine models.

In the next section, the highlights of activities carried out during the calendar year corresponding to this report are presented.

II. HIGHLIGHTS OF THE RESEARCH

This section is a brief statement of the main achievements under Grant NSG-3048 during the period from March 1, 1977 to February 28, 1978. There are two major subdivisions, according to the main thrusts of the investigation. The first of these is Local Multivariable Frequency Domain Methods; and the second is Global Nonlinear Optimal Methods.

For the most part, the wording of these paragraphs has been constrained so as to be as nontechnical as possible. Nonetheless, some readers may find it useful to review the basic introduction provided in Section I.

A. Local Multivariable Frequency Domain Methods

During the calendar year ending on February 28, the following results were achieved in the area of modern, frequency domain control of turbofan engine models.

(1) The first formal documentation of the CARDIAD method (Complex Acceptability Region for DIAgonal Dominance) was completed. See (1), Section III. Though supported principally under a theory grant from the National Science Foundation, this technique had its origin in class studies of older methods for approximate decoupling of jet engine models in the frequency domain. Almost all of the examples in this thesis were taken from F100-like engine data.

(2) The first documented studies of direct Nyquist plots of return difference determinants for jet engine models were completed. See (3), Section III. This thesis has been a helpful ancillary tool in general frequency domain design.

(3) The first frequency domain closed loop compensation and simulation of a DYNGEN turbofan engine model was achieved. See (5), Section III. As explained in

Section I, the DYNGEN simulation supplies two control inputs.

(4) The first study of polynomial techniques for exact model matching control of jet engine models in the frequency domain was reported. See (6), Section III. This paper has been pivotal in promoting the numerical advance of such techniques for applications. More will be reported in the subsequent semi-annual status report.

(5) About a given design point, linear models of the standard type are obtained from the DYNGEN simulation by the DYGABCD routine [11]. In order to use DYGABCD at off-design points, however, modifications to DYGABCD necessary to the research had to be accomplished. See (7), Section III.

(6) The CARDIAD plot was applied to a series of DYNGEN off-design point models in order to determine its utility as a method for global classification of interaction characteristics of jet engines. See (14), Section III. The results were positive.

(7) An entire conference was convened from industry, laboratories, and universities to hear speakers from several countries apply their theories to a theme problem developed from jet engine data. See (15), Section III. This meeting resulted in a book publication [12].

(8) The CARDIAD methodology was extended to the three-control-input case and applied successfully to Pratt-Whitney data for the F100 engine. See (16), Section III.

(9) A joint seminar series was established between the Department of Electrical Engineering at Notre Dame and the Energy Controls Division of the Bendix Corporation at South Bend, in areas of mutual interest. This has resulted in published work. See (17), Section III.

B. Global Nonlinear Optimal Methods

The major advances and results achieved during the past year in the area of global nonlinear optimal methods are the following.

(1) The hierarchy of analytical nonlinear models for the two spool turbofan jet engine has been expanded and refined. See (2), Section III. This effort is in

keeping with general interest in the industry concerning improvement of compact general models.

(2) A comparison has been achieved between the use of a linear affine model and a nonlinear model for time optimal control studies of a single spool engine. See (4), Section III. The results again support the search for reasonably simple nonlinear models, in the sense that they argue in favor of models whose nonlinearity is not excessively complicated.

(3) A method using linear quadratic regulator methods to obtain decoupled control has been tested on various engine models. See (8), Section III. This is also an outgrowth of the joint Notre Dame - Bendix seminar series mentioned in (9), Section IIA, above.

(4) A two time-scale scheme has been developed in order to do two-dimensional dynamic programming on a fifth order model of a jet engine. See (10), Section III. This is part of a continuing study of time-optimal control methods applied to nonlinear engine models.

(5) Convergence times in time-optimal successive approximation dynamic programming have been dramatically improved through development of a scheme for a spiral out sweep from the target. See (10), Section III.

(6) A completely automatic method for obtaining nonlinear analytical models for engine simulations has been developed and tested numerically. See (11), Section III. This approach offers considerable promise for improvement over previous methods.

(7) A discrete maximum principle has been developed for nonlinear systems having the property that the control is constrained by the present state. See (12), Section III.

(8) A family of optimal feedback control laws has been developed and simulated for a variety of models.

Further details concerning these highlights may be found in Sections IV and V. Also, as described in Section III following, a number of the documents have been included as appendices.

The next section contains a list of publications completed during the current year of the grant.

III. PUBLICATIONS

This section provides a list of the nineteen documents completed during the year March 1, 1977 through February 28, 1978. The works are ordered chronologically.

Some of the listings are followed by an alphabetical code consisting of one or more of the letters A, M, and R. The letter A signifies that the document or an abstract thereof appears as one of the appendices to this report; the letter M signifies that the document comprises a thesis for the degree of Master of Science in Electrical Engineering; and the letter R declares that the document summarizes an effort which was closely integrated with, but not directly supported by, the activities of this grant.

Completed publications from earlier years are not included in this list; but a total listing of all the grant documents has been provided as an appendix to the report. See the Table of Contents.

(1) R.M. Schafer, "A Graphical Approach to System Dominance", Technical Report EE 772, University of Notre Dame, April 1, 1977. (M,R)

(2) W.E. Longenbaker and R.J. Leake, "Hierarchy of Simulation Models for a Turbofan Gas Engine", Proceedings Eighth Annual Pittsburgh Conference on Modeling and Simulation, April 1977. (A)

(3) P.W. Hoppner, "The Direct Approach to Compensation of Multivariable Jet Engine Models", Technical Report EE 774, University of Notre Dame, May 1977, (M,R)

(4) R.R. Gejji and R.J. Leake, "Time-Optimal Control of a Single Spool Turbojet Engine Using a Linear Affine Model", Technical Report EE 7711, University of Notre Dame, June 1977.

(5) R.M. Schafer, R.R. Gejji, P.W. Hoppner, W.E. Longenbaker and M.K. Sain, "Frequency Domain Compensation of a DYNGEN Turbofan Engine Model", Proceedings Sixteenth Joint Automatic Control Conference, pp. 1013-1018, June 1977. (A)

(6) R.R. Gejji and M.K. Sain, "Application of Polynomial Techniques to Multivariable Control of Jet Engines", Proceedings Fourth IFAC Symposium on Multivariable Technological Systems, pp. 421-429, July 1977. (A)

(7) R.R. Gejji, "Use of DYGABCD Program at Off-Design Points", Technical Report EE 7703, University of Notre Dame, July 1977.

(8) E.A. Sheridan and R.J. Leake, "Non-Interactive State Request Jet Engine Control with Non-Singular B Matrix", Proceedings Twentieth Midwest Symposium on Circuits and Systems, pp. 539-543, August 1977. (R)

(9) R. Gejji, R.M. Schafer, M.K. Sain, and P. Hoppner, "A Comparison of Frequency Domain Techniques for Jet Engine Control System Design", Proceedings Twentieth Midwest Symposium on Circuits and Systems, pp. 680-685, August 1977. (A)

(10) W.E. Longenbaker and R.J. Leake, "Time Optimal Control of a Two-Spool Turbofan Jet Engine", Technical Report EE 7714, University of Notre Dame, September 1977. (A,M)

(11) R.J. Leake and J.G. Comiskey, "A Direct Method for Obtaining Nonlinear Analytical Models of a Jet Engine", Proceedings International Forum on Alternatives for Linear Multivariable Control, National Electronics Conference, Chicago, pp. 203-212, October 1977. (A)

(12) J.A. Ortega and R.J. Leake, "Discrete Maximum Principle with State Constrained Control", SIAM Journal on Control and Optimization, Vol. 15, No. 6, pp. 109-115, November 1977. (R)

(13) Michael K. Sain and V. Seshadri, "Pole Assignment and a Theorem from Exterior Algebra", Proceedings IEEE Conference on Decision and Control, pp. 291-295, December 1977. (R)

(14) R. Michael Schafer and Michael K. Sain, "Some Features of CARDIAD Plots for System Dominance", Proceedings IEEE Conference on Decision and Control, pp. 801-806, December 1977. (A)

(15) M.K. Sain, "The Theme Problem", in Alternatives for Linear Multivariable Control, M.K. Sain, J.L. Peczkowski and J.L. Melsa, Editors. Chicago: National Engineering Consortium, 1978, pp. 20-30. (A)

(16) R.M. Schafer and M.K. Sain, "Input Compensation for Dominance of Turbofan Models", in Alternatives for Linear Multivariable Control, M.K. Sain, J.L. Peczkowski, and J.L. Melsa, Editors. Chicago: National Engineering Consortium, 1978, pp. 156-169. (A)

(17) J.L. Peczkowski and M.K. Sain, "Linear Multivariable Synthesis with Transfer Functions", in Alternatives for Linear Multivariable Control, M.K. Sain, J.L. Peczkowski, and J.L. Melsa, Editors. Chicago: National Engineering Consortium, 1978, pp. 71-87. (R)

(18) R.J. Leake and M.K. Sain, "Semi-Annual Status Report, NASA Grant NSG-3048, 'Alternatives for Jet Engine Control', Supplement No. 2", March 1, 1977-August 31, 1977.

(19) R.J. Leake and M.K. Sain, "Final Technical Report, NASA Grant NSG-3048, 'Alternatives for Jet Engine Control', Supplement No. 2", March 1, 1977-February 28, 1978.

IV. LOCAL MULTIVARIABLE FREQUENCY DOMAIN METHODS

Progress on local multivariable frequency domain methods has been achieved during this grant period in the areas of Low Interaction Design, Polynomial Design, Extension of CARDIAD Method, and Multiple Setpoint studies.

Low Interaction Design

As mentioned in the Final Report for NASA Grant NSG-3048, Supplement No. 1, a promising new technique for designing dynamical compensation began to develop in the Fall of 1976. This methodology, built upon what are currently being called CARDIAD plots, was only being tentatively considered in October, 1976 when the continuation proposal for NASA Grant NSG-3048, Supplement No. 2, was being written. Based upon favorable preliminary reaction by personnel from NASA Lewis Research Center, a decision was made to investigate further the use of CARDIAD plots as a design aid for turbofan engine control in the frequency domain. In essence, this study proved to be successful enough that it really dominated the remaining time period of Supplement No. 1 and has continued through Supplement No. 2.

A great deal of the power of the CARDIAD plot arises from its simplicity. For each frequency, a circle is constructed on a planar plot. Data for the center and radius of this circle is obtained from the complex transfer function matrix of the plant. The circle may be solid or dashed. If solid, the inside of the circle defines the acceptable complex region for the value of a frequency dependent compensator element in order to achieve dominance. If dashed, the outside of the circle de-

fines the acceptable region. As the frequency follows a standard Nyquist pattern, these circles result in a CARDIAD plot. (Complex Acceptability Region for DIAgonal Dominance). This plot has been shown to speak constructively to the issue of compensator choice to reduce interaction.

As an example of the CARDIAD plot application to the turbofan engine control problem, a linear model obtained using DYGABCD on the DYNGEN digital engine simulator was used to illustrate control design at the 1977 Joint Automatic Control Conference. The paper based upon this effort, which may be seen in Appendix C, utilizes a two-input, five-state, two-output engine model in which the inputs are fuel flow and nozzle area, the states are compressor speed, fan speed, burner exit pressure, afterburner exit pressure, and high turbine inlet energy, and the outputs are thrust and high turbine inlet temperature.

Typical examples of CARDIAD plots for such engine models may be seen in Figures 2-5 of Appendix C. The investigators involved in this study have seen the same type of plots arising from a variety of engine data. This has raised the interesting question of whether there may be a meaningful concept of "engine interaction footprint" in the sense of the CARDIAD plot.

Of particular interest is the plot shown in Figure 3 of Appendix C. Students of classical control theory will immediately recognize the near semicircular nature of this plot. Such semicircular behavior has been observed frequently and serves to specify a sort of essential lead-lag classical compensator element which can achieve diagonal dominance.

Using the CARDIAD approach, it has been possible to achieve diagonal

dominance at all frequencies on typical engine models. Moreover, only simple compensators have been required to do this. While it is not possible to apply the same degree of credibility to the model itself at all frequencies, it is nonetheless of considerable theoretical interest to be able to make this accomplishment, especially for (A, B, C, D) type plant models which have the D matrix present to approximate modelling errors at high frequencies. Further insight into the significance of these steps can be obtained by examining Appendix B of the Final Report for Supplement No. 1.

Appendix C of this report also contains evidence of two other facets of the applications researches conducted under this grant. Figures 6-8 are characteristic locus plots for the plant, after it was compensated by the CARDIAD methodology. This combination of ideas, namely, the CARDIAD plot and the characteristic locus, has been quite helpful in studies conducted up to this time. Softwares were developed and experience gained with the characteristic locus on the original grant NSG-3048, as well as on Supplement No. 1.

Of additional interest also are Figures 9-11 of Appendix C. These figures deal with an aspect of frequency domain control research which may be called a "direct" approach. The term "direct" refers to a direct construction of the determinant of return difference as frequencies follow a standard Nyquist pattern. This tool really underlies all the modern frequency domain ideas; but it is usually handled obliquely, as for example by the CARDIAD idea or by the characteristic locus. Studies of the direct approach to determinant of return difference have confirmed

that it is at the very least a revealing analysis method. Figure 11 of Appendix C, for example, reveals a condition of gain limitation which is understandable in a global way not so easily visualized by separate characteristic locus plots. It should be emphasized, moreover, that diagrams of the type of Figure 11 can be drawn without any regard of plant size in terms of inputs, states, and outputs.

Efforts to use the direct approach for design, as well as for analysis, have posed nontrivial algebraic questions. Some insight has been gained, but no breakthroughs have occurred as yet.

Polynomial Design

The principal efforts and results obtained in applying polynomial design techniques to the turbofan engine control problem have been reported in the Final Report on Supplement No. 1.

During the present grant period, a paper on this work was presented at the International Federation of Automatic Control's Fourth Symposium on Multivariable Technological Systems at the University of New Brunswick in Fredericton. See Appendix D.

There is now little doubt that the control area is experiencing a resurgence of interest in transfer function methods. As part of this resurgence, grant work on polynomial design has pointed out the necessity of increased attention to numerical method. The investigators also believe that it has stimulated other workers to begin numerical studies.

The transfer function has a number of key properties which have long made it popular with control practitioners. For example, the transfer function is unique relative to similarity transformations on the state

space.

Much work remains to be done, however, on computational aspects of transfer function design.

A presentation comparing the design experiences of the investigators under this grant, in the frequency domain, was made at the 1977 Midwest Symposium on Circuits and Systems, Lubbock, Texas, in August. A copy of this brief manuscript may be seen in Appendix E.

Extension of CARDIAD Method

All the work so far mentioned in regard to the CARDIAD plot was carried out for plants having two inputs and two outputs. In this situation, it is certainly true that the plots have many interesting properties.

On the basis of this experience, which was in its final stages in May, 1977, it was decided to extend the CARDIAD theory to the three-input, three-output case. Also, the National Engineering Consortium's International Forum on Alternatives for Linear Multivariable Control, which took place in October, 1977, offered a prime opportunity to apply the theoretical extension, inasmuch as the Forum contains a Theme Problem based on a linearized model of a modern turbofan engine. See Appendix I. Assistance in the theoretical extension of CARDIAD to the three-input, three-output case was provided by support extended to Dr. Sain by the National Science Foundation under Grant ENG 75-22322. NASA support under Supplement No. 2 was focused on the turbofan application.

Appendix J, "Input Compensation for Dominance of Turbofan Models",

provides a complete description of the successful work on this extension and its application.

Technically, the extension of CARDIAD plot methods to the three-input, three-output case involved the use of a bound which provides sufficient conditions for diagonal dominance. Many possibilities exist for the selection of such a bound, and there remains considerable opportunity for further research along these lines. After examination of a number of basic bounding possibilities, an initial selection was made in such a way that the bound will extend to the case of a plant having p inputs and p outputs, where p is any positive integer greater than or equal to two, and that the bound will be tight in the place where it matters the most---where the plant is close to failing the dominance test.

From an engineering point of view, it was necessary to develop software to extend the CARDIAD idea and to establish viewpoints for studying the plots in more complicated cases. The CARDIAD analysis was divided into two phases. The first phase assumed one off-diagonal compensator element to be zero. An advantage of such a phase lies in its conceptual reduction to the situation of Appendix C, where greater design experience is available. The first-phase approach was adequate for about half of the application to the National Engineering Consortium Theme Problem. The second phase assumed both off-diagonal compensator elements to be nonzero, but drew the plot in such a way that the designer could ascertain what would happen when one of those elements was zero. This second phase approach was successful in completing the design for the Theme Problem.

A number of noteworthy points should be brought out concerning this extension research.

(1) These CARDIAD methods have been successful without assuming a fixed form of the compensator. The importance of this fact can scarcely be overemphasized. If a fixed form is assumed, it may happen that the form is inadequate to fit the essential plant characteristics; and, as a result, it can well be the case that essential insight is lost.

(2) The CARDIAD approach, applicable to design localized to just one side of the plant, as for example the input, can be used to affect outputs that are not measurable. Other methods that use compensation both at plant input and plant output often depend upon moving the output compensator around the loop---an operation which is not possible unless those outputs drive the loop. It would seem that this could be quite important in the case of key outputs such as high turbine inlet temperature and thrust.

(3) In cases studied so far, and there have been over a dozen of them, the CARDIAD plot has achieved dominance over all frequencies, even when the plant has (A, B, C, D) form and transmission does not roll off to zero at high frequencies. This design power has been accompanied by a need for only relatively simple dynamical compensation.

(4) In practice, gain selection in compensators has to be done with some care, so as not to invalidate the accuracy of the linearized model. The CARDIAD approach conveys considerable direct insight into the gains available; and does not leave the choice indirectly to an op-

timization program.

Because of these features, the investigators feel that the CARDIAD plot is helping to push back the research frontier in frequency domain approaches to approximate decoupling.

Multiple Setpoints

From the outset, the CARDIAD plot has offered much promise for the general control problem which involves linearization at multiple setpoints, design at each setpoint, and a piecing together of these designs to achieve global effects. Such technique is certainly the norm both in present-day practice and in current research for the turbofan engine.

Basically, the idea is to construct CARDIAD plots to each setpoint and to use these to study the interaction features of the nonlinear engine model over a more global operating regime. The investigators believe that such studies can be helpful in selecting setpoints for design and in constructing compensation which works toward global dominance.

Work has been proceeding along these lines, with the aid of setpoints involving two inputs and two outputs from NASA's DYNGEN engine simulator. The first documentation can be found in Appendix H.

In Appendix H, the setpoints are determined by fuel flows of 2.145, 2.31, 2.475, 2.64, and 2.75 LBM/SEC. Figures 1-10 of the appendix contain the corresponding CARDIAD plots. Consider Figures 1, 3, 5, 7 and 9, which focus on the first column. Note their clear similarity. Next consider Figures 2, 4, 5, 8 and 10. Again note their clear similarity. Because of this similarity, it was possible to design one simple compensator to achieve diagonal dominance at all five setpoints. This compensa-

tor is indicated in Section Four of Appendix C.

Research is continuing on putting together a global compensation based upon these analyses on the DYNGEN simulator.

The technique is promising and is receiving maximal attention on the project.

V. GLOBAL NONLINEAR OPTIMAL METHODS

This section is concerned with some of the details of the third year of effort on the global nonlinear optimal part of the research. As in the previous year, this part is primarily concerned with the control of a two-spool engine.

There are three main aspects of the work:

DYNGEN Simulator Operation

Turbine Engine Modelling

Nonlinear Optimal Control

DYNGEN Simulator Operations

The DYNGEN simulator, equipped with DYGABCD, has been useful in nearly all studies related to the grant, as it provides a "real world" testing ground for the various control methods under investigation. However, it is costly and has limitations. Two such limitations are the fact that it is difficult to get convergence at low rotor speeds, and that only two controls (WFB and A_8) are readily available to the user.

The automatic generation of ABCD matrices enabled by DYGABCD has been invaluable. It is felt that our work has contributed to the overall development of the simulator through feedback provided, as for example, the simple modification suggested in Mr. Gejji's memorandum. See (7), Section III.

In the early stages of the work, DYNGEN was of primary concern, but it is now fairly routine and attention has turned to other areas.

Turbine Engine Modelling

This phase of the work began with analog computer studies of a single spool engine. Then a considerable effort was spent to obtain a good analytical model for a two spool model using fundamental physical considerations. This study resulted in a hierarchy of models as reported in W.E. Longenbaker's M.S. Thesis, Appendix F, and the paper by Longenbaker and Leake presented at the Pittsburgh Conference on Modelling and Simulation, Appendix B. As indicated in the results of Longenbaker's Thesis, the models obtained were disappointing. Even linear affine models appeared to fare better. See (4), Section III.

As a result of this experience, the main emphasis in the work has now turned toward automatic generation of models by computer methods. The first effort in this direction is reported in the Chicago International Forum paper by Leake and Comiskey, Appendix G. The basic approach is to use an approximation of

$$\dot{x} = f(x,u)$$

which is of the form

$$\dot{x} = A(x,u)\ (x - g(u)).$$

This form seems to work very well for jet engine models. In the first place, there is always a unique equilibrium point for a given fixed control u, so

$$x = g(u)$$

is the equilibrium equation which is all important for steady state analysis. In the second place, jet engine A matrices rarely have poles (eigenvalues) at the origin and hence they are invertible.

This is a great help in computing such models. Suppose then that

$$f(x,u) = A(x,u)\ (x-g(u)),$$

and let

$$(x_e,\ u_e)$$

be an equilibrium pair satisfying

$$x_e = g(u_e).$$

Then

$$\frac{\partial f}{\partial x}\ (x_e,\ u_e) = A(x_e,\ u_e)\ ,$$

and

$$\frac{\partial f}{\partial u}\ (x_e,\ u_e) = -\ A(x_e,\ u_e)\ \frac{\partial g}{\partial u}\ (u_e).$$

Now it is well known that $\frac{\partial f}{\partial x}$ corresponds to the approximate system A matrix in the steady state, so in our model, A(x,u) is a running approximation of the system A matrix and it can thus be approximated by measuring the A matrix at equilibrium points of interest and interpolating.

A key point is, however, that $\frac{\partial f}{\partial u}$ corresponds to the system B matrix in the steady state, and hence

$$B(x_e,\ u_e) = -\ A(x_e,\ u_e)\ \frac{\partial g}{\partial u}\ (u_e)$$

or

$$\frac{\partial g}{\partial u}\ (u_e) = -\ A^{-1}(x_e,\ u_e)\ B(x_e,\ \ u_e)\ .$$

This is where the invertibility of A comes in.

Thus, if there is an <u>automatic</u> method of finding A and B matrices (as we have in DYGABCD) then we have an easy way to get measurements of

$$A(x,u),\ g(u),\ \text{and}\ \frac{\partial g}{\partial u}\ (u).$$

The $\frac{\partial g}{\partial u}$ term is very important because it is the DC gain of the linear model from control to state. To see this, consider the transfer function relation

$$X(s) = (sI-A)^{-1}B\ U(s).$$

Then the s = 0 DC gain relation is

$$-\ A^{-1}\ B.$$

It follows from the above discussion that use of the model form prescribed permits one to key in on

Authentic Equilibrium Values

Authentic A Matrix Values

Authentic DC Gain Values

for a global nonlinear model by measuring only

Equilibrium Values

A Matrices

B Matrices.

These measurements can usually be made by automated methods.

The Chicago paper, Appendix G, was a first attempt to use the approach. J.G. Comiskey's M.S. Thesis is to use Hermite polynomials which are well matched to $\frac{\partial g}{\partial u}$ derivative requirements.

Nonlinear Optimal Control

It is felt that W.E. Longenbaker did a comprehensive job of refining our basic successive approximation Dynamic Programming scheme and

applying it to the models he studied. Details can be found in Technical Report No. EE-7714, Appendix F, and in our Semi-Annual Status Report for the period March 1, 1977 - August 31, 1977.

VI. SPECIAL INITIATIVES RELATED TO GRANT WORK

Two special initiatives were carried out during this year. The first was a special session at the 1977 Joint Automatic Control Conference, and the second was an entire meeting, the International Forum on Alternatives for Linear Multivariable Control.

Joint Automatic Control Conference

A session "Turbofan Engine Control" was put together for this conference. Co-Chairmen and Organizers were Drs. Michael K. Sain and H. Austin Spang. The papers are listed below.

1. System Identification Principles Applied to Multivariable Control Synthesis of the F100 Turbofan Engine
   R.L. DeHoff and W.E. Hall, Jr.
   Systems Control, Inc. (Vt.)

2. Failure Detection and Correction for Turbofan Engines
   H.A. Spang, III and R.C. Corley
   General Electric Company

3. Frequency Domain Compensation of a DYNGEN Turbofan Engine Model
   R.M. Schafer, R.R. Gejji, P.W. Hoppner, W.E. Longenbaker, and M.K. Sain
   University of Notre Dame

   See Appendix C.

4. The Application of the Routh Approximation Method to Turbofan Engine Models
   W. Merrill
   NASA Lewis Research Center

5. Minimum-Time Acceleration of Aircraft Turbofan Engines
   F. Teren
   NASA Lewis Research Center

6. Optimal Controls for an Advanced Turbofan Engine
   G.L. Slater
   University of Cincinnati

International Forum on Alternatives for Linear Multivariable Control

In October, 1977, Dr. Sain was Program Chairman for an entire meeting focused in the general subject area of this grant. Approximately two hundred persons attended from industry, laboratories, and universities. About thirty papers were presented, many by invited authorities of international stature. Nearly two-thirds of these addressed themselves to a Theme Problem, Appendix I, which was derived from researches on this grant. Two publications resulted. The Proceedings contained contributed papers and abstracts of invited papers. The book [12] contained invited papers and those contributed papers which best fit in with the Forum Theme.

The Forum Program appears on the next two pages. More information can be found in [12].

SESSION 1. *Origins of the Theme Problem*
Chairman: M. K. Sain, University of Notre Dame

8:00 Engine Criteria and Models for Multivariable Control System Design
R. D. Hackney and R. J. Miller, Pratt-Whitney Aircraft Group, and L. L. Small, Air Force Aero-Propulsion Laboratory

8:30 A Practical Approach to Linear Model Analysis for Multivariable Turbine Engine Control Design
C. A. Skira, Air Force Aero-Propulsion Laboratory, and R. L. DeHoff, Systems Control, Inc. (Vt.)

SESSION 2. *Theme Session A: Inverse Nyquist Array*
Chairman: B. Lehtinen, NASA Lewis Research Center

9:00 The Inverse Nyquist Array Method
H. H. Rosenbrock and N. Munro, University of Manchester, England

10:00 Insight into the Application of the Inverse Nyquist Array Method to Turbofan Engine Control
H. A. Spang, III, General Electric Research and Development Center

10:30 BREAK

	SESSION 3-1. *Transfer Functions I* Chairman: S. Kahne, Case Western Reserve Univ.	SESSION 3-2. *Alternate Methods* Chairman: J. Gibson, Texas A & M University
11:00	Multivariable Design Problem Reduction to Scalar Design Problems B. D. O. Anderson and N. T. Hung, University of Newcastle, Australia	A New Frequency Method for Multivariable Systems R. DeSantis, Universite de Montreal
11:30	The Multivariable Nyquist Array: The Concept of Dominance Sharing G. G. Leininger, University of Toledo	Performance Analysis of Stochastic Linear Control Systems: A New Viewpoint S. R. Liberty, Texas Tech University
12:00	Input Compensation for Dominance of Turbofan Models R. M. Schafer and M. K. Sain, University of Notre Dame	An Automatic Depth and Pitch Control System for Submarines V. Nitsche, K. Luessow, and G. J. Thaler, Naval Post-Graduate School

12:30 LUNCH

SESSION 4. *Theme Session B: Complex Variable Methods*
Chairman: N. B. Nichols, Aerospace Corporation

2:00 Complex Variable Methods for Multivariable Feedback Systems Analysis and Design
A. G. J. MacFarlane, B. Kouvaritakis, and J. M. Edmunds, Cambridge University, England

3:00 The Characteristic Frequency and Characteristic Gain Design Method for Multivariable Feedback Systems
B. Kouvaritakis and J. M. Edmunds, Cambridge University, England

3:30 BREAK

	SESSION 5-1. *Transfer Functions II* Chairman: B. Doolin, NASA Ames Research Center	SESSION 5-2. *Spectral Methods* Chairman: R. DeSantis, Universite de Montreal
4:00	Linear Multivariable Control--A Problem of Specifications Z. V. Rekasius, Northwestern University	Stability and Homotopy R. Saeks, Texas Tech University and R. DeCarlo, Purdue University
4:30	Linear Multivariable Synthesis with Transfer Functions J. L. Peczkowski, Bendix Energy Controls Division and M. K. Sain, University of Notre Dame	A Compensation Procedure for the Desensitization of Multivariable Regulator Eigenvalues P. J. M. Martin, R. K. Cavin, III and J. W. Howze, Texas A M University
5:00	Application of Frequency Domain Multivariable Control Synthesis Techniques to an Illustrative Problem in Jet Engine Control L. G. Hofmann, G. L. Teper, and R. F. Whitbeck, Systems Technology, Inc.	Linear Multivariable Synthesis by Eigenvalue/Eigenvector Assignment S. Srinathkumar, NASA Langley Research Center and R. P. Rhoten, Oklahoma State University

5:30 NO HOST COCKTAIL PARTY

SESSION 6. *Theme Session C: Regulator Methods*
Chairman: S. Brodsky, Office of Naval Research

8:30 Alternatives for Linear Multivariable Control
N. Munro and S. Hirbod, University of Manchester, England

9:00 The Systematic Design of Linear Multivariable Control Systems for the Servomechanism Problem
E. J. Davison and W. S. Gesing, University of Toronto

10:00 Linear Multivariable Control Design Based on Asymptotic Regulator Properties
C. A. Harvey and G. Stein, Honeywell Systems and Research Center

10:30 BREAK

	SESSION 7-1. *Modelling* Chairman: M. Wozny, National Science Foundation	SESSION 7-2. *Model Following* Chairman: W. R. Perkins, University of Illinois	SESSION 7-3. *Comparisons* Chairman: T. E. McDonald, Los Alamos Scientific Laboratory
11:00	A Direct Method for Obtaining Nonlinear Analytical Models of a Jet Engine R. J. Leake and J. G. Comiskey, University of Notre Dame	Active Maneuver Load Control for a Control Configured Airplane N. C. Weingarten and E. G. Rynaski, Calspan Corporation	Quasi-Upper Triangular Decomposition Applied to the Linearized Control of a Turbo-fan Engine--Preliminary Results W. E. Holley, Oregon State University
11:30	A Multi-Time-Scale Design Approach for Jet Engine Control Systems A. J. Calise and B. Sridhar, Dynamics Research Corporation	A Parameter Optimization Method Applied to Engine Control System Design Y. Cheng, NASA Dryden Research Center	Reliability Considerations in Decentrally Controlled Multivariable Systems F. N. Bailey, E. B. Lee, and M. K. Sundareshan, University of Minnesota
12:00	BLS as an Alternative to Linear Control Systems R. R. Mohler and V. R. Karanam, Oregon State University	Model Algorithmic Control A. Rault, J. Richalet and J. Papon, ADERSA/GERBIOS, France, and R. Mehra and W. C. Kessel, Scientific Systems	On Alternative Methodologies for the Design of Robust Linear Multivariable Regulators H. G. Kwatny and K. C. Kalnitsky, Drexel University and TASC

12:30 LUNCH

	SESSION 8-1. *Output Feedback* Chairman: E. M. Cliff Virginia Polytechnic Institute	SESSION 8-2. *Additional Approaches* Chairman: I. Rhodes, Wash. Univ.	SESSION 8-3. *Design* Chairman: E. C. Tacker University of Houston
2:00	Output Feedback Regulator Design for Jet Engine Control Systems W. C. Merrill, NASA Lewis Research Center	Optimal Open Loop Compensator Combined with Riccati Feedback Compensator Control ... R. Froriep, D. Joos, G. Kreisselmeier, DFVLR, West Germany	A Conceptual Design Approach Using Feedforward Plus Forward Compensation N. H. McClamroch, University of Michigan
2:30	A Classical Root Locus Design Method for Multivariable Systems in State Space Form G. K. Lee, University of Connecticut, M. Sohrwardy, Ruhr-Universitat, and D. Jordan, University of Connecticut	Observing Partial States for Systems with Unmeasurable Disturbances S. H. Wang and E. J. Davison University of Colorado and University of Toronto	Computer Aided Design of Control System via Optimization David Q. Mayne, Imperial College, London, England Design of Linear Multivariable Control Systems by CIP L. L. Gresham, J. R. Mitchell, and W. L. McDaniel, Jr. Mississippi State University
3:00	Output Control via Matrix Generalized Inverse R. J. Miller, D. L. Powers, and V. Lovass-Nagy, Clarkson College	On the Design of Accurate Observers S. P. Bhattacharyya and I. G. Trindade, Universidade Federal de Rio de Janeiro and Universidade Federal Fluminense, Brazil	
3:30			

VII. REFERENCES

1. R.L. De Hoff, W. Earl Hall, Jr., R.J. Adams, and N.K. Gupta, "F100 Multivariable Control Synthesis Program", Vols. I and II, Technical Report AFAPL-TR-77-35, June 1977.

2. J.F. Sellers and C.J. Daniele, "DYNGEN-A Program for Calculating Steady-State and Transient Performance of Turbojet and Turbofan Engines", NASA Technical Note TN D-7901, April 1975.

3. R.W. Koenig and L.H. Fishbach, "GENENG-A Program for Calculating Design and Off-Design Performance for Turbojet and Turbofan Engines", NASA Technical Note TN D-6552, February 1972.

4. L.H. Fishbach and R.W. Koenig, "GENENG II-A Program for Calculating Design and Off-Design Performance of Two and Three Spool Turbofans with as Many as Three Nozzles", NASA Technical Note TN D-6553, February 1972.

5. J.G. Truxal, Automatic Feedback Control System Synthesis. New York: McGraw-Hill, 1955.

6. I.M. Horowitz, Synthesis of Feedback Systems. New York: Academic Press, 1963.

7. A.S. Boksenbom and R. Hood, "General Algebraic Method Applied to Control Analysis of Complex Engine Types", NACA Technical Note 1908, July 1949.

8. M.S. Feder and R. Hood, "Analysis for Control Application of Dynamic Characteristics of a Turbojet Engine with Tail-Pipe Burning", NACA Technical Note 2183, September 1950.

9. A.G.J. MacFarlane and I. Postlethwaite, "Characteristic Frequency Functions and Characteristic Gain Functions", International Journal of Control, Vol. 26, pp. 265-278, 1977.

10. H.H. Rosenbrock, Computer-Aided Control System Design. New York: Academic Press, 1974.

11. "DYGABCD - A Program for Calculating A, B, C, and D Matrices for Linear Descriptions of Simulated Turbojet and Turbofan Engines", NASA Lewis Research Center, Preliminary Report.

12. M.K. Sain, J.L. Peczkowski, and J.L. Melsa, Editors, Alternatives for Linear Multivariable Control. Chicago: National Engineering Consortium, 1978.

APPENDIX A

GRANT BIBLIOGRAPHY, INCEPTION TO PRESENT

(1) R.J. Leake, J.L. Melsa, and M.K. Sain, "Preliminary Proposal on Modern Approaches to Jet Engine Control", November 1, 1974.

(2) R.J. Leake, M.K. Sain, and J.L. Melsa, "Proposal to NASA for Support of a Work Entitled 'Alternatives for Jet Engine Control'", November 27, 1974.

(3) R.J. Leake and M.K. Sain, "Semi-Annual Status Report on NASA Grant NSG-3048, 'Alternatives for Jet Engine Control'", March 1, 1975 - August 31, 1975.

(4) R.J. Leake, M.K. Sain, and J.L. Melsa, "Proposal for Continuation of NASA Grant NSG-3048, 'Alternatives for Jet Engine Control'", October 1, 1975.

(5) J.C. Shearer, "An IBM 370/158 Installation and User's Guide for the DYNGEN Jet Engine Simulator", M.S. Thesis, November 1975.

(6) T.C. Brennan and R.J. Leake, "Simplified Simulation Models for Control Studies of Turbojet Engines", Technical Report EE 757, University of Notre Dame, November 1975.

(7) R.J. Leake, M.K. Sain, and J.L. Melsa, "Final Technical Report on NASA Grant NSG-3048, 'Alternatives for Jet Engine Control'", March 1, 1975 - February 29, 1976.

(8) R.R. Gejji and M.K. Sain, "Polynomial Techniques Applied to Multivariable Control of Jet Engines", Technical Report EE 761, March 1976.

(9) V. Seshadri and M.K. Sain, "Multivariable System Compensation Including Characteristic Methods for Jet Engine Control", Technical Report EE 763, May 1976.

(10) A.J. Maloney III, "Graphics Analysis of Dominance in Jet Engine Control Models", Technical Report EE 765, June 1976.

(11) M.K. Sain, R.J. Leake, R. Basso, R. Gejji, A. Maloney, and V. Seshadri, "Alternative Methods for the Design of Jet Engine Control Systems", Proceedings Fifteenth Joint Automatic Control Conference, pp. 133-142, July 1976.

(12) J.C. Shearer, W.E. Longenbaker, Jr., and R.J. Leake, "An IBM 370/158 Installation and User's Guide to the DYNGEN Jet Engine Simulator", Technical Report EE 766, July 1976.

(13) R.R. Gejji and M.K. Sain, "A Jet Engine Control Problem for Evaluating Minimal Design Software", Proceedings Midwest Symposium on Circuits and Systems, pp. 238-243, August 1976.

(14) V. Seshadri and M.K. Sain, "Interaction Studies on a Jet Engine Model by Characteristic Methodologies", Proceedings Midwest Symposium on Circuits and Systems, pp. 232-237, August 1976.

(15) R.J. Leake and M.K. Sain, "Semi-Annual Status Report on NASA Grant NSG-3048, 'Alternatives for Jet Engine Control', Supplement No. 1", March 1, 1976-August 31, 1976.

(16) R. Basso and R.J. Leake, "Computational Alternatives to Obtain Time-Optimal Jet Engine Control", Technical Report EE 767, September 1976.

(17) R. Basso and R.J. Leake, "Computational Methods to Obtain Time-Optimal Jet Engine Control", Proceedings Fourteenth Allerton Conference on Circuit and System Theory, pp. 652-661, September 1976.

(18) M.K. Sain and V. Seshadri, "A Result on Pole Assignment by Exterior Algebra", Proceedings Fourteenth Allerton Conference on Circuit and System Theory, pp. 399-407, September 1976.

(19) R.R. Gejji, "A Computer Program to Find the Kernel of a Polynomial Operator", Proceedings Fourteenth Allerton Conference on Circuit and System Theory, pp. 1091-1100, September 1976.

(20) R.J. Leake and M.K. Sain, "Proposal for Continuation of NASA Grant NSG-3048, 'Alternatives for Jet Engine Control'", October 25, 1976.

(21) R.M. Schafer, W.E. Longenbaker, and M.K. Sain, "System Dominance: A Preliminary Report on an Alternate Approach", Technical Report, University of Notre Dame, November 25, 1976.

(22) R.J. Leake and M.K. Sain, "Final Technical Report, NASA Grant NSG-3048, 'Alternatives for Jet Engine Control', Supplement No. 1", March 1, 1976 - February 28, 1977.

(23) R.J. Leake, J.G. Allen, and R.S. Schlunt, "Optimal Regulators and Follow-Up Systems Determined from Input-Output Signal Monitoring", Proceedings IEEE International Symposium on Circuits and Systems, April 1977.

(24) R.M. Schafer, "A Graphical Approach to System Dominance", Technical Report EE 772, University of Notre Dame, April 1, 1977.

(25) W.E. Longenbaker and R.J. Leake, "Hierarchy of Simulation Models for a Turbofan Gas Engine", Proceedings Eighth Annual Pittsburgh Conference on Modeling and Simulation, April 1977.

(26) P.W. Hoppner, "The Direct Approach to Compensation of Multivariable

Jet Engine Models", Technical Report EE 774, University of Notre Dame, May 1977.

(27) R.R. Gejji and R.J. Leake, "Time-Optimal Control of a Single Spool Turbojet Engine Using a Linear Affine Model", Technical Report EE 7711, University of Notre Dame, June 1977.

(28) R.M. Schafer, R.R. Gejji, P.W. Hoppner, W.E. Longenbaker, and M.K. Sain, "Frequency Domain Compensation of a DYNGEN Turbofan Engine Model", Proceedings Sixteenth Joint Automatic Control Conference, pp. 1013-1018, June 1977.

(29) R.R. Gejji and M.K. Sain, "Application of Polynomial Techniques to Multivariable Control of Jet Engines", Proceedings Fourth IFAC Symposium on Multivariable Technological Systems, pp. 421-429, July 1977.

(30) R.R. Gejji, "Use of DYGABCD Program at Off-Design Points", Technical Report EE 7703, University of Notre Dame, July 1977.

(31) E.A. Sheridan and R.J. Leake, "Non-Interactive State Request Jet Engine Control with Non-Singular B Matrix", Proceedings Twentieth Midwest Symposium on Circuits and Systems, pp. 539-543, August 1977.

(32) R. Gejji, R.M. Schafer, M.K. Sain, and P. Hoppner, "A Comparison of Frequency Domain Techniques for Jet Engine Control System Design", Proceedings Twentieth Midwest Symposium on Circuits and Systems, pp. 680-685, August 1977.

(33) W.E. Longenbaker and R.J. Leake, "Time Optimal Control of a Two-Spool Turbofan Jet Engine", Technical Report EE 7714, University of Notre Dame, September 1977.

(34) R.J. Leake and J.G. Comiskey, "A Direct Method for Obtaining Nonlinear Analytical Models of a Jet Engine", Proceedings International Forum on Alternatives for Linear Multivariable Control, National Electronics Conference, Chicago, pp. 203-212, October 1977.

(35) M.K. Sain and R.J. Leake, "Proposal for Continuation of NASA Grant NSG-3048, 'Alternatives for Jet Engine Control'", October 25, 1977.

(36) J.A. Ortega and R.J. Leake, "Discrete Maximum Principle with State Constrained Control", SIAM Journal on Control and Optimization, Vol. 15, No. 6, pp. 109-115, November 1977.

(37) Michael K. Sain and V. Seshadri, "Pole Assignment and a Theorem from Exterior Algebra", Proceedings IEEE Conference on Decision and Control, pp. 291-295, December 1977.

(38) R. Michael Schafer and Michael K. Sain, "Some Features of CARDIAD Plots for System Dominance", Proceedings IEEE Conference on Decision

and Control, pp. 801-806, December 1977.

(39) M.K. Sain, "The Theme Problem", in Alternatives for Linear Multivariable Control, M.K. Sain, J.L. Peczkowski and J.L. Melsa, Editors. Chicago: National Engineering Consortium, 1978, pp. 20-30.

(40) R.M. Schafer and M.K. Sain, "Input Compensation for Dominance of Turbofan Models", in Alternatives for Linear Multivariable Control, M.K. Sain, J.L. Peczkowski, and J.L. Melsa, Editors. Chicago: National Engineering Consortium, 1978, pp. 156-169.

(41) J.L. Peczkowski and M.K. Sain, "Linear Multivariable Synthesis with Transfer Functions", in Alternatives for Linear Multivariable Control, M.K. Sain, J.L. Peczkowski, and J.L. Melsa, Editors. Chicago: National Engineering Consortium, 1978, pp. 71-87.

(42) R.J. Leake and M.K. Sain, "Semi-Annual Status Report, NASA Grant NSG-3048, 'Alternatives for Jet Engine Control', Supplement No. 2", March 1, 1977 - August 31, 1977.

(43) R.J. Leake and M.K. Sain, "Final Technical Report, NASA Grant NSG-3048, 'Alternatives for Jet Engine Control', Supplement No. 2", March 1, 1977 - February 28, 1978.

Appendix B

"HIERARCHY OF SIMULATION MODELS FOR A TURBOFAN GAS ENGINE"

W. E. Longenbaker
R. J. Leake

EIGHTH ANNUAL PITTSBURGH CONFERENCE ON MODELING AND SIMULATION

APRIL 21-22, 1977

Benedum Engineering Hall
University of Pittsburgh

More Than 220 Papers On:

- SOCIO-ECONOMIC SYSTEMS
- ENVIRONMENTAL SIMULATION
- SIMULATION IN EDUCATION
- ECONOMIC MODELING
- MODELING AND ESTIMATION
- REGIONAL PLANNING
- BIOMEDICAL SYSTEMS
- ECOSYSTEMS
- URBAN MODELING
- ENERGY RESOURCES
- TRANSPORTATION
- AND MANY OTHER SESSIONS

Sponsored by

Department of Electrical Engineering
School of Engineering
University of Pittsburgh
Pittsburgh, Pennsylvania

In Cooperation With

The Pittsburgh Sections
of the
Institute of Electrical and Electronic Engineers
and
The Instrument Society of America
and
The Systems, Man and Cybernetics Society
The Society for Computer Simulation
The International Association for Mathematics and Computers in Simulation (formerly AICA)

Conference Committee

Michael A. Shanblatt
Leone Monticone
Chang-Eun Kim
Martin Savol
Chin Shiek
Khe-Tai Ma
Aly Abulleil
C. P. Fong
Jang G. Lee
Suk H. Lee

Conference Co-Chairmen

William G. Vogt
Marlin H. Mickle

HIERARCHY OF SIMULATION MODELS FOR A TURBOFAN GAS ENGINE

W.E.Longenbaker and R.J. Leake
Department of Electrical Engineering
University of Notre Dame
Notre Dame, Indiana 46556

ABSTRACT

This work is a comparison of successively more comprehensive simulation models of an F-100-like Turbofan jet engine. A large and elaborate computer program called DYNGEN , developed over a number of years at NASA Lewis Research Center, is employed as the most comprehensive model for analyzing steady-state and transient performance for control studies. This model employs many block data maps and includes about 25 states. In order to perform optimal control studies, low order nonlinear analytical, and linear models have been developed. This paper reports on the details of these models and presents experimental data on their relative performance.

INTRODUCTION

In this paper we consider the determination of a simplified nonlinear analytical model for a two spool turbofan jet engine. A large and elaborate (about 4000 FORTRAN statements) generalized engine simulator called DYNGEN [1,2] coded with representative block data maps, design parameters, and two spool operation is taken as the principal object to be approximated. First we present the various models and then performance comparisons are made. The models considered have been enumerated as follows.

Model 0. The actual jet engine (hypothetical.)

Model 1. The DYNGEN simulator, coded with data presumed to have been taken from experimental measurements on Model 0. This model solves more than 16 nonlinear differential equations and uses data maps and thermodynamic tables which cannot be expressed analytically.

Model 2. This is an analytically expressed set of 5 nonlinear differential equations plus about 20 static equations expressing the relationship between various engine variables. The main task in this project was to determine this model.

Model 1L5. This is a normalized 5th order linear model which is obtained numerically from Model 1, using an experimental version of a program [3] being developed at NASA Lewis Research Center.

Model 1L3. This is a normalized 3rd order linear model obtained by a hand calculated order reduction of Model 1L5.

Model 2L5. This is a normalized 5th order linear model obtained by taking partial derivatives of the analytical Model 2.

Model 2L3. This is a normalized 3rd order linear model obtained by a hand calculated order reduction of Model 2L5.

ANALYTICAL MODEL

In this section we discuss and present Model 2., a simplified nonlinear analytical model of the jet engine. There are several reasons why it is desirable to have such a model. First of all, one likes to see the basic nonlinear relationships between the engine variables in order to gain insight to their dynamical and static behavior. Secondly, such a model is invaluable in the application of optimal control techniques [4] to engine control system design. In the third place, if the model is reasonably accurate, it can be employed as a fast inexpensive nonlinear engine simulator for the evaluation of linear and nonlinear control strategies. Finally, linear models obtained by partial differentiation of this model tend to have more structure (zero entries in the ABCD matrices) then those obtained numerically, which gives the linear designer more insight. These linearizations then serve as a back up to compare with the numerical linearizations.

In the determination of Model 2. as an approximation of the DYNGEN Model 1., theoretical relationships developed in [5],[6], and [7] were employed as a starting point. Certain simplifications suggested in [8] were used; and linear, least squares, exponential, and polynomial fits to the Model 1. data about the chosen design point were made.

A 2 input, 5 state, 2 output model was developed with the following variable designations.

U_1 = fuel flow (WFB)

U_2 = nozzle area (A_8)

X_1 = compressor rotor speed (N_C)

X_2 = fan rotor speed (N_F)

X_3 = burner exit pressure (P_4)

X_4 = after burner exit pressure (P_7)

X_5 = high inlet energy (U_4)

Y_1 = thrust (FG)

Y_2 = high turbine inlet temperature (T_4)

The model is completely determined by the following specifications.

Constants

$J = AJ = 778.26$	$N \cong 20.71175$
$A_8 = 2.948255$	$C_{PC} \cong .24$
$R = RA = .0252$	$C_{PF} \cong .24$
$\gamma^* = 1.4$	$C_{VB} \cong .20279$
$P_2 = 1.$	$C_{PHT} \cong .22589$
$T_2 = 518.668$	$C_{PLT} \cong .27938$
$I_C = PMIHP = 3.8$	$\phi = \frac{BLC}{WAC} = .16 = PCBLC$
$I_F = PMILP = 4.5$	$\alpha = PCBLDU = .208$
$V_{COMB} = 1.65$	$\beta = PCBLHP = .726$
$V_{AFBN} = 49.77$	$\gamma = PCBLLP = .066$
N_C DESIGN = XNHPOS = 10070	
N_F DESIGN = XNLPOS = 9651	

Design Values

WFB = 2.75	N_C = 11899.2	FG = 15431.02
A_8 = 2.948255	N_F = 9873.94	T_4 = 2982.04
	P_4 = 23.9299	
	U_4 = 586.467	
	P_7 = 2.55007	

State Equations

$$(1)\ \frac{dN_C}{dt} = \left(\frac{30}{\pi}\right)^2 \frac{J}{I_C N_C}\left[C_{PC}WAC(T_{21}-T_3) + C_{PHT}WG50(T_4 - T_{50})\right]$$

$$(2)\ \frac{dN_F}{dt} = \left(\frac{30}{\pi}\right)^2 \frac{J}{I_F N_F}\left[C_{PF}WAF(T_2 - T_{21}) + C_{PLT}WG55(T_{50} - T_{55})\right]$$

$$(3)\ \frac{dP_4}{dt} = \frac{R\gamma^*}{V_{COMB}}\left[T_4(WA3 + WFB - WG_4)\right]$$

$$(4)\ \frac{dP_7}{dt} = \frac{R\gamma^* T_7}{V_{AFBN}}\left[WG4 - WA3 + WAF - WG7\right]$$

$$(5)\ \frac{dU_4}{dt} = \frac{C_{VB}RT_4}{V_{COMB}P_4}\left[T_4(WG4 - WFB - WA3) + \gamma^*\{T_3 WA3 - T_4 WG4 + T_4(1+\eta)WFB\}\right]$$

Nonlinear Functions Required for State Equations and Outputs

$$(1)\ CNF = \frac{N_F}{N_F DESIGN} = \frac{N_F}{9651}$$

$$(2)\ T_{21} = T_2 + 214.2732\,CNF^2 - 48.0(A_8 - 2.948255)$$

$$(3)\ CNC = \frac{N_C}{N_C DESIGN\sqrt{T_{21}/T_2}} = \frac{N_C}{10070\sqrt{T_{21}/518.668}}$$

$$(4)\ T_3 = T_{21} + 743.2722\,CNC^2 - 68\,(A_8 - 2.948255)$$

$$(5)\ T_4 = U_4/C_{VB}$$

$$(6)\ T_{50} = .727\,T_4$$

$$(7)\ P_3 = 1.05944P_4$$

$$(8)\ P_{21} = -6.20568 + .0129774\,T_{21} - .0185376\,P_3$$

$$(9)\ W_{FMAX} = 3.516739\,CNF - 63.916$$

$$(10)\ P_{FMAX} = 3.516739\,CNF - .23561$$

$$(11)\ WAF = W_{FMAX} + 28.502\left[1 - e^{-2.313268(P_{FMAX}-P_{21})}\right]$$

$$(12)\ W_{CMAX} = 137.54 - 457.987\,CNC + 564.325\,CNC^2 - 188.113\,CNC^3$$

$$(13)\ \Delta W_{CMAX} = 6.492 - 4.9747\,CNC$$

$$(14)\ P_{CMAX} = 26.43184 - 89.0484\,CNC + 109.7234\,CNC^2 - 36.5756\,CNC^3$$

$$(15)\ WAC = \frac{P_{21}}{\sqrt{T_{21}/518.668}}\left\{W_{CMAX} + \Delta W_{CMAX}\left(1 - e^{-.3662\left(P_{CMAX} - \frac{P_3}{P_{21}}\right)}\right)\right\}$$

$$(16)\ WA3 = (1-\phi)WAC = .84\,WAC$$

$$(17)\ WG50 = 301.957\,P4\sqrt{T_4}$$

$$(18)\ WG4 = WG50 - \beta\phi WAC = WG50 - .116164\,WAC$$

$$(19)\ WG55 = WG50 + \gamma\phi WAC = WG50 + .01056\,WAC$$

$$(20)\ T_{55} = 106.002 + .86154T_{50} - .10458CNC\sqrt{T_{21}/T_{50}}$$

$$(21)\ T_7 = \frac{(T_{55} + 414.582P_7)}{2.01365}$$

$$(22)\ WG7 = \frac{1121.784P_7A_8}{\sqrt{T_7}}$$

$$(23)\ FG = .02951\,WG7\sqrt{1934.415T_7 + 68558.365} + 2116.217A_8\,(.53978P_7 - 1)$$

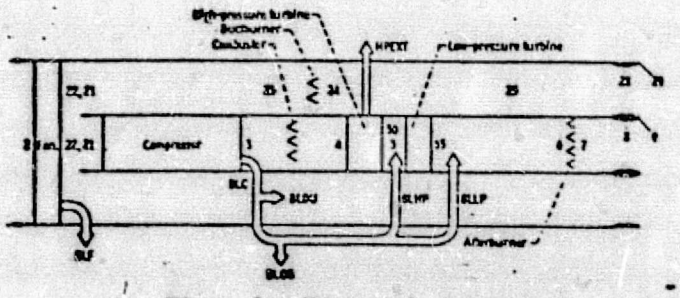

Figure 1 - Two-spool, two-stream turbofan engine

KEY

WA Air flow
WG Gas flow
P Pressure
T Temperature
U Internal Energy

Numbers refer to the location within the engine (figure 1). All variable names correspond to those which are used in DYNGEN

LINEAR MODELS

The following linear models were obtained, with thrust, (FG), as the output if there is only one output.

Model 1L5

$$A = \begin{bmatrix} -3.80 & -1.277 & 2.067 & -1.152 & 1.448 \\ 2.748 & -5.39 & 1.585 & -1.991 & 1.071 \\ 377.9 & 49.51 & -264.9 & 86.807 & 78.91 \\ 31.26 & 139.39 & -6.269 & -88.69 & 27.83 \\ -176.5 & 23.91 & -10.27 & -37.40 & -246.7 \end{bmatrix}$$

$$B = \begin{bmatrix} -.00259 & .355326 \\ .2116 & -.316176 \\ 12.54 & -13.7828 \\ -.6201 & -99.388 \\ 157.783 & 6.84396 \end{bmatrix}$$

$$C = \begin{bmatrix} -.8594 & -.1397 & .6672 & 1.167 & .1236 \\ .055591 & .00656034 & -.0018374 & .0135393 & .853914 \end{bmatrix}$$

$$D = \begin{bmatrix} -.102766 & .900938 \\ -.013839 & .020856 \end{bmatrix}$$

Eigenvalues: $-251 \pm 23j$, -96, $-5 \pm 0.8j$

Model 1L3

$$A = \begin{bmatrix} -2.4307 & -.70897 & -.81149 \\ 3.8281 & -4.9579 & -1.7235 \\ 2.4466 & 140.5 & -94.982 \end{bmatrix} \quad B = \begin{bmatrix} 1.395 & .34875 \\ 1.2585 & .27933 \\ 15.434 & -8.208 \end{bmatrix}$$

$$C = \begin{bmatrix} -.1543 & .013382 & 1.333 \end{bmatrix} \quad D = \begin{bmatrix} .2346 & .87572 \end{bmatrix}$$

Eigenvalues: -92, $-5 \pm 5j$

Model 2L5

$$A = \begin{bmatrix} -12.5487 & -1.69279 & 3.58369 & .237860 & 1.70112 \\ .833048 & -5.61346 & 1.64496 & 0.143805 & 1.30396 \\ 671.604 & 387.711 & -392.675 & -26.1602 & 160.529 \\ -104.155 & 21.1351 & 64.9255 & -67.8031 & 2.63144 \\ 50.9527 & -55.8546 & -81.2047 & -7.47450 & -105.743 \end{bmatrix}$$

$$B = \begin{bmatrix} 0.0 & 1.40762 \\ 0.0 & .758167 \\ 1.28129 & -122.314 \\ 0.0 & -48.9280 \\ 149.210 & -3.09196 \end{bmatrix}$$

$$C = \begin{bmatrix} 0.0 & 0.0 & 0.0 & 1.46096 & 0.0 \\ 0.0 & 0.0 & 0.0 & 0.0 & 1.0 \end{bmatrix}$$

$$D = \begin{bmatrix} 0.0 & 1.21383 \\ 0.0 & 0.0 \end{bmatrix}$$

Eigenvalues: -343, -154, -73, $-7.2 \pm 1.4j$

Model 2L3

$$A = \begin{bmatrix} -8.4225 & -1.254 & -.047955 \\ 2.3957 & -5.9244 & .0048499 \\ -111.51 & -97.919 & -74.905 \end{bmatrix}$$

$$B = \begin{bmatrix} 3.4058 & .79723 \\ 2.1242 & .56146 \\ 200.75 & -39.261 \end{bmatrix}$$

$$C = \begin{bmatrix} 0 & 0 & 1.461 \\ -.63298 & -.97908 & -.01486 \end{bmatrix}$$

$$D = \begin{bmatrix} 0 & 1.2138 \\ 1.072 & .15978 \end{bmatrix}$$

Eigenvalues: -74.976, $-7.138 \pm 1.1717j$

EXPERIMENTAL COMPARISONS

Figures 2 and 3 represent the nonlinear steady state operating lines of the fan and compressor respectively, as both nozzle area and fuel flow are changed. This is a detailed map in the vicinity of our nominal engine design configuration. The design point for model 2 differs from that of model 1 by less than 1/2%.

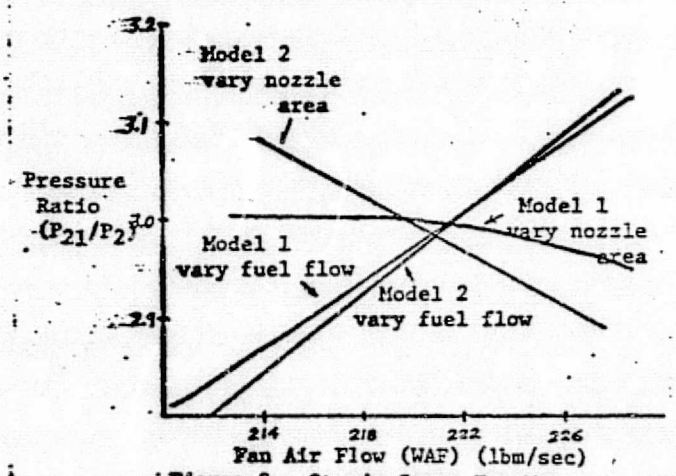

Figure 2. Steady State Fan Map

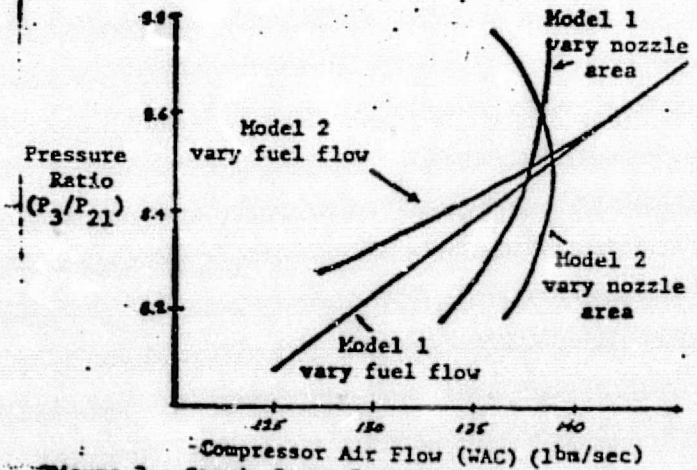

Figure 3. Steady State Compressor Map

The time responses of various states due to 5% step inputs in fuel flow and nozzle area are shown in Figures 4 and 5 respectively. Only the nonlinear models are represented. Although the deviations of the states from their design point differ by as much as a factor of two, the actual values (design plus deviation) of model 2 remain within 1% of the model 1 values. For steps in fuel of minus 20%, the states remain within 8% of each other.

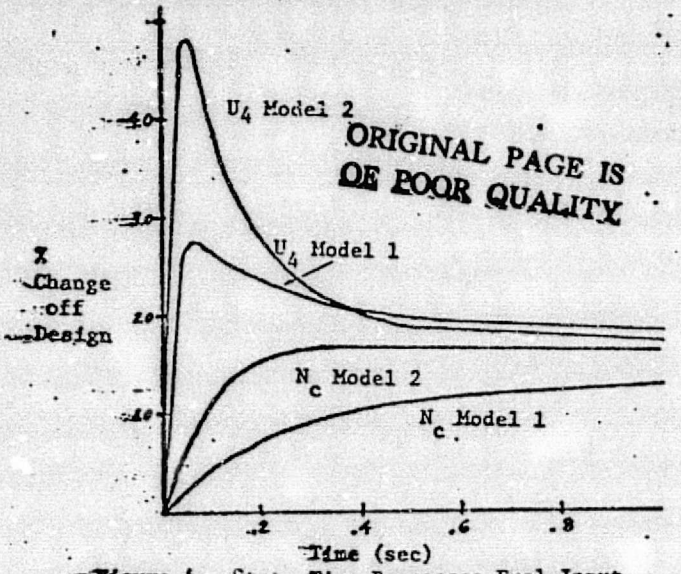

Figure 4. State Time Responses-Fuel Input

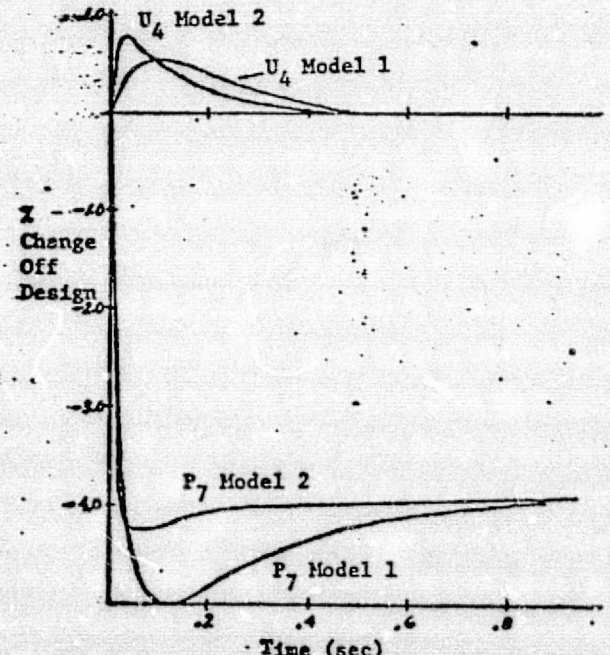

Figure 5. State Time Responses-Nozzle Area Input Step

The effects on thrust by a 5% step in fuel flow are shown in Figure 6. Model 2L5 yields results which are quite close to model 2, although, both are significantly different from model 1.

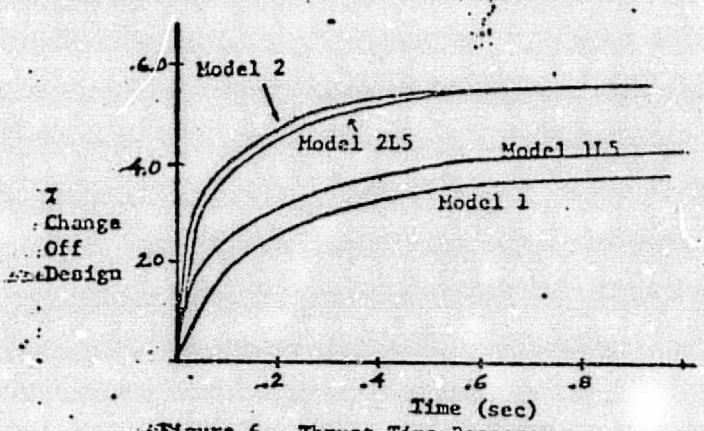

Figure 6. Thrust Time Response – Fuel Step Input

A comparison of the linear system frequency responses of nozzle area to thrust, and fuel flow to thrust, is shown in Figure 7. Models 1L5 and 2L5 match extremely well for the fuel input, but not so well for the nozzle area input. Even the lower order model 1L3 is closer in this case.

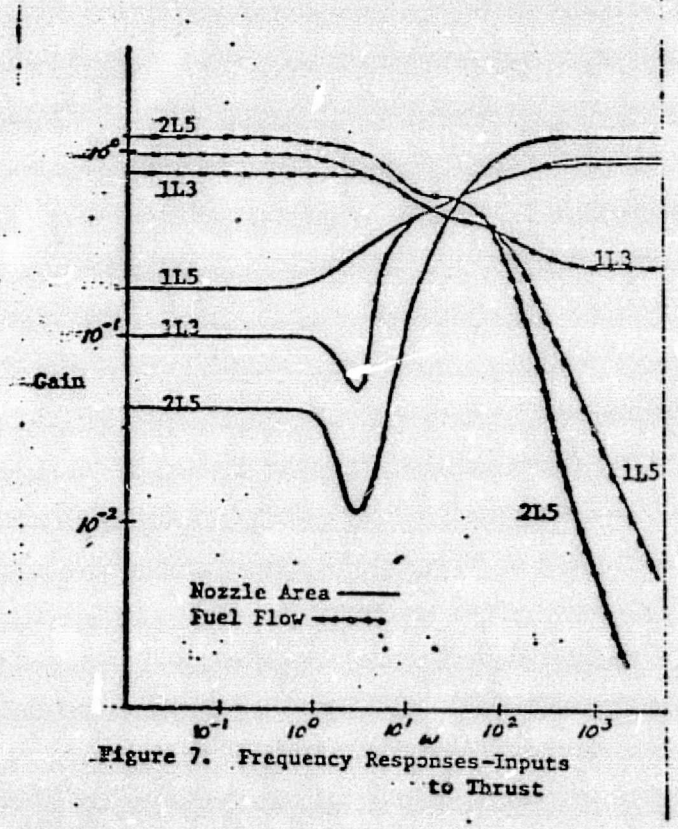

Figure 7. Frequency Responses-Inputs to Thrust

SUMMARY

To the best of the authors' knowledge, no nonlinear analytical dynamic models of a two-spool, two-stream jet engine have ever appeared in literature. Indeed, it is the value of the development of such a model which is the most important consideration in the evaluation of our work, i.e., that a good nonlinear analytical dynamic model will provide a flexibility and usefulness which is non-existent in present non-analytical jet engine simulations. Although, some significant discrepancies exist, our model yields results which are accurate to within 1%

near the design point, and which degrade to an accuracy of approximately 8% with a drop in fuel flow of 20%. The frequency response for fuel inputs of the linearized models is also in close agreement.

In conclusion, we are encouraged by our overall progress towards the development of the analytical model, however, we feel that more work is needed to further improve the accuracy of our model.

ACKNOWLEDGEMENT

This research was supported by NASA grant NSG-3048.

REFERENCES

[1] R.W. Koenig and L.H. Fishbach, "GENENG - A Program for Calculating Design and OFF-design Performance for Turbojet and Turbofan Engines", NASA TN D-6552, 1972

[2] J.F. Sellers and C.J. Daniele, "DYNGEN - A Program for Calculating Steady-state and Transient Performance of Turbojet and Turbofan Engines," NASA TN D-7901, 1975

[3] L. Geyser, "DYGABCD - A Program for Calculating Linear A,B,C and D Matrices from a Nonlinear Dynamic Engine Simulator", Technical Report in preparation at NASA Lewis Research Center, Cleveland, Ohio.

[4] R.J. Basso and R.J. Leake, "Computational Methods to Obtain Time Optimal Jet Engine Control," Allerton Conference on Circuit and System Theory 1976.

[5] K. Seldner, L.C. Geyser, H. Gold, D. Walker, and G. Burgner, "Performance and Control Study of a Low-pressure-ratio Turbojet Engine for a Drone Aircraft", NASA TM X-2537, 1972

[6] K. Seldner, J.R. Mihaloew, and R.J. Blaha, "Generalized Simulation Technique for Turbojet Engine System Analysis", NASA TN D-6610, 1972

[7] Zucrow, M.J., Aircraft and Missile Propulsion, New York, John Wiley and Sons, Inc., 1958

[8] T.C. Brennan and R. J. Leake, "Simplified Simulation Models for Control Studies of Turbojet Engines", Technical Report No. EE-757, Department of Electrical Engineering, University of Notre Dame, Notre Dame, Indiana 46556

Appendix C

"FREQUENCY DOMAIN COMPENSATION OF A DYNGEN TURBOFAN ENGINE MODEL"

R. M. Schafer
R. R. Gejji
P. W. Hoppner
W. E. Longenbaker
M. K. Sain

1977 Joint Automatic Control Conference
San Francisco, California
June 22-24, 1977

FREQUENCY DOMAIN COMPENSATION OF A DYNGEN TURBOFAN ENGINE MODEL*

R. M. SCHAFER, R. R. GEJJI, P. W. HOPPNER,
W. E. LONGENBAKER and M. K. SAIN
Department of Electrical Engineering
University of Notre Dame
Notre Dame, Indiana 46556

Abstract

Following Rosenbrock's ideas regarding the advantages of dominance in linear multivariable control systems, a new graphical technique is used for the design of compensators that achieve dominance. The technique is illustrated with an application to the problem of designing compensators for a linear turbofan-engine model. The resulting design is put into perspective by examining it in the light of two other multivariable frequency-domain methods. One, MacFarlane's method of characteristic loci, is used to realize a final design for stability and low interaction. The other is a direct technique based upon the algebraic expansion of the determinant of the return difference in terms of it's elements. Results from simulations carried out on the NASA DYNGEN software are included.

1. Introduction

Recent years have witnessed a renewal of interest in frequency domain design methods for linear multivariable control systems. The preponderance of these ideas are closely related to classical Nyquist constructions on the determinant of return difference. In this paper, we use three such methods to design a compensator for a two-input, five-state, two-output linear model of a modern two-spool turbofan jet engine obtained from the DYNGEN digital jet engine simulation.

Rosenbrock [1] has related the classical Nyquist construction on the determinant of return difference to corresponding classical constructions on the diagonal elements of the return difference--provided these diagonal elements "dominate" their rows or columns in an appropriate manner. Focussing the design interest on achieving dominance in this sense, Section 3 presents a new graphical technique to help with this aspect of design. Next, Section 4 utilizes the generalized Nyquist plots to obtain an acceptable compensator design. The ideas of generalized Nyquist plots were introduced by MacFarlane [2], who related the determinant of the return difference to it's spectrum when regarded as an appropriate linear operator.

In Section 5, we utilize a direct technique which emphasizes the algebraic relationship between the elements of the return difference and it's determinant. Typically, when it achieves user satisfaction, this method does so with greater speed, and fewer concepts, than it's competitors. The jet engine model is introduced in Section 2, which also establishes the notation for succeeding sections. Finally, in Section 6, we give results of simulations to evaluate the performance of the system.

* This work was supported in part by the National Science Foundation under Grant ENG 75-22322 and in part by the National Aeronautics and Space Administration under Grant NSG 3048.

2. Jet Engine Model and Return Difference Determinant

The linear model used for the study is based upon data obtained from a DYNGEN simulation. It is specified by the equations

$$\dot{x} = Ax + Bu \tag{1}$$

$$y = Cx + Du \tag{2}$$

where x, u, y denote the state, input and output vectors respectively. The inputs are fuel flow and nozzle area; the five states are compressor rotor speed, fan rotor speed, burner exit pressure, afterburner exit pressure and high pressure turbine inlet energy; while thrust and high pressure turbine inlet temperature constitute the two outputs.

We next consider the problem of designing controllers for the plant. The underlying feedback control scheme is shown in Fig. 1. G(s), the plant,

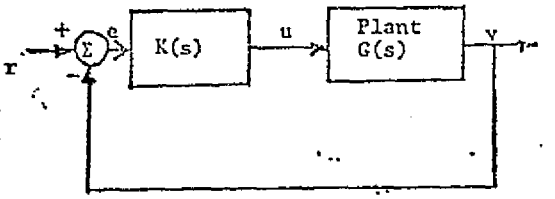

Fig. 1 Feedback Control Scheme

represents the jet engine model, that is,

$$G(s) = C(sI - A)^{-1}B + D. \tag{3}$$

K(s) represents the rational compensator to be designed. G(s) can be computed as:

$$G(s) = \frac{\begin{bmatrix} -502s^5-3.64E5s^4 & 4104s^5+1.93E6s^4 \\ -1.78E7s^3+6.15E9s^2 & +1.69E8s^3-1.44E10s^2 \\ +1.26E11s+6.25E11 & -6.77E10s+6.59E10 \\ -14.554s^5+1.33E5s^4 & 20.46s^5+1.69E4s^4 \\ +4.96E7s^3+3.7E9s^2 & +7.03E6s^3+1.12E9s^2 \\ +2.82E10s+4.95E10 & +5.63E9s+5.41E8 \end{bmatrix}}{s^5+4609.57s^4+1.184E5s^3+7.31E6s^2 \\ +6.52E7s+1.62E8} \tag{4}$$

Central to the application of Nyquist type ideas to multivariable systems is the return difference matrix, which in this case becomes [I+G(s)K(s)]. It's principal use arises from the relation of the closed loop characteristic polynomial (CLCP) to the open loop characteristic polynomial (OLCP) which can be stated, in the manner of [1], as

$$\frac{CLCP}{OLCP} = \det[I+G(s)K(s)], \qquad (5)$$

where equality is understood up to a real constant. Of primary concern here is the behavior of det(I+GK) for values of s on the standard Nyquist contour (SNC), which encircles the open right half plane clockwise with indentations into the left half plane around poles and zeros on the imaginary axis. In practice, plots are made for values of s on the positive imaginary axis. Stability can then be determined from plots of det(I+GK) in conjunction with knowledge of the open loop characteristic polynomial. Also interesting, of course, is the use of such plots to aid in the choice of a suitable K(s).

3. CARDIAD Plots and Dominance [3,4]

The CARDIAD (Compensator Acceptability Region for DIAgonal Dominance) plot is a graphical approach to the problem of choosing a compensator that will achieve system dominance. A system is said to be row (column) dominant [1] if the magnitude of each diagonal element of the open loop transfer function matrix is greater than the sum of the magnitudes of the off diagonal elements of the row (column) at all frequencies. In the 2x2 case being considered in this paper, the dominance condition reduces to the magnitude of the diagonal element being greater than the magnitude of the off diagonal element of the row (column). Consonant with the Rosenbrock approach, the CARDIAD plot analysis is applied to the inverse of the plant G(s). As a notational point, the inverse plant transfer function matrix will be denoted by $\hat{G}(s)$ and the inverse precompensator by $\hat{K}(s)$.

The specific application to the jet engine design problem involves trying to find a compensator $\hat{K}(s)$ such that $\hat{K}(s)\hat{G}(s)$ is row dominant. Without loss of generality, the form of $\hat{K}(s)$ will be restricted to

$$\hat{K}(s) = \begin{bmatrix} 1 & \beta_1(s) \\ \beta_2(s) & 1 \end{bmatrix} \qquad (6)$$

where

$$\beta_i(s) = x_i(s) + jy_i(s), \quad i = 1,2. \qquad (7)$$

If $\hat{G}(s)$ and $\hat{K}(s)$ are each evaluated at a frequency jw_o, the equation for dominance of the i^{th} row of $\hat{K}(s)\hat{G}(s)$ becomes a function $f_i(x_i,y_i)$ which describes a paraboloid in three-space. The intersection of this paraboloid and the complex plane is a circle which is the locus of the values of x_i and y_i such that the magnitude of the diagonal element of the i^{th} row of $\hat{K}(s)\hat{G}(s)$ is equal to the magnitude of the off diagonal element of the row. Minima and maxima analysis of the function f_i reveals that values of x_i and y_i on one side of the circle will make the system dominant, whereas values which lie on the other side of the circle will not. In the CARDIAD plots, this differentiation is made by drawing a solid circle if the acceptable values of x_i and y_i lie inside and dashed circles if the acceptable region is outside.

If the above procedure is repeated over a range of frequencies for each row of the system, and the circles of intersection drawn, a plot describing the acceptable values of the complex number $x_i + jy_i$ for each frequency results. In this way, the acceptable range of the function $\beta_i(s)$ such that the i^{th} row of $\hat{K}(s)\hat{G}(s)$ is dominant is described.

The analysis of the CARDIAD plot for a given row of $\hat{G}(s)$ proceeds as follows. If the origin of the plot is contained inside all solid circles and is excluded by all dashed circles, the row of $\hat{G}(s)$ is dominant uncompensated. If the row of $\hat{G}(s)$ is not dominant uncompensated, the CARDIAD plot is next checked to see if there is a constant entry β_i that will make $\hat{K}(s)\hat{G}(s)$ dominant at all frequencies. For this to be the case, there must be a point on the real axis that is included in all solid circles and excluded by all dashed circles.

If there exists no constant β_i such that the i^{th} row of $\hat{K}(s)\hat{G}(s)$ is dominant at all frequencies, the CARDIAD plot is used as a guide to design a frequency dependent $\beta_i(s)$ that will achieve dominance. This is accomplished by realizing a function $\beta_i(s)$ whose value at jw_o lies inside the circle associated with the same frequency in the CARDIAD plot if that circle is solid, or outside if that circle is dashed. This approach is illustrated by considering the DYNGEN problem.

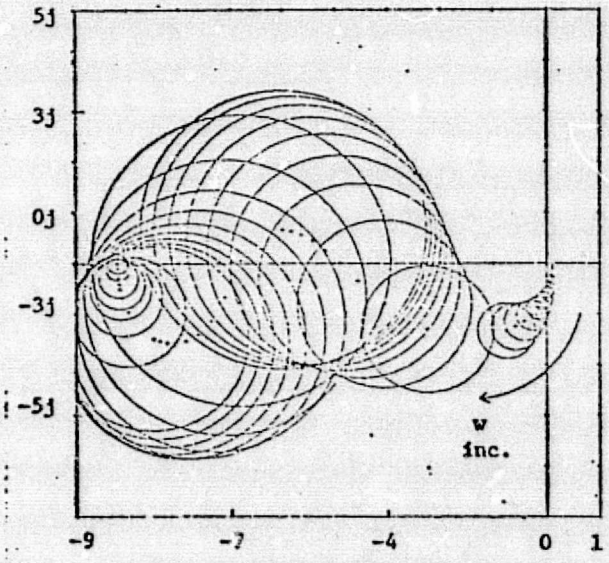

Fig. 2 CARDIAD Plot Row 1 Uncompensated

The initial CARDIAD plots of $\hat{G}(s)$ indicate that row 2 of $\hat{G}(s)$ is dominant uncompensated since the plot consists only of dashed circles, which all exclude the origin. The plot for row 1, however, shows that this row is not dominant uncompensated and also that there is no constant entry in the off diagonal element of row 1 of $\hat{K}(s)$ that will make the row dominant at all frequencies. This is easily seen since all the circles in this plot are solid and there is no point on the x axis that is included in all the circles. Moreover, the plot hints that there will be difficulty finding a $\beta_1(s)$

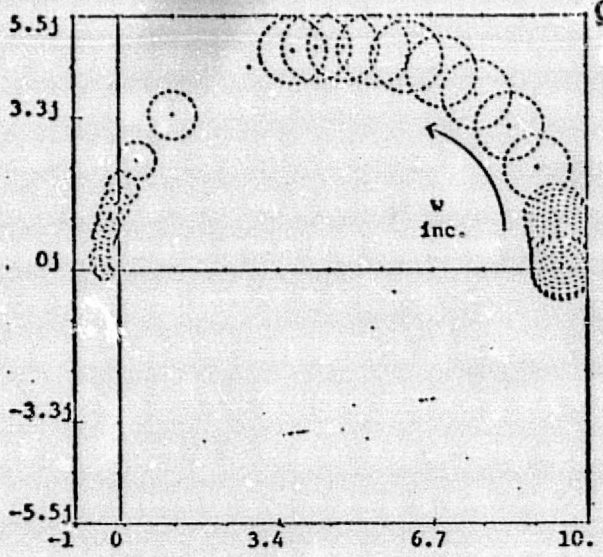

Fig. 3 CARDIAD Plot Row 2
Uncompensated

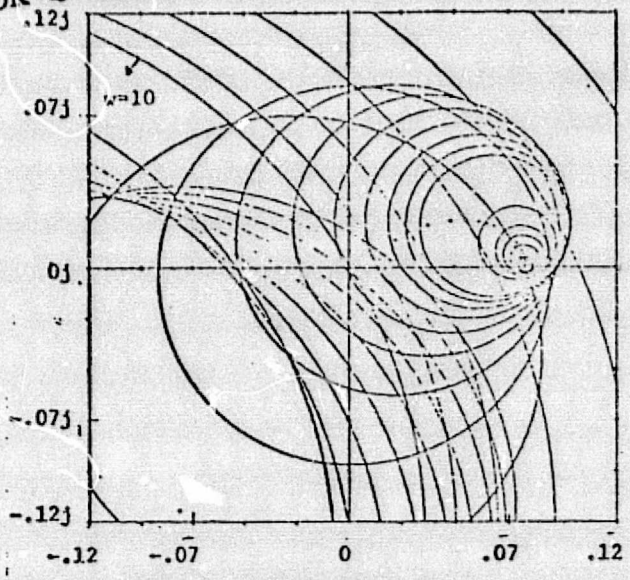

Fig. 4 CARDIAD Plot Row 1
Compensated

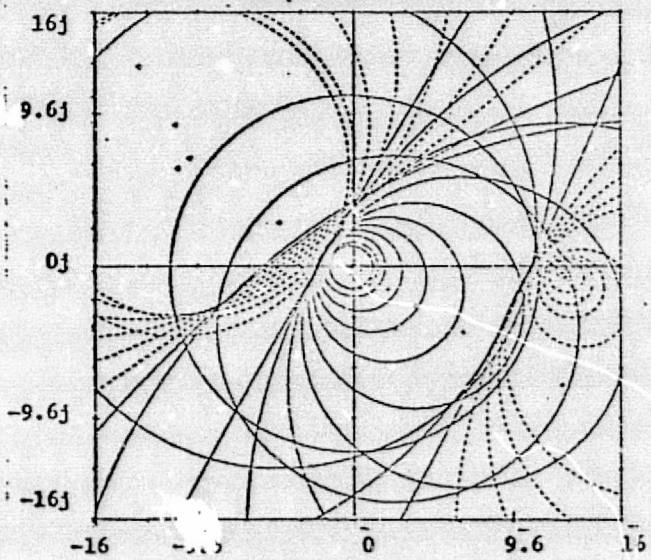

Fig. 5 CARDIAD Plot Row 2
Compensated

that will make this row of $\hat{K}(s)\hat{G}(s)$ dominant because of the complexity of the plot and the small radii of the low frequency circles which necessitate a very close fit.

To facilitate the process of finding a compensator that will make $\hat{K}(s)G(s)$ dominant, the system was first precompensated with

$$\hat{K}_1 = \begin{bmatrix} 0 & 1 \\ 1 & 0 \end{bmatrix}.$$

Space limitations do not allow the CARDIAD plots of $\hat{K}_1\hat{G}(s)$ to be included, but the new plots are the same shape as the CARDIAD plots of $\hat{G}(s)$ with two major changes. The row 1 plot of $\hat{K}_1\hat{G}(s)$ is the same shape as the row 2 plot of $\hat{G}(s)$ with dashed circles changed to solid circles. Similarly, the row 2 plot of $\hat{K}_1G(s)$ is the same shape as the row 1 plot of $\hat{G}(s)$ with the solid circles changed to dashed circles.

The problem of finding a $\hat{K}_2(s)$ such that $\hat{K}_2(s)\hat{K}_1\hat{G}(s)$ is dominant is now simplified. Since row 2 of $\hat{K}_1\hat{G}(s)$ is now dominant uncompensated, the off diagonal term in the second row of $\hat{K}_2(s)$ is left a zero, with the provision that if it later proves helpful in compensation, the entry may be chosen to be any constant that lies outside all of the circles. To make row 1 of $\hat{K}_1\hat{G}(s)$ dominant, the off diagonal entry in row 1 of $\hat{K}_2(s)$ must follow the semicircular path through the complex plane described by the CARDIAD plot for this row. A fit was made to this shape and the resulting $K_2(s)$ was

$$\hat{K}_2(s) = \begin{bmatrix} 1 & \dfrac{9.4798 + 0.2494s}{1. - 1.2359s} \\ 0 & 1 \end{bmatrix} \qquad (8)$$

The CARDIAD plots of $\hat{K}_2(s)\hat{K}_1\hat{G}(s)$ are considerably more complex than the previous plots. The plot for row 2 shows that the row is dominant at all frequencies since the origin is included by all solid circles and excluded by all dashed circles. The CARDIAD plot for row 1 shows that the row is clearly not dominant at all frequencies. Dominance is lost at w=10, is regained as w=90, and is lost again at w=700. It is perhaps possible to find a better choice of $K_2(s)$ that will make row 1 dominant at all frequencies, but the dominance achieved by the above $K_2(s)$ proved to be sufficient.

An interesting feature of the CARDIAD plot is illustrated in the final plot for row 2. Close analysis of this plot shows that there are three occurrences of solid circles changing to dashed circles or dashed circles changing to solid. When these transitions occur, the paraboloid is inverting and the circle of intersection degenerates to a line. These lines occur when the other row changes from being dominant to not dominant or vice versa. Thus, each change in dominance of row 1 causes a change in the type of circle being drawn in the plot of row 2.

4. Design Using Characteristic Loci

Another approach to design, due to A.G.J.MacFarlane, uses the locus of the eigenvalues of G(s)K(s), called the characteristic loci (C.L.), for values of s on the SNC. This method is based on the relation of the determinant of the return difference to eigenvalues of G(s)K(s). In order to assess stability from the C.L. plots, for s=jw, w positive, one must count the clockwise encirclements of the critical point (-1,0) made by the C.L. plots and sum all these up. The closed loop system is stable if this sum equals -po, where po is the number of zeros of OLCP enclosed by the SNC. As an approximate measure of interaction, we compare the eigenvalue plots with plots of the diagonal elements of Q(s)=G(s)K(s). For a noninteracting system with Q(s) a diagonal matrix, these would be identical. In our design example, Q(s) is a 2x2 matrix, and therefore we will be looking at plots of two eigenvalues $\lambda_1(s)$, $\lambda_2(s)$ and the two diagonal elements $q_{11}(s)$, $q_{22}(s)$.

First, an examination of the C.L. plots of the uncompensated system revealed that, without compensation, the closed loop system is unstable. The plots are not included due to lack of space, but conclusions drawn from them are given. Control problems for the uncompensated model were complicated by the existence of considerable interaction, and large gains at high frequencies. An additional difficulty was that one of the eigenvalues was negative at zero frequency. This tended to limit the response speed of the closed loop system. It appeared on the C.L. plots that, from a stability viewpoint, the frequency range of interest is in the vicinity of 10 rps. This gives justification for use of the compensator given in the previous section. As a practical matter, our goal is to achieve as rapid a response as possible to a step input, without suffering any overshoot. Heavy emphasis is placed also on steady state accuracy.

To remove the right half plane pole in $\hat{K}_2$, we choose K_3 arbitrarily as diag (1/s,(-1+1.2359s)/s). The resulting $K(s)=K_1*K_2*K_3$ becomes

$$K(s) = \frac{\begin{bmatrix} 0 & -1+1.2359s \\ 1 & 9.4798+0.2494s \end{bmatrix}}{s} \qquad (9)$$

The diagonal nature of $K_3(s)$ does not affect dominance. Moreover, an examination of the (1,1) and (1,2) elements of G(s) reveals that if the 0 in K(s) is changed to 9, we can significantly reduce the high frequency magnitude of $q_{11}(s)$ while simultaneously boosting the low frequency magnitude. This is in accordance with the freedom specified for K_2 previously. The modified K(s) gives rise to the plots of Fig. 6 and 7.

Since dominance is not affected by diagonal compensators, the problem becomes that of independently shaping q_{11} and q_{22} by means of single loop techniques. In order to reduce high frequency gain in q_{22} without appreciably affecting low frequency behavior, we use lag compensation. A little bit of cut and try led finally to $K_4(s)$=diag.(0.44E-4, (-s-0.1)/(2000s+10)). The plots corresponding to $K=K_1*K_2*K_3*K_4$ are not shown. The λ_1 and q_{11} plot is essentially that of λ_1 in Fig. 6 scaled by a factor of 0.44E-4. Similarly, the q_{22} plot inverted and scaled by 0.0005. (By inversion we mean reflection through both axes.) The plot for λ_2 is shown in Fig. 8.

5. The Direct Method of Analysis

Direct methods of multivariable Nyquist analysis concern themselves with the algebraic relationship between the elements of return difference and its determinant. For an NxN return difference, the most basic of these relationships is

$$\det(I+GK) = 1+\sum_{i=1}^{N} \{\sum \text{ ixi principal minors of } CK\}. \qquad (10)$$

For the example of this paper, (10) takes the form

$$1+\{(G_{11}K_{11}+G_{12}K_{21})+(G_{21}K_{12}+G_{22}K_{22})\} + \det(GK). \qquad (11)$$

In (10) and (11) we note the advantage of minute detail and the disadvantage of nonrecursive construction. Considerable interest attaches to the removal of this disadvantage, which can be accomplished by methods drawn from the results of exterior algebra [5]. Consider the recursion (where tr denotes trace)

$$\alpha_0 = 1 \qquad (12a)$$

$$\alpha_r = -\frac{1}{r}\sum_{p=0}^{r-1} \alpha_p \, tr(GK)^{r-p} \qquad (12b)$$

for $1 \le r \le N$. It can be shown that

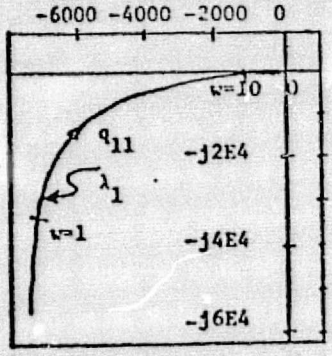

Fig. 6 First C.L. plot for $GK_1K_2K_3$.

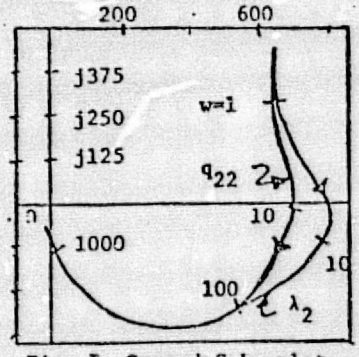

Fig. 7 Second C.L. plot for $GK_1K_2K_3$.

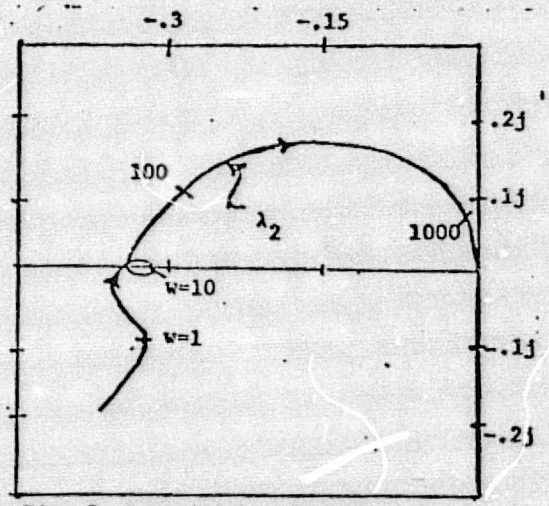

Fig. 8 Second C.L. plot for $GK_1K_2K_3K_4$.

$$\det(I+GK) = \sum_{i=0}^{N} (-1)^i a_i . \qquad (13)$$

The direct approaches differ appreciably from methods described in preceding sections, in that they address themselves directly to the image of det(I+GK) on the SNC, without any particular concern for such issues as dominance or interaction. Alternate insights accrue from such plots, which we illustrate here for the engine design example. All plots are drawn for the final return difference as developed in the sections preceding.

Fig. 9 indicates the five constituents of a det(I+GK) plot as developed in (11), while Fig. 10 presents the corresponding two constituents according to (13). Fig. 11 contains the total Nyquist plot, which is obtained by adding the individual curves in either of the two prior figures. Revealed in this plot, Fig. 11 is a feature not so readily noticeable in the earlier plots, namely conditional stability. It appears, therefore, that the availability of a variety of graphical tools is in the multivariable case every bit as valuable as in the more classical, one-input, one-output situation.

It is readily seen in Fig. 11 that the plot encircles -1+j0 twice in a counterclockwise direction. Therefore, the system is shown to be stable because the open loop characteristic polynomial has a double zero at the origin.

Further exploratory studies of direct methods as design aids are available elsewhere [6].

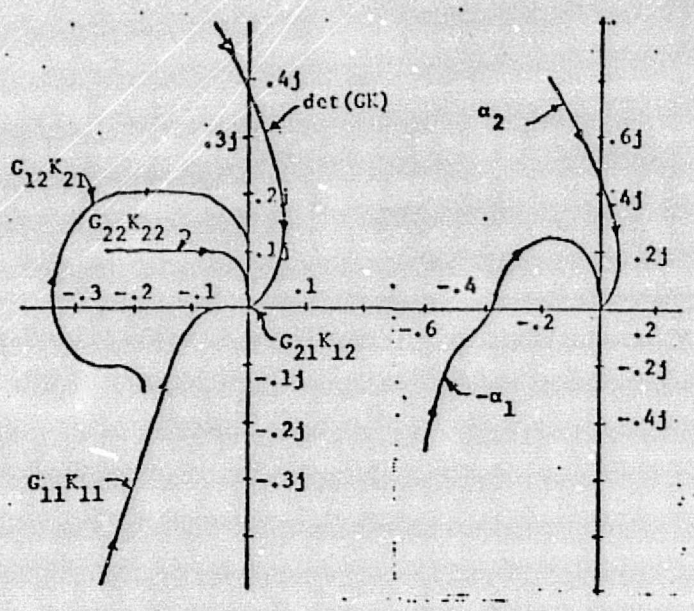

Fig. 9 The Nyquist Plot of the Elements of Det(I+GK), According to Expansion Eq. (11).

Fig. 10 The Nyquist Plot of the Elements of Det(I+GK) According to Expansion, Eq. (13).

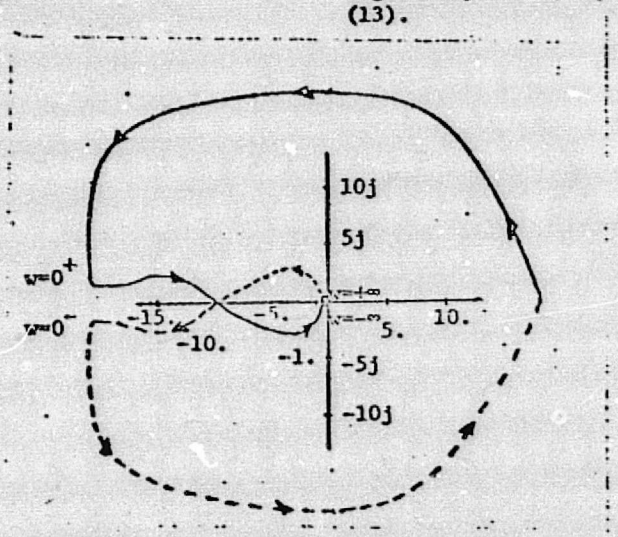

Fig. 11 Nyquist Plot of Det(I+GK).

6. Simulation Results

Closed-loop time responses were obtained both by using the linear model simulation and by implementing the compensator on DYNGEN, a jet engine simulation program developed by the NASA Lewis Research Center [7].

DYNGEN is a versatile digital program which analyzes steady-state and transient performance of turbojet and turbofan engines. It uses a sixteenth order system to model this example, and solves the state differential equations by a modified Euler method. The user need only supply appropriate component performance maps and design-point information, and then write the control subroutines. Implementation of the compensator required first order functions to perform integration and lead-lag compensation.

The linear model used in this study was also obtained from DYNGEN. By utilizing a special control subroutine written by NASA, called DYGABCD [8], models can be derived using whatever states the user desires. DYNGEN thus possesses the capability to determine linear models for the engine with any order up to sixteen.

Fig. 12 shows the response of the linear model to a step input in the first channel. Thrust has a rise time (10%-90%) of 1.04 seconds with no overshoot occurring. High pressure turbine inlet temperature increases to a maximum of 0.105 at approximately 0.9 seconds, then gradually decreases.

Similar, and even better, results occur when the compensator is employed in the DYNGEN simulation using a one percent step. Thrust rise time is 0.88 seconds, and the turbine temperature reaches a maximum increase of 0.097.

The linear and nonlinear responses were not in such close agreement for a step input in the second channel. The linear model shows turbine temperature slowly ramping up (Fig. 13) as the change in thrust is held to a minimum. DYNGEN produces similar results for the turbine temperature response; however thrust experiences a strong decrease before rising to zero. At this writing, it is believed that the five states chosen for the DYGABCD model do not adequately describe local engine behavior for the second channel equipped with the present controller.

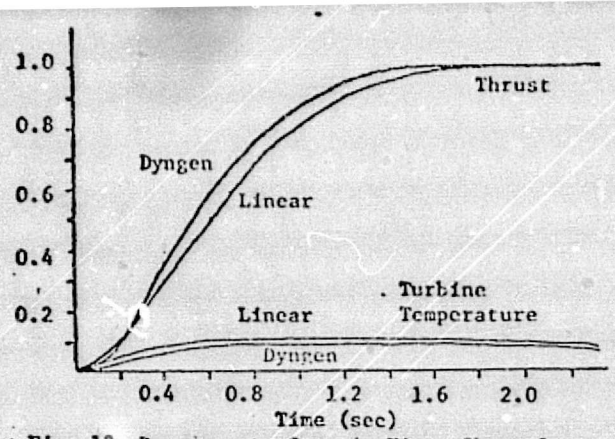

Fig. 12 Response to Step in First Channel

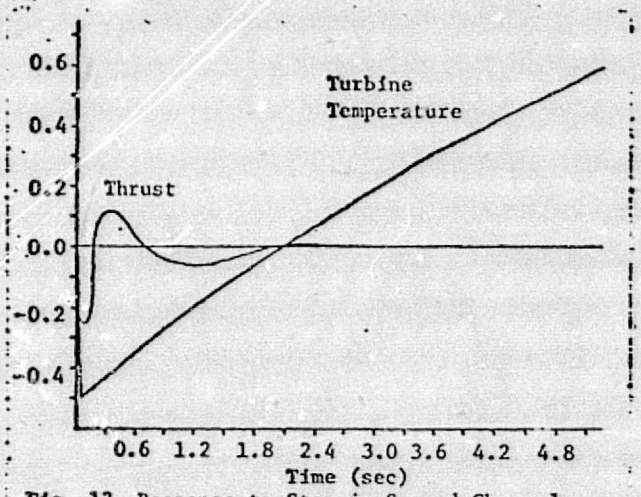

Fig. 13 Response to Step in Second Channel

7. Conclusions

This paper has demonstrated the usefulness of the new CARDIAD plot approach to designing compensators for complex plants. The DYNGEN simulation for a step in channel 1 has shown that acceptable responses can be obtained using linear compensators. An ordered collection of these may make global control feasible. For steps in channel 2, conclusive evidence was not obtained. We suspect that this is due to inadequacy of the linear model in describing the plant. This important factor of selecting an appropriate linear model is often overlooked. But, as we have seen, it turns out to be crucial in practical applications.

The method of CARDIAD plots can be generalized to plants with more than two inputs and outputs by considering a family of compensators with 1's on the diagonal and only one non-zero off-diagonal term. As stated in [1], except for changes in the ordering of inputs or outputs, such a study is exhaustive.

8. References

[1] H. H. Rosenbrock, Computer-Aided Control System Design. London: Academic Press, 1974.

[2] A. G. J. MacFarlane, and J. J. Belletrutti, "The Characteristic Locus Design Method," Automatica, Vol. 9, No.5, pp. 575-588, September 1973.

[3] R. M. Schafer, W. E. Longenbaker and M. K. Sain, "System Dominance," Preliminary Report Department of Electrical Engineering, University of Notre Dame, Notre Dame, Indiana, November 1976.

[4] R. M. Schafer, "A Graphical Approach to System Dominance," M. S. Thesis, Department of Electrical Engineering, University of Notre Dame, Notre Dame, Indiana, May 1977.

[5] W. H. Greub, Multilinear Algebra. New York: Springer, 1967.

[6] P. W. Hoppner, "The Direct Approach to Compensation of Multivariable Jet Engine Models," M. S. Thesis, Department of Electrical Engineering, Notre Dame, Indiana, May 1977.

[7] J. F. Sellers and C. J. Daniele, "DYNGEN-A Program for Calculating Steady-State and Transient Performance of Turbojet and Turbofan Engines," NASA Technical Note, NASA TN D-7901, Washington, D.C., April 1975.

[8] L. C. Geyser, "NASA Preliminary Report on DYGABCD," April 1976.

Appendix D

APPLICATION OF POLYNOMIAL TECHNIQUES TO MULTIVARIABLE CONTROL OF JET ENGINES

R. R. Gejji
M. K. Sain

APPLICATION OF POLYNOMIAL TECHNIQUES TO MULTIVARIABLE CONTROL OF JET ENGINES *

R. R. Gejji and M. K. Sain
Department of Electrical Engineering
University of Notre Dame
Notre Dame, Indiana
U.S.A.
46556

SUMMARY

This paper describes a complete case study of the application of the theory of minimal design to multivariable control of jet engines. The minimal design problem is approached from the viewpoint of polynomial modules, and computational experience with PL/I and FORMAC-PL/I software is discussed. The complete minimal design solution exhibits flexibilities not apparent in early industry studies, and a new approach to pole assignment can be used to advantage in this situation.

1. INTRODUCTION

One way to approach the design of linear multivariable control systems is to express system specifications in terms of a desired closed loop transfer function matrix. A question which is often raised about such an approach is the practicality of making such a specification. Another, related, question concerns the possibility of determining the existence of realizable compensators to achieve the specification. When such compensators do exist, there are the very practical issues of giving a finite enumeration of them, of determining whether they have fixed poles, and of assigning one or more of the non-fixed poles. Of special interest, as it turns out, for the issue of pole assignment is the idea of minimality, in the state-space sense, of a proposed solution in the context of all possible solutions.

This paper provides a thorough case study of such a design approach when applied to realistic numerical models associated with an F-100-like turbofan engine. Specifications are accomplished by means of the methods of linear optimal control theory, according to procedures already worked out in the jet engine industry. The remaining tasks are addressed by regarding the design as a problem in free polynomial modules. A special feature of the application lies in its attention to compensators of simple structure, with a view to the use of a graded collection of them for the purpose of global engine control.

Section 2 describes the basic design problem, once specifications are made. Section 3 provides the discussion of the jet engine application, with particular attention paid to the manner of making the specifications and to the formulation of the main design problem for the jet engine application. Section 4 explains how to cast the design problem in terms of free polynomial modules, and Section 5 describes floating point computational experience gained in applying extended precision PL/I software to solve the jet engine problem in the free module context. Section 6 outlines the corresponding experience associated with an exact rational calculation made with FORMAC-PL/I software.

The results of Section 6 show that considerably greater compensator design freedom is available than had been apparent from early industry studies. Using these results, a new pole placement design procedure based on alternating multilinear algebra achieves in Section 7 a minimal pole placement solution not possible by those earlier industry methods.

Section 8 closes with remarks designed to place the work in historical perspective, to reference the literature, and to assess the merits of polynomial methods for control system design in the near term.

2. THE MINIMAL DESIGN PROBLEM

Suppose that F is a given field. For the jet engine control problem, F is taken to be R, the field of real numbers; however, a great deal of the algorithmic nature of the discussion is more general than that, and is so stated. The set of polynomials which are of interest is F[s], namely those polynomials in the variable s with coefficients in the field F. The fact that F[s] is a principal ideal domain ring is well known, as is the equally pertinent fact that F[s] has a quotient field F(s). More intuitively, F(s) is often described as the field of rational functions in s having coefficients in F.

The design problems of interest in the sequel are conventionally stated in terms of F(s); however, Section 4 explains how such problems may be re-converted back to a corresponding F[s] form.

Principal interest centers upon the minimal design problem (MDP), which can be described as follows. Let $G: V_1 \to V_2$ be a linear operator for finite-dimensional F(s)-vector spaces V_1 and V_2. G is regarded as realizable if its matrix is proper. Now let $G_1: V_2 \to V_3$ and $G_2: V_1 \to V_3$ be given linear operators, where V_3 is also a finite-dimensional F(s)-vector space. MDP consists in determining whether there are realizable linear operators G which make the diagram in fig. 1 commute and, if so, to find one whose minimal realization is of least dimension among all such realizable operators. Intuitively,

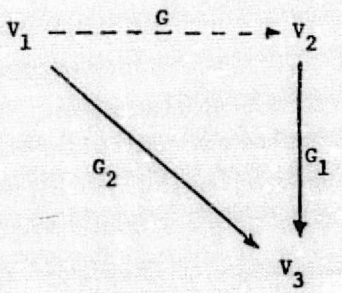

Fig. 1. Minimal Design Problem

the operators G_1 and G_2 derive from the given plant and from the specifications, while G represents the compensators to be designed.

Beyond the basic MDP, several additional issues are of practical importance. Among these should be included

* This work was supported in part by the National Science Foundation under Grants GK-37285 and ENG 75-22322 and in part by the National Aeronautics and Space Administration under Grant NSG 3048.

(i) a finite enumeration of all possible solutions, (ii) determination of any fixed poles in the matrix of G, and (iii) methods for assigning the poles of G which are not fixed. The answers to these questions resolve such issues as the availability of solutions with varying degrees of integration. From a conceptual viewpoint, these ideas are developed further in Sections 4 and 7, whereas the computational issues are discussed in Sections 5 and 6.

Next in order of presentation, however, is the statement of a minimal design problem for jet engine control.

3. JET ENGINE APPLICATION

In this section, we demonstrate the practicality of the minimal design approach in the context of jet engine control. The basic plant is a version of the F-100 turbofan engine. Inputs are jet exhaust area and main burner fuel flow; states are fan inlet temperature, main burner pressure, fan speed, high compressor speed, and afterburner pressure; and outputs are thrust and high-turbine inlet temperature. The linearized model approximates the small signal behavior of these engine variables in a neighborhood of 47° Power Lever Angle (PLA). This corresponds to a point approximately midway between engine idle and maximum nonafterburning power. The plant is specified by the four matrices A_p, B_p, C_p, D_p in (1) and (2).

$$\dot{\delta x} = A_p\, \delta x + B_p\, \delta u \tag{1}$$

$$\delta y = C_p\, \delta x + D_p\, \delta u \tag{2}$$

Table 1 lists these matrices for our example. The attempt to design simple compensators for linear control over a specified region is part of a strategy for global control of the engine using a graded collection of these.

Table 1

State Description Matrices for Jet Engine (PLA=47°)

Matrix	Matrix Elements				
A_p	-57.096	3.613	-10.211	- 5.481	- 2.715
	19.832	-72.34	30.295	40.972	15.327
	0.66	4.496	- 3.601	- 0.011	- 2.808
	1.326	2.313	- 0.809	- 3.032	- 0.821
	0.882	0.703	2.922	1.471	- 4.596
B_p		1.017		39.792	
		- 0.125		4.181	
		- 0.077		- 0.382	
		- 0.088		- 0.565	
		- 3.563		- 0.785	
C_p	- 0.037	0.031	- 0.016	- 0.042	1.368
	1.081	0.149	- 0.057	0.001	- 0.086
D_p		0.546		0.018	
		- 0.013		- 0.086	

We next examine how engine control specifications can be obtained from linear optimal control theory. In fig. 2, the compensators,

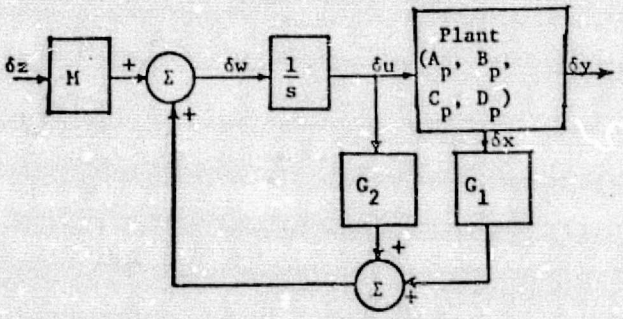

Fig. 2. Linear Optimal Control

specified by gain matrices G_1 and G_2 are chosen with the objective of minimizing the performance index of (3).

$$J = \frac{1}{2}\int_0^\infty (\delta y^T Q \delta y + \delta u^T R \delta u + \delta \dot{y}^T S \delta \dot{y})\,dt \tag{3}$$

where superscript T denotes matrix transposition. The weighting matrices Q,R, and S are listed in table 2.

Table 2

Weighting Matrices
with Optimal Integral Control Solution

Matrix	Matrix Elements				
Q	50,000	0			
	0	10,000			
R	550	0			
	0	175			
S	0	0			
	0	20,000			
L	0.509	0.268	1.979	2.171	2.098
	-2.137	-0.377	- 0.223	- 0.776	- 0.227
H	8.329		- 1.126		
	-2.811		- 1.842		

At this point, a minimal design problem can be brought into play. The control scheme of fig. 3 is seen to be more desirable because it incorporates output feedback and enjoys the concomitant advantage of zero steady state error, even in the presence of plant parameter variation.

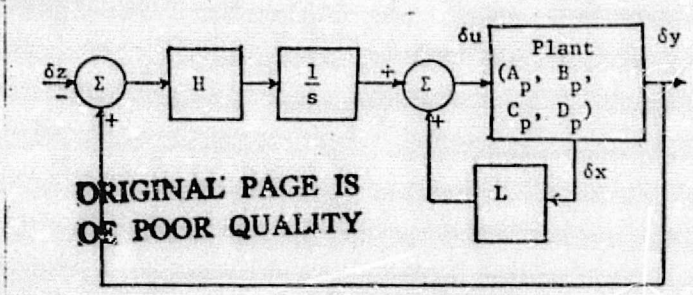

Fig. 3. Optimal Integral Control

One relates the performance of the two control schemes by equating, in both, the Laplace transform of the variable δu, as written in terms of the respective state variables. This leads to the following equations, which may be solved for L and H, the values of which have been listed in table 2.

$$M = -H \tag{4}$$

$$[L:H]\begin{bmatrix} A_p & \vdots & B_p \\ \cdots & & \cdots \\ C_p & \vdots & D_p \end{bmatrix} = [G_1 \vdots G_2] \tag{5}$$

That this is nothing but a form of the minimal design problem can be seen by evaluating the 2x2 closed loop transfer function matrices T(s) and T'(s) for the two systems in figs. 2 and 3. In fig. 2,

$$T(s) = P_1(s)\,[sI - P_2(s)]^{-1} M \tag{6}$$

where

$$P_1(s) = C_p(sI-A_p)^{-1} B_p + D_p \tag{7}$$

$$P_2(s) = G_1(sI-A_p)^{-1} B_p + G_2. \tag{8}$$

In fig. 3, on the other hand,

$$T'(s) = -P_1(s)\,[sI-P_3(s)]^{-1} H \tag{9}$$

where

$$P_3(s) = HP_1(s) + sL(sI-A_p)^{-1} B_p. \tag{10}$$

Now, rewrite (6) using (4) as

$$T(s) = -P_1(s)\,[sI-P_2(s)]^{-1} H. \tag{11}$$

The relationship between (9) and (11) now depends upon that between (8) and (10).

Comparison of $P_3(s)$ and $P_2(s)$, with the aid of (5) and (7), establishes the equality of the two transfer functions T(s) and T'(s).

We can then pose questions regarding the existence of compensators other than H and L to achieve the same performance as attained in fig. 3, and what, if any, advantages such compensators would have over that scheme. To do this, we consider fig. 4, which is a more general scheme of control based on fig. 3.

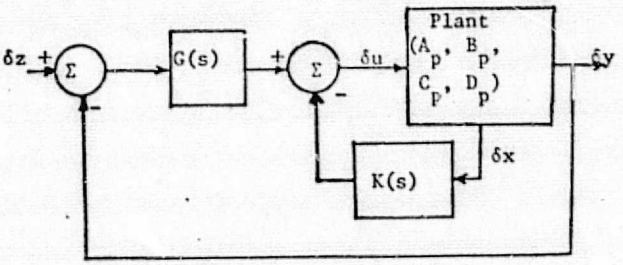

Fig. 4. Generalized Compensation Scheme

Our objective is to design compensators G(s) and K(s) to achieve exactly the transfer function T(s) = T'(s) between δz and δy. This means that we must have

$$(I + P_4(s))^{-1} P_4(s) = T(s) \tag{12}$$

where we have introduced

$$P_4(s) = P_1(s)\,(I+K(s)P_5(s))^{-1}\,G(s) \tag{13}$$

and

$$P_5(s) = (sI-A_p)^{-1}\,B_p. \tag{14}$$

From (12), we obtain the equivalent condition

$$P_4(s) = (I+P_4(s))\,T(s), \tag{15}$$

which can be restated in the manner

$$P_1(I+KP_5)^{-1}G = \{I+P_1(I+KP_5)^{-1}G\}T. \tag{16}$$

From table 1, D_p is clearly invertible; and so the linear dynamical system P_1 has a unique linear dynamical inverse system P_1^{-1}, which we designate $\hat{P}_1$. Thus (16) is equivalent to

$$G(I-T) - K\,P_5\hat{P}_1T = \hat{P}_1T \tag{17}$$

which in turn can be written

$$[(I-T^T) \;\vdots\; -T^T\hat{P}_1^TP_5^T]\begin{bmatrix}G^T\\ \cdots\\ K^T\end{bmatrix} = T^T\hat{P}_1^T. \tag{18}$$

Some simplification can be achieved at this point if we take advantage of the fact that the matrix $T^T(s)$ has an inverse $\hat{T}^T(s)$. Then (18) can be cleared in its right member so that

$$[P_1^T(\hat{T}^T-I) \;\vdots\; -P_5^T]\begin{bmatrix}G^T\\ \cdots\\ K^T\end{bmatrix} = I \tag{19}$$

Now compare (19) with fig. 1, from which it becomes clear that G_2 is the identity map, or that our control system minimal design problem turns out to be a version of the minimal inverse system problem. Writing

$$\begin{bmatrix}G^T(s)\\ \cdots\\ K^T(s)\end{bmatrix} = N(s)D^{-1}(s), \tag{20}$$

and

$$[P_1^T(s)(\hat{T}^T(s)-I) \;\vdots\; -P_5^T(s)] = \frac{M(s)}{d(s)}, \tag{21}$$

where N(s), D(s), and M(s) are matrices over R[s], and where d(s) ∈ R[s], we can put (21) in the polynomial form

$$[M(s) \;\vdots\; -d(s)I]\begin{bmatrix}N(s)\\ \cdots\\ D(s)\end{bmatrix} = 0 \tag{22}$$

Equation (22) is a polynomial "kernel" problem, equivalent to the design problem of fig. 4. By comparing figs. 3 and 4, we can trivially establish that a solution to the problem does indeed exist. Our goal in the sequel is to give a finite enumeration of all possible solutions and to study their pole assignment possibilities relative to the structure of fig. 4.

We remark here on a special feature of (20), in that it implies a common set of dynamics for both compensators. Suppose that a suitable solution of (22) leads us to matrices A_g, B_g, C_g, D_g and A_k, B_k, C_k, and D_k such that

$$G(s) = C_g(sI-A_g)^{-1}B_g + D_g \tag{23}$$

$$K(s) = C_k(sI-A_k)^{-1}B_k + D_k. \tag{24}$$

In a typical situation, $D_g = 0$; and it can be shown that

$$A_g = A_k; \qquad C_g = C_k.$$

Fig. 5 then shows how such a control scheme can be realized.

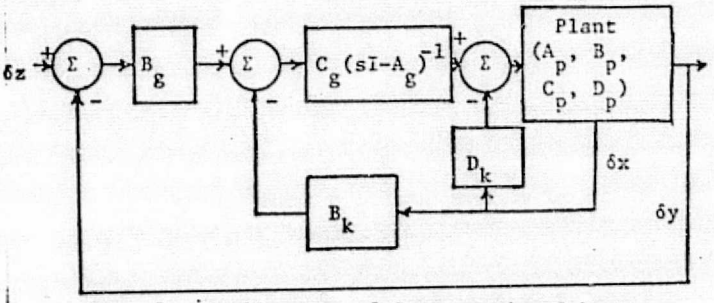

Fig. 5. Realization of Compensation Scheme

Finally, we make the observation that (22) can be completely solved, and a minimal solution computed by algorithms given in the Appendix. The next section deals with the theoretical foundation of these algorithms; and subsequent sections describe their application to (22).

4. FREE MODULAR APPROACH TO MDP

In matrix form, the minimal design problem of fig. 1 reduces to solving an equation

$$G_1(s)G(s) = G_2(s) \tag{25}$$

for the various realizable G(s), where $G_1(s)$ and $G_2(s)$ are given. Section 3 provided a nontrivial illustration of (25) in (19), where

$$G_1(s) = [P_1^T(s)\{\hat{T}^T(s)-I\} \;\vdots\; -P_5^T(s)] \tag{26}$$

$$G_2(s) = I, \tag{27}$$

and where the field F was R, the real numbers.

The free modular approach to MDP is based upon the recognition that, as a set,

$$F(s) \subset F[s] \times F[s],$$

which, in turn, suggests that it may be possible to express (25) in terms of F[s]. A convenient way to bring this about, as illustrated in (20), is to write

$$G(s) = N(s)\,D^{-1}(s), \tag{28}$$

where N(s) and D(s) have their elements in F[s]. It is easy to see that every G(s) has representation in the form (28). Similar representations could be adopted for $G_i(s)$, i = 1,2, but the presentation can be simplified if the choice

$$G_i(s) = \frac{M_i(s)}{d_i(s)} \qquad i = 1, 2 \tag{29}$$

is made, with $d_i(s) \in F[s]$, i = 1,2 and $M_i(s)$ having elements in F[s], i = 1,2. Equation (25) is then clearly the same as

$$\frac{M_1(s)}{d_1(s)}\,N(s)D^{-1}(s) = \frac{M_2(s)}{d_2(s)}, \tag{30}$$

which, in turn, is equivalent to

$$[d_2(s)M_1(s) \;\vdots\; -d_1(s)M_2(s)]\begin{bmatrix}N(s)\\ \cdots\\ D(s)\end{bmatrix} = 0, \tag{31}$$

an equation written over F[s]. For the jet engine

problem, (22) corresponds to (31). Let

$$\hat{t}_i(s) = \begin{bmatrix} \hat{n}_i(s) \\ \hline \hat{d}_i(s) \end{bmatrix} \tag{32}$$

denote the ith column of

$$\begin{bmatrix} N(s) \\ \hline D(s) \end{bmatrix}.$$

Then

$$[d_2(s)M_1(s) \vdots -d_1(s)M_2(s)]\ \hat{t}_i(s) = 0, \tag{33}$$

and every candidate tc construct a solution (28) can be traced to such $\hat{t}_i(s)$.

Thus MDP is quite closely related to the homogeneous equation

$$[d_2(s)M_1(s) \vdots -d_1(s)M_2(s)]\ t(s) = 0. \tag{34}$$

The purpose of this section is to explain briefly an appropriate algebraic interpretation of (34). This interpretation is based upon generalizing the notion of the n-dimensional F(s)-vector space $F(s)^n$ to that of a rank-n F[s]-module $F[s]^n$. As a vector space, $F(s)^n$ satisfies the usual axioms, with scalars taken from the field F(s). As a module, $F[s]^n$ satisfies exactly the same set of axioms, but with scalars taken from the principal ideal domain ring F[s]. Despite this close similarity, F[s]-modules do not behave in exactly the same way as vector spaces. But there is a class of them, known as finite-rank free modules, which have a great similarity to finite-dimensional vector spaces in that they have a basis, which can be defined in the usual way using concepts of span and independence. $F[s]^n$, for example, is said to be free on the basis

$$\{(0, \ldots, 0, \underset{\text{ith position}}{1}, 0, \ldots, 0);\ i = 1,2,\ldots,n\}. \tag{35}$$

Morphisms of F[s]-modules are defined analogously to linear operators on vector spaces; and, when domain and codomain are finite-rank free modules, the basis concept is used in the usual way to define a matrix for the morphism. This, then, is the interpretation to be given to the $p \times q$ matrix

$$[d_2(s)M_1(s) \vdots -d_1(s)M_2(s)] \tag{36}$$

in (34), namely the interpretation of a morphism

$$M: F[s]^q \to F[s]^p \tag{37}$$

of finite-rank free F[s]-modules. As a submodule of the finite-rank free module $F[s]^q$ over the principal ideal domain F[s], the kernel of M is also free, and thus the solution to (34) is tantamount to finding a basis for this kernel. The process for calculating such a basis is provided by Algorithm 1 in the Appendix.

If a basis

$$t_1(s), t_2(s), \ldots, t_\rho(s) \tag{38}$$

for Ker M has been computed, MDP solution then depends upon a determination of whether these basis elements can be used, through (32) and (28), to construct realizable G(s) matrices---and, if they can, to find G(s) whose minimal realizations are smallest and to assign poles wherever possible. It turns out to be convenient to answer these questions in terms of a reduced basis, whose definition is as follows. Let

$$t_i(s) = \sum_{j=0}^{k_i} t_{i,j} s^j \tag{39}$$

where $t_{i,j} \in F^q$, $t_{i,k_i} \neq 0$, and $i = 1,2,\ldots,\rho$. Then the basis (38) is said to be reduced if the matrix

$$[t_{1,k_1} \vdots t_{2,k_2} \vdots \ldots \vdots t_{\rho,k_\rho}] \tag{40}$$

has rank ρ. Algorithm 2 in the Appendix reduces a basis.

With these notions, the MDP Algorithm in the Appendix solves MDP. The issue of pole assignment is taken up in Section 7.

5. FLOATING POINT EXPERINECE

In view of the material presented in the previous section, we are ready to take a closer look at (22). The matrix $[M(s) \vdots -d(s)I]$ turns out to be a 2 x 9 matrix of polynomials in R[s]. Lack of space prevents us from reproducing all the numbers here, but fig. 6 shows that the typical element is a thirteenth degree polynomial. We also note the large variation in the magnitudes of the coefficients of the polynomials.

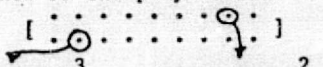

1.17 E10 s^3	-1.37 E10 s^2
+4.40 E10 s^4	-4.99 E10 s^3
+4.06 E10 s^5	-4.21 E10 s^4
+1.18 E10 s^6	-1.07 E10 s^5
-1.24 E9 s^7	+1.49 E9 s^6
-1.26 E9 s^8	+1.99 E9 s^7
-2.07 E8 s^9	+1.99 E8 s^8
-5.55 E6 s^{10}	+6.93 E6 s^9
-4.80 E4 s^{11}	+8.33 E4 s^{10}
-7.09 E1 s^{12}	+2.38 E2 s^{11}
+4.5 E-1 s^{13}	-1.00 E0 s^{12}

Fig. 6. Polynomial Matrix

In this section, we report on FORTRAN and PL/I softwares developed to implement the MDP Algorithm on a digital computer, and our experience in the application of the software to the jet engine control problem described earlier in the paper. Both the programs use floating point arithmetic to implement the MDP Algorithm, considered over the field of real numbers. The FORTRAN version, using double precision arithmetic, affords 15 digits of precision (decimal) on an IBM 370/158 computer. The PL/I version, using extended precision arithmetic, carries 33 significant digits. Our jet engine minimal design problem comes down to the question of determining the rank-seven kernel of a module morphism whose domain has rank nine, and whose matrix representation in the usual basis contains thirteenth degree polynomials. In our experience, the principal difficulties arise from roundoff error occurring as a result of finite representation of real numbers in the computer.

There are two noteworthy features of the floating point KERPO (KERnel of a Polynomial Operator) software. First, it provides the user some control over the number of digits considered significant during internal computer arithmetic. In actual problems, this appeared as the critical factor in obtaining acceptable solutions from the computer. Second, it performs a verification of the computed results up to four significant digits. Any discrepancy so pointed up, one attempts to rectify by varying the number of digits considered significant. In the case of the jet engine problem, after making several runs, we obtained an (apparently) acceptable solution from the PL/I version by setting the threshold for loss of significance near eleven digits. We can compare this solution with the known solution to the problem, represented by fig. 3. To do this, we proceed as follows.

The complete solution to the kernel problem appears in the form of seven elements in a rank nine module, which are the required reduced basis for the kernel. Represented in the usual manner, five of these contained polynomials of degree k_i one or less. It is interesting to note that the existence of such elements can be predicted by the following argument. We interpret fig. 3

to yield a solution to the kernel problem, of the form (41).

$$\begin{bmatrix} N \\ \hline D \end{bmatrix} = \begin{bmatrix} -H^T \\ \hline -sL^T \\ \hline sI \end{bmatrix} \qquad (41)$$

On the assumption that all solutions can be generated from the kernel basis, the logical conclusion is that the two columns of (41) can be represented as a linear combination of the five first degree elements in the reduced kernel basis. Interestingly enough, the question of determining this transformation can itself be represented as another kernel problem in polynomial modules. However, attempts to generate such a transformation turned out to be unsatisfactory.

As an alternative approach to verifying the KERPO solution, we used two of the five first degree basis elements to realize a second order dynamical control scheme for the jet engine, along the lines of fig. 5. From fig. 5, we could then obtain a state description for the overall closed loop system, which we then compared with the corresponding optimal integral control scheme system of fig. 3. This comparison was based on the first few Markov parameters. Table 3 shows this comparison for two of these parameters.

Table 3

Comparison of KERPO Results with Optimal Integral Control

Markov Parameter	KERPO Solution	Optimal Integral Control
CB	-4.4968 0.64815 -0.13348 -0.17304	-4.4969 0.64814 -0.13348 -0.17305
CAB	2631.6 1348 20693 10890	70.451 3.544 129.15 95.573

We note that our solution appears to have identified the B and C matrices correctly, while it is in error so far as the A matrix is concerned. On the basis of this evidence, we conjecture that roundoff error incurred in implementing the Euclidean division algorithm has the most serious impact on the correctness of the solution. This is because, intuitively, the effect of the A matrix in the state space corresponds to multiplication by 's' in the module. Since, in our case, the factors by which the matrix columns are multiplied are computed via the division algorithm, we hypothesize this to be the source of the error.

In order to solve the jet engine minimal design problem, then, one has the option of developing floating-point software which has increased sophistication or of switching to softwares which permit exact rational calculations. The next section reports on the latter method.

6. EXACT RATIONAL SOLUTION

One way to avoid the difficulties of finite machine representation of real numbers is to consider the numbers of table 1 as being rational instead of real numbers. It is then possible to get an exact solution to the jet engine problem, using softwares such as FORMAC or ALTRAN. These have the capability of rational and symbolic manipulation with an essentially unlimited degree of precision. Naturally, as the calculation proceeds, one would expect the integer size to increase quite a bit. As a consequence, the storage requirements and computer time needed to manipulate these would also be substantial. In this section we give evidence as to the magnitude of these, especially to contrast with the requirements for the floating point calculations. This yields valuable insight into the tradeoffs involved in terms of computer usage needed to solve typical realistic jet engine control problems from the polynomial approach. The results reported here are based upon FORMAC software written to implement, in rational arithmetic, the procedure of the Appendix, on an IBM 370/158 computer.

Starting with the numbers of table 1, together with the L and H matrices of table 2, we go through the calculations outlined in Section 3, and arrive at an exact rational-coefficient version of the kernel problem of (22). By applying the MDP Algorithm, conceived now over the field Q of rational numbers, we are led finally to an exact reduced basis for the corresponding exact 2 x 9 matrix over Q[s]. The seven basis elements turn out to contain polynomials of degree k_i equal to one and no polynomials of higher degree. Note that this means the floating point software missed at least two elements of first degree in the reduced basis. Rounded to fit in the available space, the seven basis elements obtained from exact software are indicated in table 4.

We would now like to compare the computer resources needed for the floating point calculation with those required for the exact calculation.

In the floating point software, a sort of trial and error process was used to optimize the calculation by varying the threshold for loss of significance. Though this software did not reach a satisfactory answer for the jet engine problem, we have allotted from our experience about seven runs of two CPU minutes each to this calculation. Each run occupied 400K bytes of memory.

Next consider the exact calculation. This software occupied 300K bytes of memory and executed the jet engine calculation in 135 minutes CPU time. However, the great majority of this time turns out to be consumed in Algorithm 2, which computes a reduced basis. This suggests strongly that more research on the reduction process---a common one in the literature ---could have a considerably greater than average effect on practical applications of the method. Except for the reduction, the remaining part of the calculation is just about an order of magnitude away from being very reasonable; and improvements of that order can be expected to occur in the near term, either through hardware or software advances.

A comparison is made in table 5. Here it is seen

Table 5

Comparison of Floating Point and Exact Solutions

Resource	Floating Point	Exact	
	Algorithms 1 and 2	Algorithm 1	Algorithm 2
Memory	400K bytes	300K bytes	300K bytes
CPU	14 minutes(average)	18 minutes	117 minutes

that, on the average, the difference between floating point and exact softwares was about an order of magnitude in computing time.

For the exact solution, it is of interest also to examine integer sizes at various stages in the calculation. Such a summary has been made in table 6. Note

Table 6

Integer Size During Exact Solution

Stage of Computation	No. of Decimal Digits in Typical Integer
1. State Matrices For Plant	4
2. Plant Transfer Function	14
3. Inverse of Closed Loop System (T)	33
4. Kernel Problem (2 x 9 matrix)	45
5. After Algorithm 1	150
6. 20% through Algorithm 2	270
7. 60% through Algorithm 2	250
8. Final Reduced Basis	160

Table 4

(Rounded) Reduced Basis from Exact Solution

2.443E-3	0.0	0.0	0.0	0.0	0.0	0.0
1.601E-3	0.0	0.0	0.0	0.0	0.0	6.565E-4
-3.824E-2 1.125E-3s	-7.199E-5 -6.649E-6s	4.494E-4 1.288E-5s	4.146E-4 1.188E-5s	4.146E-4 5.151E-6s	4.146E-4 5.834E-6s	0.0 5.806E-4s
-7.898E-3 1.87 E-4s	-6.41 E-4 -1.331E-5s	0.0 3.653E-6s	0.0 3.322E-6s	0.0 -2.571E-6s	0.0 -1.768E-6s	0.0 8.467E-5s
-1.526E-3 6.54 E-4s	9.685E-5 -6.621E-5s	2.893E-6 -4.642E-5s	0.0 -4.423E-5s	0.0 -2.416E-5s	0.0 -1.847E-5s	0.0 -1.314E-4s
0.0	5.081E-4	4.794E-4 1.843E-4s	4.479E-4 1.713E-4s	0.0 -4.245E-5s	0.0 -3.076E-5s	0.0 1.279E-5s
0.0	0.0	0.0	-2.217E-6	-3.491E-5 +3.131E-6s	0.0 7.438E-6s	0.0 -1.421E-4s
0.0	0.0	0.0	0.0	0.0	1.622E-5	0.0 9.972E-5s
2.935E-2 8.69 E-4s	2.949E-4	-4.416E-4	-4.068E-4	-2.25 E-4	-2.434E-4	0.0 2.955E-4s

that integer size before and after Algorithm 2 is about the same, while it nearly doubles during Algorithm 2. This also suggests that improvements in the efficiency of Algorithm 2 may be possible.

Finally, we summarize by commenting that the floating point software used on the order of 4×10^8 byte seconds of computing power, but eventually did not yield an acceptable solution. On the other hand, the exact rational software required on the order of 2.4×10^9 byte seconds of computing resources and led to an exact solution.

7. COMPENSATOR POLE ASSIGNMENT

The exact rational software discussed in Section 6 obtained the reduced basis, $t_i(s)$, $1 \le i \le 7$, with

$$t_i(s) = \begin{bmatrix} n_i(s) \\ d_i(s) \end{bmatrix} \tag{42}$$

of table 4. From (20), where $G^T(s)$ is 2 x 2 and $K^T(s)$ is 5 x 2, we see that the matrix N(s) must be 7 x 2 while D(s) is 2 x 2. Accordingly,

$$\left[\frac{N(s)}{D(s)}\right]$$

is a 9 x 2 matrix, which means from (32) that two kernel elements

$$\hat{t}_i(s) = \begin{bmatrix} \hat{n}_i(s) \\ \hline \hat{d}_i(s) \end{bmatrix}, \quad i = 1,2 \tag{43}$$

must be chosen to effect a design. These elements (43) will be linear combinations of the reduced basis elements (42). If

$$[\hat{t}_1(s) \vdots \hat{t}_2(s)]$$

has a linear dynamical interpretation as described in the Appendix, then $N(s)D^{-1}(s)$ has a minimal realization whose state matrix has a characteristic polynomial

$$|D(s)| = |\hat{d}_1(s) \vdots \hat{d}_2(s)|. \tag{44}$$

Now let

$$\hat{d}_i(s) = \sum_{k=1}^{7} f_{ik}\, d_k(s), \; f_{ik} \in R, \; i = 1,2. \tag{45}$$

Then

$$|D(s)| = \left| \sum_{k=1}^{7} f_{1k}\, d_k(s) \vdots \sum_{j=1}^{7} f_{2j} d_j(s) \right| = \sum_{k=1}^{7} \sum_{j=1}^{7} f_{1k} f_{2j} \, |d_k(s) \vdots d_j(s)|, \tag{46}$$

by elementary properties of determinants. This shows that the characteristic polynomial of the state matrix in a minimal realization of $N(s)D^{-1}(s)$ can be viewed as a linear combination of the determinants $|d_k(s) \vdots d_j(s)|$.

Table 4 makes it clear that $|D|$ must have degree at least two; and so, since

$$|d_1 \vdots d_6| = -1.4092974E\text{-}8s - 4.7599915E\text{-}7 \tag{47a}$$

$$|d_1 \vdots d_7| = -8.6656773E\text{-}8s^2 - 2.9268875E\text{-}6s \tag{47b}$$

$$|d_6 \vdots d_7| = 2.9060023E\text{-}8s. \tag{47c}$$

with the polynomials in (47) serving as a basis for $R_2[s]$, the R-subspace of R[s] consisting of polynomials of degree two or less, it is possible to construct an arbitrary polynomial

$$|D(s)| = b_1 s^2 + b_2 s + b_3, \tag{48}$$

for $b_i \in R$, i = 1,2,3 by forming an appropriate linear combination

$$\beta_1 |d_1 \vdots d_6| + \beta_2 |d_1 \vdots d_7| + \beta_3 |d_6 \vdots d_7|; \tag{49}$$

$\beta_i \in R$, i = 1,2,3. The β_i's are uniquely determined by the b_i's. To complete a minimal design (48), it is only necessary to calculate f_{1k} and f_{2j} for k and j = 1,6,7. But certain results from the exterior algebra, referenced in Section 8, permit the calculation of (f_{11}, f_{16}, f_{17}) and (f_{21}, f_{26}, f_{27}) as the basis of the kernel of the matrix $[\beta_3, -\beta_2, \beta_1]$. Space precludes a complete treatment of the theory, so we turn to the jet engine example.

We make the selection

$$|D(s)| = s^2 + 2s + 2, \tag{50}$$

not so much because these dynamics are most desirable, but rather because the industry methods described in Section 3 could not be used to achieve (50) in a minimal design. Thus, by solving this case, we establish potential superiority for MDP over existing industry techniques.

Starting then, with (50) and working backwards, we can calculate β_i, i = 1,2,3 and thence (f_{11}, f_{16}, f_{17}) as well as (f_{21}, f_{26}, f_{27}). These calculations were performed using exact arithmetic again. The results are presented here after rounding. First we obtain,

$$\beta_1 = -4.202E6 \tag{51a}$$

$$\beta_2 = -1.154E7 \tag{51b}$$

$$\beta_3 = -1.095E9. \tag{51c}$$

Next, the needed f_{ij}'s are obtained from the basis for the kernel of $[\beta_3, \beta_2, \beta_1]$. A workable set of f_{ij}'s is,

$$f_{11} = \beta_2/\beta_3 \quad (52a)$$

$$f_{21} = -\beta_1/\beta_3 \quad (52b)$$

$$f_{16} = f_{27} = 0 \quad (52c)$$

$$f_{26} = f_{17} = 1 \quad (52d)$$

The f_{ij}'s were, in our application, further scaled by a factor of 10^5 to obtain the compensator gains as reasonable numbers. This can be done without upsetting the compensator pole placement to be achieved. Eqs. (45) and (42) can then be solved for $\hat{t}_1$ and $\hat{t}_2$ of (43). The 9 x 2 matrix $[t_1 : t_2]$, which represents our solution, is seen to be,

$$\begin{bmatrix} 2.573 & -0.937 \\ 1.687 & 65.039 \\ 1.769s + 1.183 & 57.634s + 14.665 \\ 0.0202s - 8.32 & 8.395s + 3.029 \\ -1.158s - 1.607 & -13.396s + 0.585 \\ -3.076s & 1.279s \\ 0.744s & -14.214s \\ 1.622 & 9.972s \\ 0.915s + 6.582 & 29.213s - 11.258. \end{bmatrix} \quad (53)$$

A number of procedures exist which lead directly from the matrix $[t_1 : t_2]$ to a state-space realization for the compensators $G(s)^{-1}$ and $K(s)$. Referring then to fig. 5 and eqs. (23) and (24), we find the matrices A_g, B_g, C_g, B_k and D_k for a final solution of the problem. These are listed in Table 7, after rounding.

Table 7

Compensator Realizations

Matrix	Elements				
A_g	-2.0	-0.1626			
	12.298	0			
B_g	2.5732	1.686			
	-0.9369	65.039			
C_g	-3.2	0.1			
	1.092	0			
B_k	-11.727	-9.725	2.888	5.944	0.824
	36.416	3.28	-13.66	-37.83	9.147
D_k	0.119	0.777	2.363	9.973	-3.806
	1.932	0.022	-1.265	-3.36	0.813

The solution given in table 7 was verified by comparing the corresponding Markov parameters for the closed loop systems of figs. 5 and 3. An exact calculation comparing the first two Markov parameters, showed these to be identical for both systems. Another, non-exact calculation, which verified the first six Markov parameters, showed agreement to four digits. The first two of these were listed in the second column of table 3.

Step responses obtained from the closed loop system of fig. 5, using the numbers of table 7, are shown in fig. 7.

A visual comparison of fig. 7, with similar plots obtained for the optimal integral control system of fig. 3 showed them to be identical. Hence the latter set is not included here. It might be interesting to examine the distribution of closed loop poles, which is given below.

-138.43	-4.47 + 0.986 i
- 78.38	-1.678 ± 0.238 i
-0.136.	

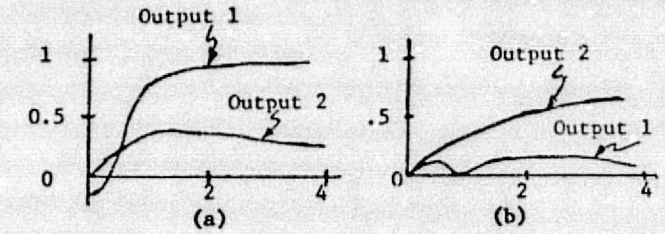

Fig. 7 Unit Step Responses. (a) Step on Input 1 (b) Step on Input 2.

As a final note in this section, it can be pointed out that the fixed poles in a compensator solution are the zeros of the greatest common divisor of the polynomials $\{|d_i : d_j|, i, j = 1,2,\ldots,7\}$. It is clear from the pairings (1,6), (1,7), (6,7) of our example that this GCD is 1, and thus that there are no fixed poles in the jet engine application.

8. REMARKS

8.1 Conclusions

Considerable work has been done in the control systems area on polynomial design methods. Regardless of which viewpoint one takes toward the definition of such problems, their solution is usually assumed to proceed according to algorithms of the type described in the Appendix. Conceptually, this theory has achieved considerable maturity, and so it seems appropriate to conduct an extensive case study of its application to a realistic problem. This is the reason for the jet engine control analyses carried out in this paper.

The conclusions are generally positive in nature, though with some temporary limitations. On the positive side, Sections 3 and 7 show that MDP is a problem relevant to the jet engine control industry and that the MDP Algorithm offers a significant improvement in flexibility of design over existing algorithms in that industry. The application problem detailed herein provides a realistic and nontrivial test case for workers in the area of computer solution of polynomial problems. A first limitation clearly occurs in Algorithm 2, which is a popular and well known theoretical algorithm. Both in terms of integer growth and relative CPU time, this reduction algorithm points to a need for further research. Following such an improvement, it would appear that the second limitation is overall CPU time for an exact solution. Though the cost of such time would be a small part of overall design cost, it appears desirable to reduce this time by an order of magnitude. Since such a reduction seems to be a near-term possibility by hardware or software advances, it would seem that polynomial methods may soon be ready to play a greater role in everyday practical design.

8.2 Historical Remarks

The original stimulus for this work was the paper of Wang and Davison [1] in 1973, in which a minimal inverse system problem was solved. That work subsequently led to the algorithm of Forney [2] phrased in rational vector spaces. Together, these works then led to the free-modular MDP Algorithm [3] which has been applied here. The jet engine application has been motivated by Michael and Farrar [4], whence arose our numerical data. A report on KERPO in double-precision FORTRAN has been presented [5], as has a more complete treatment of the pole assignment approach [6] in Section 7. Background reading on the algebraic aspects of the paper is available in [7]; and the exact proposition needed in Section 7 can be found in Chapter XV, Section 8, Proposition 15 of [8]. Further references to related

polynomial works have been cited in [3].

REFERENCES

1. S. H. Wang and E. J. Davison, "A Minimization Algorithm for the Design of Linear Multivariable Systems," IEEE Transactions on Automatic Control, Vol. AC-18, pp. 220-225, June 1973.
2. G. D. Forney, Jr., "Minimal Bases of Rational Vector Spaces, with Applications to Multivariable Linear Systems," SIAM Journal on Control, Vol. 13, pp. 493-520, May 1975.
3. M. K. Sain, "A Free-Modular Algorithm for Minimal Design of Linear Multivariable Systems," Proceedings IFAC 6th World Congress, Part IB, pp. 9.1-1--9.1-7, August 1975.
4. G. J. Michael and F. A. Farrar, "An Analytical Method for the Synthesis of Nonlinear Multivariable Feedback Control," Report M941338-2, United Aircraft Research Laboratories, June 1973.
5. R. R. Gejji, "A Computer Program to Find the Kernel of a Polynomial Operator," Proceedings Fourteenth Allerton Conference on Circuit and System Theory, September 1976.
6. V. Seshadri and M. Sain, "An Approach to Pole Assignment by Exterior Algebra," Proceedings Fourteenth Allerton Conference on Circuit and System Theory, September 1976.
7. M. K. Sain, "The Growing Algebraic Presence in Systems Engineering: An Introduction," IEEE Proceedings, Vol. 64, pp. 96-111, January 1976.
8. S. MacLane and G. Birkhoff, Algebra. London: The Macmillan Co., 1967.

APPENDIX

Let

$$M : F[s]^q \to F[s]^p \tag{A.1}$$

be a morphism of free modules. In the appendix, we describe how a reduced basis for the kernel of M can be obtained and used to solve MDP. For a more complete discussion, the reader is referred to [3]. Solutions are obtained in the form of the $q \times \ell$ matrix

$$\begin{bmatrix} N(s) \\ \hline D(s) \end{bmatrix} \tag{A.2}$$

over $F[s]$.

We change notation slightly by letting M be the $h \times q$ matrix representing the morphism M. The technique is to choose $q \times q$ unimodular $F[s]$-matrices to post-multiply M. A matrix is unimodular if it has a non-zero determinant that is an element of F. Mathematically,

$$U : F[s]^q \to F[s]^q \tag{A.3}$$

is unimodular if $|U| \neq 0, \in F$. Such an operation is equivalent to a change of basis in $F[s]^q$ and leads to a representation of M in the new basis. The following elementary column operations are examples of such transformations. The column operations are, (1) interchanging two columns of M; (2) adding an $F[s]$-multiple of one column of M to another; (3) multiplication of a column of M by a non-zero element of F.

Given the $p \times q$ matrix M, the following algorithm leads to a basis for Ker M. The basis elements are represented in the usual manner.

Algorithm 1

Step 1. To the $p \times q$ matrix M, adjoin a $q \times q$ identity matrix to form

$$\begin{bmatrix} M \\ \hline I \end{bmatrix}. \tag{A.4}$$

Step 2. By elementary column operations, reduce (A.4) to the form

$$\left[\begin{array}{c|c} E_{11} & 0 \\ \hline E_{21} & E_{22} \end{array}\right] \tag{A.5}$$

where E_{11} has p rows, has no zero columns and is in an echelon form.

Step 3. Then the columns of E_{11} are a basis for the image of M, and the columns of E_{22} are a basis for the kernel of M (Ker M).

Now, let b_i, $i = 1,2,\ldots,n$ be the columns of E_{22} obtained from Algorithm 1 as a basis for Ker M. Then by application of further unimodular transformations, we can get an equivalent basis for Ker M which is reduced in the sense of Section 4. Notice that we have introduced the notation b_i for elements of the basis before reduction, to avoid confusion with t_i, $i = 1,2,\ldots n$, which was assumed to be a reduced basis in Section 4. The algorithm below is used to reduce the kernel basis. However, the procedure is more general in nature and can be used to reduce n linearly independent elements in $F[s]^q$ regardless of their origin. This one is typical of procedures described in the literature for doing these kinds of calculations. However, as has been pointed out in the paper, it is this part of the computation that consumes the major portion of computer time. Any research aimed at achieving efficiency in the reduction process is, therefore, the most likely to have a significant payoff in terms of making the MDP method of control system design tractable in the near term.

Algorithm 2

Write each b_i, $i = 1,2,\ldots, n$ in the manner

$$b_i = \sum_{j=0}^{\ell_i} b_{i,j} s^j \tag{A.6}$$

where $b_{i,j} \in F^q$ and $b_{i,\ell_i} \neq 0$. We shall say the list $b_1, b_2,\ldots, b_n$ is reduced if the matrix

$$[b_{1,\ell_1}\ b_{2,\ell_2} \cdots b_{n,\ell_n}] \tag{A.7}$$

has rank n. Then, perform:

Step 1. If the list $b_1, b_2,\ldots, b_n$ of linearly independent elements is reduced, stop; otherwise, continue.

Step 2. Determine field elements f_i in F, $1 \leq i \leq n$, which are not all zero and which satisfy

$$\sum_{i=1}^{n} f_i\, b_{i,\ell_i} = 0. \tag{A.8}$$

Step 3. For the set of integers i having f_i non-zero, determine an i, denoted by i_{max}, for which ℓ_i is a maximum, denoted by ℓ_{max}.

Step 4. Perform the elementary column operation: Replace $b_{i_{max}}$ by

$$\sum_{i=1}^{n} f_i\, b_i s^{(\ell_{max} - \ell_i)}$$

Return to Step 1.

The question that remains is how the reduced basis may be used to obtain linear dynamical solutions to MDP. Let MDP take the form (A.9) when stated over $F[s]$.

$$M \begin{bmatrix} N \\ \hline D \end{bmatrix} = 0. \tag{A.9}$$

Now, in any solution

$$\begin{bmatrix} N \\ \hline D \end{bmatrix}$$

of (A.9), each of the ℓ columns will be contained in the kernel of M. All solutions pairs (N,D) can, thus, be built up as linear combinations of elements in a basis for Ker M. Under what conditions will a solution pair (N,D) yield a minimal solution?

Without loss of generality, we may assume that for any candidate pair (N,D) the ℓ columns of

$$\left[\frac{N}{D}\right]$$

are reduced, because if they are not, a unimodular transformation V on $F[s]^{\ell}$, chosen according to Algorithm 2, will produce an equivalent pair $(\hat{N},\hat{D})$ such that the columns of

$$\left[\frac{\hat{N}}{\hat{D}}\right]$$

are reduced and

$$ND^{-1} = NV(DV)^{-1} = \hat{N}\hat{D}^{-1}. \tag{A.10}$$

Then, we make the following comments, offered without proof.

(1) $N(s)D^{-1}(s)$ can be realized by a linear dynamical system if ND^{-1} is a matrix of proper rational functions. In such a situation, there exists a realization A,B,C,E, all matrices over F, such that

$$\begin{aligned} G(s) &= N(s)D^{-1}(s) \\ &= C(sI-A)^{-1}B + E. \end{aligned} \tag{A.11}$$

Equivalently, we also say that a pair (N,D) has a linear dynamical interpretation if the ℓ columns of

$$\left[\frac{N}{D}\right]$$

are reduced and furthermore, letting the i^{th} column be

$$\hat{t}_i = \left[\frac{\hat{n}_i}{\hat{d}_i}\right], \quad i = 1,2,\ldots,\ell, \tag{A.12}$$

these ℓ columns, when expressed as

$$\hat{t}_i = \sum_{j=0}^{m_i} \hat{t}_{i,j}s^j, \quad \hat{t}_{i,m_i} \neq 0 \tag{A.13}$$

are such that the last ℓ rows of the matrix

$$[\hat{t}_{1,m_1}\ \hat{t}_{2,m_2} \cdots \hat{t}_{\ell,m_\ell}] \tag{A.14}$$

have full rank.

Being concerned with finding a realization with the least order of dynamics, we state two more properties.

(2) If the property in (1) is satisfied, then the determinant $|D(s)|$ is related to the minimal realization, being an F-multiple of the corresponding characteristic polynomial $|sI-A)|$. Also,

(3) The columns of

$$\left[\frac{N}{D}\right]$$

when expressed as in (A.13), yield the number of dynamical elements in the minimal realization as

$$\sum_{i=1}^{\ell} m_i.$$

With these notions, let t_i, $i = 1,2,\ldots,n$ be the reduced basis obtained from Algorithm 2. Then, MDP reduces to generating ℓ elements in Ker M which have a linear dynamical interpretation, with minimum order dynamics. For this, we can use the MDP Algorithm.

MDP Algorithm

Step 1. Apply Algorithm 1 to obtain a basis

$$b_i, \quad 1 \leq i \leq n \tag{A.15}$$

for Ker M.

Step 2. Apply Algorithm 2 to the elements of (A.15), to form a reduced basis,

$$t_i, \quad 1 \leq i \leq n. \tag{A.16}$$

Step 3. Express the reduced basis (A.16) in this manner

$$t_i = \sum_{j=0}^{k_i} k_{i,j}s^j, \quad t_{i,k_i} \neq 0 \tag{A.17}$$

for $i = 1,2,\ldots,n$. Form the matrix

$$[t_{1,k_1}\ t_{2,k_2} \cdots t_{n,k_n}]. \tag{A.18}$$

If the rank of the matrix formed from the last ℓ rows of (A.18) is not equal to ℓ, stop; MDP has no solution; otherwise, continue.

Step 4. From the elements of (A.16) in the reduced basis select ℓ elements

$$t_{i_1}, t_{i_2}, \ldots, t_{i_\ell}$$

with the properties

(i) the rank of the matrix formed from the last ℓ rows of

$$[t_{i_1,k_{i_1}}\ t_{i_2,k_{i_2}} \cdots t_{i_\ell,k_{i_\ell}}]$$

is equal to ℓ; and

(ii) $\sum_{j=0}^{\ell} k_{i_j}$ is a minimum.

As a matter of fact, more solutions to MDP may be possible. Any elements $\hat{t}_1, \hat{t}_2, \ldots, \hat{t}_\ell$ in Ker M, which admit a linear dynamical interpretation and achieve the minimum order dynamics predicted in (ii) above, are a solution to MDP through the equations

$$\left[\frac{N}{D}\right] = [\hat{t}_1\ \hat{t}_2 \cdots \hat{t}_\ell] \tag{A.19}$$

and

$$G(s) = N(s)D^{-1}(s). \tag{A.20}$$

Now, in the jet engine problem, n is 7 and ℓ is 2. The two needed columns of

$$\left[\frac{N}{D}\right]$$

were generated in Section 7 to satisfy the pole placement requirement.

Appendix E

"A COMPARISON OF FREQUENCY DOMAIN TECHNIQUES FOR JET ENGINE CONTROL SYSTEMS DESIGN"

M. K. Sain
R. M. Schafer
R. R. Gejji
P. W. Hoppner

A COMPARISON OF FREQUENCY DOMAIN TECHNIQUES FOR JET ENGINE CONTROL SYSTEM DESIGN

R. Gejji, R. M. Schafer, M. K. Sain, & P. Hoppner
Department of Electrical Engineering
University of Notre Dame
Notre Dame, Indiana 46556

Abstract

Present research efforts in the area of linear multivariable control systems include activities which will probably reestablish frequency domain methods as frequently used tools for design. Two notable branches of this activity are polynomial methods and return-difference-determinant methods. This paper sketches some features of these approaches, in the context of a numerical example from turbofan engine control.

1. INTRODUCTION

State variable methods for the design of linear multivariable control systems are well established as a major tool in the applications. Variants of the linear quadratic regulator theory are probably the most successful, with a variety of other techniques such as pole placement, decoupling, and geometric regulator theory also available. Even today, however, linear quadratic regulator theory still requires a somewhat indirect thought process, a feature it shares with many optimization methods; and much of the remaining technique is synthesis oriented instead of design oriented.

Accordingly, some modern re-emergence of frequency domain thought has occurred---especially for design. Broadly depicted, this work involves polynomial methods and return-difference-determinant methods. This paper records certain studies of these ideas, on a common illustration from turbofan engine control. Brevity precludes in-depth treatment; we rely instead on the illustrations and the references.

2. ILLUSTRATIVE PROBLEM

The turbofan engine model chosen for the illustrations has two control inputs--fuel flow and exhaust area, five states--fan turbine inlet temperature, main burner pressure, fan speed, high compressor speed, and augmentor pressure, and two outputs--thrust and high turbine inlet temperature. In traditional (A,B,C,D) form, the state description [1] is given by the matrices at the top of the following column, at a power lever angle of 47°. For the sequel the corresponding matrix G(s), namely $C(sI-A)^{-1}B+D$, is recorded.

$$A = \begin{bmatrix} -57.096 & 3.613 & -10.211 & -5.481 & -2.715 \\ 19.832 & -72.340 & 30.295 & 40.972 & 15.327 \\ .660 & 4.496 & -3.601 & -.011 & -2.808 \\ 1.326 & 2.313 & -.809 & -3.032 & -.821 \\ .882 & .703 & 2.922 & 1.471 & -4.596 \end{bmatrix}$$

$$B = \begin{bmatrix} 39.792 & 1.017 \\ 4.181 & -.125 \\ -.382 & -.077 \\ -.565 & -.088 \\ -.785 & -3.563 \end{bmatrix} \qquad D = \begin{bmatrix} .018 & .546 \\ -.086 & -.013 \end{bmatrix}$$

$$C = \begin{bmatrix} -.037 & .031 & -.016 & -.042 & 1.368 \\ 1.081 & .149 & -.057 & .001 & -.086 \end{bmatrix}$$

The design problem is to select compensators for G(s), in a loop under unity negative feedback of the plant outputs. Fast step responses with small overshoot are of interest.

3. POLYNOMIAL METHODS [2]

Polynomial methods take advantage of the fact that action of the A-matrix and the s-variable are closely related in a module theoretic sense [3]. Not yet well advanced computationally, polynomial methods nonetheless offer considerable insight into system structure. As is to be expected, they resemble the geometric methods in this regard.

$$G(s) = \frac{\begin{bmatrix} (.018s^5 + .145s^4 - 92.05s^3 & (.546s^5 + 71.9s^4 + 2247s^3 \\ -396.9s^2 + 29801s + 95491) & -1943.s^2 - 16855s - 12495) \\ (-.036s^5 + 31.63s^4 + 3321.5s^3 & (-.013s^5 - .437s^4 + 68.2s^3 \\ + 25500s^2 + 76068s + 78277) & + 1703.3s^2 + 1742.9s - 3532.2) \end{bmatrix}}{s^5 + 140.7s^4 + 5337.6s^3 + 38691s^2 + 119690s + 133389}$$

As an example, consider the selection of $K_1(s)$ and $K_2(s)$ in Figure 1 in order to achieve a specified closed loop performance T(s). Such a specification is, of course, a nontrivial issue in its own right. A complete treatment of such a specification can be found in [2]. Relying upon the algebraic interpretation of a transfer function as a pair of polynomials, such a design problem can be converted to a kernel calculation in R[s]-modules, where R[s] denotes polynomials in s with coefficients in the real number field R. Considerable manipulation must be carried out to set up this kernel problem, which turns out to involve a 2x9 matrix of polynomials up to the thirteenth degree, as shown below.

$$\begin{bmatrix} \cdot & \cdot & \cdot & \cdot & \cdot & \cdot & \cdot & \odot & \cdot \\ \cdot & \odot & \cdot & \cdot & \cdot & \cdot & \cdot & \cdot & \odot \end{bmatrix}$$

1.17 E10 s^3	-1.37 E10 s^2
+4.40 E10 s^4	-4.99 E10 s^3
+4.06 E10 s^5	-4.21 E10 s^4
+1.18 E10 s^6	-1.07 E10 s^5
-1.24 E9 s^7	+1.49 E9 s^6
-1.26 E9 s^8	+1.99 E9 s^7
-2.07 E8 s^9	+1.99 E8 s^8
-5.55 E6 s^{10}	+6.93 E6 s^9
-4.80 E4 s^{11}	+8.33 E4 s^{10}
-7.09 E1 s^{12}	+2.38 E2 s^{11}
+4.5 E-1 s^{13}	-1.00 E0 s^{12}

Solution involves automorphic transformations on the domain of the map represented by this matrix to determine seven "reduced basis" elements, shown below which serve to describe the kernel. From these, construction of $K_1(s)$ and $K_2(s)$ involves two linear combinations of these seven module elements, and standard realization methodology. Using first, sixth, and seventh elements, and the assumptions

$$C_{K_1} = C_{K_2} \quad A_{K_1} = A_{K_2}, \quad D_{K_1} = 0,$$

realizations can be found in the manner

Compensator Realizations

Matrix	Elements				
A_{K_1}	-2.0	-0.1626			
	12.298	0			
B_{K_1}	2.5732	1.686			
	-0.9369	65.039			
C_{K_1}	-3.2	0.1			
	1.092	0			
B_{K_2}	-11.727	-9.725	2.888	5.944	0.824
	36.416	3.28	-13.66	-37.83	9.147
D_{K_2}	0.119	0.777	2.363	9.973	-3.806
	1.932	0.022	-1.265	-3.36	0.813

Responses to unit steps in the two reference channel are shown in Figures 2 and 3.

Solution of a problem by polynomial methods involves at this time nontrivial computational overhead, which is discussed in greater detail in [2]. It is likely, however, that advances in software and hardware will soon reduce this overhead. Advantages of the method include a finite enumeration of all solutions for a given T(s), and perhaps eventually a finite description of all possible performances.

2.443E-3	0.0	0.0	0.0	0.0	0.0	0.0
1.601E-3	0.0	0.0	0.0	0.0	0.0	6.565E-4
-3.824E-2	-7.199E-5	4.494E-4	4.146E-4	4.146E-4	4.146E-4	0.0
1.125E-3s	-6.649E-6s	1.288E-5s	1.188E-5s	5.151E-6s	5.834E-6s	5.806E-4s
-7.898E-3	-6.41 E-4	0.0	0.0	0.0	0.0	0.0
1.87 E-4s	-1.331E-5s	3.653-6s	3.322E-6s	-2.571E-6s	-1.768E-6s	8.467E-5s
-1.526E-3	9.685E-5	2.893E-6	0.0	0.0	0.0	0.0
6.54 E-4s	-6.621E-5s	-4.642E-5s	-4.423E-5s	-2.416E-5s	-1.847E-5s	-1.314E-4s
0.0	5.081E-4	4.794E-4	4.4794E-4	0.0	0.0	0.0
		1.843E-4s	1.713E-4s	-4.245E-5s	-3.076E-5s	1.279E-5s
0.0	0.0	0.0	-2.217E-6	-3.491E-5	0.0	0.0
				+3.131E-6s	7.438E-6s	-1.421E-4s
0.0	0.0	0.0	0.0	0.0	1.622E-5	0.0
						9.972E-5s
2.935E-2	2.949E-4	-4.416E-4	-4.068E-4	-2.25 E-4	-2.434 E-4	0.0
8.69 E-4s						2.955E-4s

4. RETURN-DIFFERENCE-DETERMINANTS [4]

The present computational situation for polynomial methods makes alternate frequency domain approaches of interest.

If we set K_2 to zero and denote K_1 by K, we have the archetypal unity negative feedback precompensation problem. If K is assumed to have state description (A_K, B_K, C_K, D_K), then a combined state description (A_C, B_C, C_C, D_C) for

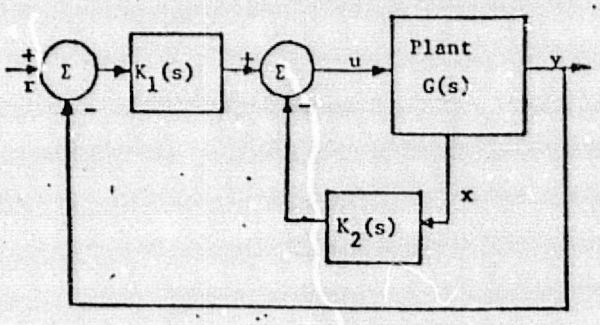

Fig. 1
Compensation Scheme for Polynomial Design

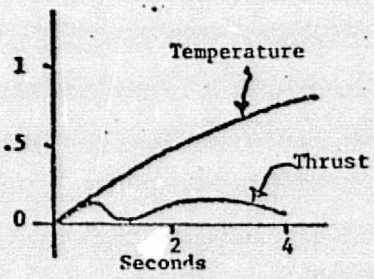

Fig. 3
Closed Loop Response to Unit Step in
Commanded Temperature; Polynomial Design

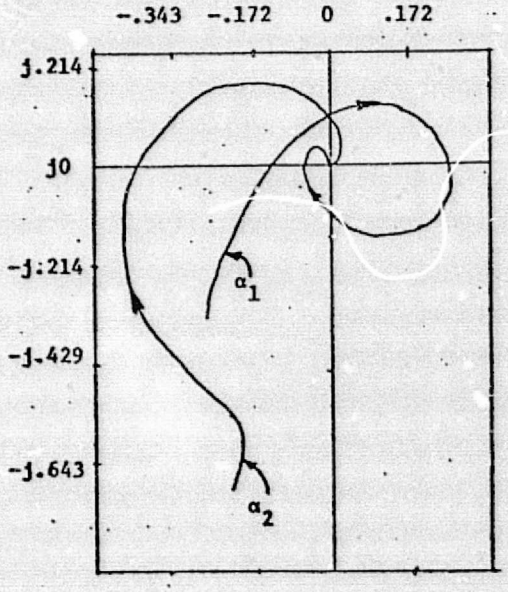

Fig. 5
Nyquist Plots for Compensated System;
Alpha Expansion

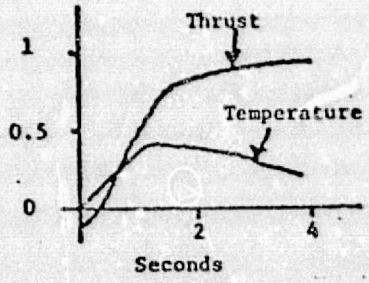

Fig. 2
Closed Loop Response to Unit Step in
Commanded Thrust; Polynomial Design

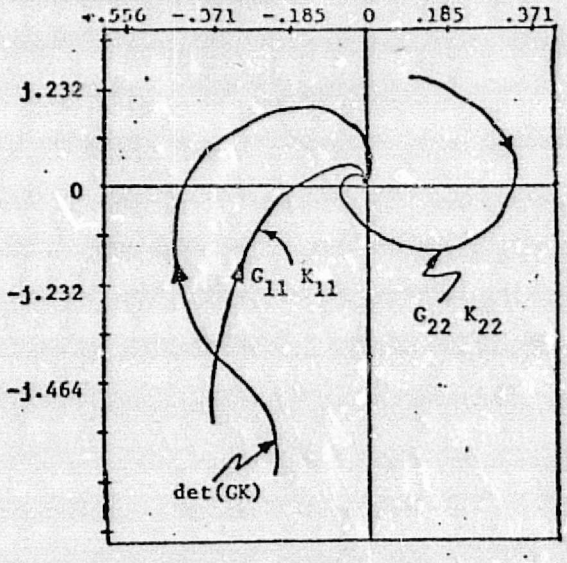

Fig. 4
Nyquist Plots for Compensated System;
Direct Expansion

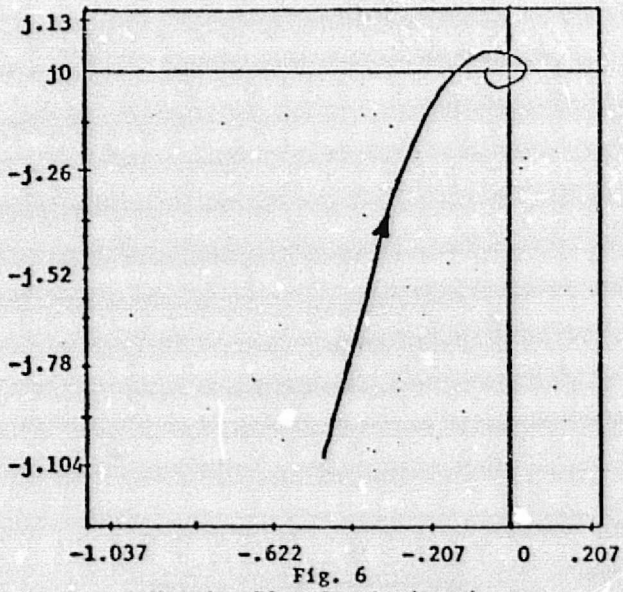

Fig. 6
Nyquist Plot for det(I+GK)

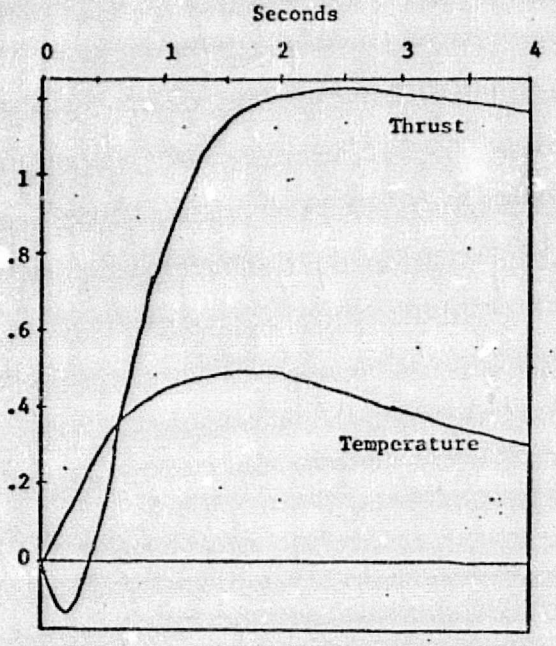

Fig. 7
Same as Fig. 2 for Direct Approach Design

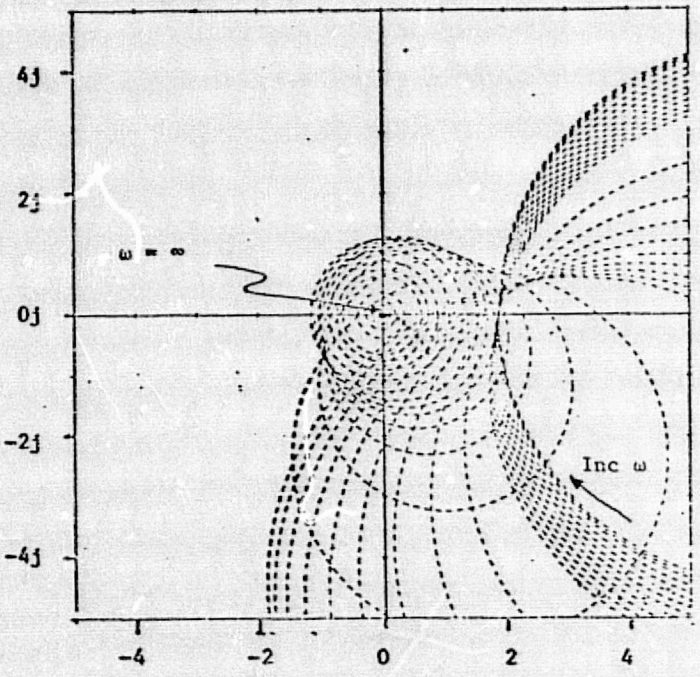

Fig. 9
CARDIAD Plot, Column 1, Uncompensated

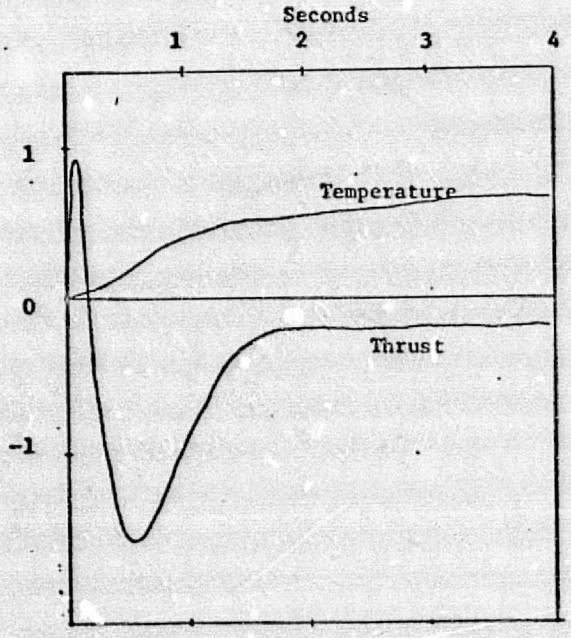

Fig. 8
Same as Fig. 3 for Direct Approach Design

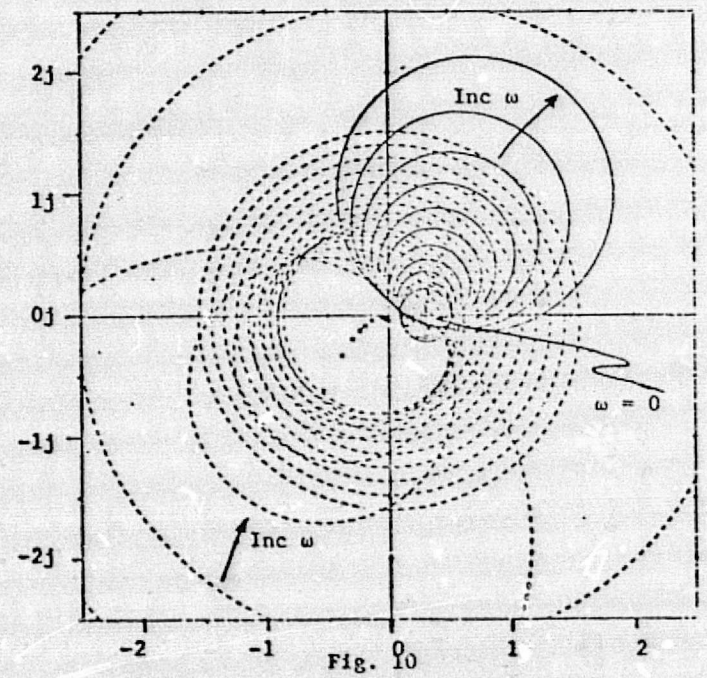

Fig. 10
CARDIAD Plot, Column 2, Uncompensated

the loop can be obtained by an isomorphism on the product of the state spaces X and X_K associated with the plant and compensator, respectively, provided that the gain matrix DD_K has no negative unit eigenvalues. For this situation, one has the important relationship that

$$|I+DD_K|\ |sI-A_C|=|I+GK|\ |sI-A|\ |sI-A_K|,$$

upon which a Nyquist study can be based. We refer

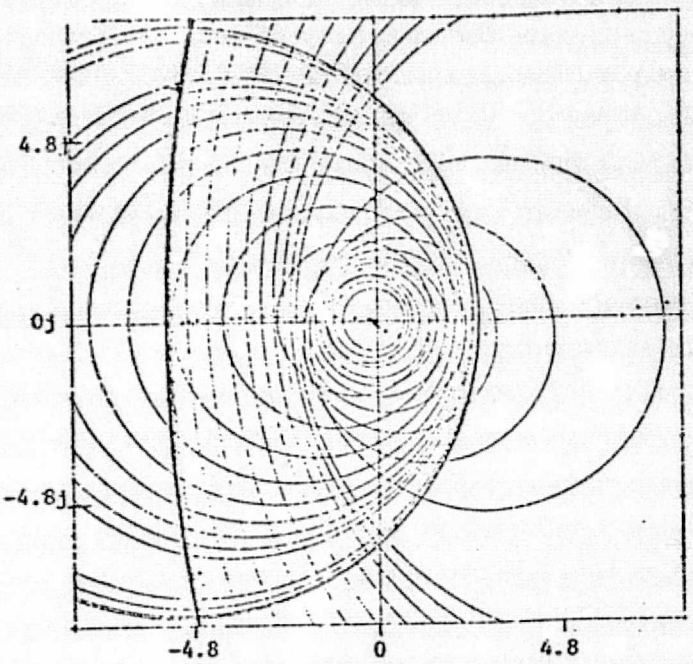

Fig. 11
CARDIAD Plot, Column 1, Compensated System

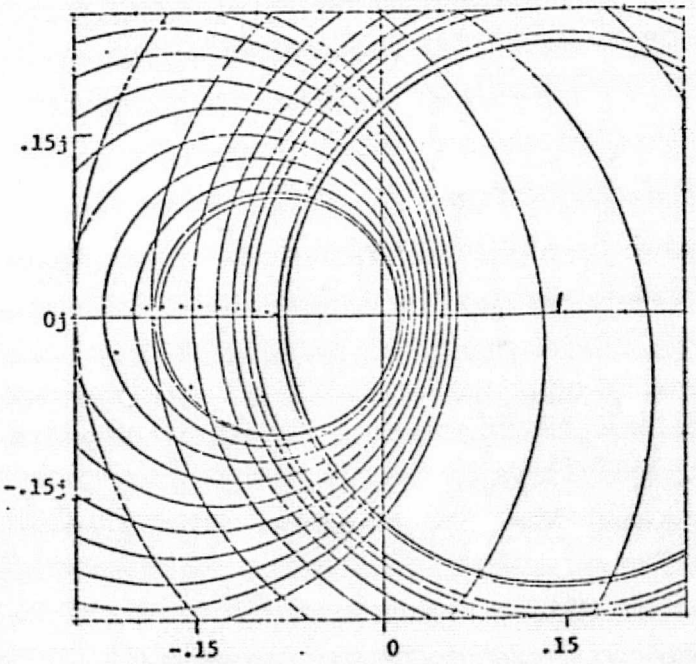

Fig. 12
CARDIAD Plot, Column 2, Compensated System

to such studies as return-difference-determinant methods, because of the presence of $|I+GK|$ in a key role.

Construction of a Nyquist plot is related to the expansion chosen for the return-difference-determinant. The obvious expansion, shown for the present illustrative case, is

$$1 + G_{11}K_{11} + G_{12}K_{21} + G_{21}K_{12} + G_{22}K_{22} + |GK|;$$

and a less obvious, more recursive expansion in an NxN case is

$$\sum_{i=0}^{N} (-1)^i \alpha_i,$$

where

$$\alpha_0 = 1,$$

and

$$\alpha_i = (-1/i) \sum_{p=0}^{i-1} \alpha_p \, \text{trace}(GK)^{i-p},$$

for $i \geq 1$.

Design based upon Nyquist plots of $|I+GK|$ is made challenging by the intricate way in which the compensator K relates to the determinant. At present, only introductory design studies based upon the expansions above have been made [4]. An illustration is the compensator

$$K(s) = \begin{bmatrix} \frac{1}{s} & 0 \\ 0 & \frac{1000(s+1)}{s(s+200)} \end{bmatrix},$$

which was chosen by a cut-and-try method to increase the speed of response of the second output. Figures 4 and 5 show the terms in the "obvious" and "a" expansions for the compensated system, with Figure 6 indicating the sum, exclusive of the unit term in each expansion. Closed loop responses to reference steps in each channel are shown in Figures 7 and 8. Though the temperature response in Figure 8 is acceptable, the thrust response in Figure 7 exhibits overshoot; and considerable interaction is evident.

In current practice, plots such as Figure 6 tend to be the most useful. Design technique tends to focus upon reducing the interaction evident in these results, which brings us to the next topic.

5. CARDIAD--A DOMINANCE APPROACH [5]

In making a Nyquist plot of the determinant of return difference, H. H. Rosenbrock, [7] has established that $|I+GK|$ encirclements can be counted as the algebraic sum of the encirclements of the diagonal elements of return difference (I+GK)--provided that a condition of "dominance" holds on (I+GK). This means, in our case, that the off-diagonal element in a column is smaller in magnitude than the diagonal element, as a function of frequency ($s=j\omega$). Related to this stability oriented usage of the dominance idea is a corresponding requirement on the loop transmission GK, which is used to help with decoupling closed loop performance.

Selection of K(s) for this latter purpose, so that $G(j\omega)K(j\omega)$ is dominant on its columns, has been widely studied for the case in which K(s) is restricted to be a constant matrix. Much less has been accomplished relative to the choice of a dynamic K(s).

A new technique for this purpose is the CARDIAD

plot, acronymed for Compensator Acceptability Region for Diagonal Dominance. Compensators

$$K(j\omega) = \begin{bmatrix} 1 & x_2(j\omega)+jy_2(j\omega) \\ x_1(j\omega)+jy_1(j\omega) & 1 \end{bmatrix}$$

are assumed, without loss of generality for precompensation. A CARDIAD plot for column one of the uncompensated system is shown in Figure 9. Each circle corresponds to a particular frequency ω, and acceptable (x_1,y_1) pairs must be outside dashed circles at the frequency in question. Note that $y_1 = 0$ and x_1 suitably negative will be acceptable for all frequencies. Figure 10 shows a CARDIAD plot for column two. Acceptable (x_2,y_2) pairs must be inside solid circles at the frequency in question.

The simple compensator

$$K(s) = \begin{bmatrix} 1 & \dfrac{.7s + .44}{.05s + 1} \\ -10 & 1 \end{bmatrix}$$

achieves dominance at all frequencies in both columns, as can be seen in Figures 11 and 12, which consist only of solid circles each of which includes the origin.

More detailed information about an application of this method to design and simulation of a turbofan engine control can be found in [6].

6. DISCUSSION

Recent activities in frequency domain analysis and design of linear multivariable control systems suggest a certain resurgence of this viewpoint in useful new ways. Though somewhat limited by space constraints, we have tried to give a glimpse of some of these methods in the context of a numerical model from the turbofan engine area. Focus has been on polynomial methods, which bear close resemblance to geometric control methods in an abstract algebraic sense, and upon methods related to the determinant of return difference. The CARDIAD plot, a new dynamical approach to dominance, has been illustrated.

ACKNOWLEDGMENTS

This work was supported in part by the National Science Foundation under Grant ENG 75-22322 and in part by the National Aeronautics and Space Administration under Grant NSG 3048.

REFERENCES

1. C. J. Michael and F. A. Farrar, "An Analytic Method for the Synthesis of Nonlinear Multivariable Control," United Technologies Research Laboratories, Report M941338-2, East Hartford, Connecticut, June 1973.

2. R. R. Gejji and M. K. Sain, "Application of Polynomial Techniques to Multivariable Control of Jet Engines," Preprints Fourth IFAC International Symposium on Multivariable Technological Systems, pp. 421-429, June 1977.

3. S. MacLane and G. Birkhoff, Algebra. London: The Macmillan Co., 1967.

4. P. W. Hoppner, "The Direct Approach to Compensation of Multivariable Jet Engine Models," Tech. Rept. EE-779, Notre Dame, Indiana, April 25, 1977.

5. R. M. Schafer, "A Graphical Approach to System Dominance," Tech. Rept. EE-778, Notre Dame, Indiana, March 26, 1977.

6. R. M. Schafer, R. R. Gejji, P. W. Hoppner, W. E. Longenbaker, and M. K. Sain, "Frequency Domain Compensation of a DYNGEN Turbofan Engine Model," Proc. 1977 Joint Automatic Control Conference, pp. 1013-1018.

7. H. H. Rosenbrock, Computer-Aided Control System Design. New York: Academic Press, 1974.

Appendix F

"TIME OPTIMAL CONTROL OF A TWO-SPOOL TURBOFAN JET ENGINE"

W. E. Longenbaker
R. J. Leake

TIME OPTIMAL CONTROL OF A TWO-SPOOL TURBOFAN JET ENGINE

by

W. E. Longenbaker and R. J. Leake

Department of Electrical Engineering
University of Notre Dame

Technical Report No. EE-7714

September 1977

* This research was supported by the National Aeronautics and Space Administration under Grant NSG-3048.

ABSTRACT

This work explores an alternative to existing methods which are commonly used to design controls for jet engines. Whereas most modern designs implement piecewise-linear quadratic regulators, this represents an attempt to obtain a global nonlinear optimal control for a two-spool turbofan jet engine.

A necessary starting point, therefore, is to have a good nonlinear model on which to perform the control studies. Unfortunately, the only accurate existing models of jet engines are (1) linear analytical models valid only for small regions, or (2) massive nonlinear, non-analytical computer programs which attempt to match experimental data. What is needed for this study is something which lies between these two extremes, i.e., a nonlinear, analytical model.

A fifth order nonlinear model was developed in this study which correctly models most of the qualitative behavior of the jet engine, but which fails to achieve strong numerical agreement with DYNGEN, a reliable non-analytical simulator. Several linear models were derived, both from the nonlinear analytical model, and also from DYNGEN. A time optimal control problem was formulated, subject to various constraints. Dynamic Programming theory and the Successive Approximations technique were explored, and applied to the problem of interest, while several improvements in the numerical programming were introduced. Analytical and numerical results were obtained for several models, both constrained and unconstrained. Finally, these results were tested on the two principal simulators, DYNGEN and the analytical nonlinear model.

The study successfully achieved time optimal feedback control laws for various models of the two-spool turbofan jet engine. Furthermore, valuable insight into the nature of the problem was obtained, and much

useful computer software was developed. However, an optimal control law obtained from any model can only be as good as the model itself. For this reason, more work is needed to develop a better nonlinear analytical model of the two-spool turbofan jet engine.

TABLE OF CONTENTS

CHAPTER I

INTRODUCTION

This work explores an alternative to existing methods which are commonly used to design controls for jet engines. Whereas most modern designs implement piecewise-linear quadratic regulators, this represents an attempt to obtain a global nonlinear optimal control for a two-spool turbofan jet engine.

A necessary starting point, therefore, is to have a good nonlinear model on which to perform the control studies. Unfortunately, the only accurate existing models of jet engines are (1) linear analytical models valid only for small regions, or (2) massive nonlinear, non-analytical computer programs which attempt to match experimental data. What is needed for this study is something which lies between these two extremes, i.e., a nonlinear, analytical model.

Finally, after a suitable model(s) of the F-100-like jet engine is obtained, a time-optimal control can be calculated. This control will be determined subject to various constraints. It will be derived using Dynamic Programming and the Successive Approximations technique.

CHAPTER II

TWO SPOOL TURBOFAN JET ENGINE MODELS

2.1 Introduction

In this chapter, a hierarchy of models for a two spool turbofan jet engine is discussed. The configuration for this engine has been specified by NASA Lewis Research Center personnel. A preliminary version of this work is given in reference [1] and has also been reported in [2]. The models have been classified as follows:

Model 0. The actual jet engine (hypothetical).

Model 1. The DYNGEN [3] simulation program, coded with data presumed to have been taken from experimental measurements on Model 0. This model solves 16 nonlinear differential equations and uses data maps and thermodynamic tables which cannot be expressed analytically.

Model 2. This model involves the primary thrust of this chapter, and is a 5th order nonlinear analytical model. It includes the 5 state differential equations which govern the dynamic behavior of the system, along with 20 algebraic equations which express the relationship between various engine variables.

In addition to these nonlinear models, several linear models have been developed. Their original purpose was to provide an indirect method to compare Models 1 and 2. Subsequently, they also became important in the determination of a time-optimal control for the jet engine, when comparisons showed marked differences between Models 1 and 2.

Model 1L5. This is a normalized 5th order linear model which is obtained numerically from Model 1, using the experimental DYGABCD [4] program of L. Geyser.

Model 1L3. This is a normalized 3rd order linear model obtained by means of an order reduction performed on Model 1L5.

Model 1L2. This is the corresponding 2nd order reduction of Model 1L3.

Model 2L5. This is a normalized 5th order linear model obtained by taking partial derivatives of the analytical Model 2.

Model 2L3. This is a normalized 3rd order linear model obtained by means of an order reduction performed on Model 2L5.

Model 2L2. This is the corresponding 2nd order reduction of Model 2L3.

2.2 Model 2 Development

There are several purposes for the development of Model 2. First, it enables one to readily see the basic nonlinear relationships between the engine variables. This allows one to gain insight into their static and dynamic behavior. Second, it is fundamental that an analytical model be available for the application of optimal control techniques. Finally, linear models obtained by partial differentiation of this model tend to have more structure (zero entries in the ABCD matrices) than those obtained numerically. This in turn gives the linear control designer more insight.

Model 2 was intended to be an approximation of Model 1, based on the specified engine configuration. Theoretical relationships developed in references [5], [6], and [7] were employed as a starting point and certain simplifications suggested in [8] were used. In various situations, least squares and exact fits were made to theoretical forms, and if a theoretical form was unavailable, polynomial, linear, and exponential forms were used, whatever seemed to best fit the situation.

In most cases, the variables used in Model 2 correspond to those of Model 1. A letter key provides consistency among the variable names in the following manner:

P a pressure

T a temperature

U a specific energy

V a volume

W a flow

Similarly, numbers in the variable names identify engine locations as per figure 2.1. Table 2.1 is a list of all variables used.

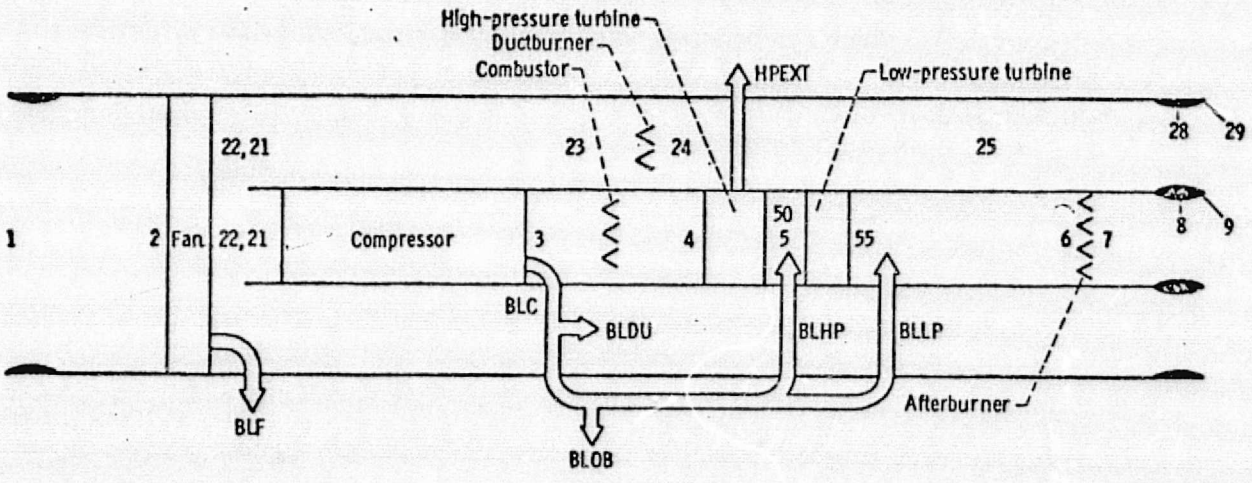

FIGURE 2.1. Jet Engine Diagram

Before delving into the details of the model, certain decisions had to be made regarding the choice of state variables and the order of the system. There is no general agreement as to what the order of a jet engine system is. It is a physical, not mathematical, entity and thus, every mathematical model is an approximation to the reality. Naturally, the higher the order of the model, the more accurate the approximation should be. The order that was selected (5th) was a function of the accuracy required by the control study to follow. This contrasts with the DYNGEN 16th order model, but is not an excessively low choice, for even first order models could yield reasonable results.

The most obvious states to choose are the rotor speeds, (1) N_C and (2) N_F. The other selections were (3) the burner pressure, P_4, a variable which is strongly affected by changes in fuel, WFB; (4) the burner internal energy, U_4, a variable which is related by a constant to the burner temperature; and (5) the afterburner pressure, P_7, a variable which is strongly affected by changes in the nozzle area, A_8.

Table 2.2 gives a listing of the inputs, states and outputs. In actual existing control systems, inputs (1) and (2) are used, along with movable guide vanes mounted throughout the compressor and fan stages. These vanes cause changes in the air flow in a manner similar to the bleeds used in the model.

Tables 2.3, 2.4, and 2.5 respectively are listings of the constants used in the model, the design values corresponding to the specified engine configuration, and the nonlinear state equations. Note that the state equations are formulated in terms of intermediate variables which have a very real physical interpretation.

Table 2.6 is a listing of these nonlinear relationships existing between the state variables and the intermediate variables. Some of

TABLE 2.1

SYMBOLS FOR VARIABLES

Symbol	Variable Description
A_8	nozzle area
CNC	corrected compressor rotor speed
CNF	corrected fan rotor speed
FG	thrust
N_C	compressor rotor speed
N_F	fan rotor speed
P_{CMAX}	compressor pressure ratio at surge
P_{FMAX}	fan pressure ratio at surge
P_{21}	fan exit (compressor inlet) pressure
P_3	compressor exit pressure
P_4	combustor exit pressure
P_7	afterburner exit pressure
T_{21}	fan exit (compressor inlet) temperature
T_3	compressor exit temperature
T_4	combustor exit temperature
T_{50}	high pressure turbine exit temperature
T_{55}	low pressure turbine exit temperature
T_7	afterburner exit temperature
U_4	combustor internal energy
WAC	compressor airflow rate
WAF	fan airflow rate
WA3	airflow rate into combustor
W_{CMAX}	maximum compressor airflow rate
ΔW_{CMAX}	correction term for maximum compressor airflow rate
WFB	fuel flow rate into combustor
W_{FMAX}	maximum fan airflow rate
WG4	gaseous flow rate out of combustor
WG50	gaseous flow rate out of high pressure turbine
WG55	gaseous flow rate out of low pressure turbine
WG7	gaseous flow rate out of afterburner
ZC	compressure surge margin
ZF	fan surge margin

TABLE 2.2

INPUT, STATE, AND OUTPUT VARIABLES

	Variable Description	Symbol
u_1	fuel flow	WFB
u_2	nozzle area	A_8
x_1	compressor rotor speed	N_C
x_2	fan rotor speed	N_F
x_3	burner exit pressure	P_4
x_4	afterburner exit pressure	P_7
x_5	high pressure turbine inlet energy	U_4
y_1	thrust	FG
y_2	high pressure turbine inlet temperature	T_4

TABLE 2.3

CONSTANTS

Symbol	Description	Value
J(AJ)	mechanical equivalent of heat	778.26
G	force of gravity	32.174049
R(RA)	gas constant	.0252
γ*	ratio of specific heats	1.4
P_2	fan inlet pressure	518.668
I_C(PMIHP)	high pressure rotor polar moment of inertia	3.8
I_F(PMILP)	low pressure rotor polar moment of inertia	4.5
V_{COMB}	combustor volume	1.65
V_{AFBN}	afterburner volume	49.77
CVMNOZ	nozzle thrust coefficient	.9494
N_CDESIGN (XNHPDS)	high pressure rotor design speed	10070
N_FDESIGN (XNLPDS)	low pressure rotor design speed	9651
N	combustor efficiency	20.71175
C_{PC}	compressor specific pressure	.24
C_{PF}	fan specific pressure	.24
C_{VB}	combustor specific volume	.20279
C_{PHT}	high pressure turbine specific pressure	.22589
C_{PLT}	low pressure turbine specific pressure	.27938
ϕ(PCBLC)	percent of compressor exit air bled for cooling	.16
α(PCBLDU)	percent of bleed air which leaks into fanduct	.208
β(PCBLHP)	percent of bleed air put into high pressure turbine	.726
γ(PCBLLP)	percent of bleed air put into low pressure turbine	.066

TABLE 2.4

DESIGN EQUILIBRIUM VALUES

Variable	Value	Variable	Value
WFB	2.75	PFMAX	3.3624
A_8	2.948255	WAF	221.573
N_C	11899.1	W_{CMAX}	54.4151
N_F	9873.95	ΔW_{CMAX}	1.5805
P_4	23.9299	P_{CMAX}	10.270
U_4	586.467	WAC	137.649
P_7	2.55142	WA3	115.625
CNF	1.02310	WG50	134.364
T_{21}	742.957	WG4	118.375
CNC	.98730	WG55	135.818
T_3	1467.47	T55	1789.15
T_4	2892.04	T_7	1413.81
T_{50}	2103.47	WG7	224.323
P_3	25.3522	FG	13431.02
P_{21}	2.9960	ZC	.8143
W_{FMAX}	203.123	ZF	.8333

TABLE 2.5

STATE EQUATIONS

State #	State Equation
(1)	$\frac{dN_C}{dt} = \left(\frac{30}{\pi}\right)^2 \frac{J}{I_C N_C} [C_{PC} WAC(T_{21} - T_3) + C_{PHT} WG50(T_4 - T_{50})]$
(2)	$\frac{dN_F}{dt} = \left(\frac{30}{\pi}\right)^2 \frac{J}{I_F N_F} [C_{PF} WAF(T_2 - T_{21}) + C_{PLT} WG55(T_{50} - T_{55})]$
(3)	$\frac{dP_4}{dt} = \frac{R\gamma^*}{V_{COMB}} [T_4 WA3 + WFB - WG4]$
(4)	$\frac{dP_7}{dt} = \frac{R\gamma^* T_7}{V_{AFBN}} [WG4 - WFB - WA3]$
(5)	$\frac{dU_4}{dt} = \frac{C_{VB} R T_4}{V_{COMB} P_4} [T_4\{WG4 - WFB - WA3\} + \gamma^*\{T_3 WA3 - T_4 WG4 + T_4(1+\eta)WFB\}]$

TABLE 2.6a

FUNCTIONAL RELATIONSHIPS BETWEEN VARIABLES

Eq. #	Equation
(1)	$CNF = \frac{N_F}{N_F DESIGN} = \frac{N_F}{9651}$
(2)	$T_{21} = T_2 + 214.2732\ CNF^2 - 48(A_8 - 2.948255)$
(3)	$CNC = \frac{N_C}{N_C DESIGN\ \sqrt{T_{21}/T_2}} = \frac{N_C}{10070\ \sqrt{T_{21}/518.668}}$
(4)	$T_3 = T_{21} + 743.2722\ CNC^2 - 68(A_8 - 2.948255)$
(5)	$T_4 = U_4/C_{VB}$
(6)	$T_{5U} = .727\ T_4$
(7)	$P_3 = 1.05944\ P_4$
(8)	$P_{21} = -6.20568 + .0129774\ T_{21} - .0185376\ P_3$
(9)	$W_{FMAX} = 261.01\ CNF - 63.196$
(10)	$P_{FMAX} = 3.516739\ CNF - .23561$
(11)	$WAF = W_{FMAX} + 28.502\ \ 1 - e^{-2.313268(P_{FMAX}-P_{21})}$
(12)	$W_{CMAX} = 137.54 - 457.987\ CNC + 564.325\ CNC^2 - 188.113\ CNC^3$
(13)	$\Delta W_{CMAX} = 6.492 - 4.9749\ CNC$
(14)	$P_{CMAX} = 26.43184 - 89.0484\ CNC + 109.7243\ CNC^2 - 36.5756\ CNC^3$
(15)	$WAC = \frac{P_{21}}{\sqrt{T_{21}/518.668}}\ \ W_{CMAX} + \Delta W_{CMAX}(1 - 3^{-.3662(P_{CMAX} - \frac{P_3}{P_{21}})}$

TABLE 2.6b

FUNCTIONAL RELATIONSHIPS BETWEEN VARIABLES

Eq. #	Equation
(16)	$WA3 = (1 - \phi)WAC = .84\ WAC$
(17)	$WG50 = 301.957\ P4/\sqrt{T_4}$
(18)	$WG4 = WG50 - \beta\phi WAC = WG50 - .11616\ WAC$
(19)	$WG55 = WG\ 50 + \gamma\phi WAC = WG50 + .01056\ WAC$
(20)	$T_{55} = 106.002 - .86154\ T_{50} - .10458\ CNC\sqrt{T_{21}T_{50}}$
(21)	$T_7 = .49661\ T_{55} + 205.886\ P_7$
(22)	$WG7 = \dfrac{1121.786\ P_7 A_8}{\sqrt{T_7}}$
(23)	$FG = .02951\ WG7\sqrt{1934.415\ T_7 + 68558.365} + 2116.217\ A_8(.53978\ P_7 - 1)$
(24)	$ZC = \dfrac{(P_3/P_{21}) - 1}{P_{CMAX} - 1}$
(25)	$ZF = \dfrac{P_{21} - 1}{P_{FMAX} - 1}$

these can be readily observed in a DYNGEN listing, while others are far more obscure. Equations (9) through (15) are approximations to the fan and compressor block data maps.

2.3 Linearization and Order Reductions of Model 2

Model 2L5 was obtained through a very tedious and time-consuming hand-calculated linearization. The partial derivative of each state equation and nonlinear function was calculated, and then combined together to form a linear model. This linear model was then normalized as follows.

Let A be n x n and let B be n x m. Then each state derivative may be written

$$\dot{x}_i = \sum_{j=1}^{n} a_{ij} x_j + \sum_{j=1}^{m} b_{ij} u_j \qquad (2.3\text{-}1)$$

Let the values of x at the design point be denoted $\hat{x}$, and denote the normalized state variable as $\bar{x}$:

$$\bar{x}_i = \frac{x_i}{\hat{x}_i} \qquad (2.3\text{-}2)$$

Similarly for the controls:

$$\bar{u}_i = \frac{u_i}{\hat{u}_i} \qquad (2.3\text{-}3)$$

Combine (2.3-2) and (2.3-3) with (2.3-1),

$$(\bar{x}_i \dot{\hat{x}}_i) = \sum_{j=1}^{n} a_{ij} \bar{x}_j \hat{x}_j + \sum_{j=1}^{m} b_{ij} \bar{u}_j \hat{u}_j \qquad (2.3\text{-}4)$$

and simplify, resulting in

$$\dot{\bar{x}}_i = \sum_{j=1}^{n} \left(a_{ij} \frac{\hat{x}_j}{\hat{x}_i}\right) \bar{x}_j + \sum_{j=1}^{m} \left(b_{ij} \frac{\hat{u}_j}{\hat{x}_i}\right) u_j \qquad (2.3\text{-}5)$$

Thus, elements of the normalized matrices are obtained by

$$\bar{a}_{ij} = a_{ij} \frac{\hat{x}_j}{\hat{x}_i} \qquad (2.3\text{-}6)$$

and

$$\bar{b}_{ij} = b_{ij} \frac{\hat{u}_j}{\hat{x}_i} \qquad (2.3\text{-}7)$$

The normalized linear Model 2L5 is given in Table 2.7. The eigenvalues of Model 2L5 are (1)(2) $-7.2264 \pm 1.3913j$, (4) -73.554, (5) -153.27, and (3) -343.11. The numbered eigenvalues can be associated with the state of like number, as they bear a loose resemblance with the diagonal terms. Note that all eigenvalues are negative, and the model is clearly stable.

It seems quite reasonable that lower order models would be almost as accurate, suggested by the clear difference in the magnitudes of the eigenvalues. They will also be much easier to use to perform Dynamic Programming studies, saving much storage space and c.p.u. time. As mentioned above, the eigenvalues show that the states which will be eliminated as the order is decreased, are $P_4(3)$, then $U_4(5)$, then $P_7(4)$.

The method used to perform the order reduction is to first rearrange the states into partitions of "states to keep", X1, and "states to eliminate", X2.

$$\begin{bmatrix} \dot{X1} \\ X2 \end{bmatrix} = \begin{bmatrix} A_{11} & A_{12} \\ A_{21} & A_{22} \end{bmatrix} \begin{bmatrix} X_1 \\ X_2 \end{bmatrix} + \begin{bmatrix} B_1 \\ B_2 \end{bmatrix} \underline{u} \qquad (2.3\text{-}8)$$

Now set the derivative of X_2 equal to zero, since their dynamic behavior is to be eliminated. Thus,

$$A_{21}\, X_1 + A_{22}\, X_2 + B_2\, \underline{u} = 0 \qquad (2.3\text{-}9)$$

Solving for X_2,

$$X_2 = -A_{22}^{-1}\{A_{21}\, X_1 - B_2\, \underline{u}\} \qquad (2.3\text{-}10)$$

X_2 is now replaced in equation (2.3-8) by its expression in (2.3-10), yielding

$$\dot{X}_1 = (A_{11} - A_{12}\, A_{22}^{-1} A_{21})\; X_1 + (B_1 - A_{12}\, A_{22}^{-1} B_2)\underline{u} \qquad (2.3\text{-}11)$$

Application of this method yields Models 2L3 and 2L2 per Tables 2.8 and 2.9 respectively. Note that the most important eigenvalues have not changed significantly in the model reductions.

2.4 Linearizations and Order Reductions of Model 1

As previously mentioned, linear models obtained from Model 1 will be useful in comparing with those obtained from Model 2. In addition, it should yield a good model of the DYNGEN simulator in the area of the design point.

The general method for obtaining numerical linearizations of Model 1 is outlined in reference [10], including all the necessary program inputs. Additional insight into the selection of states for low order models is provided by DYGABCD. This stems from the identification technique used in DYGABCD, which is to perturb the inputs and states one at a time, and then measure the changes in each state derivative. A loose hierarchy of states in terms of their importance in the model is obtained by measuring how much each state perturbation affects the fan speed (which is certainly one of the most important states). A close resemblance with the choice of states for Model 2 occurs.

TABLE 2.7

MODEL 2L5

Matrix	Matrix Elements					Eigenvalues
A	-12.549	-1.6928	3.584	.23786	1.7011	-343.11
	.83305	-5.6135	1.645	.14381	1.304	-153.27
	671.66	387.71	-392.67	-26.16	160.53	-73.554
	-104.15	21.135	64.925	-67.803	2.6314	-7.2264 ± 1.3913j
	50.953	-55.855	-81.205	-7.4745	-105.74	
B	=	0	1.4078			
		0	.75817			
		1.2813	-122.31			
		0	-48.928			
		149.21	-3.092			
C	0	0	0	1.461	0	
	0	0	0	0	1	
D		0	1.2138			
		0	0			

TABLE 2.8

MODEL 2L3

Matrix	Matrix Elements			Eigenvalues
A	-8.4226	-1.2541	-.047955	-72.576
	2.3957	-5.9244	.0048531	-7.1663 ± 1.2441j
	-11.566	56.677	-72.562	
B		3.406	.79722	
		2.1241	.56161	
		31.486	-64.49	
C	0	0	1.461	
	-.63298	-.97907	-.01486	
D		0	1.2138	
		1.072	.1598	

TABLE 2.9

MODEL 2L2

Matrix	Matrix Elements	Eigenvalues
A	-8.415 -1.2916 2.3949 -5.9206	-7.1678 ± 1.2401j
B	3.3852 .83984 2.1262 .5573	
C	-.23288 1.1412 -.63061 -.99068	
D	.63396 -.084644 1.0656 .17301	

TABLE 2.10

MODEL 1L5

Matrix	Matrix Elements					Eigenvalues
A	-3.8	-1.277	2.067	-1.152	1.448	-251.51 ± 23.147j
	2.748	-5.39	1.585	-1.991	1.071	-96.366
	377.9	49.51	-264.9	86.807	78.91	-5.0491 ± .83858j
	31.26	139.39	-6.269	-88.69	27.83	
	-176.5	23.91	-10.27	-37.4	-246.7	
B		-.00259	.3553			
		.2116	-.31618			
		12.54	-13.774			
		-.6201	-99.3			
		157.78	6.84			
C	-.8594	-.1397	.6672	1.167	-.1236	
	.055591	.00656	-.001837	.01354	.85391	
D		-.10277	.90094			
		-.013839	.020856			

TABLE 2.11

MODEL 1L3

Matrix	Matrix Elements	Eigenvalues
A	-2.4307 -.70897 -.81149 3.8281 -4.9579 -1.7235 2.4466 140.5 -94.982	-92.242 -5.0644 ± .86196j
B	1.395 .30875 1.2585 -.35303 15.434 -98.208	
C	.034897 -.0083832 1.3734 -.60014 .081353 -.12635	
D	-.023854 .86846 .52351 .046147	

TABLE 2.12

MODEL 1L2

Matrix	Matrix Elements	Eigenvalues
A	-2.4516 -1.91 3.7857 -7.5073	-4.9795 ± .91478j
B	1.2631 1.1483 .97844 1.429	
C	.070274 2.0232 -.60339 -.10555	
D	.19932 -.55158 .50298 .17879	

Table 2.10 details the results for Model 1L5 after normalization. Inspection shows that Models 1L5 and 2L5 do not closely match on an element-by-element basis, although there is not great disparity between the eigenvalues of the two models.

Order reductions of Model 1L5 were performed by the same method detailed in section 2.3, rather than direct use of DYGABCD. It was felt that Model 1L5 was a reasonable approximation to the DYNGEN simulator at the design point, and it was desired not to rely heavily on an experimental program. Tables 2.11 and 2.12 list Models 1L3 and 1L2 respectively. Again, the eigenvalues do not change appreciably after the order reduction.

2.5 Comparison of Model Responses

Concurrent with the development of Model 2 was the development of a computer program describing Model 2 (see Appendix). It employs an Euler integration and was used with a time step (DT) of .001, very suitable in light of the values of the eigenvalues of the linear models. DYNGEN was run with time steps of .01 and higher, for it employs a modified Euler technique [3] which allows larger increments to be used. In addition, the linear models were tested on program ABCD (see Appendix), with a Runga-Kutta integration. Figures 2.2, 2.3, and 2.4 show various time responses of Models 1 and 2. Unfortunately, the responses shown are the closest Models 1 and 2 came towards agreement. The linear responses are evidence that the linearization and order reductions were correctly calculated.

Comparisons of the various linear models are given in figures 2.5, 2.6, 2.7, and 2.8. There seems to be better agreement between models for the frequency responses involving the high pressure turbine inlet temperature (T_4).

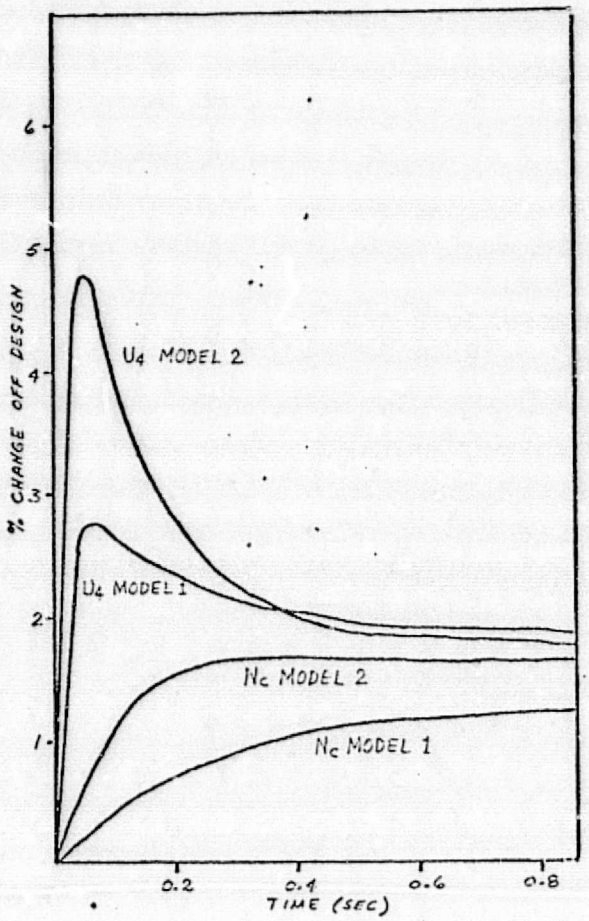

FIGURE 2.2. State Time Responses - Fuel Input

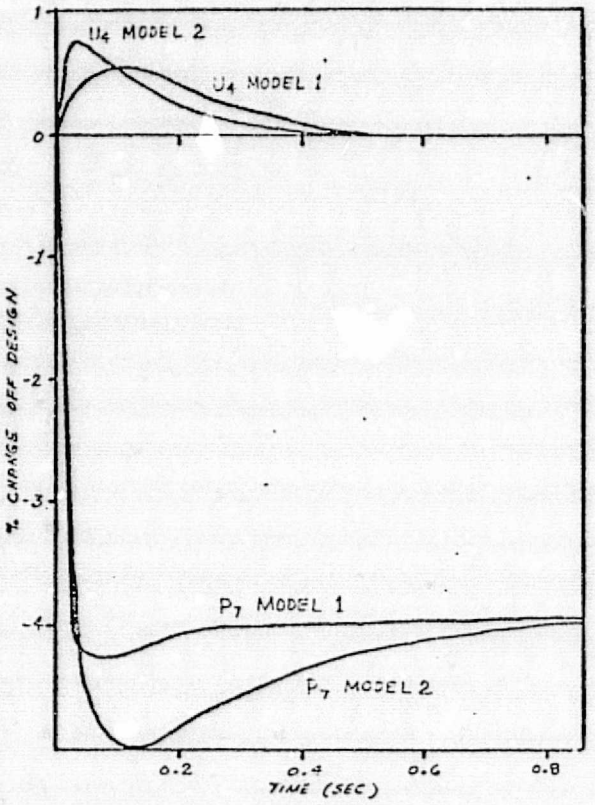

FIGURE 2.3. State Time Responses - Nozzle Input

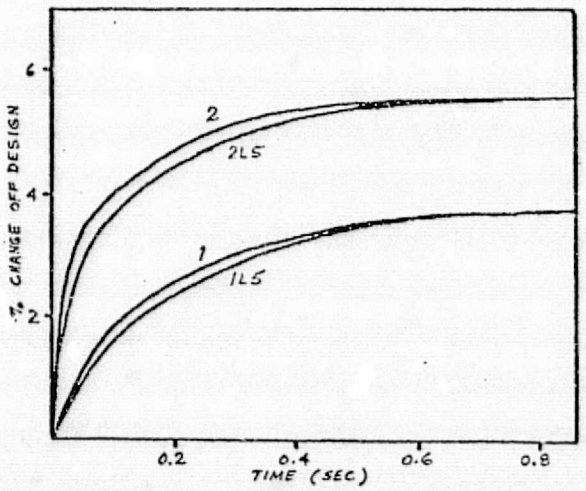

FIGURE 2.4. Thrust Time Response - Fuel Input

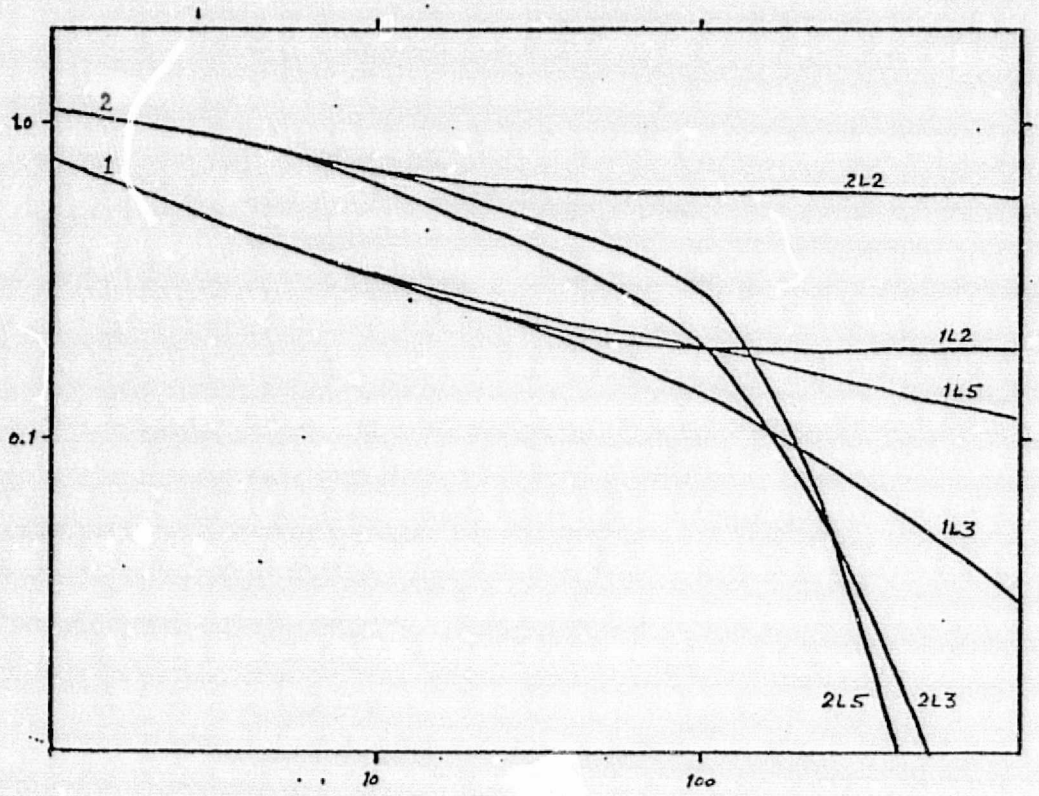

FIGURE 2.5. Magnitude Frequency Response - WFB to FG

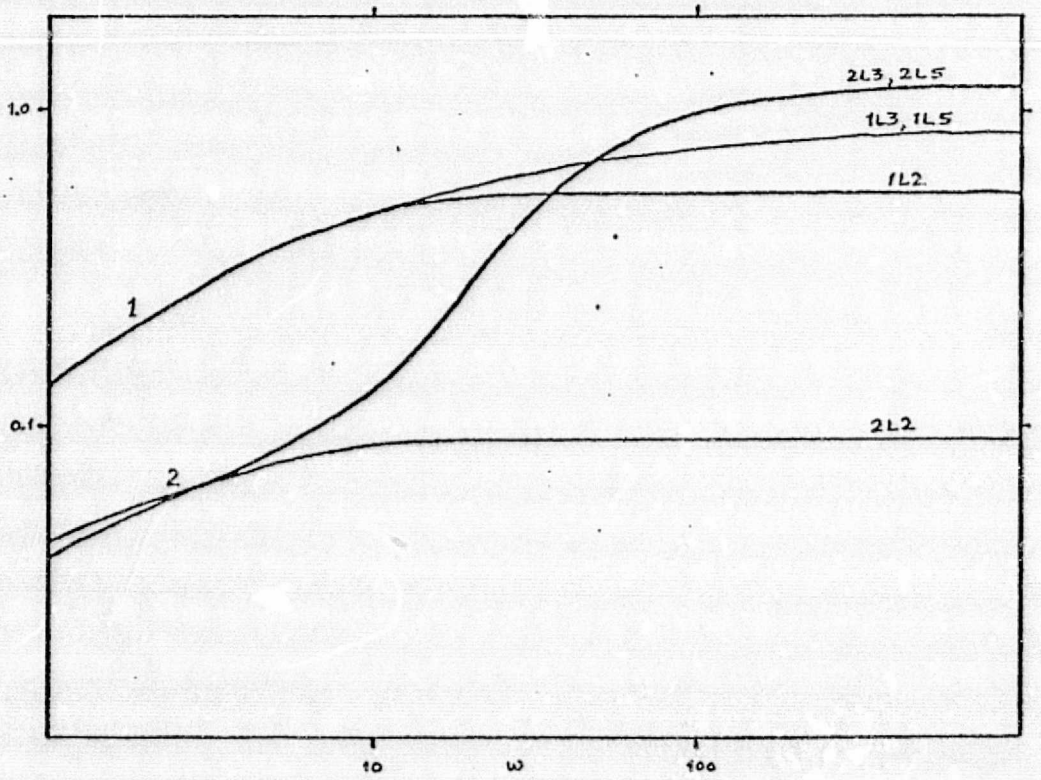

FIGURE 2.6. Magnitude Frequency Response - Ag to FG

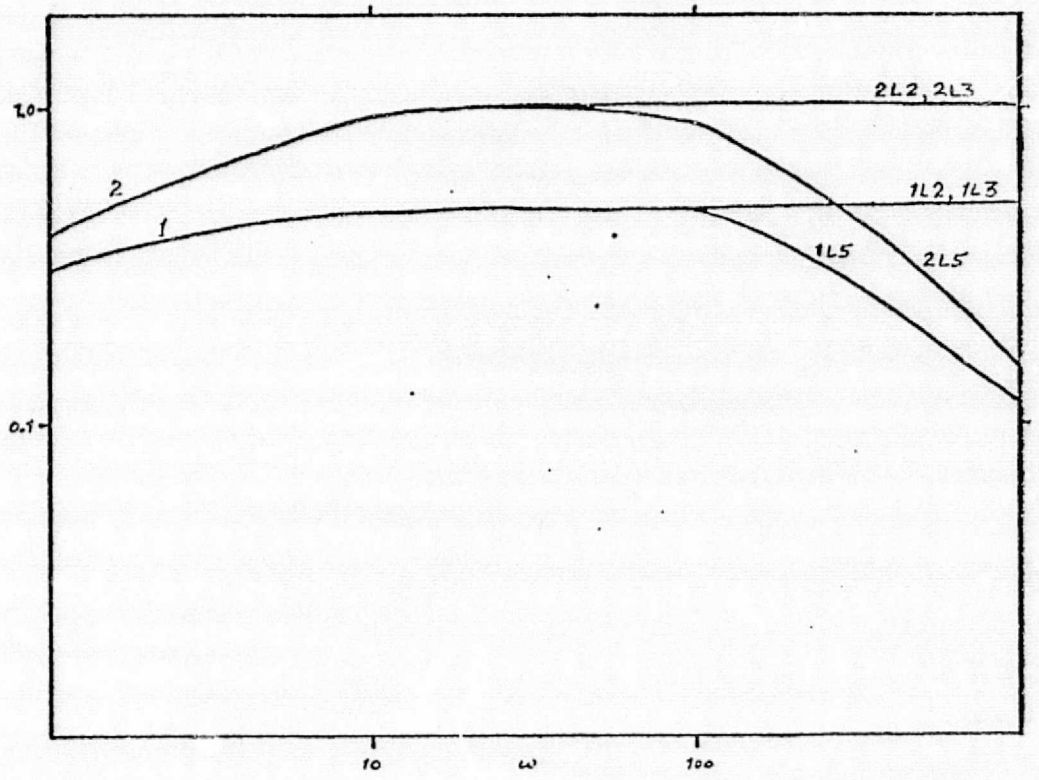

FIGURE 2.7. Magnitude Frequency Response - WFB to T_4

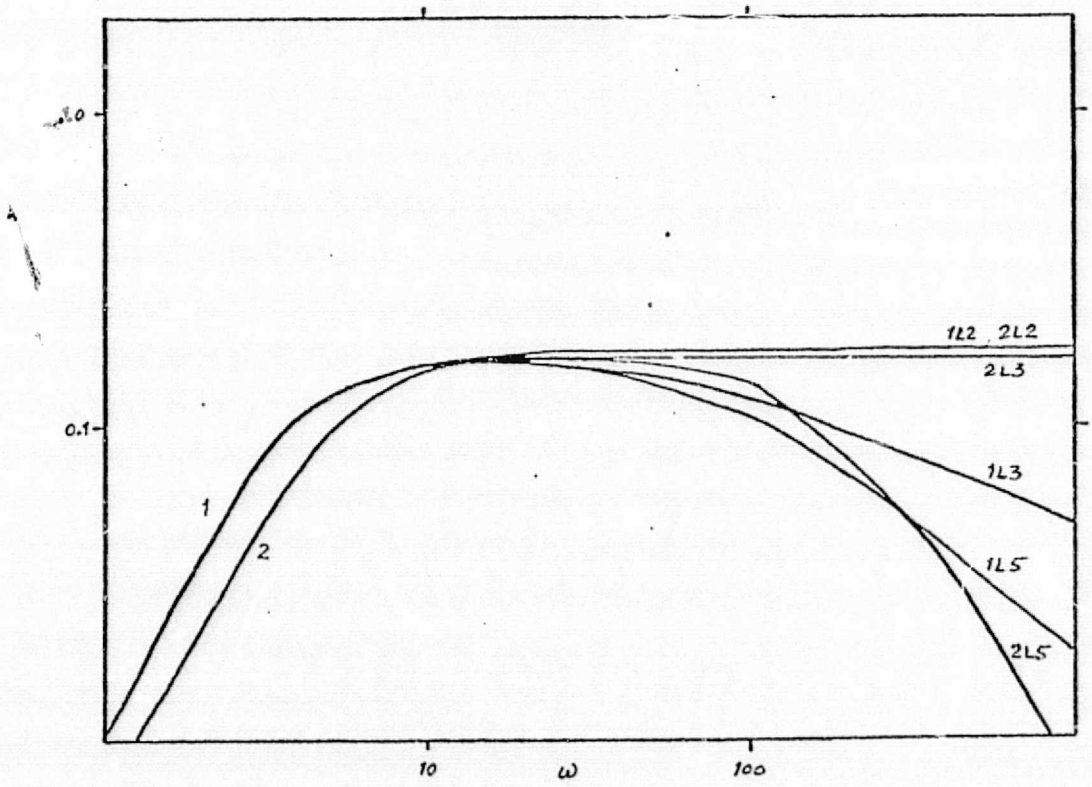

FIGURE 2.8. Magnitude Frequency Response - A_8 to T_4

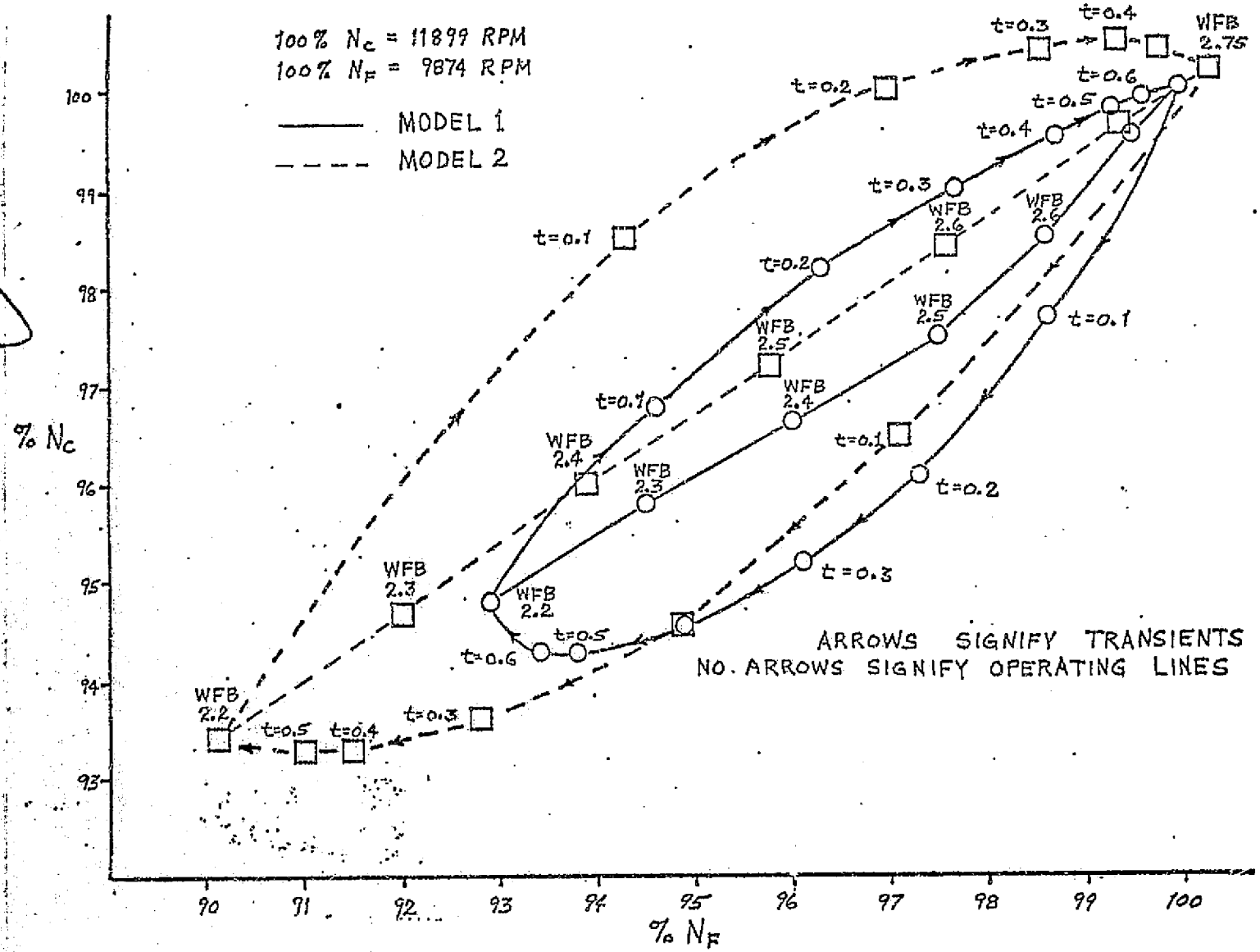

FIGURE 2.9. State Space Trajectories - Model 1 vs. Model 2

Figure 2.9 is yet another comparison of Models 1 and 2. It shows the steady state equilibriums of both models as fuel is varied. It is not surprising that a change in fuel in Model 2 produces a corresponding change in steady state which is greater than Model 1 would produce. This follows since Model 2L2 is known to have higher eigenvalues than Model 1L2. Also shown are transients for step inputs between a low thrust point and a high thrust point (the design point).

CHAPTER III

THE TIME OPTIMAL CONTROL PROBLEM

3.1 Introduction

In light of the disagreements between models found in Chapter II, no single model will be relied upon to determine a time optimal control law for the jet engine. The control problem is to determine a controller which will drive a model from a low thrust equilibrium to the design point, in minimum time, and subject to certain constraints, as yet undetermined. In addition, it is desired that the controller be determined by feedback control law, for the usual reasons: reduced sensitivity to plant variations; control over system stability; and regarding programming aspects, the ease at which a global solution can be obtained.

3.2 Statement of the Problem

The necessary first step is to reformulate the models as discrete time systems. Let

$$x(t + \Delta t) = x(t) + \Delta t \cdot f(x(t), u(t)) \tag{3.2-1}$$

represent the system with starting time k and terminal time N. It is understood that

$$f(x(t), u(t)) = Ax(t) + B\,u(t) . \tag{3.2-2}$$

for linear models. Let x(k) be the starting state and let the terminal time N be defined as the first instant at which the system state reaches the designated target set S. All x(t) are εX, the state set. The performance index

$$J(x,\underline{u}) = \sum_{t=k}^{N-\Delta t} \Delta t \tag{3.2-3}$$

$$t = k,\ k + \Delta t, \ldots,\ N-\Delta t$$

is to be minimized with $u(t) \varepsilon U$, the control set, and $\underline{u}$ defined as the control sequence.

$$\underline{u} = u(k),\ u(k + \Delta t), \ldots u(N-\Delta t) \tag{3.2-4}$$

Furthermore, the minimization is subject to hard constraints of the form

$$g_i\ (x(t),\ u(t)) \leq c_i \tag{3.2-5}$$

3.3 Constraint Determination

The final step in a complete formulation of the control problem lies in the determination of the g_i and c_i of equation (3.2-5). There is a strong intuitive need for such constraints, for the physical jet engine has very real performance limitations. Brennan and Leake [8] have chosen turbine inlet temperature and surge margin as constraint variables in their studies of the drone engine, and similar constraints have been chosen for this study: (1) high pressure turbine inlet temperature (T4); (2) compressor surge margin (Z_c); and (3) fan surge margin (Z_F). The surge margin of a compressor or fan is defined as

$$Z = \frac{(P_{out}/P_{in}) - 1}{P_{max} - 1} \tag{3.3-1}$$

If either the surge margin or the turbine temperature is too high, the constraints will be violated. By definition, let

$$T_4 = g_1\ (x(t),\ u(t)) \tag{3.3-2}$$

$$Z_c = g_2\ (x(t),\ u(t)) \tag{3.3-3}$$

$$Z_F = g_3\ (x(t),\ u(t)) \tag{3.3-4}$$

The next step is to determine g_i for each model.

Model 2 presents no difficulty whatsoever since all three constraint variables are defined in the Chapter II development. It will be an easy matter to incorporate these equations into subsequent control tests.

The constraints are harder to determine for the linear models, and a starting point is needed. Control studies by Basso and Leake [12] have used constraints which were strictly functions of the states. However, such is not the case here. Simulations of both Models 1 and 2 show T_4 and Z_c to have very little steady state change over a wide range of state space, yet step inputs elicit strong overshoots from both variables. Clearly the constraints must be functions of both the states and the inputs.

Once again, DYGABCD was used to obtain linear expressions for the constraint variables. An order reduction was performed (per Chapter II) yielding the g_i for Model 1L2:

$$T_4 = -.61059\, x_1 - .10759\, x_2 + .50292\, u_1 + .17689\, u_2 \quad (3.3\text{-}5)$$

$$Z_c = -.20154\, x_1 - .45813\, x_2 + .20423\, u_1 + .14724\, u_2 \quad (3.3\text{-}6)$$

$$Z_F = -.58229\, x_1 + .46872\, x_2 + .18877\, u_1 - .92545\, u_2 \quad (3.3\text{-}7)$$

Constraint functions were not determined for the other linear models, since Dynamic Programming solutions (see Chapter V) subject to constraints were only obtained using Model 1L2 and Model 2.

The final task remaining is to determine reasonable values for c_i of the constraint equations. These c_1 will play a fundamental role in the optimal control solutions of Chapter V, for they are hard constraints which will often affect the control chosen. After studying results of DYNGEN simulations, it was decided to use the following values:

$$c_1 = .150 \quad (3.3\text{-}8)$$

$$c_2 = .105 \quad (3.3\text{-}9)$$

$$c_3 = .080 \quad (3.3\text{-}10)$$

CHAPTER IV

THE DYNAMIC PROGRAMMING METHOD

4.1 Introduction

It has been pointed out in Chapter III that a feedback control law is desired, rather than an open loop control. Furthermore, the Dynamic Programming method has been extensively used in such situations to obtain numerical solutions. One of the more recent examples of its application is found in reference [12], where Basso and Leake have successfully obtained a feedback control law for a single spool turbojet engine. Use of Dynamic Programming methods to solve time optimal problems was shown to involve a successive approximations technique.

4.2 Dynamic Programming Theory

The basic applications of the Dynamic Programming method are fixed time, free right end problems. Let

$$x(t + \Delta t) = x(t) + f(x(t), u(t)) \qquad (4.2\text{-}1)$$
$$\text{with } u(t) \in U$$

The starting time k is known, and the terminal time N is known. The target set is any $x(N) \in X$. The object is to find

$$V_k(x) = \min J_k(x,\underline{u}) \qquad (4.2\text{-}2)$$

for a given initial state x, where

$$J_k(x,\underline{u}) = K(x(N)) + \sum_{t=k}^{N-\Delta t} L(x(t),u(t)\ t) \qquad (4.2\text{-}3)$$

Rewriting:

$$J_k(x,\underline{u}) = K(x(N)) + L(x,u(k),k) + \sum_{t=k+\Delta t}^{N-\Delta t} L(x(t),u(t),t) \qquad (4.2\text{-}4)$$

$$J_k(x,\underline{u}) = L(x,u(k),k) + J_{k+\Delta t}(x(k+\Delta t),\underline{u}) \qquad (4.2\text{-}5)$$

The Principle of Optimality states that in order for the entire state trajectory to be optimal from k to N, it has to be optimal from $k + \Delta t$ to N. Thus, equation (4.2-4) can be reformulated as

$$J_k(x,\underline{u}) = L(x,u(k),k) + V_{k + \Delta t}(x(k + \Delta t)) \tag{4.2-6}$$

which leads to

$$V_k(x) = \min_{u(k)} \{L(x,u(k),k) + V_{k + \Delta t}(x(k + \Delta t))\} \tag{4.2-7}$$

Since the minimization really only concerns $u(k)$, ($u(k + \Delta t)$ .... $u(N - \Delta t)$ are previously determined), $u(k)$ can be defined as u, and Bellman's Equation results:

$$V_k(x) = \min_{u} \{L(x,u,k) + V_{k + \Delta t}(x + f(x,u))\} \tag{4.2-8}$$

The boundary condition is

$$V_N(x) = K(x(N)) \tag{4.2-9}$$

These equations are necessary and sufficient for optimality.

4.3 Successive Approximations Technique

The task is to fit the time optimal problem (i.e., free time, fixed right end), into a form which can utilize the basic Dynamic Programming method. This was developed by Leake, Liu, and Richardson in references [13] and [14], and later applied by Basso and Leake in [12].

As per [12], let $V_k^n(x)$ be any function such that $V_k^n(x) \geq V_k(x)$ and let $v^n(x,k)$ be a control law which results when performing the minimization.

$$\min_{u \in U} [L(x,u,k) + V_{k + \Delta t}^n(x + f(x,u))] \quad (x,k) \notin S \tag{4.3-1}$$

It is shown in [14] that if $V_k^{n+1}(x)$ is the performance index resulting from $V^n(x,k)$, then

$$V_k(x) \leq V_k^{n+1}(x) \leq V_k^n(x) \tag{4.3-2}$$

and further that $V_k^n(x)$ converges monotonically to $V_k(x)$ in a finite number of steps, although each (x,k) may require a different number of steps. Thus, it is concluded in [12] that

$$V_k^{n+1}(x) = \min_{u \in U} [L(x,u,k) + V_k^n(x + f(x,u))] \qquad (x,k) \notin S \tag{4.3-3}$$

which very closely parallels Bellman's Equation. The only difference is that in the solution of the fixed time, free right end problem, equation (4.2-8) is relating two performance indices for the same state, but separated by Δt in time; whereas, equation (4.3-3) is relating two performance indices for the same state, and the same time k, one being a better approximation than the other.

It now appears that the time optimal free time free right end problem can be successfully solved, using the existing Dynamic Programming method. Indeed this is true for all practical purposes; however, there is a slight discrepancy between the successive approximation theory and its application to Dynamic Programming. To be specific, it is a fallacy to conclude that equation (4.3-3) guarantees that (4.3-2) be true. By definition, V_k^{n+1} is the cost which results when applying $V^n(x,k)$, until the target set S is reached, which is not equation (4.3-3). For example, let

$$V_k^0(x) = V_{max} \qquad (x,k) \notin S \tag{4.3-4}$$

and

$$V_k^{\,o}(x) = 0. \qquad (x,k) \in S \tag{4.3-5}$$

Then, if x is sufficiently far away from S, it is quite possible that there exists no $v(x,k) \in U$ which will enable the equation

$$V_k^{\,o}(x + f(x,u)) = 0 \tag{4.3-6}$$

to be true, i.e., the control could not cause the system to reach the target set in a time of Δt. Since equation (4.3-4) is true for all $(x,k) \in S$, then

$$V_k^{\,1}(x) = \min_{u \in U} [L(x,u,k)] + V_k^{\,o}(x) \tag{4.3.7}$$

and equation (4.3-2) is no longer valid. In practical situations, however, the method used in [12] and also used in Chapter V of this study, using equation (4.3-3), will still converge.

A further simplification can be made when the control problem is time-independent, which is the case in this study (see section 3.2). Equation (4.3-3) simplifies to

$$V^{n+1}(x) = \min_{u \in U} [L(x,u) + V^n(x + f(x,u))] \qquad (x,k) \in S \tag{4.3-8}$$

4.4 Technique Refinements

One way of assuring that equation (4.3-2) will always be true is to replace (4.3-8) with

$$V^{n+1}(x) = \min \begin{cases} V^n(x) \\ \min\limits_{u \in U} [L(x,u) + V^n(x + f(x,u))] \end{cases} \tag{4.3-9}$$

Rewriting this in terms of the problem as described in Chapter III,

$$V^{n+1}(x) = \min \begin{cases} V^n(x) \\ \min\limits_{u \in U} [\Delta t + V^n(x + f(x,u))] \end{cases} \tag{4.3-10}$$

A successive approximation problem allows still another departure from the basic Dynamic Programming problem (fixed time, free right end). Let us examine how equation (4.2-8), describing a fixed time problem, would be implemented on a computer. $V_{N-\Delta t}(x)$ would be calculated for all $x \in X$, and stored; $V_{N-2\Delta t}(x)$ would be calculated and stored, and so forth. Therefore, each iteration has a specific time associated with it. However, in the successive approximations technique, either all approximations are concerned with the same time, or the problem is time independent. In Basso and Leake [12], $V^1(x)$ was calculated for all $x \in X$ and stored in an array. Then $V^2(x)$ was calculated, and after that had been completed for all $x \in X$, $V^2(x)$ replaced $V^1(x)$ in the array, and so forth. It would be more efficient to immediately change each $V^1(x)$ to the just-calculated $V^2(x)$ in a state-by-state manner. In reality then, the approximations for V changes much more rapidly, for one does not wait until the completion of the sweep through state space before using information derived during that sweep. In this manner, new information becomes available at a faster rate, speeding up the convergence to V(x).

Furthermore, if one starts the state space sweep at the target, and slowly moves away from the target, convergence will occur still faster. By starting near the target, one is testing controls for states which can probably reach the target in a time of the order of Δt. Since $V^o(x)$ for the target is equal to zero, while guesses for $V^o(x)$ at other states must be made safely higher than the unknown solution, it is a benefit to start at a point where the information is the best, letting the information propagate outward to other states. Figure 4.1 shows the logic for this state search. This logic requires the target to lie at the center of the state space.

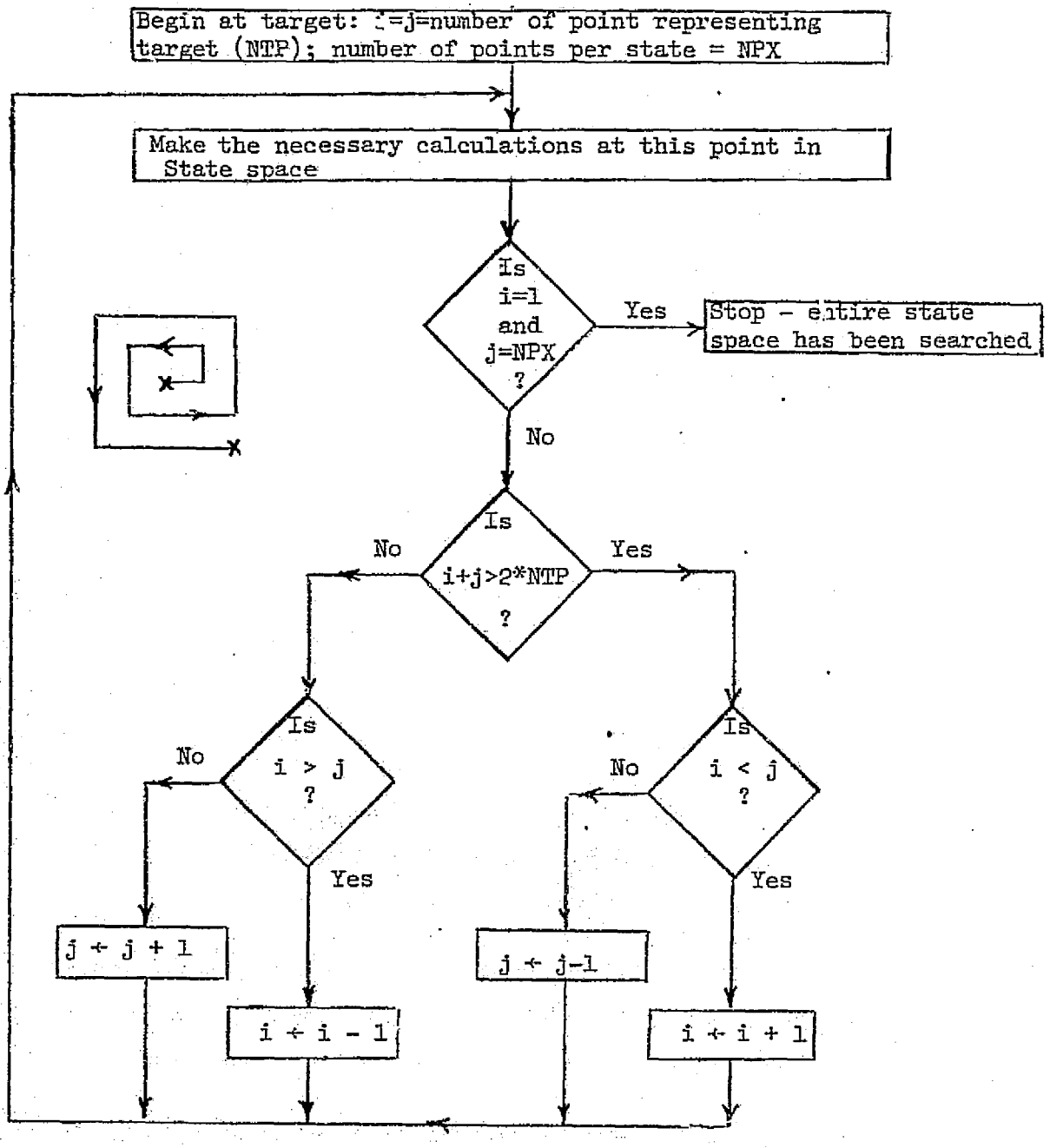

FIGURE 4.1. State Searching Algorithm

TABLE 4.1

A COMPARISON OF COSTS FOR "FAST UPDATE" SUCCESSIVE APPROXIMATIONS vs. THE "SLOW UPDATE" METHOD

($V(x)_{slow}$ is listed first for each state)

Iteration #6		X_1			
		0.85	0.95	1.05	1.15
X_2	1.15	0.5463 0.4680	0.3825 0.3530	0.2733 0.2513	0.2925 0.2678
	1.05	0.4024 0.3658	0.2222 0.2156	0.1378 0.1354	0.2674 0.2525
	0.95	0.3101 0.2890	0.1578 0.1519	0.2190 0.2126	0.3726 0.3410
	0.85	0.3477 0.3102	0.2968 0.2643	0.3920 0.3498	0.5184 0.4480

As proof of the numerical superiority of this "fast update" method, Table 4.1 compares Dynamic Programming results for $V^6(x)$, one obtained through regular "do loop" sweeps through state space, the other by the "fast update" method. Both started with the same $V^o(x)$. Note that the superscript on the cost function no longer refers to the approximation number, but serves as a record of how many sweeps through state space have been made. In the fast update of Table 4.1, there will have been $6p^2$ approximations made, where p is the number of discrete points for each state in this second order system. Of course, c.p.u. time is virtually identical for both programs.

Since the number of actual approximations in the fast update method is equal to the number of the sweep through state space times the number of points in state space, the finer the quantization, the more benefit is derived through use of the fast update method. An alternative explanation is that the old method (do loops) makes you wait even longer before obtaining new information, when you increase the quantization of the state space.

4.5 General Program Structure

One of the first considerations is c.p.u. time. This is a function of the number of points in control space and state space, as well as the time increment Δt which is used. (It should also be mentioned that this refers to c.p.u. time on an IBM 370/158 computer). In this study, individual programs were limited to 14 minutes, 59 seconds, to avoid additional job control language complications which occur for higher times. Thus, single Dynamic Programming solutions may be the result of several program runs. Near the end of the time limit, each job stores cost information on disk to be used by a subsequent job as a starting point,

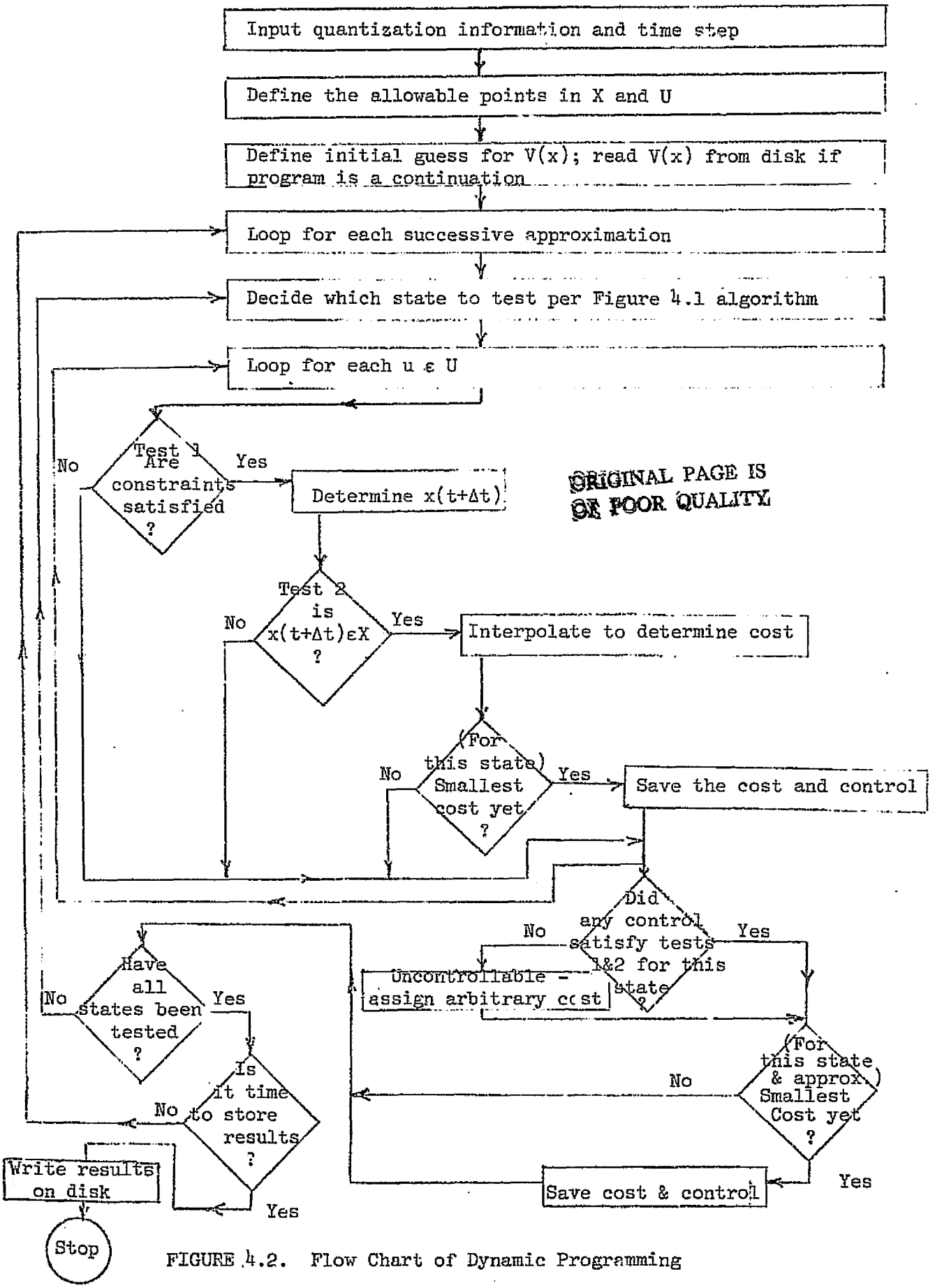

FIGURE 4.2. Flow Chart of Dynamic Programming

$V^o(x)$. In addition, control information is stored, so that the optimal feedback control law will be easily accessed by the simulators in Chapter VI.

Dynamic Programming is generally best-written in a somewhat ad hoc fashion. The number of subscripts in an array is dependent on the order of the system, and interpolation schemes will differ according to the dimension of state space. However, there still remains a basic structure to the program. Figure 4.2 shows a flow chart, while the actual program is contained in the Appendix. Note the absence of a "do loop" for searching the state space. Also, the target cost is set to zero and left there, never allowing interpolation errors due to quantization to occur. When controls are tested for possible violation of constraints, the values of the "present state" $x(t)$ are used. However, the "future state" $x(t + \Delta t)$ is used when testing whether or not a particular control takes the state outside of the state set X. The interpolation scheme is a standard method as used in reference [12] for two dimensions, and is analogously extended for third order models (Model 2L3 in particular).

CHAPTER V

OPTIMAL CONTROL LAWS

5.1 Basic Problem Considerations

In order to compare control studies of the linear models of Chapter II with studies of the nonlinear Model 2, linear affine models must be formulated. If the linear description of the system is

$$\dot{x} = Ax + Bu \tag{5.1-1}$$

and the equilibrium values at the target are designated as $\hat{x}$ and $\hat{u}$, then the linear affine system is

$$\dot{x} = (\dot{x} - \hat{x}) = A(x - \hat{x}) + B(u - \hat{u}) \tag{5.1-2}$$

Similarly the constraint variables become

$$(y - \hat{y}) = C(x - \hat{x}) + D(u - \hat{u}) \tag{5.1-3}$$

where $\hat{y}$ is the equilibrium of the constraint variable. Since all the linear models found in Chapter II were normalized, $\hat{x} = \hat{u} = \hat{y} = 1$.

The time increment Δt (henceforth known as DT) for the linear models was selected based on the eigenvalues of each system. In all cases, DT = .01 seemed to be an acceptable choice, and convergence of the approximations did occur with this value.

Quantization of the control and state spaces must be considered next. In general, one would like as fine a quantization as possible, but practical limitations on the cpu time will dictate a compromise. It is desirable that the quantization of the state space be small enough such that the program does not rely too heavily on interpolation. However, if the state quantization becomes too small, DT must also be decreased. In other words, the amount by which a state can change in a time step DT will also have a bearing on the state quantization. For

example, at a point in state space near the target, it is possible that the true optimal cost V(x) could be less than DT, if the state quantization is too fine.

The presence of constraints is important, for one desires small enough quantization to ascertain when the constraints are affecting the choice of control. If quantization is coarse, it may be much harder to recognize that a control is riding a constraint.

A big factor in an optimal control solution is the definition of the control set U, not only as regards the quantization, but also the maximum and minimum values. These, of course, are chosen to reflect a true physical situation, and as such, it is expected that they influence the resultant control law. In these studies, the controls were limited such that

$$0.5 \leq \text{WFB} \leq 1.4 \tag{5.1-4}$$

$$0.7 \leq \text{A8} \leq 1.2 \tag{5.1-5}$$

Again, these are normalized values. The state set, X, does not affect the solution for the states of interest, as long as these states are sufficiently far from the boundaries of X.

5.2 Model 2L3 Unconstrained

The basic choice of $V^o(x)$ for all models was

$$V^o(x) = \min \begin{cases} V_{max} = .70 \\ c_1(x_1 - 1)^2 + c_2(x_2 - 1)^2 + c_3 \end{cases}$$

with the c_i chosen such that $V^o(x) \geq V(x)$. Whether or not this condition was satisfied was easily recognized by the success or failure of the $V^n(x)$ to converge to a solution.

		N_C												
		0.90	0.92	0.94	0.96	0.98	1.00	1.02	1.04	1.06	1.08	1.10		
		*	*	*	*	*	*	*	*	*	*	*		
	1.10	*	0.50	0.50	0.50	0.50	0.50	0.50	0.50	0.50	0.50	0.50	0.50	* 1.10
	1.08	*	0.50	0.50	0.50	0.50	0.50	0.50	0.50	0.50	0.50	0.50	0.50	* 1.08
	1.06	*	0.50	0.50	0.50	0.50	0.50	0.50	0.50	0.50	0.50	0.50	0.50	* 1.06
	1.04	*	0.50	0.50	0.50	0.50	0.50	0.50	0.50	0.50	0.50	0.50	0.50	* 1.04
	1.02	*	0.50	0.50	0.50	0.60	0.60	0.50	0.50	0.50	0.50	0.50	0.50	* 1.02
N_F	1.00	*	0.50	1.30	1.30	1.30	1.20	1.00	0.80	0.70	0.70	1.40	1.40	* 1.00
	0.98	*	1.40	1.40	1.40	1.40	1.40	1.40	1.40	1.40	1.40	1.40	1.40	* 0.98
	0.96	*	1.40	1.40	1.40	1.40	1.40	1.40	1.40	1.40	1.40	1.40	1.40	* 0.96
	0.94	*	1.40	1.40	1.40	1.40	1.40	1.40	1.40	1.40	1.40	1.40	1.40	* 0.94
	0.92	*	1.40	1.40	1.40	1.40	1.40	1.40	1.40	1.40	1.40	1.40	1.40	* 0.92
	0.90	*	1.40	1.40	1.40	1.40	1.40	1.40	1.40	1.40	1.40	1.40	1.40	* 0.90
			*	*	*	*	*	*	*	*	*	*	*	
			0.90	0.92	0.94	0.96	0.98	1.00	1.02	1.04	1.06	1.08	1.10	

FIGURE 5.1-A. Model 2L3 - Optimal Control Law (1 Control)

N_F	N_C = 0.90	0.92	0.94	0.96	0.98	1.00	1.02	1.04	1.06	1.08	1.10	N_F
1.10	0.2425	0.2374	0.2325	0.2275	0.2220	0.2159	0.2091	0.2015	0.1928	0.1831	0.1727	1.10
1.08	0.2286	0.2231	0.2172	0.2107	0.2034	0.1951	0.1856	0.1746	0.1619	0.1485	0.1391	1.08
1.06	0.2140	0.2072	0.1997	0.1911	0.1811	0.1693	0.1553	0.1389	0.1215	0.1139	0.1145	1.06
1.04	0.1977	0.1893	0.1793	0.1674	0.1530	0.1352	0.1139	0.0915	0.0900	0.0990	0.1120	1.04
1.02	0.1795	0.1684	0.1545	0.1374	0.1153	0.0872	0.0574	0.0709	0.0922	0.1129	0.1312	1.02
1.00	0.1587	0.1430	0.1231	0.0976	0.0621	0.0	0.0621	0.0975	0.1229	0.1425	0.1559	1.00
0.98	0.1344	0.1170	0.0977	0.0785	0.0664	0.0872	0.1152	0.1371	0.1540	0.1671	0.1772	0.98
0.96	0.1210	0.1093	0.1011	0.1015	0.1162	0.1355	0.1530	0.1673	0.1787	0.1880	0.1959	0.96
0.94	0.1277	0.1260	0.1306	0.1425	0.1566	0.1700	0.1816	0.1913	0.1994	0.2063	0.2126	0.94
0.92	0.1512	0.1569	0.1665	0.1772	0.1874	0.1965	0.2044	0.2113	0.2172	0.2226	0.2277	0.92
0.90	0.1810	0.1885	0.1967	0.2044	0.2115	0.2178	0.2234	0.2285	0.2330	0.2373	0.2415	0.90
	0.90	0.92	0.94	0.96	0.98	1.00	1.02	1.04	1.06	1.08	1.10	

FIGURE 5.1-B. Model 2L3 - Cost (1 Control)

N_F		0.90	0.92	0.94	0.96	0.98	1.00	1.02	1.04	1.06	1.08	1.10		
		*	*	*	*	*	*	*	*	*	*	*		
1.10	*	0.50 0.70	0.50 0.70	0.50 0.70	0.50 0.70	0.50 0.70	0.50 0.70	0.50 0.70	0.50 0.70	0.50 0.70	0.50 0.70	0.50 0.70	*	1.10
1.08	*	0.50 0.70	0.50 0.70	0.50 0.70	0.50 0.70	0.50 0.70	0.50 0.70	0.50 0.70	0.50 0.70	0.50 0.70	0.50 0.70	0.50 0.70	*	1.08
1.06	*	0.50 0.70	0.50 0.70	0.50 0.70	0.50 0.70	0.50 0.70	0.50 0.70	0.50 0.70	0.50 0.70	0.50 0.70	0.50 0.70	0.50 0.70	*	1.06
1.04	*	0.50 0.70	0.50 0.70	0.50 0.70	0.50 0.70	0.50 0.70	0.60 0.70	0.50 0.70	0.50 0.70	0.50 0.70	0.50 0.70	0.50 0.70	*	1.04
1.02	*	0.50 0.70	0.50 0.70	0.60 0.70	0.60 0.70	0.70 0.70	0.60 0.80	0.50 0.80	0.50 0.70	0.50 0.70	0.50 0.70	0.50 1.20	*	1.02
1.00	*	0.50 0.70	1.30 0.90	1.30 0.90	1.30 1.00	1.40 1.20	1.00 1.00	0.60 0.80	0.70 1.00	0.70 1.20	1.40 1.20	1.40 1.20	*	1.00
0.98	*	1.40 1.20	1.40 1.20	1.40 1.20	1.40 1.20	1.40 1.20	1.40 1.20	1.40 1.20	1.40 1.20	1.40 1.20	1.40 1.20	1.40 1.20	*	0.98
0.96	*	1.40 1.20	1.40 1.20	1.40 1.20	1.40 1.20	1.40 1.20	1.40 1.20	1.40 1.20	1.40 1.20	1.40 1.20	1.40 1.20	1.40 1.20	*	0.96
0.94	*	1.40 1.20	1.40 1.20	1.40 1.20	1.40 1.20	1.40 1.20	1.40 1.20	1.40 1.20	1.40 1.20	1.40 1.20	1.40 1.20	1.40 1.20	*	0.94
0.92	*	1.40 1.20	1.40 1.20	1.40 1.20	1.40 1.20	1.40 1.20	1.40 1.20	1.40 1.20	1.40 1.20	1.40 1.20	1.40 1.20	1.40 1.20	*	0.92
0.90	*	1.40 1.20	1.40 1.20	1.40 1.20	1.40 1.20	1.40 1.20	1.40 1.20	1.40 1.20	1.40 1.20	1.40 1.20	1.40 1.20	1.40 1.20	*	0.90
		*	*	*	*	*	*	*	*	*	*	*		
		0.90	0.92	0.94	0.96	0.98	1.00	1.02	1.04	1.06	1.08	1.10		

N_C

FIGURE 5.2-A. Model 2L3 - Optimal Control Law (2 Controls)

N_F		0.90	0.92	0.94	0.96	0.98	1.00	1.02	1.04	1.06	1.08	1.10		
	*												*	
1.10	*	0.2269	0.2215	0.2163	0.2112	0.2059	0.2002	0.1937	0.1861	0.1775	0.1676	0.1562	*	1.10
1.08	*	0.2134	0.2074	0.2014	0.1952	0.1884	0.1805	0.1712	0.1604	0.1475	0.1324	0.1203	*	1.08
1.06	*	0.1967	0.1918	0.1846	0.1766	0.1671	0.1558	0.1422	0.1257	0.1056	0.0951	0.0944	*	1.06
1.04	*	0.1827	0.1744	0.1652	0.1539	0.1401	0.1232	0.1019	0.0754	0.0719	0.0808	0.0946	*	1.04
1.02	*	0.1648	0.1544	0.1414	0.1246	0.1035	0.0764	0.0416	0.0550	0.0769	0.0984	0.1167	*	1.02
1.00	*	0.1443	0.1302	0.1105	0.0852	0.0512	0.0	0.0511	0.0849	0.1100	0.1276	0.1419	*	1.00
0.98	*	0.1201	0.1022	0.0821	0.0617	0.0495	0.0762	0.1031	0.1238	0.1395	0.1517	0.1617	*	0.98
0.96	*	0.1034	0.0910	0.0822	0.0836	0.1029	0.1228	0.1393	0.1526	0.1633	0.1722	0.1800	*	0.96
0.94	*	0.1078	0.1066	0.1129	0.1279	0.1428	0.1557	0.1665	0.1755	0.1832	0.1900	0.1963	*	0.94
0.92	*	0.1317	0.1393	0.1509	0.1622	0.1722	0.1808	0.1882	0.1947	0.2005	0.2058	0.2111	*	0.92
0.90	*	0.1631	0.1720	0.1806	0.1883	0.1951	0.2010	0.2064	0.2112	0.2158	0.2202	0.2247	*	0.90
	*												*	
		0.90	0.92	0.94	0.96	0.98	1.00	1.02	1.04	1.06	1.08	1.10		

N_C

FIGURE 5.2-B. Model 2L3 - Cost (2 Controls)

The program was originally developed using only one control, WFB. Subsequently, the A8 control was added but constraints were not yet considered. Figures 5.1 and 5.2 present the results, showing a single cross section of the three-dimensional state space, as defined by the plane $x_3(P_7) = 1$.

It is interesting that the control law WFB(x) remains basically unchanged with the addition of the second input. However, the benefit derived by its addition is clearly evident, since the two-input system reaches the target roughly 10% faster than the one-input system, for any given state.

Another significant result is that the optimal control solution for Model 2L3 is virtually the same for a given x_1 and x_2, regardless of the choice of x_3. The largest difference occurs at ($x_1 = 1$, $x_2 = 1$, $x_3 = 1$) where $V(x) = 0.0161$ seconds, as opposed to $V(x) = 0$ at the target ($x_1 = 1$, $x_2 = 1$, $x_3 = 1$). The farther that x_1 and x_2 are from the target, the smaller the difference becomes. This suggests that a second order model would be satisfactory to use, and, indeed, it comes as no surprise considering the eigenvalue information garnered in Chapter II. P_7 (afterburner pressure) reacts so quickly that it only slightly alters the cost when x_3 is far from the target.

5.3 Optimal Control Theory

Henceforth, it is assumed that second order models of the jet engine are entirely suitable for this study. Considering the low order of the system, it was decided that analytical optimal control theory might provide good insight into the ultimate feedback controller solution, at the same time providing a means to check the accuracy of the numerical program. The analytical approach is examined here.

Let us first restate the general problem in continuous time:

Minimize

$$J(x_o, u_{[t_o,t]}, t) = K(x(t_1)) + \int_{t_o}^{t_1} L(x(t),u(t),t)dt \qquad (5.3\text{-}1)$$

such that

$$\dot{x} = f(x,u,t) \qquad (5.3\text{-}2)$$

where t_o = the starting time

t_1 = the time at which the target set S is reached

$x_o = x(t_o)$

$u(t) \in U$, the control set

$(x(t_1),t,) \in S$

$u_{[t_o,t]}$ = the continuous control over the interval from t_o to t

Note that the constraints $g_i(x(t),u(t))$ are excluded from the problem in this analytical study.

For the problem of interest, equations (5.3-1) and (5.3-2) can be restated as:

Minimize

$$J(x_o,u_{[t_o,t]},t) = \int_{t_o}^{t_1} dt \tag{5.3-3}$$

Such that

$$\dot{x} = A(x - \vec{1}) + B(u - \vec{1}) \tag{5.3-4}$$

$$U = \{u(t): u_{min} \leq u(t) \leq u_{max}\}$$

$$S = \{(x(t_1),t_1): x = \vec{1}\}$$

There are two principal analytical approaches to solve this problem, and both employ the Hamiltonian H defined as:

$$H(x,p,u,t) = < p,f(x,u,t) > + p_o L(x,u,t) \tag{5.3-5}$$

where p is known as the adjoint variable, and p_o equals 1 in this case.

The first approach [14] states that if an infinum J^* exists for equation (5.3-3),

$$J^*(x_o,t_o) = \inf_{u_{[t_o,t,]}} J(x_o,t_o) \tag{5.3-6}$$

then it solves the Hamilton-Jacobi equation

$$\frac{\partial J^*(x_o,t_o)}{\partial t} + H^*\left(x, \frac{\partial J^{*T}(x_o,t_o)}{\partial x}, t\right) = 0$$

$$(x_o,t_o) \notin S \tag{5.3.7}$$

$$J^*(x_o,t_o) = K(x_o,t_o) \quad \text{for} \quad (x_o,t_o) \in S \tag{5.3-8}$$

Solution of equation (5.3-7) will yield a control $v^*(x, \frac{\partial J^{*T}(x_o,t_o)}{\partial x}, t)$. If this control does carry $(x(t_o),t_o)$ to S, the target set, then the control is optimal. Often the control law reduces to $v^*(x)$, i.e., a pure state feedback control law. This is similar to Dynamic Programming, and, in fact, Bellman's equation (4.2-8) is actually a discretization of the Hamilton-Jacobi equation (5.3-7).

In this case, an easier analytical approach is through application of the Minimum Principle [9] and the Hamilton Canonical Equations. Pontryagin's Minimum Principle states the Hamiltonian must be a minimum as a necessary condition for optimality, i.e.,

$$H(x^*,p^*,u^*,t) \leq H(x,p,u,t) \quad \forall\, u \in U \tag{5.3-9}$$

where u^* is the optimal control. The Canonical Equations state that

$$\dot{p} = -\frac{\partial H^T}{\partial x} \tag{5.3-10}$$

$$\dot{x} = \frac{\partial H^T}{\partial p} \tag{5.3-11}$$

such that

$$< p,dx > - Hdt - p_o\, dK\Big|_{t_1} = 0 \tag{5.3-12}$$

where the differentials of equation (5.3-12) are consistent with the problem constraints. Equation (5.3-12) is known as the Transversality Condition [14].

For the problem of interest,

$$H = < p, Ax + Bu > + 1 = < A^T p, x > + < B^T p, u > + 1 \qquad (5.3\text{-}13)$$

where p,x, and u are vectors. To minimize (5.3-13), u must lie at an extreme point of its control set, depending on the signs of $(B^T p)_1$ and $(B^T p)_2$ i.e.,

$$u^* = \begin{cases} (1)\ u_{1\,\max}\ u_{2\,\max} & \text{if } (B^T p)_1 = - \quad (B^T p)_2 = - \\ (2)\ u_{1\,\min}\ u_{2\,\max} & \text{if } (B^T p)_1 = + \quad (B^T p)_2 = - \\ (3)\ u_{1\,\min}\ u_{2\,\min} & \text{if } (B^T p)_1 = + \quad (B^T p)_2 = + \\ (4)\ u_{1\,\max}\ u_{2\,\min} & \text{if } (B^T p)_1 = - \quad (B^T p)_2 = + \end{cases} \qquad (5.3\text{-}14)$$

Thus we obtain the usual "bang-bang" solution, so characteristic of many time optimal control problems. It is now certain that the controls will ride the boundaries of the control set U. The problem lies in determining what control is applied when, and for how long. This leads one to a switching point analysis.

In reference [11], Pontryagin shows a method for such an analysis. Equation (5.3-14) shows that if the trajectory of p (the adjoint system) is known, then the switchings are known. Thus Pontryagin delves into an analysis of the adjoint system, employing various transformations and translations to obtain

$$\dot{p}_1 = - \lambda p_1 - \mu p_2 \qquad (5.3\text{-}15)$$

$$\dot{p}_2 = \mu p_1 - \lambda p_2 \qquad (5.3\text{-}16)$$

where λ and μ describe the complex eigenvalues $\lambda + \mu j$ as per Chapter II. Further analysis of equations (5.3-15) and (5.3-16) yields the time intervals for which each control will be applied.

5.4 Model 2L2 Unconstrained

For Model 2L2, unconstrained, controls (1) and (3) as per equation (5.3-14) have time intervals of approximately 1.27 seconds, while controls (2) and (4) have time intervals of 0.00149 seconds. From this information, state space trajectories can be constructed. Since the solutions of (5.3-15) and (5.3-16) are basically sinusoids, the sequence of controls will begin at a particular control, depending on its location in state space, and follow the control sequence in numerical order (and repeating) for the specified time intervals, until the target is reached. This, naturally means that the first and last intervals may be shorter than the others.

Let us first construct trajectories for a number of initial points in state space, given that only a single control is applied. As shown in Figures 5.3 through 5.6, each set of trajectories has a point of singularity, which is the equilibrium point of the system with the given control applied. Each "x" mark shows a time interval of 0.1 second. As the figures show, there exists a single trajectory for each control which will pass through the target. Let us start at the target, and reconstruct the trajectory for each control, going backwards in time (Figure 5.7). Considering the optimal control knowledge embodied in equation (5.3-14), it is clear that the final stage of any optimal trajectory must necessarily follow part or all of one of these arcs, in order to reach the target. Furthermore, if the last stage of an optimal trajectory follows the trajectory due to control i to the target, then it necessarily was moving in accordance with control law i-1 prior to the switching. In this way, figure 5.8 can be constructed. There will occur at most two switchings in the optimal control law for the area of state space which is of interest in this problem.

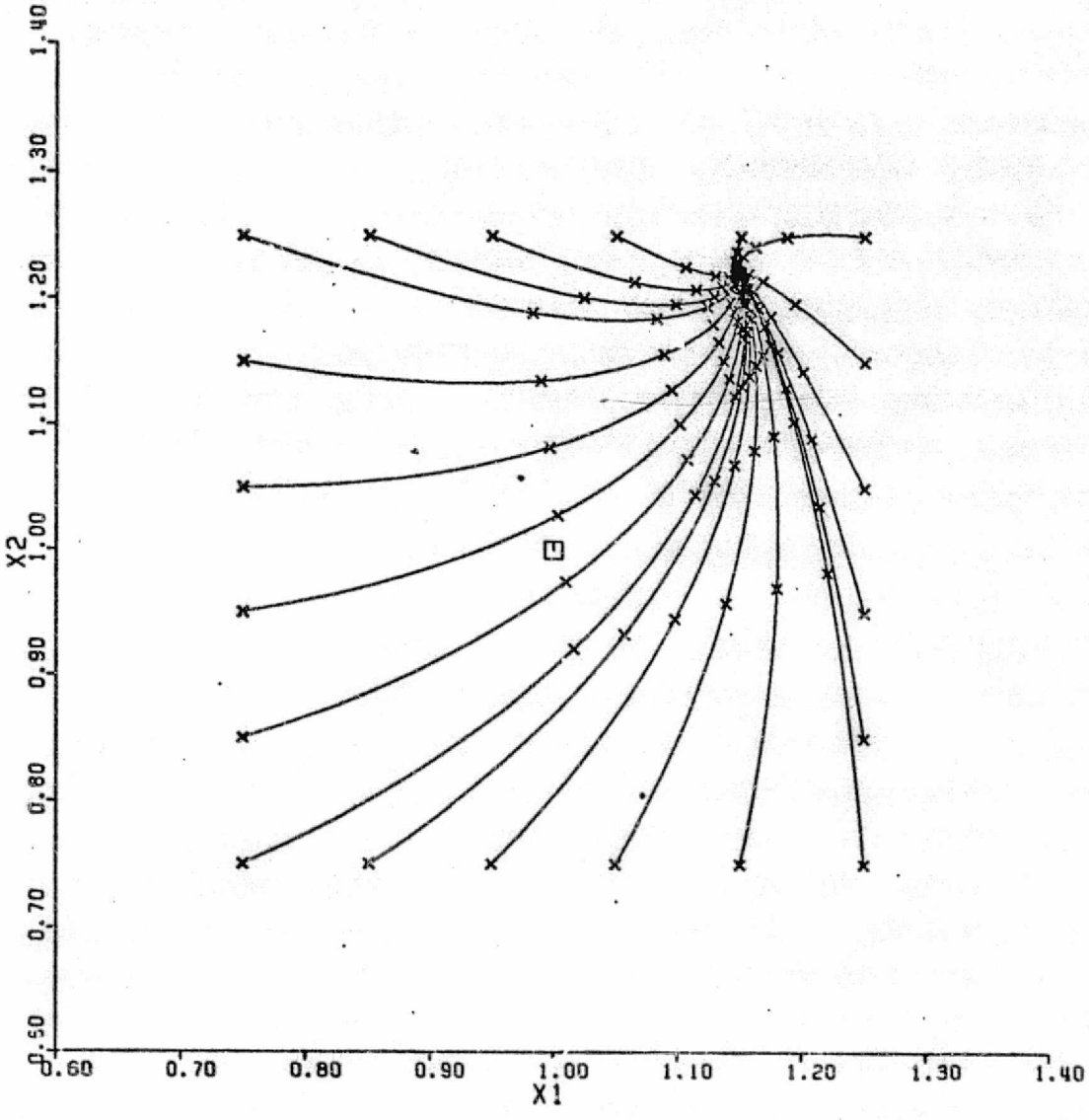

FIGURE 5.3. Model 2L2 - Control (1) Trajectories

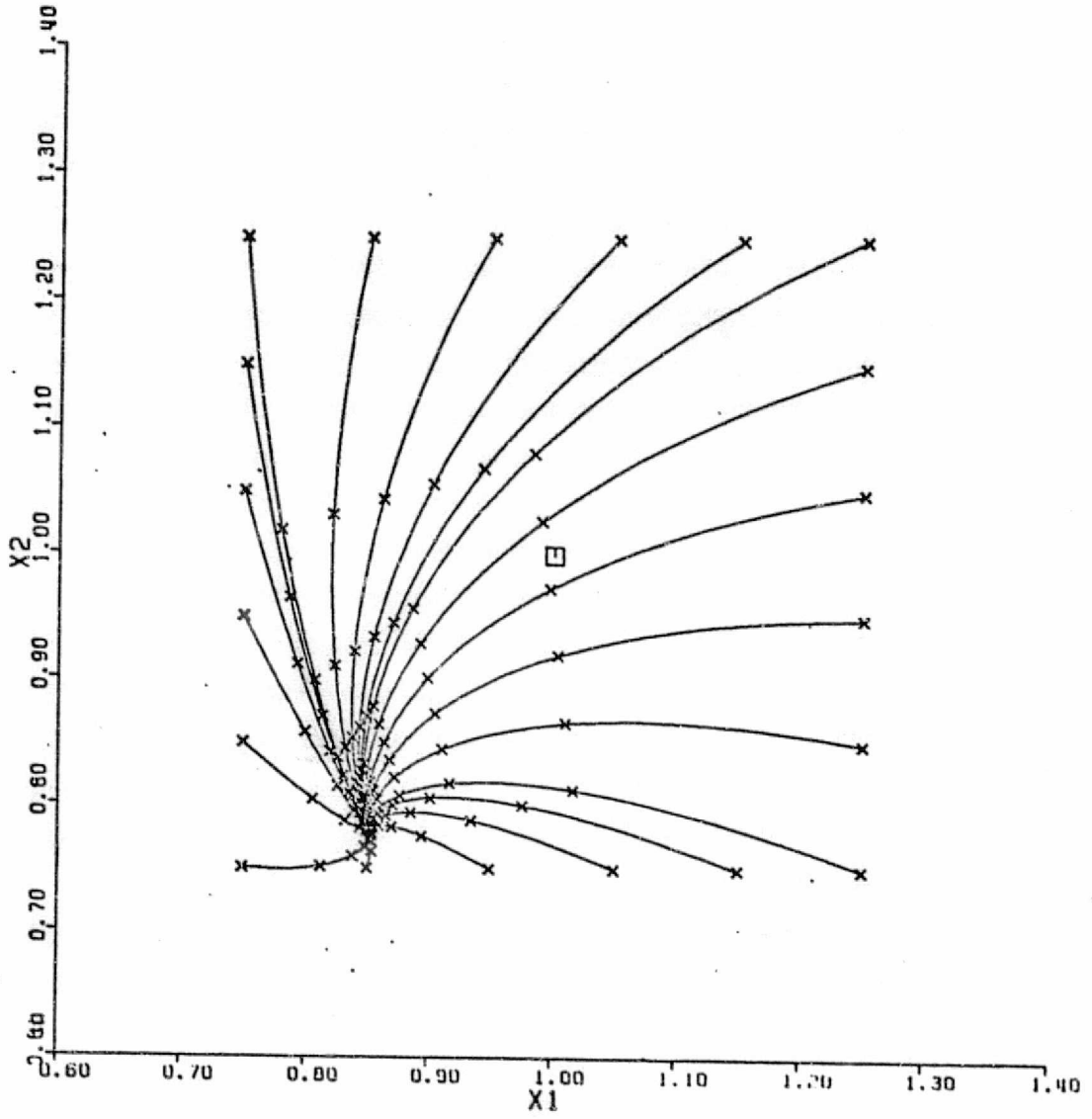

FIGURE 5.4. Model 2L2 - Control (2) Trajectories

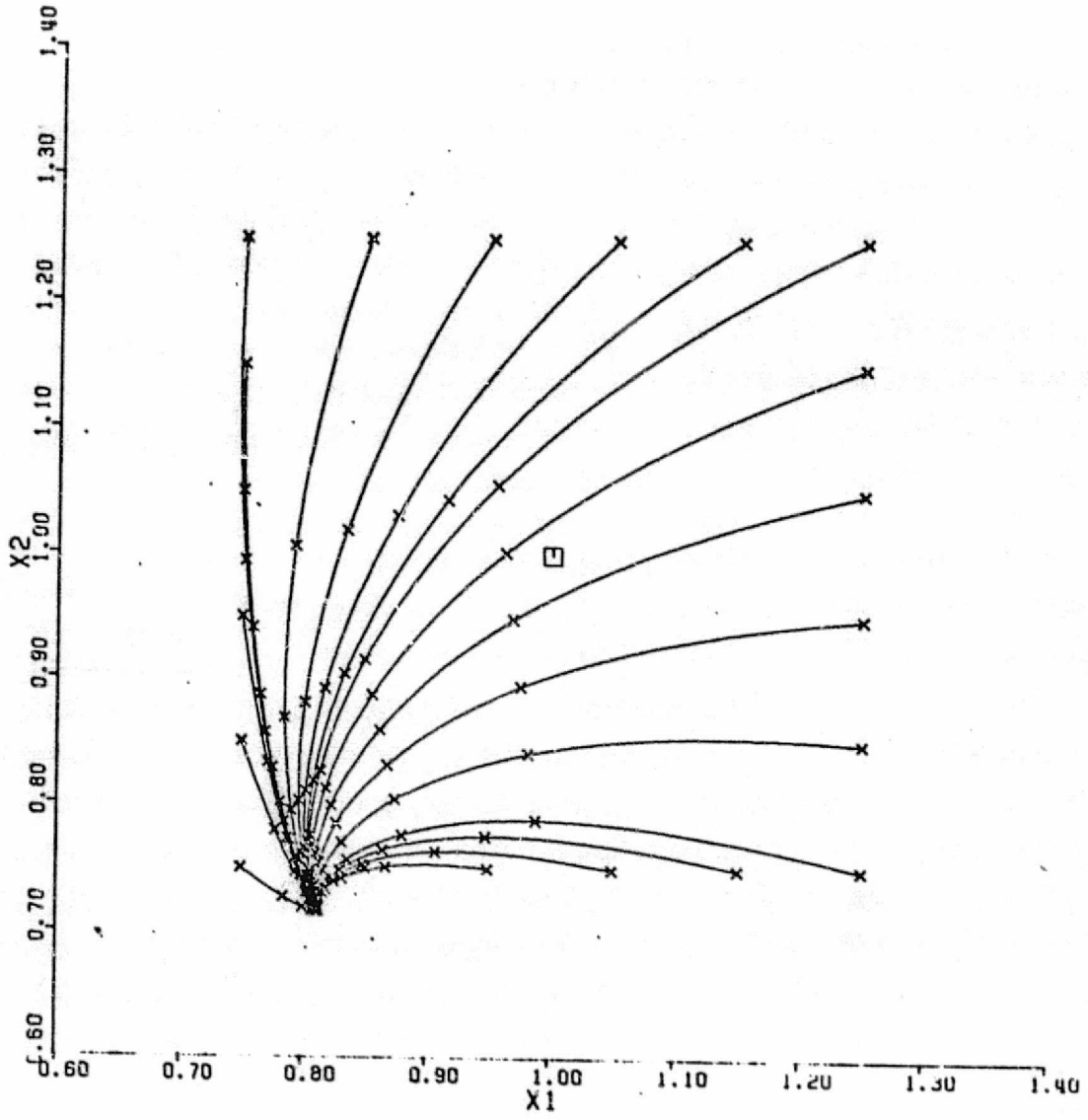

FIGURE 5.5. Model 2L2 - Control (3) Trajectories

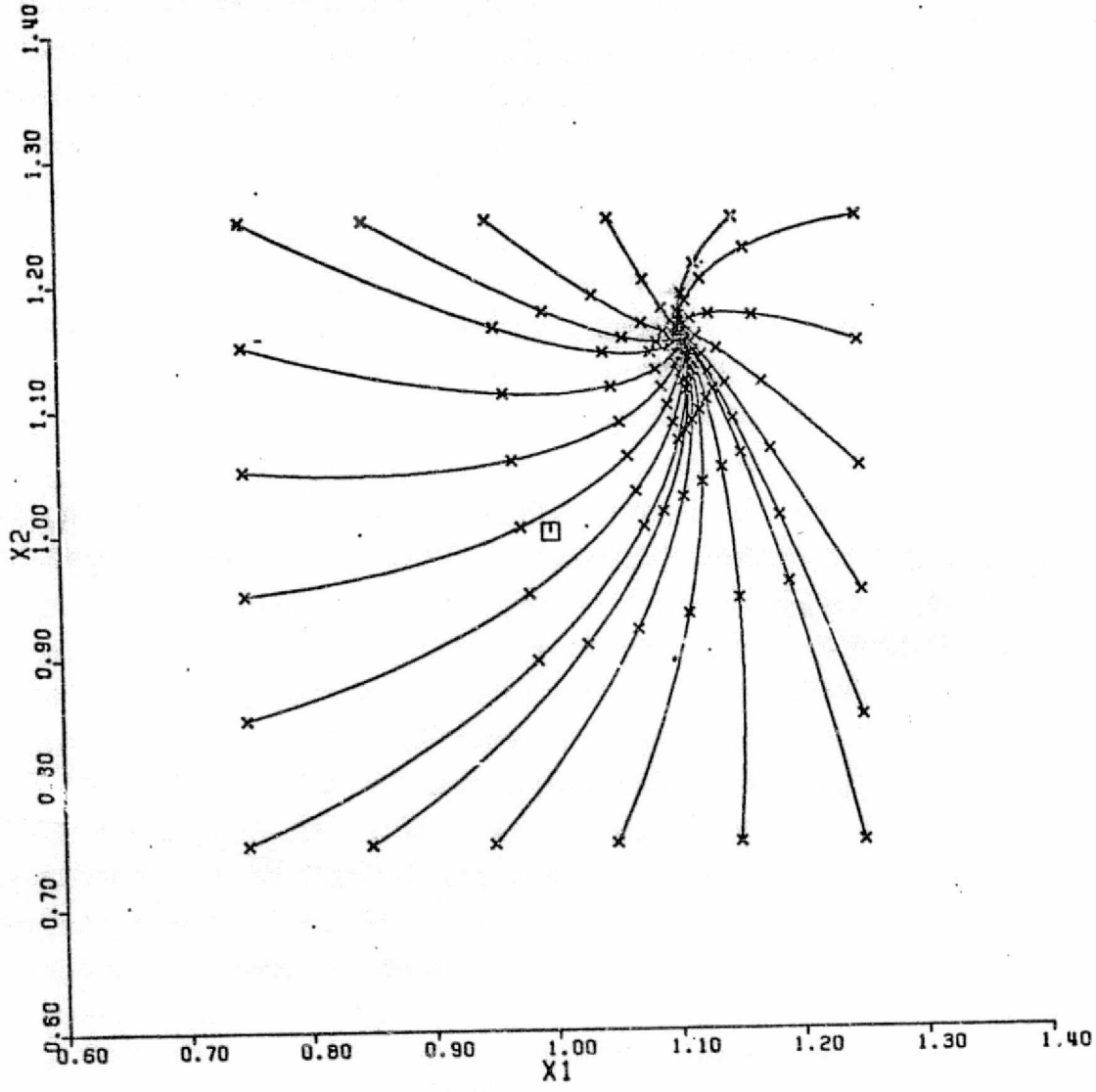

FIGURE 5.6. Model 2L2 - Control (4) Trajectories

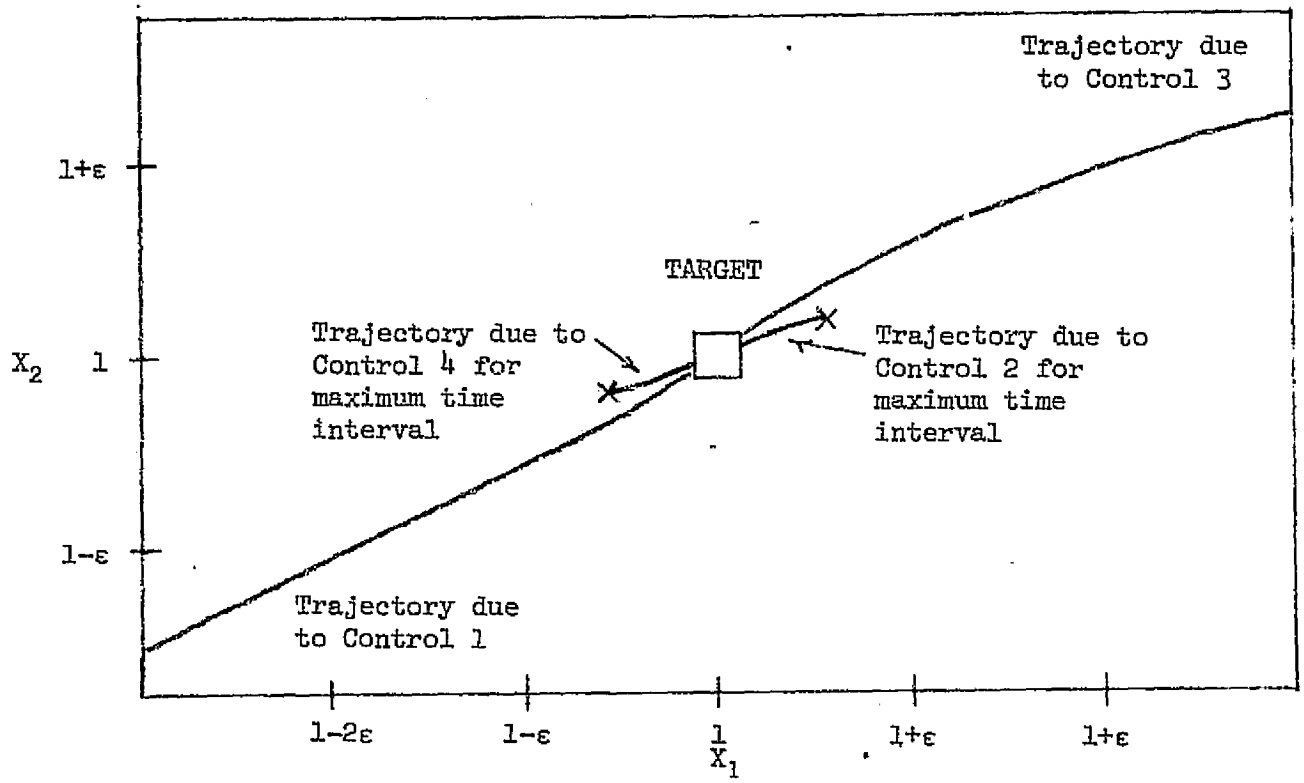

FIGURE 5.7. Model 2L2 - Optimal Control Synthesis

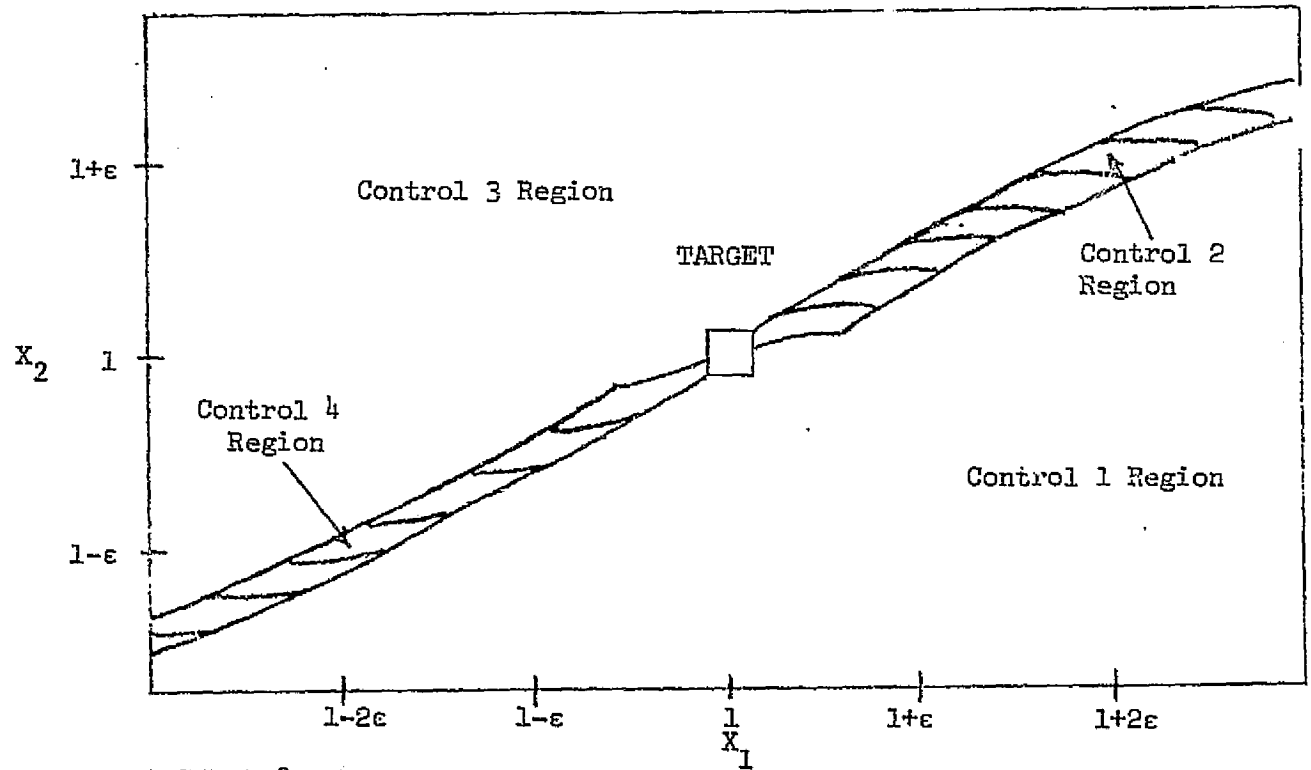

FIGURE 5.8. Model 2L2 - Optimal Control Synthesis

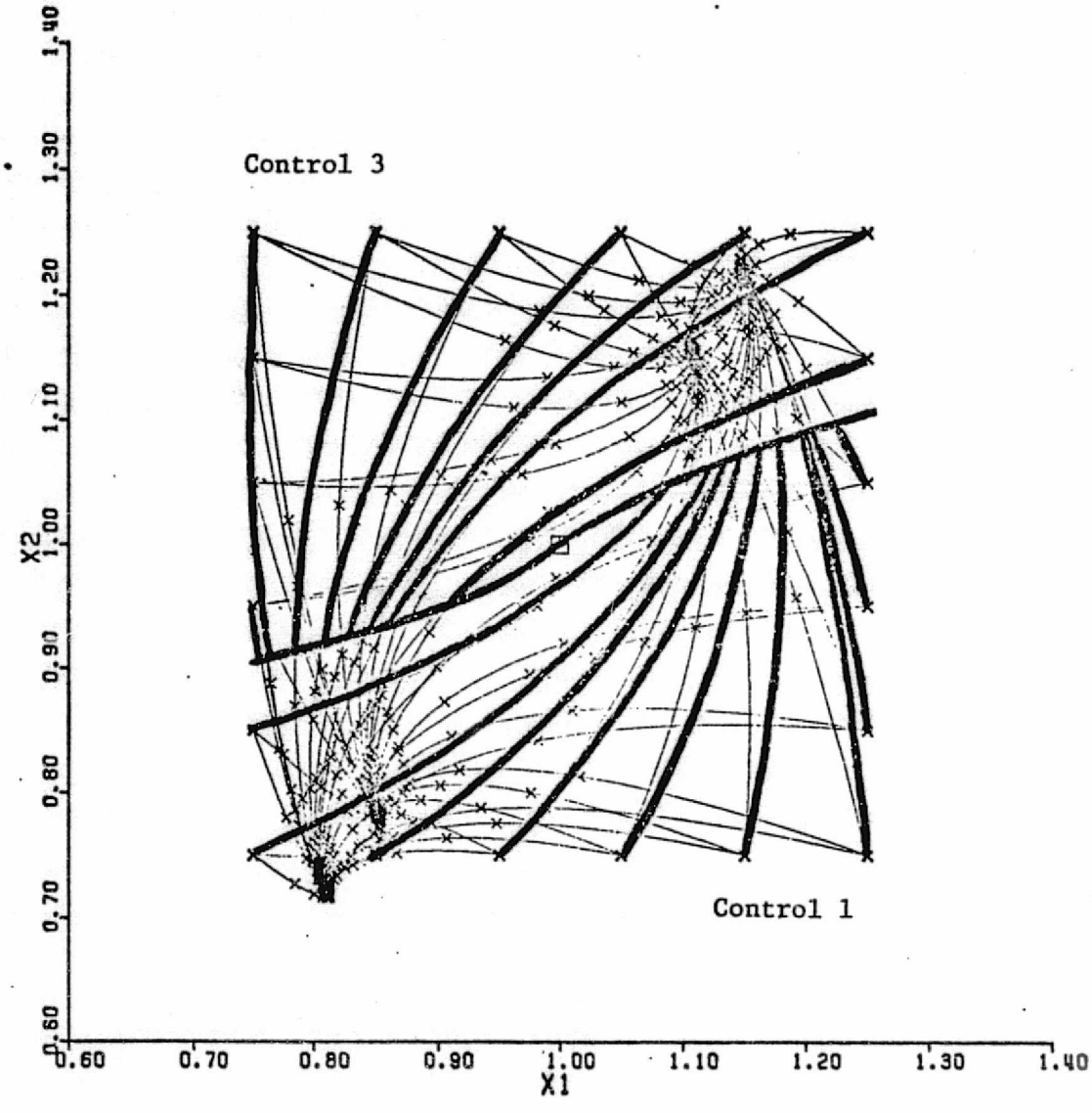

FIGURE 5.9. Model 2L2 - Optimal Control Synthesis

By plotting the four trajectory systems on one graph, a composite picture is obtained, showing the optimal trajectories for the entire state space. This is shown in Figure 5.9. Due to the relatively short time interval for which controls (2) and (4) are applied, they have a negligible effect on the solution. In fact, for the scales used in figure 5.9, these control regions do not appear.

As an example, suppose the initial state is (1.05, 0.75). Control (1) would be applied for approximately 0.2 seconds, then control (2) for 0.00149 seconds, and finally control (3) for approximately 0.06 seconds. Control (2) could have been eliminated for all practical purposes. In fact, that is precisely what occurs in the Dynamic Programming for the problem.

The Dynamic Programming results for Model 2L2, unconstrained, are shown in Figure 5.10. In general, there seems to be good agreement between the analytical study and the numerical results when considering the amount of time necessary to reach the target, V(x). The control laws, however, are not exactly the same. While the Dynamic Programming results show controls (1) and (3) to be optimum in the same areas (for the most part) as the analytical results, the boundary areas between the control regions do not agree as well as had been desired

This is accounted for by a simple explanation. For some states, there exist control laws (in the Dynamic Programming results) which are not theoretically optimal. But when these control laws are applied, they yield costs which are so close to the optimal cost that, in a numerical study subject to interpolation error, a non-optimal cost with a corresponding non-optimal control law may be chosen over an optimal cost with a corresponding optimal control law. Thus, although the

N_C

N_F	0.90	0.92	0.94	0.96	0.98	1.00	1.02	1.04	1.06	1.08	1.10	N_F
1.10	0.50 0.70	0.50 0.70	0.50 0.70	0.50 0.70	0.50 0.70	0.50 0.70	0.50 0.70	0.50 0.70	0.50 0.70	0.50 0.70	0.50 0.70	1.10
1.08	0.50 0.70	0.50 0.70	0.50 0.70	0.50 0.70	0.50 0.70	0.50 0.70	0.50 0.70	0.50 0.70	0.50 0.70	0.50 0.70	0.50 0.70	1.08
1.06	0.50 0.70	0.50 0.70	0.50 0.70	0.50 0.70	0.50 0.70	0.50 0.70	0.50 0.70	0.50 0.70	0.50 0.70	0.50 0.70	0.50 0.70	1.06
1.04	0.50 0.70	0.50 0.70	0.50 0.70	0.50 0.70	0.55 0.70	0.55 0.70	0.50 0.70	0.50 0.70	0.50 0.70	0.50 0.70	0.50 0.70	1.04
1.02	0.50 0.70	0.50 0.70	0.60 0.70	0.65 0.70	0.65 0.70	0.70 0.70	0.50 0.70	0.50 0.70	0.50 0.70	0.50 0.70	0.50 1.20	1.02
1.00	0.50 0.70	1.35 0.70	1.35 0.70	1.40 0.70	1.40 0.70	1.00 1.00	0.60 1.20	0.65 1.20	0.65 1.20	1.40 1.20	1.40 1.20	1.00
0.98	1.40 1.20	1.40 1.20	1.40 1.20	1.40 1.20	1.40 1.20	1.35 1.20	1.35 1.20	1.40 1.20	1.40 1.20	1.40 1.20	1.40 1.20	0.98
0.96	1.40 1.20	1.40 1.20	1.40 1.20	1.40 1.20	1.40 1.20	1.40 1.20	1.40 1.20	1.40 1.20	1.40 1.20	1.40 1.20	1.40 1.20	0.96
0.94	1.40 1.20	1.40 1.20	1.40 1.20	1.40 1.20	1.40 1.20	1.40 1.20	1.40 1.20	1.40 1.20	1.40 1.20	1.40 1.20	1.40 1.20	0.94
0.92	1.40 1.20	1.40 1.20	1.40 1.20	1.40 1.20	1.40 1.20	1.40 1.20	1.40 1.20	1.40 1.20	1.40 1.20	1.40 1.20	1.40 1.20	0.92
0.90	1.40 1.20	1.40 1.20	1.40 1.20	1.40 1.20	1.40 1.20	1.40 1.20	1.40 1.20	1.40 1.20	1.40 1.20	1.40 1.20	1.40 1.20	0.90
	0.90	0.92	0.94	0.96	0.98	1.00	1.02	1.04	1.06	1.08	1.10	

FIGURE 5.10-A. Model 2L2 (Unconstrained) - Optimal Control Law

N_F	0.90	0.92	0.94	0.96	0.98	1.00	1.02	1.04	1.06	1.08	1.10	N_F
1.10	0.2215	0.2170	0.2124	0.2076	0.2024	0.1967	0.1902	0.1827	0.1741	0.1643	0.1530	1.10
1.08	0.2087	0.2034	0.1978	0.1917	0.1849	0.1771	0.1678	0.1570	0.1443	0.1294	0.1174	1.08
1.06	0.1946	0.1882	0.1812	0.1732	0.1637	0.1524	0.1389	0.1225	0.1027	0.0922	0.0916	1.06
1.04	0.1790	0.1710	0.1618	0.1505	0.1367	0.1199	0.0989	0.0726	0.0691	0.0781	0.0920	1.04
1.02	0.1614	0.1510	0.1379	0.1213	0.1004	0.0734	0.0385	0.0522	0.0743	0.0958	0.1140	1.02
1.00	0.1411	0.1267	0.1071	0.0821	0.0485	0.0	0.0488	0.0824	0.1073	0.1250	0.1383	1.00
0.98	0.1169	0.0992	0.0794	0.0592	0.0474	0.0737	0.1006	0.1212	0.1369	0.1491	0.1591	0.98
0.96	0.1007	0.0884	0.0797	0.0811	0.1004	0.1202	0.1367	0.1500	0.1606	0.1695	0.1773	0.96
0.94	0.1052	0.1041	0.1103	0.1254	0.1402	0.1531	0.1638	0.1729	0.1805	0.1873	0.1935	0.94
0.92	0.1291	0.1367	0.1484	0.1597	0.1695	0.1781	0.1855	0.1920	0.1978	0.2031	0.2083	0.92
0.90	0.1605	0.1695	0.1780	0.1857	0.1924	0.1984	0.2037	0.2085	0.2131	0.2174	0.2219	0.90
	0.90	0.92	0.94	0.96	0.98	1.00	1.02	1.04	1.06	1.08	1.10	

N_C

FIGURE 5.10-B. Model 2L2 (Unconstrained) - Cost

difference between controls (1) and (3) is large, (where one would be optimal and the other non-optimal), application of each at the particular state (in the vicinity of a boundary) will yield costs which are nearly equal.

5.5 Model 1L2 Unconstrained

Switching point analysis (per Section 5.3) for Model 1L2 shows that controls (1) and (3) have maximum time intervals of 1.22 seconds, while controls (2) and (4) have maximum intervals of 0.49 seconds. In this case, a maximum of one switching may occur for the state space areas of interest. Figures 5.11 through 5.14 show the various trajectories for each control. In this case, the singularity points are not as close together as they were for Model 2L2, and thus the different controls cause much different trajectories to occur. Recall that in Section 5.4, the close proximity of two singularities revealed that two controls both had the same general effect on the state trajectory, but one control was always slightly better for a much larger area of the state space.

The composite effect is shown in Figure 5.15. These results are dramatically different from those of Model 1L2, which is not surprising since the relative magnitudes of elements in the B matrices of the two models is very different.

Although the results are not included in this work, it is a relatively easy job to devise a controller based strictly on these analytical results. Simple knowledge of several points along each of the four main trajectories (which completely define the control regions) will allow one to fit a curve to each boundary. In this way, the control is applied according to the region of state space, continuously testing as the trajectory moves throughout state space. This would be

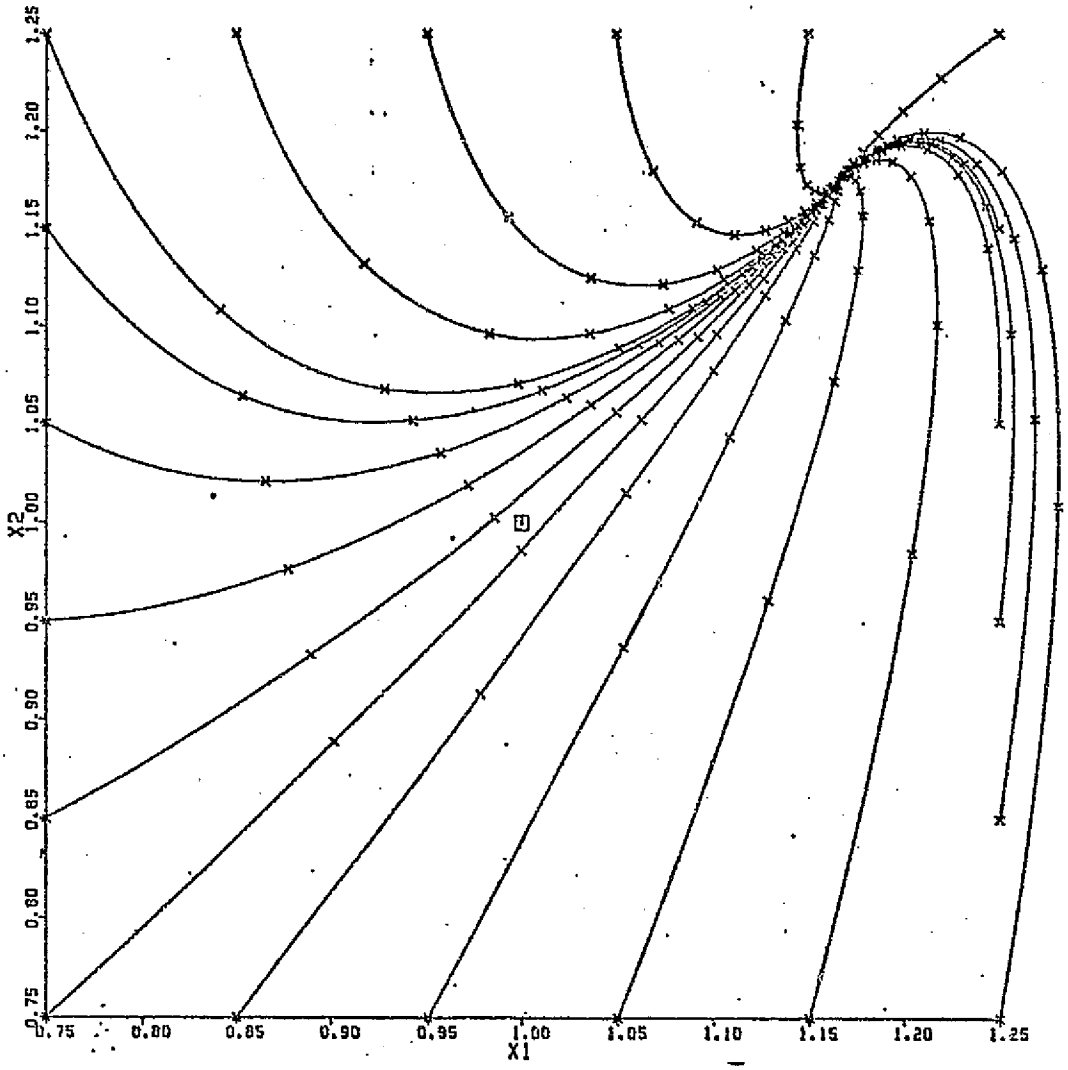

FIGURE 5.11. Model 1L2 - Control (1) Trajectories

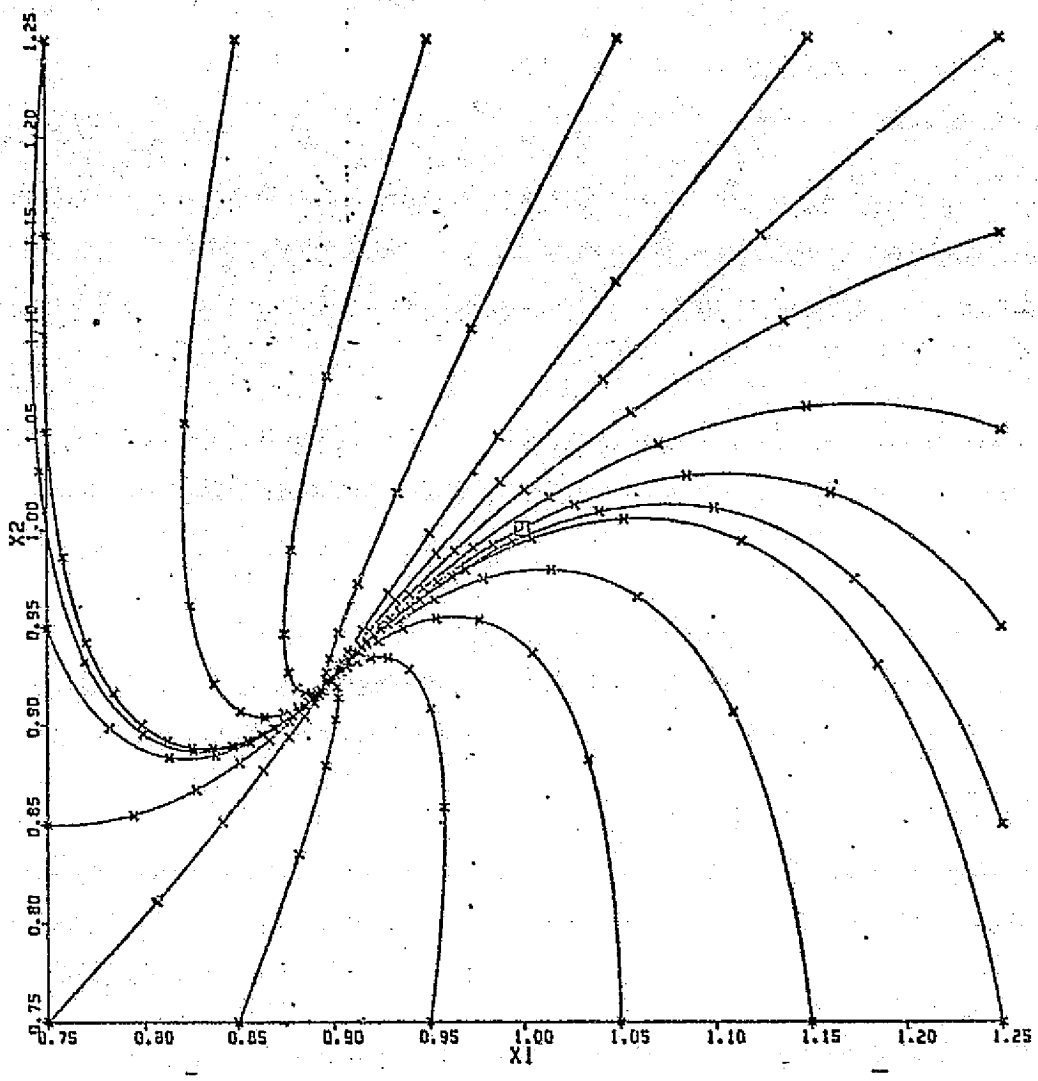

FIGURE 5.12. Model 1L2 - Control (2) Trajectories

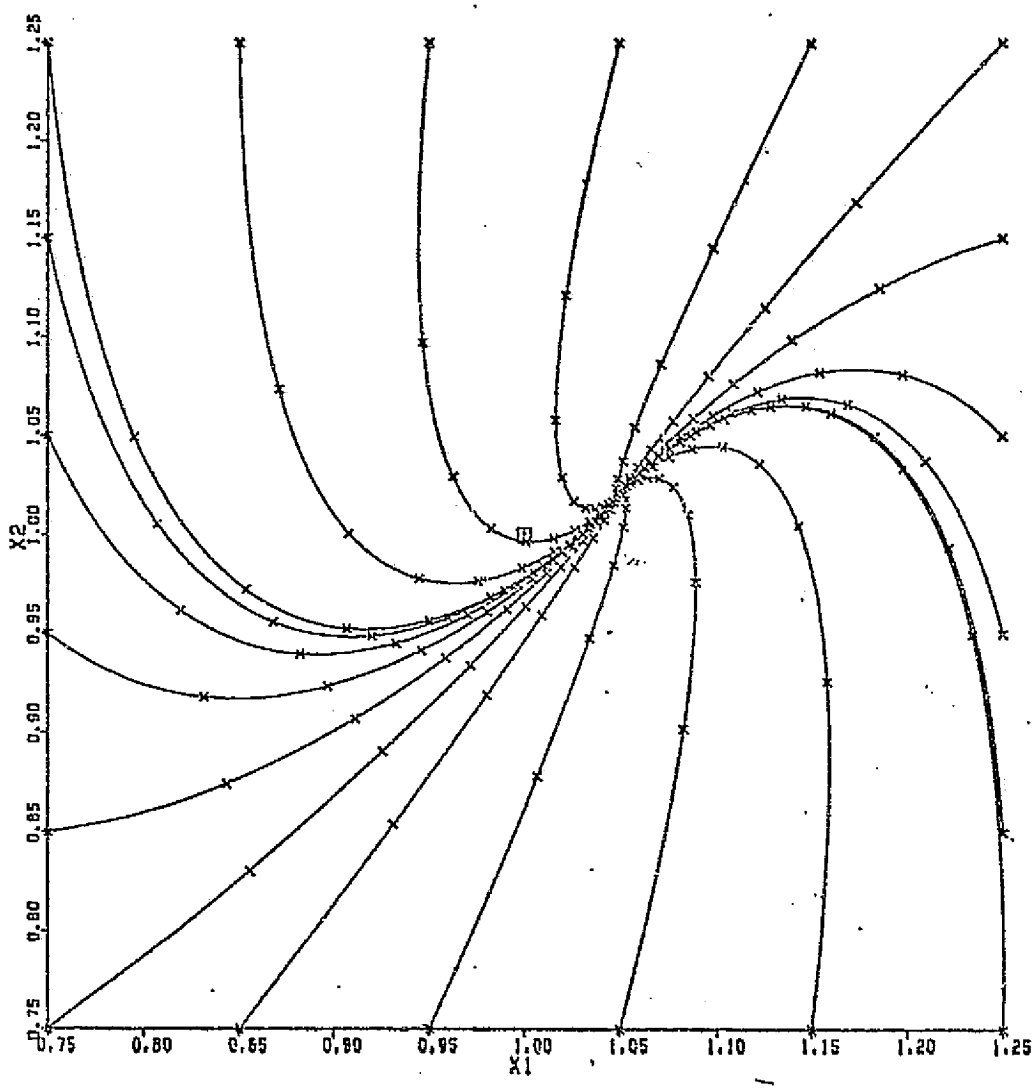

FIGURE 5.13. Model 1L2 - Control (3) Trajectories

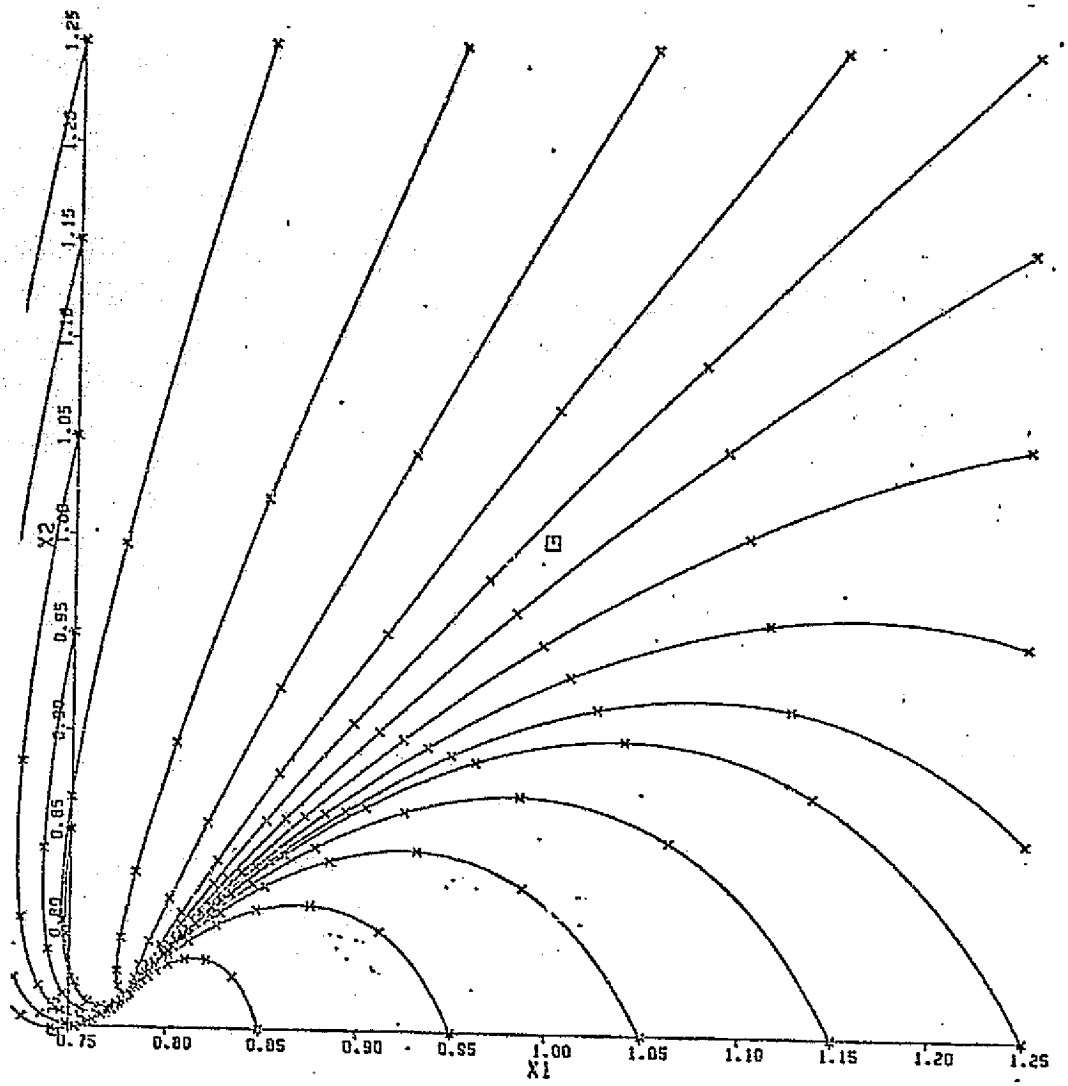

FIGURE 5.14. Model 1L2 - Control (4) Trajectories

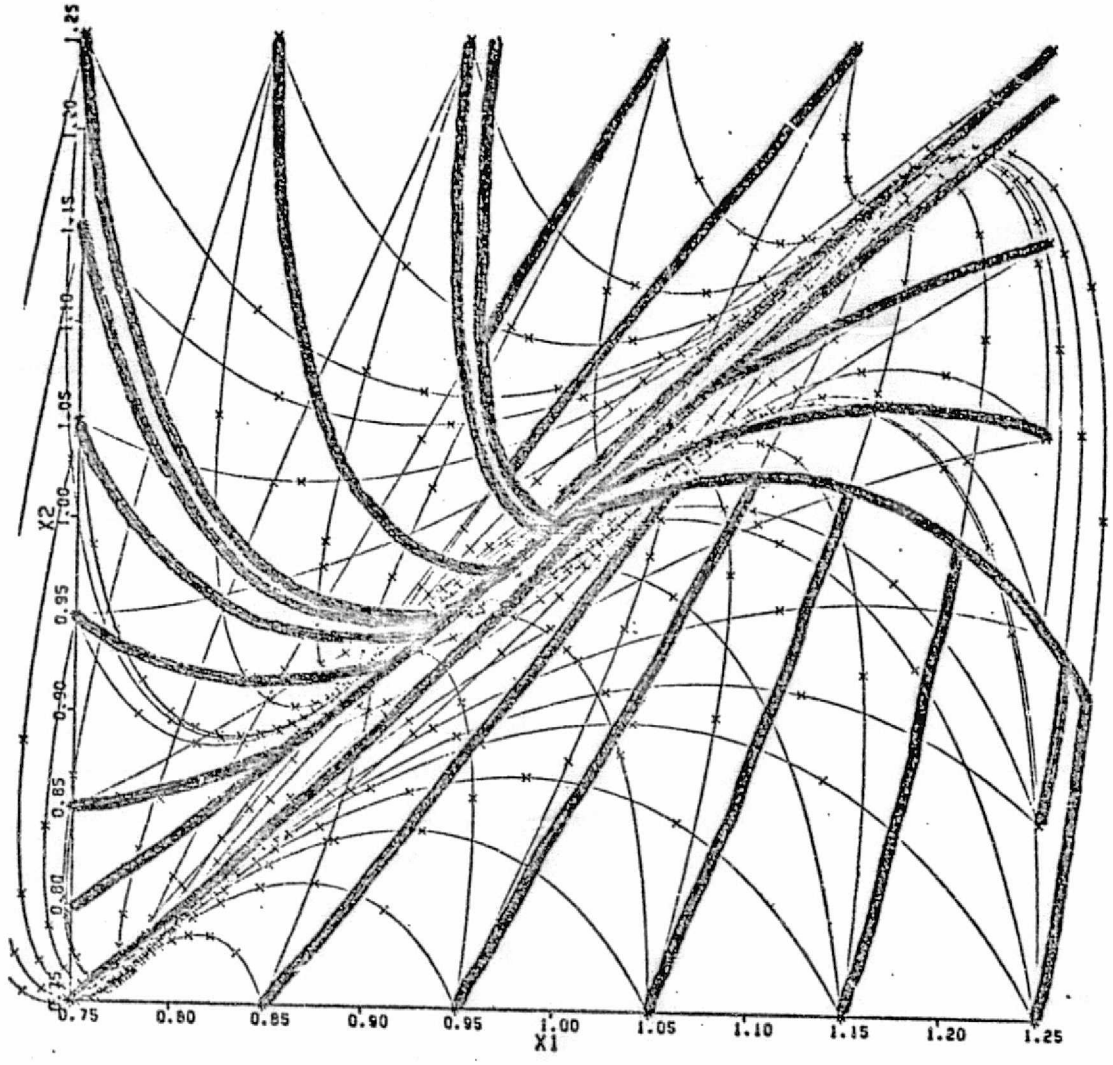

FIGURE 5.15. Model 1L2 - Optimal Control Synthesis

N_C

N_F	0.90	0.92	0.94	0.96	0.98	1.00	1.02	1.04	1.06	1.08	1.10	N_F
1.10	1.40 0.70	1.40 0.70	1.40 0.70	1.40 0.70	1.40 0.70	1.10 0.70	0.70 0.70	0.50 0.70	0.50 0.70	0.50 0.70	0.50 0.70	1.10
1.08	1.40 0.70	1.40 0.70	1.40 0.70	1.40 0.70	1.40 0.70	1.10 0.70	0.50 0.70	0.50 0.70	0.50 0.70	0.50 0.70	0.50 0.70	1.08
1.06	1.40 0.70	1.40 0.70	1.40 0.70	1.40 0.70	1.40 0.70	1.10 0.70	0.50 0.70	0.50 0.70	0.50 0.70	0.50 0.70	0.50 0.70	1.06
1.04	1.40 0.70	1.40 0.70	1.40 0.70	1.40 0.70	1.40 0.70	1.05 0.70	0.50 0.70	0.50 0.70	0.50 0.70	0.50 0.70	0.50 0.70	1.04
1.02	1.40 0.70	1.40 0.70	1.40 0.70	1.40 0.70	1.40 0.70	1.05 0.70	0.50 0.70	0.50 0.70	0.50 0.70	0.50 0.70	0.50 0.70	1.02
1.00	1.40 1.20	1.40 1.20	1.40 1.10	1.40 1.00	1.40 0.90	1.00 1.00	0.50 1.20	0.50 1.20	0.50 1.20	0.50 1.15	0.50 1.20	1.00
0.98	1.40 1.20	1.40 1.20	1.40 1.20	1.40 1.20	1.40 1.20	1.40 1.20	1.35 1.20	1.30 1.20	0.50 1.20	0.50 1.20	0.50 1.20	0.98
0.96	1.40 1.20	1.40 1.20	1.40 1.20	1.40 1.20	1.40 1.20	1.30 1.20	1.30 1.20	1.35 1.20	1.30 1.20	0.50 1.20	0.50 1.20	0.96
0.94	1.40 1.20	1.40 1.20	1.40 1.20	1.40 1.20	1.40 1.20	1.30 1.20	1.30 1.20	1.35 1.20	1.35 1.20	1.30 1.20	0.50 1.20	0.94
0.92	1.40 1.20	1.40 1.20	1.40 1.20	1.40 1.20	1.40 1.20	1.35 1.20	1.35 1.20	1.40 1.20	1.40 1.20	1.40 1.20	1.25 1.20	0.92
0.90	1.40 1.20	1.40 1.20	1.40 1.20	1.40 1.20	1.40 1.20	1.40 1.20	1.40 1.20	1.40 1.20	1.40 1.20	1.40 1.20	1.40 1.20	0.90
N_F	0.90	0.92	0.94	0.96	0.98	1.00	1.02	1.04	1.06	1.08	1.10	N_F

FIGURE 5.16-A. Model 1L2 (Unconstrained) – Optimal Control Law

N_C

N_F	0.90	0.92	0.94	0.96	0.98	1.00	1.02	1.04	1.06	1.08	1.10	N_F
1.10	0.2928	0.2775	0.2616	0.2450	0.2281	0.2102	0.1910	0.1718	0.1562	0.1486	0.1505	1.10
1.08	0.2786	0.2618	0.2439	0.2251	0.2053	0.1842	0.1620	0.1421	0.1311	0.1324	0.1439	1.08
1.06	0.2634	0.2447	0.2244	0.2026	0.1791	0.1535	0.1282	0.1117	0.1118	0.1259	0.1464	1.06
1.04	0.2469	0.2260	0.2027	0.1769	0.1483	0.1159	0.0901	0.0873	0.1058	0.1315	0.1579	1.04
1.02	0.2290	0.2054	0.1785	0.1475	0.1111	0.0675	0.0552	0.0835	0.1170	0.1481	0.1756	1.02
1.00	0.2096	0.1828	0.1514	0.1134	0.0653	0.0	0.0605	0.1052	0.1406	0.1702	0.1955	1.00
0.98	0.1908	0.1625	0.1308	0.0969	0.0674	0.0709	0.1135	0.1470	0.1741	0.1970	0.2174	0.98
0.96	0.1770	0.1509	0.1253	0.1054	0.1018	0.1222	0.1542	0.1804	0.2024	0.2213	0.2382	0.96
0.94	0.1706	0.1501	0.1344	0.1291	0.1391	0.1618	0.1869	0.2082	0.2265	0.2427	0.2572	0.94
0.92	0.1720	0.1588	0.1529	0.1576	0.1729	0.1937	0.2142	0.2319	0.2475	0.2615	0.2743	0.92
0.90	0.1801	0.1740	0.1757	0.1858	0.2021	0.2204	0.2374	0.2525	0.2660	0.2784	0.2898	0.90
	0.90	0.92	0.94	0.96	0.98	1.00	1.02	1.04	1.06	1.08	1.10	

FIGURE 5.16-B. Model 1L2 (Unconstrained) - Cost

the method utilized in a controller simulation, if constraints did not need to be considered.

The Dynamic Programming results for Model 1L2, unconstrained, are shown in Figure 5.16. Again, while there is excellent agreement on V(x) between the analytical and the numerical results, the optimal control laws do not precisely agree, for the same reasons as mentioned in Section 5.4.

5.6 Model 1L2 Constrained

Analytical results are not possible when the constraints, as developed in Chapter III, are considered. Basically, these state-control constraints may be interpreted as control constraints which vary as a function of the state. Furthermore, it is not clear which constraints affect the control law at a given state merely by studying the trajectory of an optimal solution. If the constraints were functions of the state only (as was the case in reference [12]), the optimal trajectory would easily reveal when the control was riding a state constraint.

The Dynamic Programming results for Model 1L2, constrained, are presented in Figure 5.17, and the effects of the constraints are seen in Figure 5.18. Note that each of the constraints has an effect on the optimal feedback control law for some area of state space. In fact, there is only a small region of state space where the constraints do not affect the solution. The main impact of these constraints is that the control law no longer even resembles a bang-bang controller, but instead is a continuously changing function. The more finely quantized that the control set U becomes, the smoother the control law will be.

N_C

N_F	0.90	0.92	0.94	0.96	0.98	1.00	1.02	1.04	1.06	1.08	1.10	N_F
1.10	0.60 0.95	0.65 0.95	0.50 0.90	0.55 0.90	0.60 0.90	0.65 0.90	0.50 0.85	0.50 0.85	0.50 0.85	0.50 0.85	0.50 0.80	1.10
1.08	0.65 0.95	0.70 0.95	0.55 0.90	0.60 0.90	0.65 0.90	0.70 0.90	0.55 0.85	0.50 0.85	0.50 0.85	0.50 0.85	0.50 0.80	1.08
1.06	1.15 1.05	0.50 0.90	0.55 0.90	0.65 0.90	0.70 0.90	0.50 0.85	0.60 0.85	0.65 0.85	0.50 0.85	0.50 0.80	0.50 0.80	1.06
1.04	1.15 1.05	1.05 1.00	0.60 0.90	0.70 0.90	0.75 0.90	0.60 0.90	0.65 0.85	0.50 0.85	0.50 0.80	0.50 0.80	0.50 0.80	1.04
1.02	1.15 1.05	1.10 1.00	1.15 1.00	0.75 0.90	0.80 0.90	0.85 0.90	0.50 0.85	0.50 0.80	0.50 1.10	0.50 1.20	0.50 1.20	1.02
1.00	1.15 1.05	1.15 1.00	1.20 1.00	1.20 1.00	1.25 1.00	1.00 1.00	0.50 1.20	0.50 1.20	0.50 1.20	0.50 1.20	0.50 1.20	1.00
0.98	1.15 1.05	1.15 1.10	1.20 1.05	1.15 1.20	1.15 1.20	1.15 1.20	1.15 1.20	1.15 1.20	1.10 1.20	0.65 1.20	0.50 1.20	0.98
0.96	1.15 1.05	1.10 1.20	1.15 1.15	1.15 1.20	1.15 1.20	1.20 1.20	1.20 1.20	1.20 1.20	1.25 1.20	1.30 1.20	1.30 1.20	0.96
0.94	1.10 1.15	1.10 1.20	1.15 1.15	1.15 1.20	1.15 1.20	1.20 1.20	1.20 1.20	1.25 1.20	1.25 1.20	1.30 1.20	1.30 1.20	0.94
0.92	1.10 1.15	1.10 1.20	1.10 1.20	1.15 1.20	1.15 1.20	1.15 1.20	1.20 1.20	1.20 1.20	1.25 1.20	1.25 1.20	1.25 1.20	0.92
0.90	1.10 1.10	1.05 1.20	1.05 1.20	1.10 1.20	1.10 1.20	1.10 1.20	1.15 1.20	1.15 1.20	1.20 1.20	1.20 1.20	1.20 1.20	0.90
	0.90	0.92	0.94	0.96	0.98	1.00	1.02	1.04	1.06	1.08	1.10	

FIGURE 5.17-A. Model 1L2 (Constrained) - Optimal Control Law

N_C

N_F	0.90	0.92	0.94	0.96	0.98	1.00	1.02	1.04	1.06	1.08	1.10	N_F
1.10	0.4219	0.4076	0.3919	0.3750	0.3567	0.3360	0.3107	0.2812	0.2474	0.2095	0.1728	1.10
1.08	0.4045	0.3885	0.3706	0.3513	0.3296	0.3037	0.2719	0.2345	0.1909	0.1483	0.1380	1.08
1.06	0.3851	0.3667	0.3463	0.3235	0.2964	0.2628	0.2215	0.1712	0.1212	0.1199	0.1471	1.06
1.04	0.3633	0.3417	0.3178	0.2895	0.2543	0.2089	0.1508	0.0919	0.1022	0.1374	0.1703	1.04
1.02	0.3391	0.3126	0.2831	0.2465	0.1985	0.1316	0.0564	0.0860	0.1288	0.1641	0.1936	1.02
1.00	0.3134	0.2799	0.2402	0.1897	0.1180	0.0	0.0735	0.1232	0.1603	0.1904	0.2159	1.00
0.98	0.2882	0.2490	0.2017	0.1435	0.0843	0.0899	0.1351	0.1694	0.1969	0.2199	0.2398	0.98
0.96	0.2648	0.2225	0.1748	0.1309	0.1192	0.1481	0.1796	0.2053	0.2268	0.2454	0.2621	0.96
0.94	0.2453	0.2050	0.1681	0.1508	0.1641	0.1905	0.2142	0.2341	0.2516	0.2673	0.2816	0.94
0.92	0.2328	0.2004	0.1808	0.1833	0.2025	0.2237	0.2420	0.2582	0.2729	0.2864	0.2989	0.92
0.90	0.2315	0.2099	0.2054	0.2163	0.2338	0.2505	0.2654	0.2790	0.2916	0.3034	0.3144	0.90
	0.90	0.92	0.94	0.96	0.98	1.00	1.02	1.04	1.06	1.08	1.10	

FIGURE 5.17-B. Model 1L2 (Constrained) - Cost

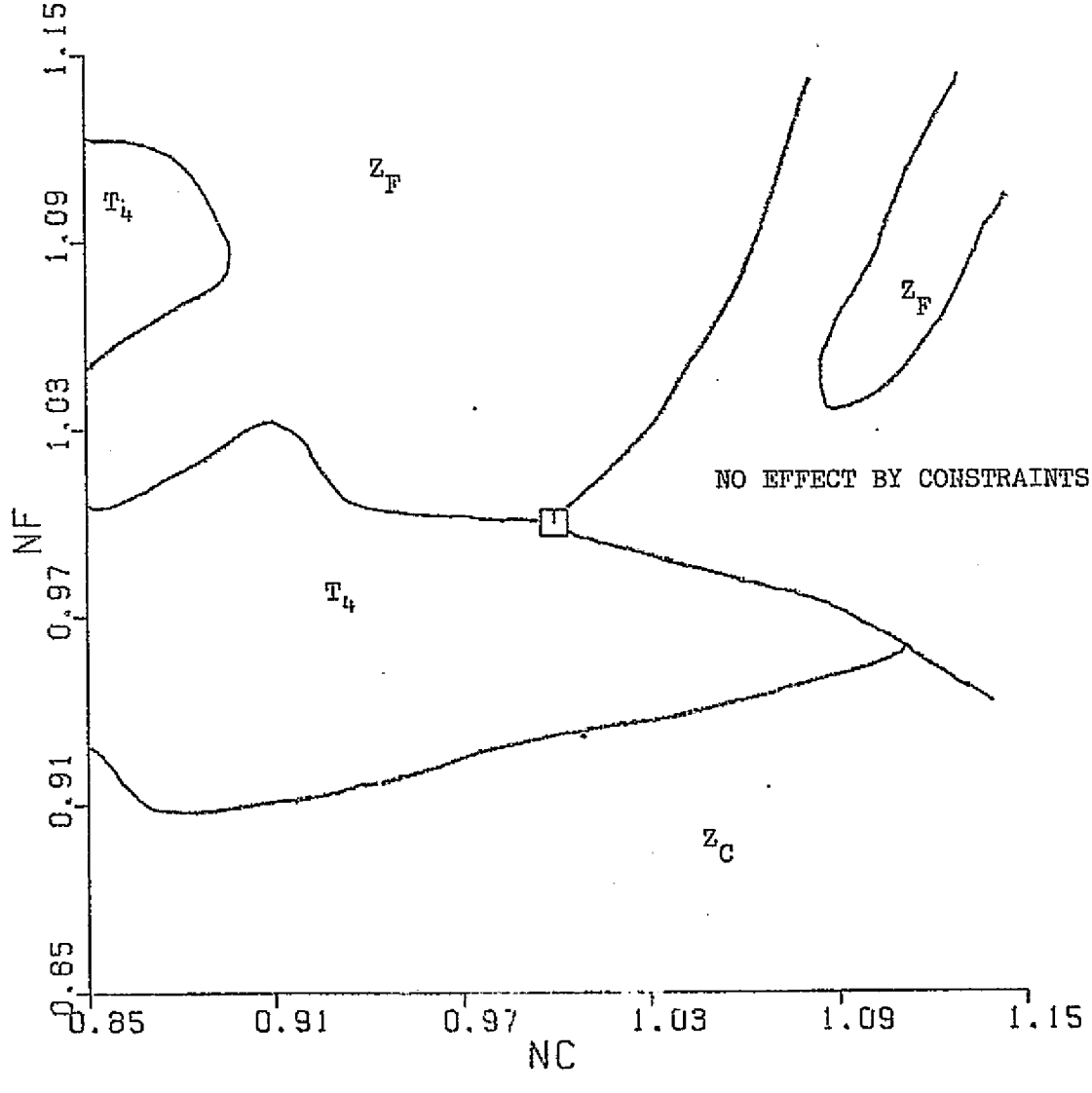

FIGURE 5.18. Effects of Constraints on Model 1L2 Optimal Control Law

5.7 Model 2 Unconstrained

After sufficiently analyzing the linear models, it now remains to study the nonlinear Model 2. No attempt will be made here at a nonlinear system analysis, which would be more complicated than the linear analysis outlined in Section 5.3. Furthermore, while the Dynamic Programming theory remains unchanged, the actual programming gets much more complicated.

If Model 2 could be embodied in 5 state equations, each a function of state variables and inputs, there still would be no significant difference in programming difficulty from the linear models. Unfortunately, Model 2 consists of many equations involving many intermediate variables, and the number of operations required for each point in state space is dramatically increased. In fact, a fifth order solution would require a prohibitive amount of c.p.u. time, and is automatically ruled out. A method must now be found to reduce the order of the system, preferably to second order. Ideally, one desires to set the derivatives of the unwanted state variables to zero, just as was done in Sections 2.3 and 2.4 with the linear models. However, it is impossible to obtain a closed form solution for all the intermediate variables, with state variables 3,4, and 5 eliminated. This leads us to consider iterative solutions.

If equations 1 through 25 of Table 2.6 are to be solved (which is necessary to evaluate the state derivatives), then values for P_4, U_4 and P_7 must somehow be determined. Recall that Dynamic Programming involves a determination of $x(t + \Delta t)$ for a given x and a given u. The first attempt, then, was to supply an initial guess for the eliminated states (P_4, U_4, and P_7), holding N_C, N_F, and the controls fixed, and iterate

until a steady-state solution was reached.

This method failed for several reasons. If one undergoes this iteration process for each state and each control on every successive approximation, c.p.u. time is extremely high. Alternatively, if one stores all the steady state values for P_7, P_4, and U_4 for each state and each control after the first approximation (eliminating the need to iterate on subsequent approximations) a prohibitively high amount of memory is required. Furthermore, if an initial guess for the eliminated states is not close to the actual steady-state solution, instabilities will occur and the system blows up. All of which requires us to look for another solution.

As a compromise to the problems encountered in determining values for the eliminated states, linear approximations are obtained from Model 2L5 and an order reduction is performed. This eliminates any instability problems and also drastically reduces c.p.u. time. The resulting equations are

$$P_4 = 1.4663\ x_1 + .53032\ x_2 + .40998\ u_1 - .18155\ u_2 \qquad (5.7\text{-}1)$$

$$P_7 = -.15936\ x_1 + .78107\ x_2 + .43393\ u_1 - .88875\ u_2 \qquad (5.7\text{-}2)$$

$$U_4 = -.63063\ x_1 - .99071\ x_2 + 1.0656\ u_1 + .17300\ u_2 \qquad (5.7\text{-}3)$$

These equations are then converted to linear affine for utilization by the program.

The Dynamic Programming computer program for Model 2 is found in the Appendix. It is divided into four subroutines: (1) the main program, which is basically the Dynamic Programming method as outlined in Figure 4.2, along with the constants used in Model 2 per Table 2.3; (2) the static relations of Model 2 per Table 2.6; (3) the dynamic relations of

N_C

N_F	0.90	0.92	0.94	0.96	0.98	1.00	1.02	1.04	1.06	1.08	1.10	N_F
1.10	1.30 1.00	0.50 1.10	0.50 1.00	0.50 1.00	0.50 1.00	0.50 1.00	0.50 1.00	0.50 1.00	0.50 1.00	0.50 1.00	0.50 1.00	1.10
1.08	1.10 1.00	0.50 1.00	0.50 1.00	0.50 1.00	0.50 1.00	0.50 1.00	0.50 1.00	0.50 1.00	0.50 1.00	0.50 1.00	0.50 0.90	1.08
1.06	1.40 1.00	0.50 1.00	0.50 1.00	0.50 1.00	0.50 1.00	0.50 1.00	0.50 1.00	0.50 1.00	0.50 1.00	0.50 0.90	0.50 0.80	1.06
1.04	1.40 0.90	0.50 1.00	0.50 1.00	0.50 1.00	0.50 1.00	0.50 1.00	0.50 1.00	0.50 1.00	0.50 0.80	0.50 0.70	0.50 0.70	1.04
1.02	1.40 0.90	0.50 1.00	0.50 1.00	0.50 1.00	0.50 1.00	0.50 1.00	0.50 0.90	0.50 0.70	0.50 0.70	0.60 0.70	0.90 0.70	1.02
1.00	1.40 0.90	1.40 0.90	1.40 0.90	1.40 0.90	1.40 0.90	1.00 1.00	0.80 0.70	0.80 0.70	0.90 0.70	0.90 0.70	1.30 0.70	1.00
0.98	1.40 0.90	1.40 0.90	1.40 1.00	1.40 1.20	1.40 1.20	1.40 0.70	1.40 0.70	1.40 0.70	1.40 0.70	1.40 0.70	1.30 0.70	0.98
0.96	1.40 1.00	1.40 1.20	1.40 1.20	1.40 1.20	1.40 1.20	1.40 0.70	1.40 0.70	1.40 0.70	1.40 0.70	1.40 0.70	1.30 0.70	0.96
0.94	1.40 1.20	1.40 1.20	1.40 1.20	1.40 1.20	1.40 1.20	1.40 1.20	1.40 0.70	1.40 0.70	1.40 0.70	1.40 0.70	1.30 0.70	0.94
0.92	1.40 1.20	1.40 1.20	1.40 1.20	1.40 1.20	1.40 1.20	1.40 1.20	1.40 1.20	1.40 1.20	1.40 0.70	1.40 0.70	1.30 0.70	0.92
0.90	1.40 1.20	1.40 1.20	1.40 1.20	1.40 1.20	1.40 1.20	1.40 1.20	1.40 1.20	1.40 1.20	1.40 0.70	1.40 0.70	1.20 0.70	0.90
	0.90	0.92	0.94	0.96	0.98	1.00	1.02	1.04	1.06	1.08	1.10	

FIGURE 5.19-A. Model 2 (Unconstrained) - Optimal Control Law

N_C

N_F	0.90	0.92	0.94	0.96	0.98	1.00	1.02	1.04	1.06	1.08	1.10	N_F
1.10	0.2420	0.2332	0.2246	0.2160	0.2074	0.1986	0.1895	0.1795	0.1685	0.1559	0.1416	1.10
1.08	0.2245	0.2148	0.2052	0.1956	0.1859	0.1755	0.1642	0.1515	0.1366	0.1193	0.1056	1.08
1.06	0.2054	0.1946	0.1839	0.1730	0.1613	0.1483	0.1334	0.1156	0.0945	0.0832	0.0802	1.06
1.04	0.1844	0.1723	0.1602	0.1471	0.1322	0.1144	0.0929	0.0670	0.0620	0.0668	0.0768	1.04
1.02	0.1611	0.1475	0.1331	0.1162	0.0954	0.0689	0.0363	0.0444	0.0601	0.0772	0.0920	1.02
1.00	0.1350	0.1196	0.1008	0.0769	0.0453	0.0	0.0553	0.0629	0.0833	0.0997	0.1120	1.00
0.98	0.1089	0.0923	0.0734	0.0543	0.0391	0.0572	0.0782	0.0950	0.1089	0.1205	0.1303	0.98
0.96	0.0935	0.0807	0.0703	0.0679	0.0812	0.0960	0.1092	0.1205	0.1303	0.1389	0.1471	0.96
0.94	0.0951	0.0912	0.0934	0.1037	0.1146	0.1247	0.1336	0.1415	0.1487	0.1553	0.1625	0.94
0.92	0.1131	0.1168	0.1246	0.1327	0.1403	0.1473	0.1536	0.1594	0.1648	0.1702	0.1767	0.92
0.90	0.1383	0.1440	0.1500	0.1556	0.1609	0.1658	0.1704	0.1748	0.1792	0.1839	0.1906	0.90
	0.90	0.92	0.94	0.96	0.98	1.00	1.02	1.04	1.06	1.08	1.10	

FIGURE 5.19-B. Model 2 (Unconstrained) - Cost

Model 2 per Table 2.5, minus the eliminated state variables; and (4) equations for determination of P_4, P_7 and U_4, per equations (5.7-1), (5.7-2) and (5.7-3). Note that subroutines XSLOW and MODEL2 utilize the unnormalized system, while the main program and XFAST utilize the normalized system. Thus conversions from one system to the other are made at several points in the program.

It is also important to note that, even though c.p.u. time has been cut as much as possible, it still takes up to five times longer to obtain a Dynamic Programming Solution for Model 2 than for the linear models. For this reason, it is important to use as much c.p.u. time as possible per job run, but still leaving enough time to insure that the results are stored on disk before the allotted program time limit is exceeded. The program itself insures that the results are safely stored, by measuring how much c.p.u. time is required for the first successive approximation, and then using that information to decide when to write the results on disk.

The first results presented in Figure 5.19 are for Model 2, unconstrained, and are normalized values. The control law is similar to the solution for Model 2L2, unconstrained, but the cost is less than the Model 2L2 cost for most points in state space. It is somewhat surprising that nozzle area does not ride the limits of U at several states.

5.8 Model 2 Constrained

Figure 5.20 shows the Dynamic Programming results for Model 2 with the constraint limits as specified in equations (3.3-8),(3.3-9), and (3.3-10), and using equations 23, 24, and 25 of Table 2.6. While the control can actually only ride one constraint at a time, there is a large area of state space where both T_4 and Z_c are very near their

N_C

N_F	0.90	0.92	0.94	0.96	0.98	1.00	1.02	1.04	1.06	1.08	1.10	N_F
1.10	0.50 1.20	0.50 1.20	0.50 1.15	0.50 1.15	0.50 1.15	0.50 1.15	0.50 1.15	0.50 1.15	0.50 1.10	0.50 1.10	0.50 1.10	1.10
1.08	0.50 1.15	0.50 1.15	0.50 1.15	0.50 1.15	0.50 1.10	0.50 1.10	0.50 1.10	0.50 1.10	0.50 1.10	0.50 1.10	0.50 1.05	1.08
1.06	0.50 1.10	0.50 1.10	0.50 1.10	0.50 1.10	0.50 1.10	0.50 1.10	0.50 1.05	0.50 1.05	0.50 1.05	0.50 1.05	0.50 1.05	1.06
1.04	0.50 1.10	0.50 1.10	0.50 1.05	0.50 1.05	0.50 1.05	0.50 1.05	0.50 1.05	0.50 1.05	0.50 1.05	0.50 1.00	0.50 1.00	1.04
1.02	1.05 1.00	1.05 1.00	0.50 1.05	0.50 1.05	0.50 1.05	0.55 1.05	0.50 1.00	0.50 1.00	0.50 1.00	0.80 0.95	0.75 0.95	1.02
1.00	1.05 1.15	1.05 1.15	1.10 0.95	1.10 1.00	1.10 1.05	1.00 1.00	0.70 1.20	0.75 1.20	0.90 0.90	1.10 0.90	1.20 0.90	1.00
0.98	1.05 1.05	1.05 1.10	1.05 1.15	1.10 0.95	1.10 1.05	1.05 1.20	1.10 1.10	1.15 0.95	1.15 0.85	1.15 0.85	1.20 0.85	0.98
0.96	1.05 0.95	1.05 1.00	1.05 1.05	1.05 1.10	1.05 1.10	1.10 1.00	1.10 1.05	1.10 1.05	1.15 0.85	1.15 0.95	1.15 1.00	0.96
0.94	1.00 1.10	1.05 0.90	1.05 0.95	1.05 1.05	1.05 1.05	1.10 0.85	1.10 0.95	1.10 1.00	1.15 0.80	1.15 0.80	1.15 0.95	0.94
0.92	1.00 1.00	1.00 1.05	1.05 0.85	1.05 0.90	1.05 1.00	1.05 1.00	1.10 0.85	1.10 0.90	1.10 0.95	1.10 0.95	1.15 0.00	0.92
0.90	1.00 0.90	1.00 0.95	1.00 1.00	1.00 1.00	1.05 0.90	1.05 0.95	1.05 0.95	1.10 0.80	1.10 0.85	1.10 0.90	1.10 0.90	0.90
	0.90	0.92	0.94	0.96	0.98	1.00	1.02	1.04	1.06	1.08	1.10	

FIGURE 5.20-A. Model 2 (Constrained) - Optimal Control Law

N_C

N_F	0.90	0.92	0.94	0.96	0.98	1.00	1.02	1.04	1.06	1.08	1.10	N_F
1.10	0.2677	0.2605	0.2526	0.2444	0.2356	0.2261	0.2157	0.2045	0.1915	0.1769	0.1605	1.10
1.08	0.2509	0.2425	0.2335	0.2238	0.2129	0.2012	0.1881	0.1733	0.1559	0.1361	0.1223	1.08
1.06	0.2325	0.2227	0.2120	0.2000	0.1866	0.1715	0.1539	0.1330	0.1088	0.0993	0.1012	1.06
1.04	0.2123	0.2006	0.1873	0.1722	0.1548	0.1341	0.1084	0.0789	0.0778	0.0899	0.1064	1.04
1.02	0.1895	0.1753	0.1583	0.1385	0.1146	0.0826	0.0453	0.0609	0.0864	0.1093	0.1275	1.02
1.00	0.1660	0.1455	0.1227	0.0960	0.0586	0.0	0.0550	0.0921	0.1183	0.1378	0.1509	1.00
0.98	0.1819	0.1611	0.1395	0.1172	0.0947	0.0869	0.1146	0.1353	0.1509	0.1636	0.1724	0.98
0.96	0.2133	0.1938	0.1748	0.1580	0.1470	0.1452	0.1586	0.1705	0.1792	0.1874	0.1933	0.96
0.94	0.2462	0.2286	0.2121	0.1976	0.1904	0.1887	0.1942	0.2000	0.2040	0.2090	0.2126	0.94
0.92	0.2785	0.2617	0.2470	0.2349	0.2262	0.2236	0.2240	0.2261	0.2271	0.2298	0.2310	0.92
0.90	0.3086	0.2929	0.2789	0.2675	0.2571	0.2525	0.2508	0.2494	0.2485	0.2490	0.2491	0.90
	0.90	0.92	0.94	0.96	0.98	1.00	1.02	1.04	1.06	1.08	1.10	

FIGURE 5.20-B. Model 2 (Constrained) - Cost

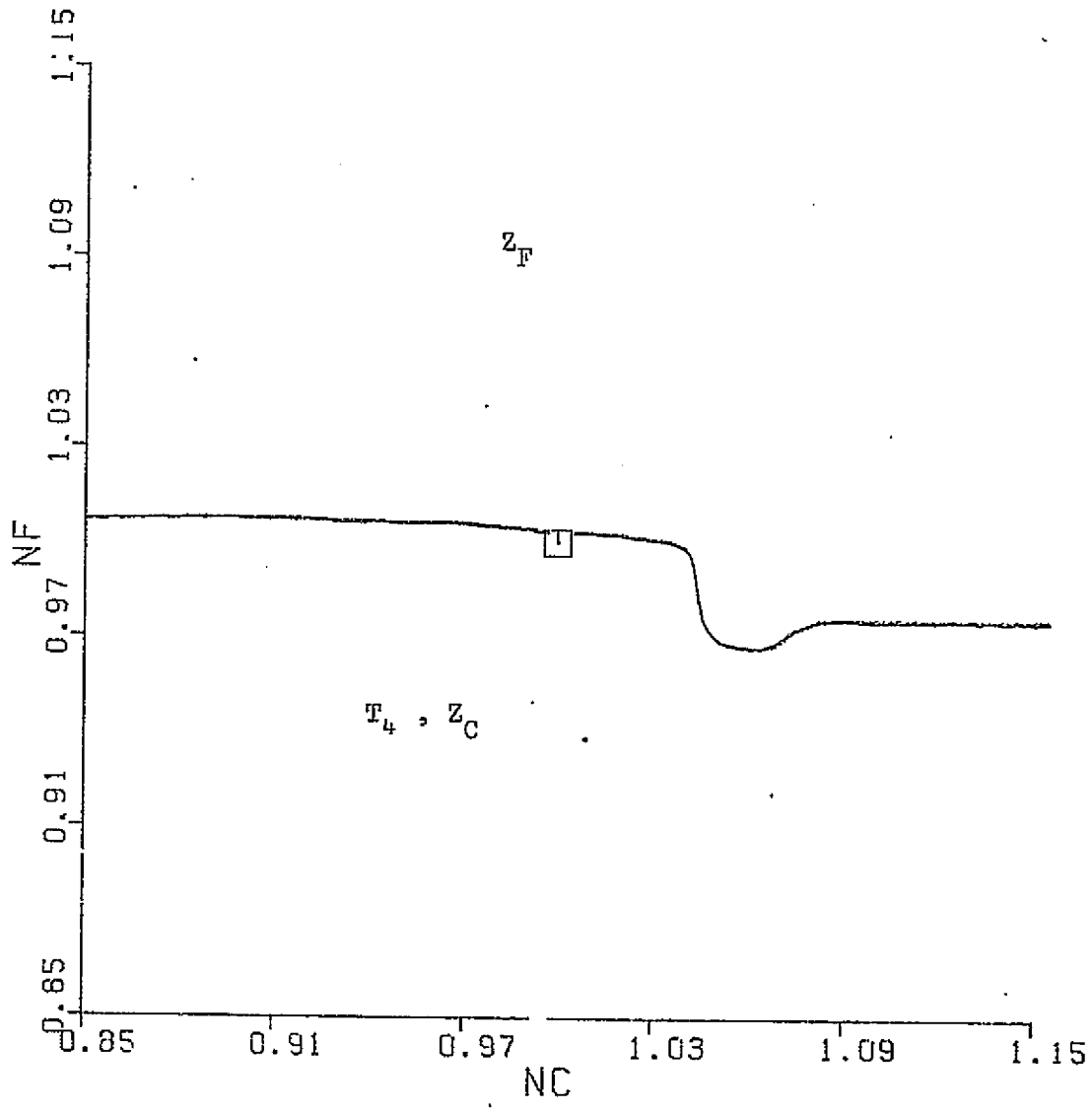

FIGURE 5.21. Effects of Constraints on Model 2 Optimal Control Law

respective limits, and thus they both are shown as affecting the solution in Figure 5.21. If only the constraint closest to its limit is shown, it would result in at least 10 smaller regions. In fact, it is unrealistic to show these smaller regions, since the somewhat coarse quantization of U used in this study will have a strong effect on which constraint the controls are rising. The result is an almost random choice as to which constraint (Z_c or T_4) that the controls ride (in the T_4-Z_c region). Note also that the constraints affect the solution much differently than they did for Model 1L2 in Figure 5.18.

This Dynamic Programming solution requires approximately 90 minutes of c.p.u. time, using a 225-point state space search, and a 209-point control space search.

CHAPTER VI

CONTROLLER SIMULATIONS

6.1 Introduction

Now that feedback control laws have been obtained for several models, both constrained and unconstrained, any state (N_C, N_F) can be driven to the specified target in (approximately) minimum time. Thus, initial starting states can be chosen which reflect low-thrust conditions for both Model 1 and Model 2. The simulators read the feedback control law from its disk storage and change the fuel flow and the nozzle area accordingly. This will necessarily involve an interpolation scheme to decide where the trajectory lies in state space, and is accomplished using the same scheme as employed in the Dynamic Programming. It is desirable that the quantization of the control law be as fine as possible for these purposes, but limits on c.p.u. time once again lead to a compromise.

Interpolation will often lead to error when you are interpolating in a region of state space where the control laws change abruptly. Obviously, the optimal control which is desired is either one extreme or the other, and not something in-between. In this case, the interpolation scheme could be overridden by an analytical test, similar to that which was mentioned in Section 5.5. Such considerations have not been implemented in this study.

The addition of constraints, and their resultant "smoothing" effect on the original "bang-bang" control law, will reduce the number of abrupt changes in the control law. Hence, the interpolation scheme is expected to be more reliable when applying a control law which was derived subject to constraints.

There is another very fundamental consideration for the controller simulations. While the optimal control law at some arbitrary state (x_1, x_2) is quite possibly the same, or nearly the same as that for state $(x_1 + \varepsilon, x_2 + \delta)$, $(\varepsilon, \delta$ small), this is not at all true near the target. The optimal control law at the target is simply $(u_1 = 1, u_2 = 1)$ for the normalized system. However, this law is only valid for that single point in state space which defines the target. The state $(x_1 = 1 + \varepsilon, x_2 = 1 + \delta)$ will have an entirely different law.

In reality, we will consider the target to be some small region, not an infinitesimally small point. As far as the simulations are concerned, this small target region has already been determined by the quantization used in the Dynamic Programming. Whenever both states are within Δx (the quantization size) of the target, the simulator will begin to interpolate on the control law $(u_1 = 1, u_2 = 1)$ for the target. This will cause the states to be slowly eased towards the target, which might be considered unacceptable, depending on how large a region of state space is involved. For this reason, these simulations determine approximate times at which the target point is reached, and exact times at which the target area is reached.

Since all the Dynamic Programming solutions involve normalized values, both simulators must convert to the unnormalized system. All plotted figures in this chapter are normalized, for purposes of comparison.

Although the specified goal is to take a low-thrust starting state to the high-thrust target state in minimum time, the nature of an optimal control study (and in particular, the Dynamic Programming method) is that it is more concerned with state space and the time domain. As such,

no plots of thrust are presented, although thrust plots would be very necessary in frequency domain transfer function studies of linear systems. It is assumed here that satisfactory output responses are obtained when the system constraints are not violated.

The choice of the initial state for the following simulations is somewhat affected by the peculiarities of the DYNGEN (Model 1) computer program. Specification of the initial conditions is determined by an "off-design point" (see reference [10]), which is generally determined by specification of WFB and A8. Ideally, it would be desirable to choose a starting state as far from the target as possible, in order to demonstrate the usefulness of the global feedback control law. This often would involve specification of an extremely low WFB, and is easily accomplished. However, the control law at this point will be a much higher WFB, and results in convergence problems once the transient simulation has begun. The success or failure of the simulation to converge is strongly controlled by the TOLALL and DT variables (see reference [10] and the program inputs given in the Appendix) and amounts to much trial-and-error technique. Even these variables cannot totally control the convergence difficulties, and further changes in the DYNGEN program itself are sometimes required, as explained in [3].

Due to the above considerations, a somewhat high initial condition is used in the simulations, the feeling being that lower initial conditions would require an unacceptable amount of tampering with the tapes on which DYNGEN is stored. For similar reasons, no control laws which were obtained from unconstrained models are tested on DYNGEN.

6.2 Model 2 Simulation Utilizing Model 2L2 (Unconstrained) Control Law

The Model 2 controllers are implemented using the program shown in the Appendix. Figures 6.1 through 6.4 show the results of a simulation utilizing the Model 2L2 (unconstrained) control law, which was presented in Section 5.4. The starting state chosen corresponds to a thrust of approximately 80% of design thrust. The effects of interpolation on the control law are readily seen in Figure 6.1, showing the inputs versus time. After 0.08 seconds, the controls are slowly eased towards their normalized design values (WFB = 1, A8 = 1). Figure 6.2 reveals an overshoot of approximately 100% for compressor speed (N_C) and 30% for fan speed (N_F), certainly not a desirable response for a jet engine. Unfortunately, elimination of the constraints in the determination of the control law has resulted in these undesirable consequences, as shown in Figure 6.3. Turbine inlet temperature (T_4) has skyrocketed to 550% of its design value in only 0.02 seconds, and the surge margins have also reached intolerable levels. The state space trajectory, as shown in Figure 6.4, agrees remarkably well with the optimal trajectories which were analytically determined and presented in Figure 5.9 of the previous chapter. The time it takes to reach the target is also in agreement with the cost results as presented in Figure 5.10, approximately 0.12 seconds.

6.3 Model 2 Simulation, Utilizing Model 2 (Unconstrained) Control Law

Figures 6.5 through 6.8 represent the results when utilizing the Model 2 (unconstrained) control law, as determined in Section 5.7. The same initial state is used here as for the linear controller of Section 6.2, and with remarkably close results. The control laws are slightly different, but the resulting state and constraint variable

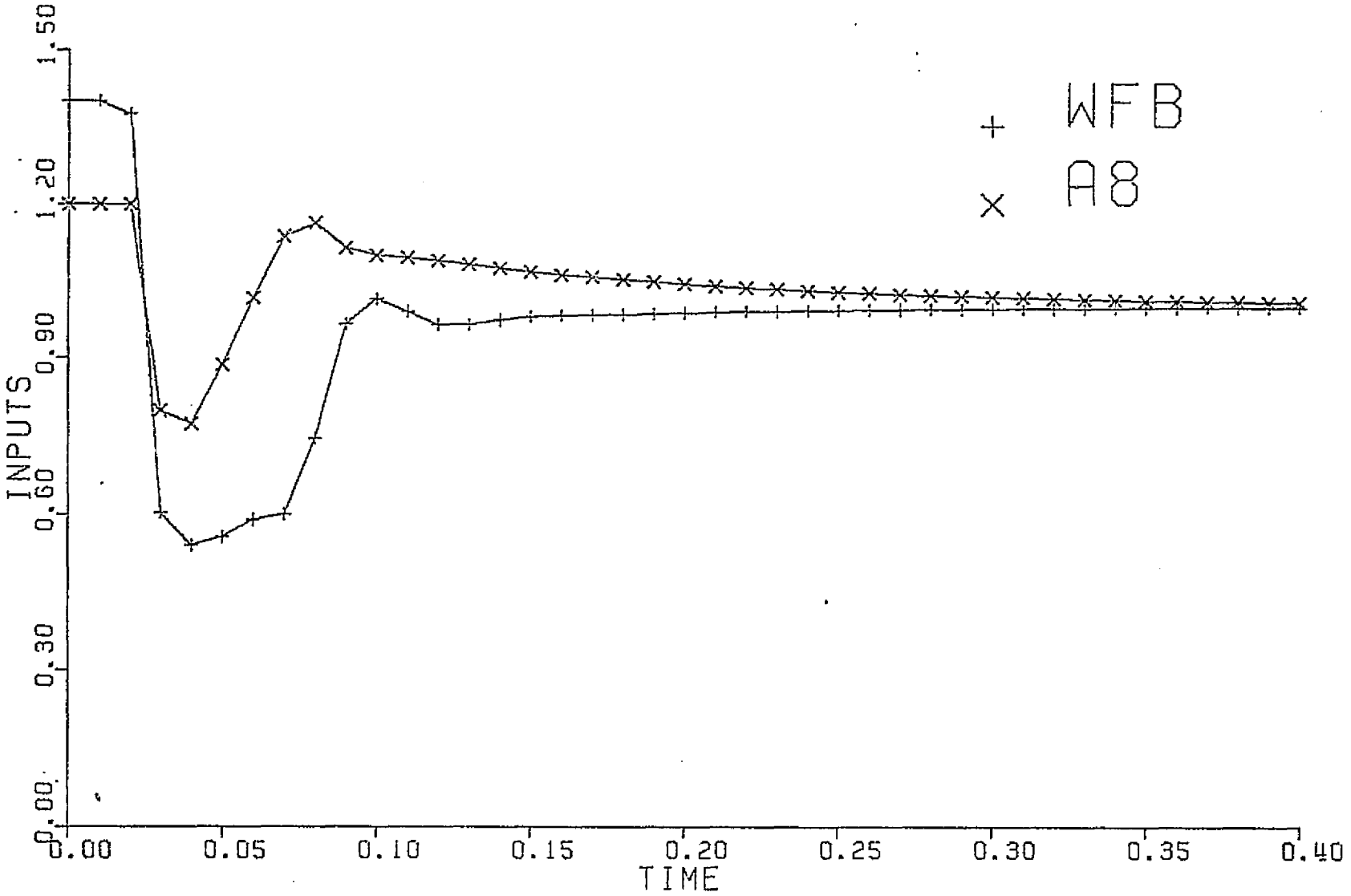

FIGURE 6.1. Model 2 Simulation Utilizing Model 2L2 (Unconstrained) Control Law; Δx (Quantization) = .02

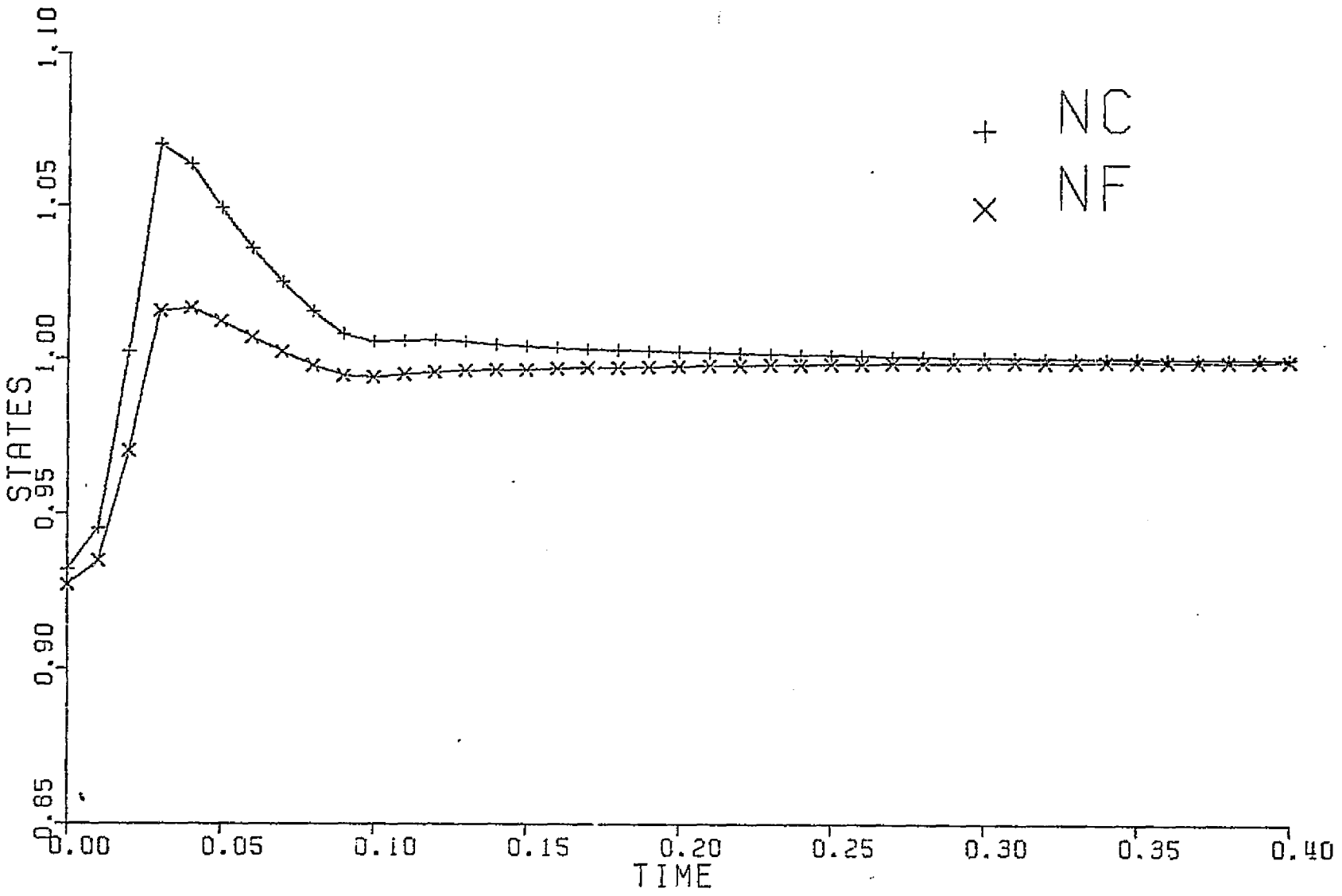

FIGURE 6.2. Model 2 Simulation Utilizing Model 2L2 (Unconstrained) Control Law; Δx (Quantization) = .02

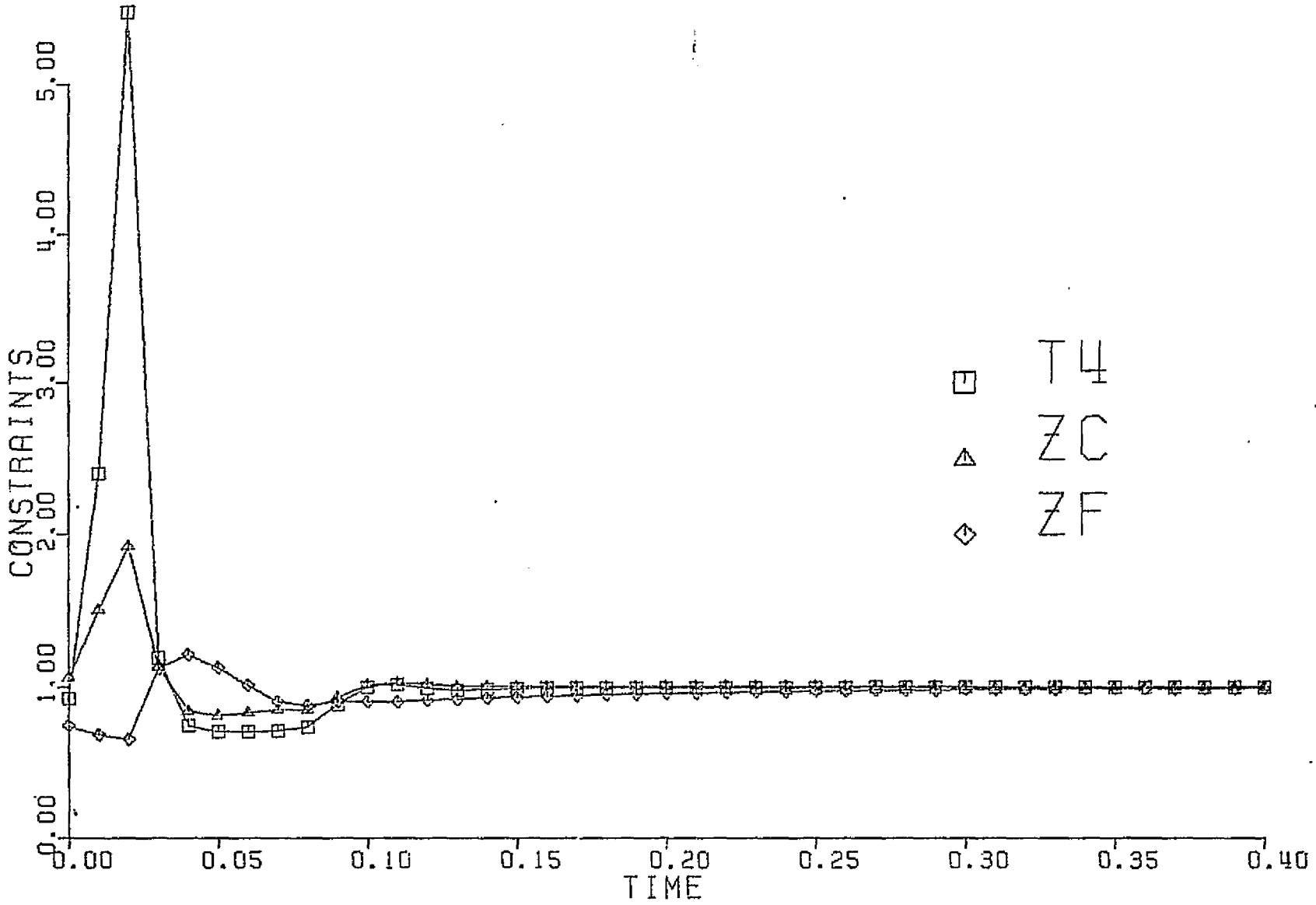

FIGURE 6.3. Model 2 Simulation Utilizing Model 2L2 (Unconstrained) Control Law; Δx (Quantization) = .02

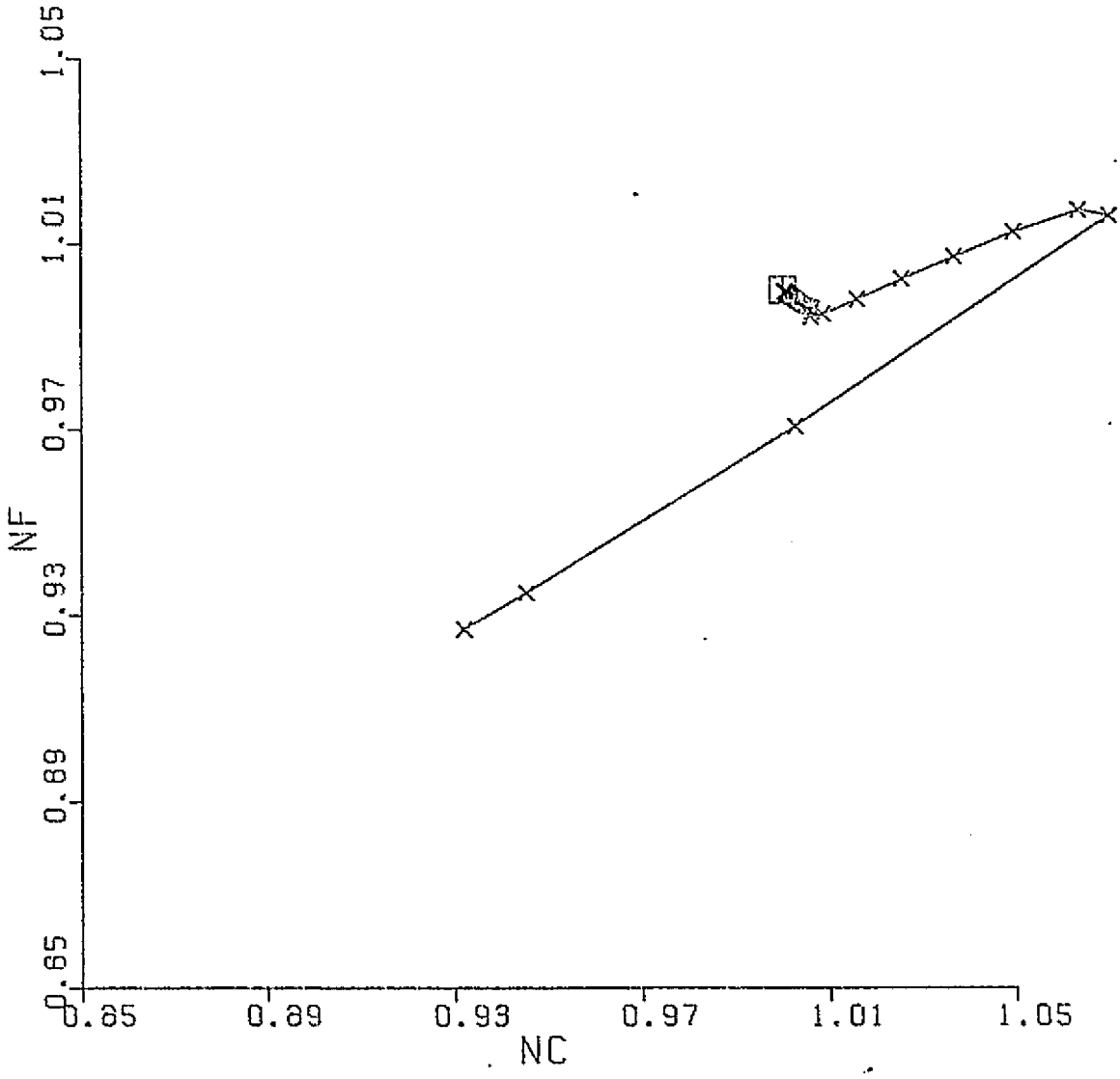

FIGURE 6.4. Model 2 Simulation Utilizing Model 2L2 (Unconstrained) Control Law; Δx (Quantization) = .02; marks indicate .01 second intervals

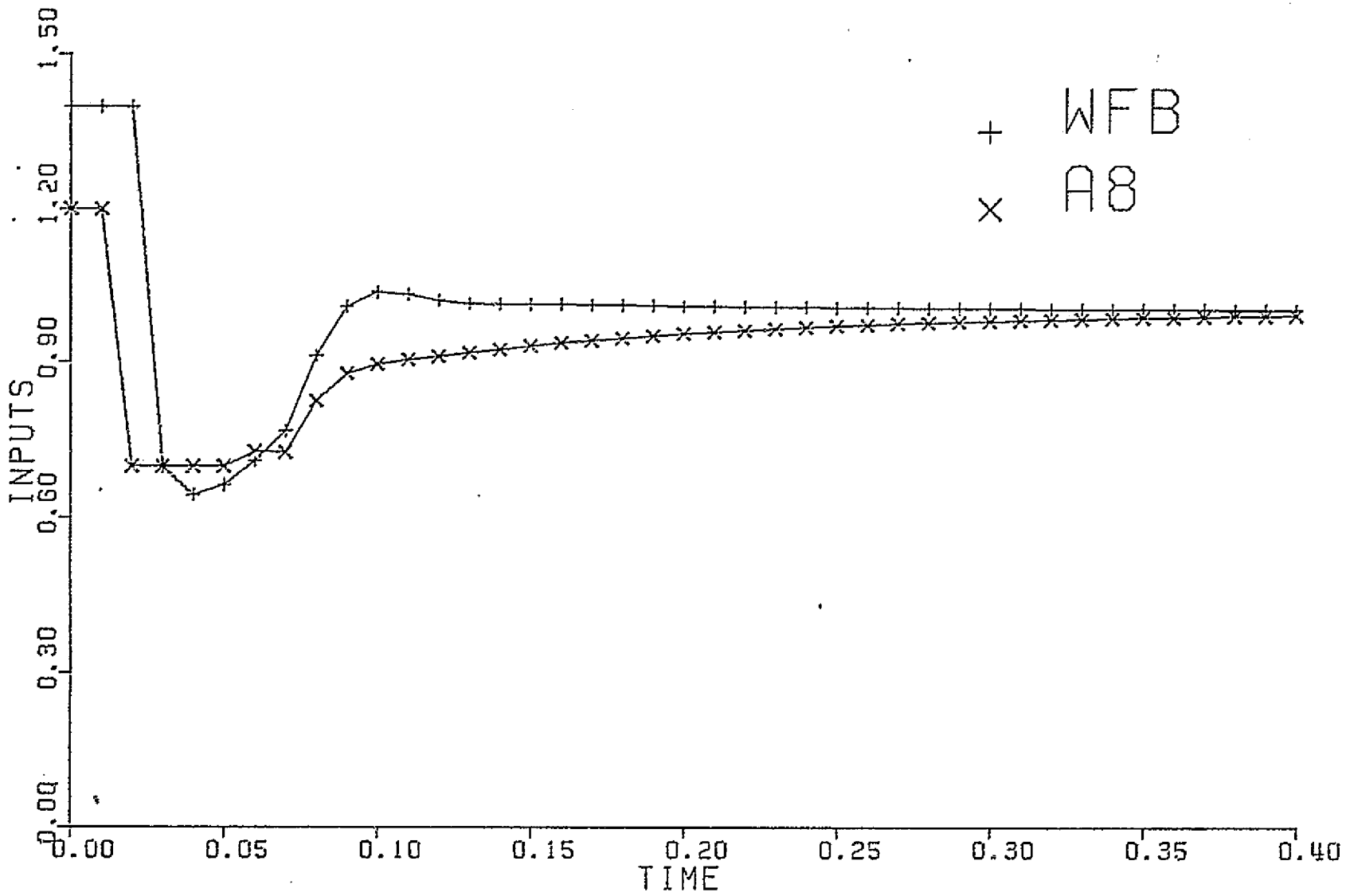

FIGURE 6.5. Model 2 Simulation Utilizing Model 2 (Unconstrained) Control Law; Δx (Quantization) = .02

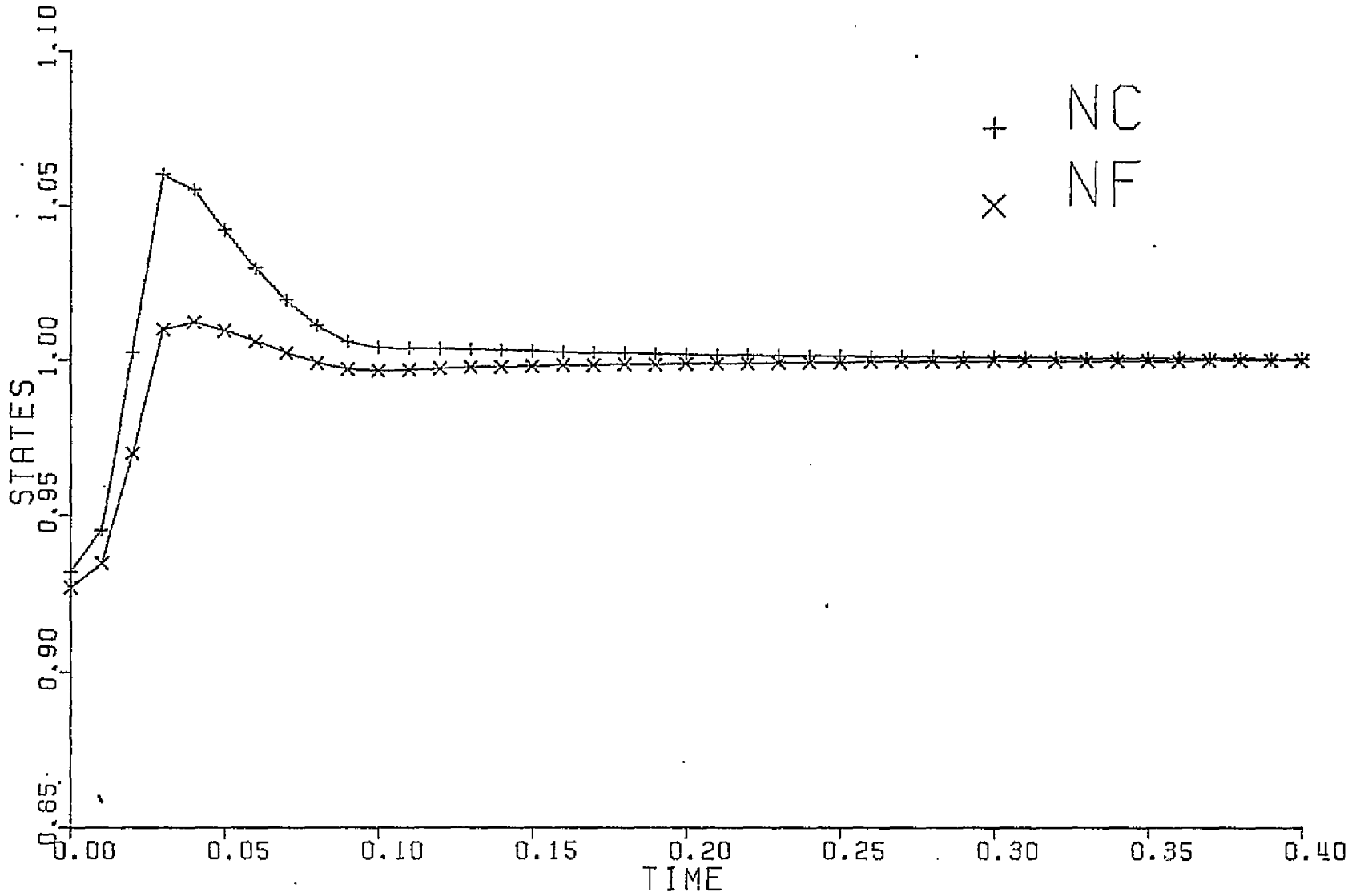

FIGURE 6.6. Model 2 Simulation Utilizing Model 2 (Unconstrained) Control Law; Δx (Quantization) = .02

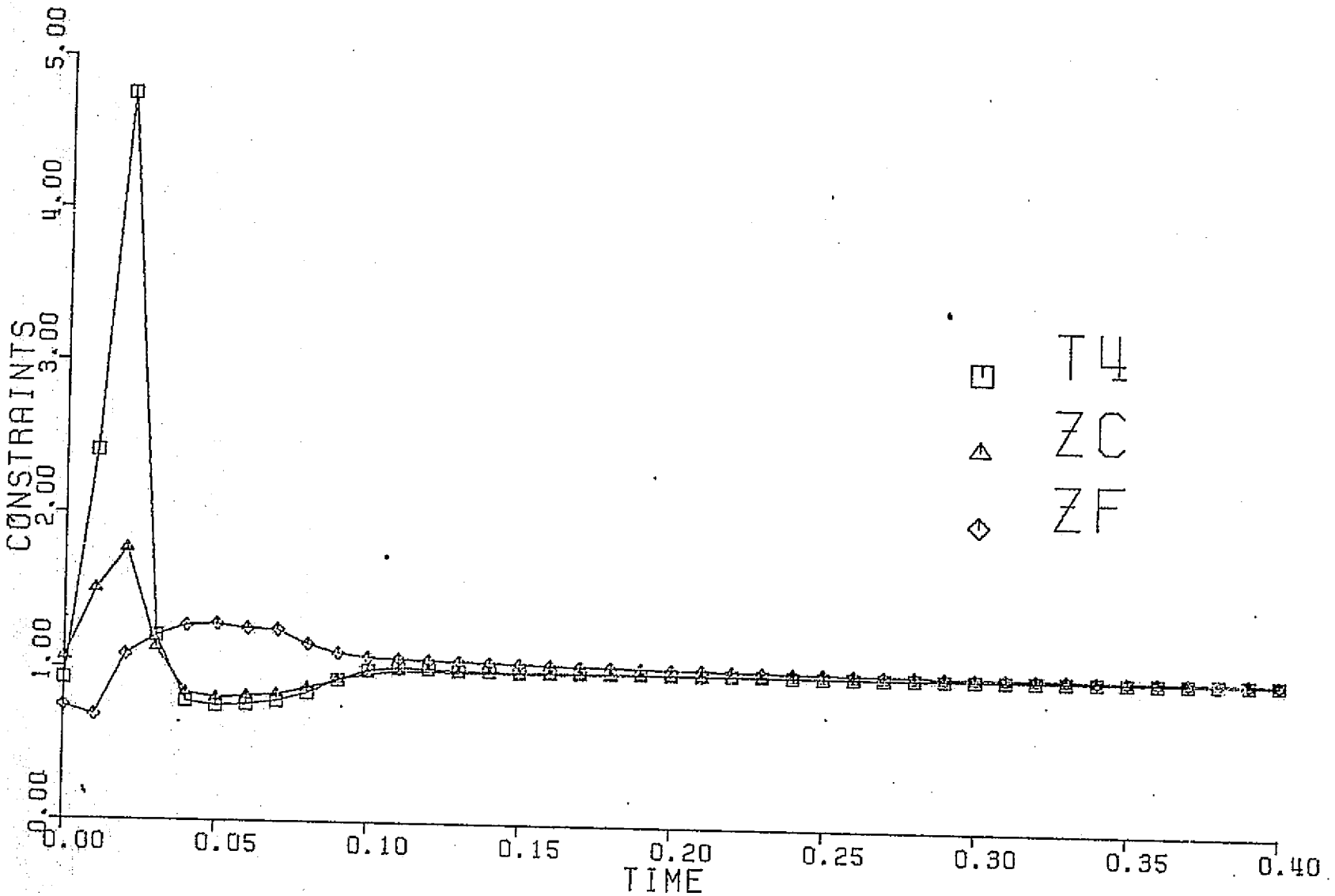

FIGURE 6.7. Model 2 Simulation Utilizing Model 2 (Unconstrained) Control Law; Δx (Quantization) = .02

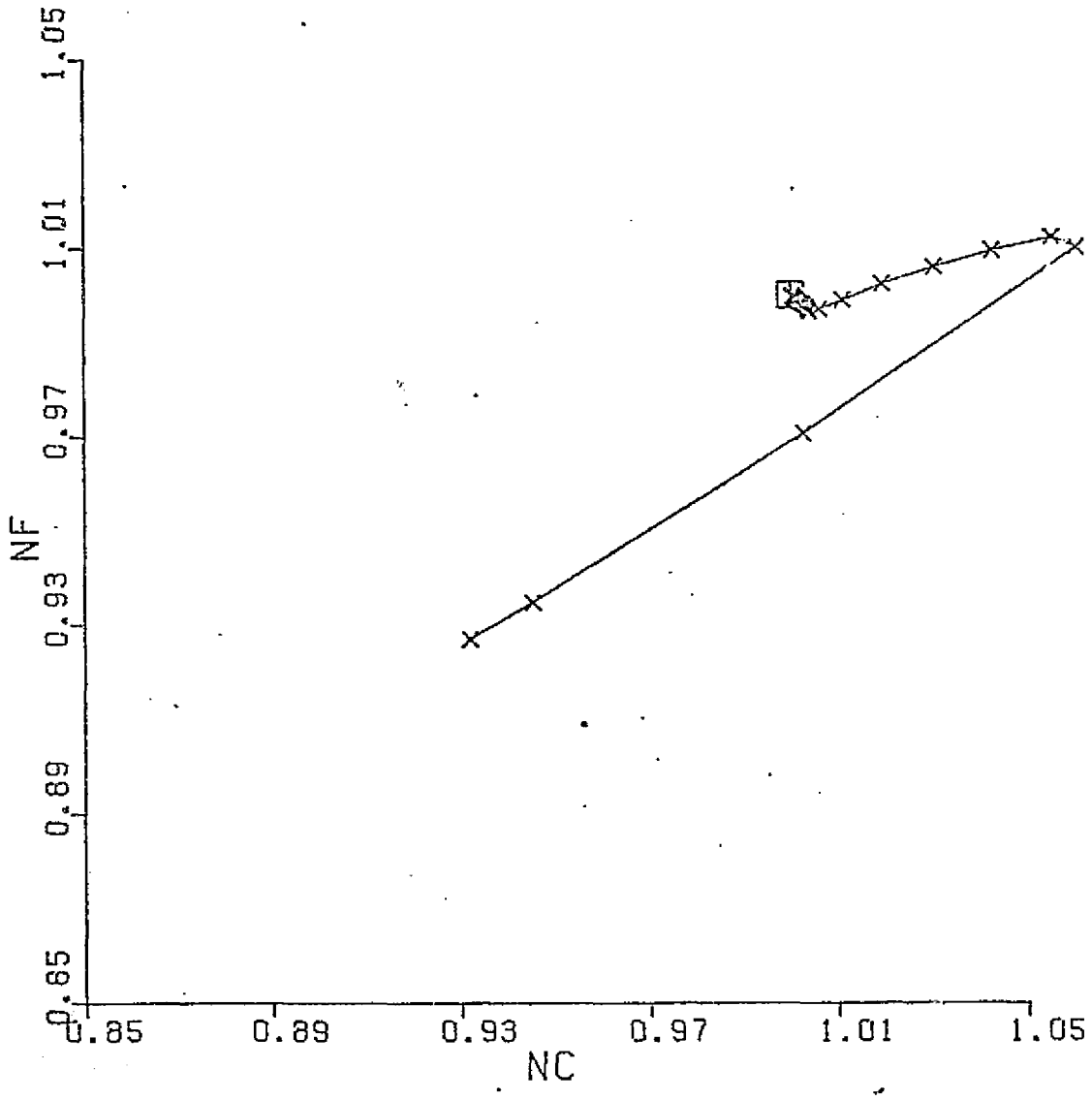

FIGURE 6.8. Model 2 Simulation Utilizing Model 2 (Unconstrained) Control Law; Δx (Quantization) = .02; marks indicate .01 second intervals

trajectories are quite similar to the trajectories produced with the Model 2L2 control law. This is certainly striking evidence that Model 2 is a nearly linear system.

6.4 Model 2 Simulation, Utilizing Model 2 (Constrained) Control Law

The effects of constraints on the control law can be quite clearly demonstrated. Figures 6.9 through 6.12 represent the results of the Model 2 simulation, utilizing the Model 2 (constrained) control law, as developed in Section 5.8. The starting state corresponds to a thrust of approximately 74% of the design value. The controls are considerably smoothed out, and Figure 6.10 shows that the state-time trajectories proceed to the target much slower and less abruptly, than was the case in the previous two sections. However, the constraints are now at acceptable levels, as evidenced by Figure 6.11. Furthermore, the control is riding both the turbine temperature and compressor surge margin constraints from the time = 0.02 seconds to time = 0.16 seconds. This agrees with the constraint analysis as shown in Figure 5.21 of the previous chapter. Unfortunately, the constraint limits, as given in equations (3.3-8), (3.3-9), and (3.3-10) are slightly exceeded, even in this simulation. This is not entirely unexpected, when considering the rather important fact that the effects of three state variables are not seen in these results. Recall that the optimal control law was derived (see Section 5.7), out of necessity, by employing linear approximations for states (3), (4), and (5) of Model 2 (see Table 2.5). The simulation of the controller as presented in this section uses no such approximation, and hence, some variation is expected. Furthermore, the choice of initial conditions for states (3), (4), and (5) introduces yet another consideration, and in fact, the particular choices for this simulation were somewhat arbitrary. Regardless of these slight

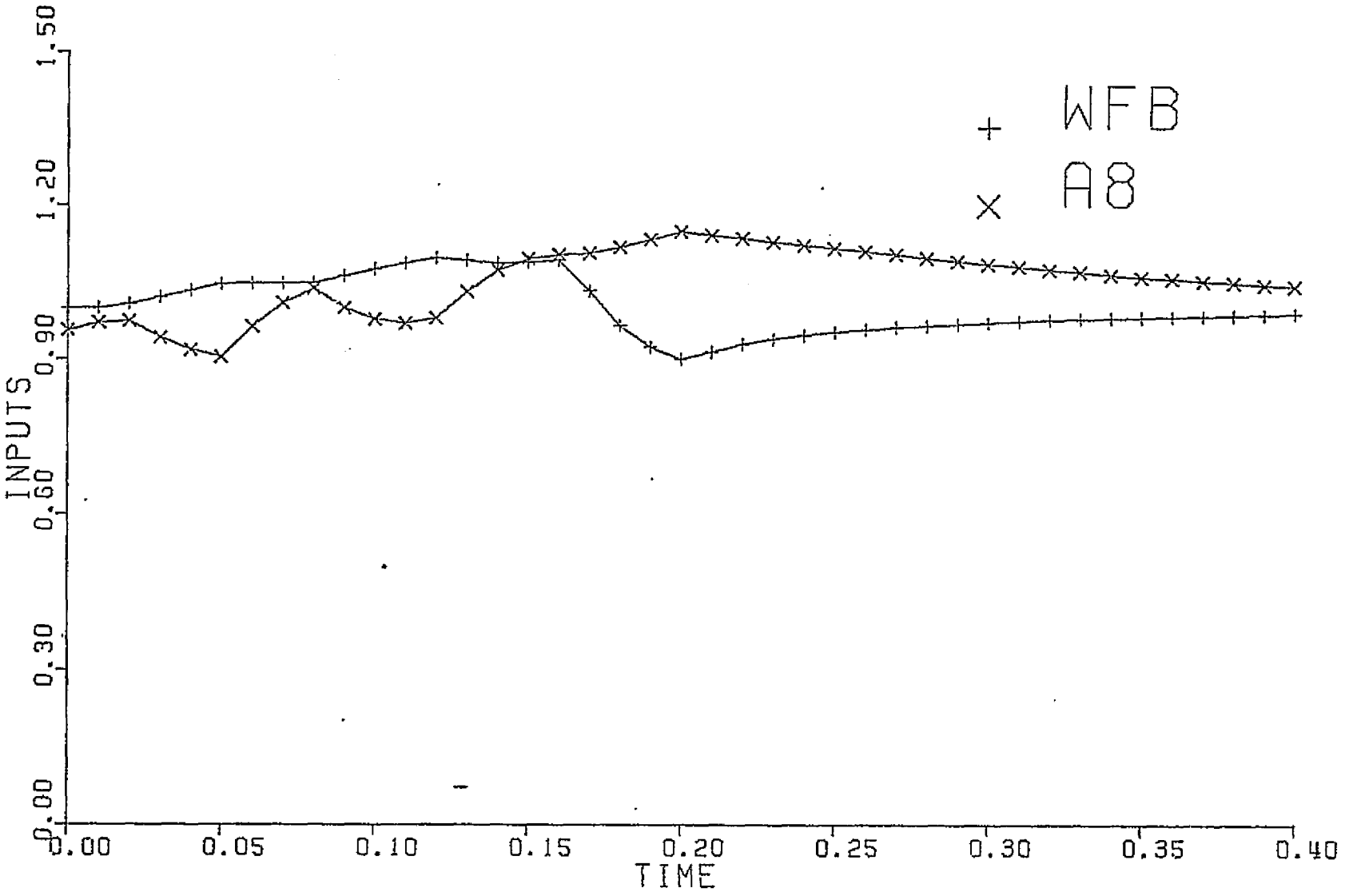

FIGURE 6.9. Model 2 Simulation Utilizing Model 2 (Constrained) Control Law;
Δx (Quantization) = .02

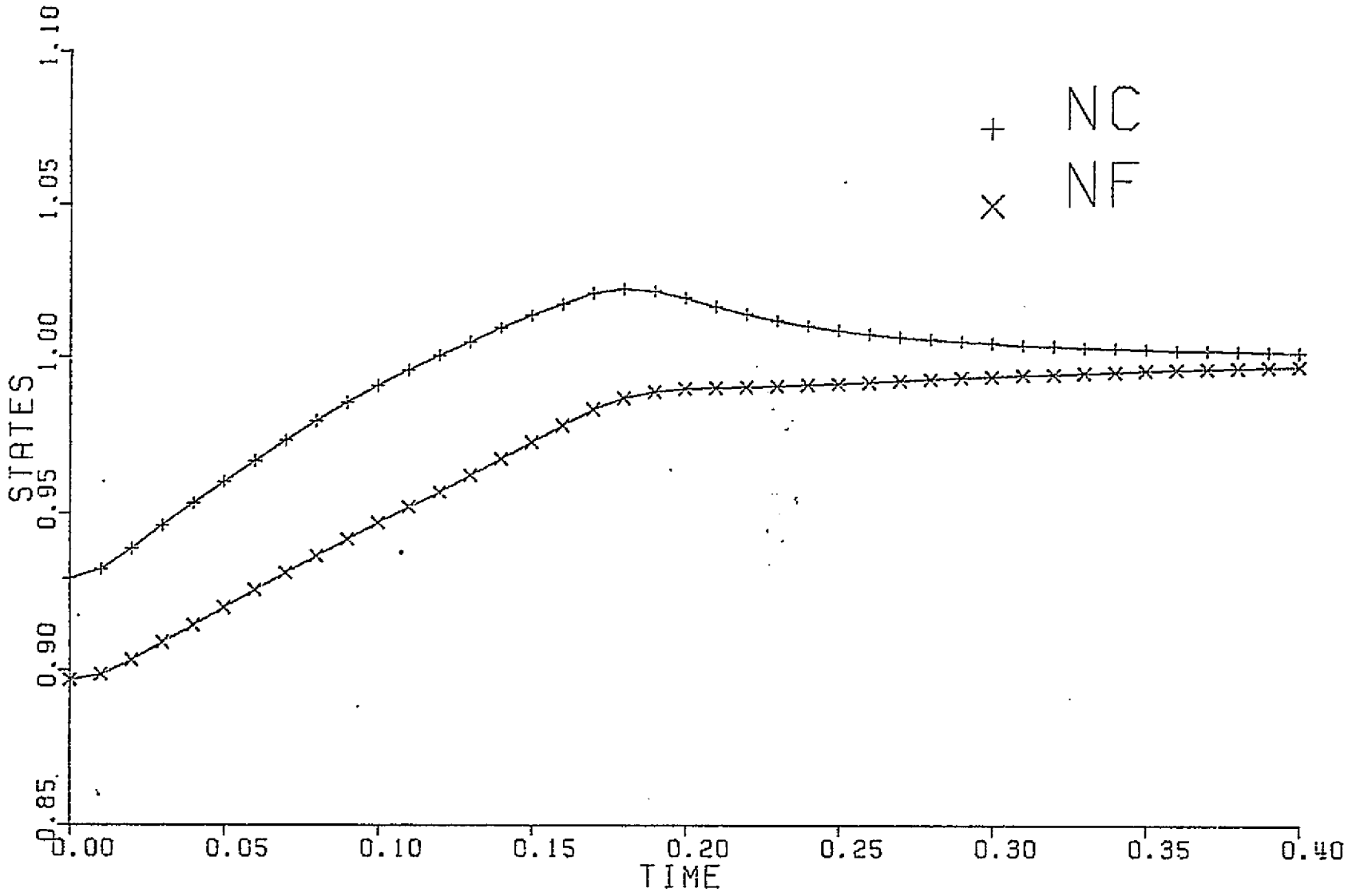

FIGURE 6.10. Model 2 Simulation Utilizing Model 2 (Constrained) Control Law; Δx (Quantization) = .02

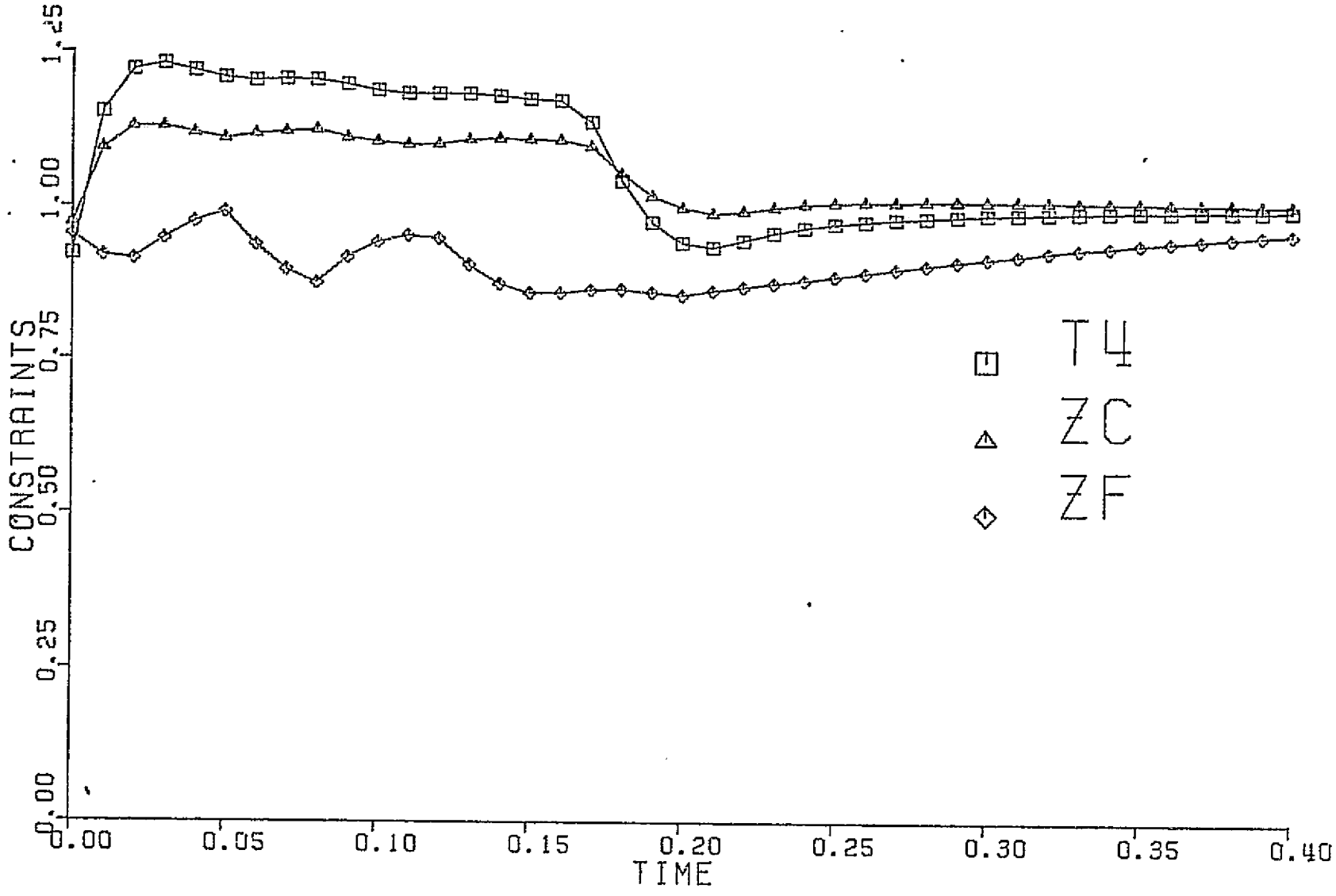

FIGURE 6.11. Model 2 Simulation Utilizing Model 2 (Constrained) Control Law; Δx (Quantization) = .02

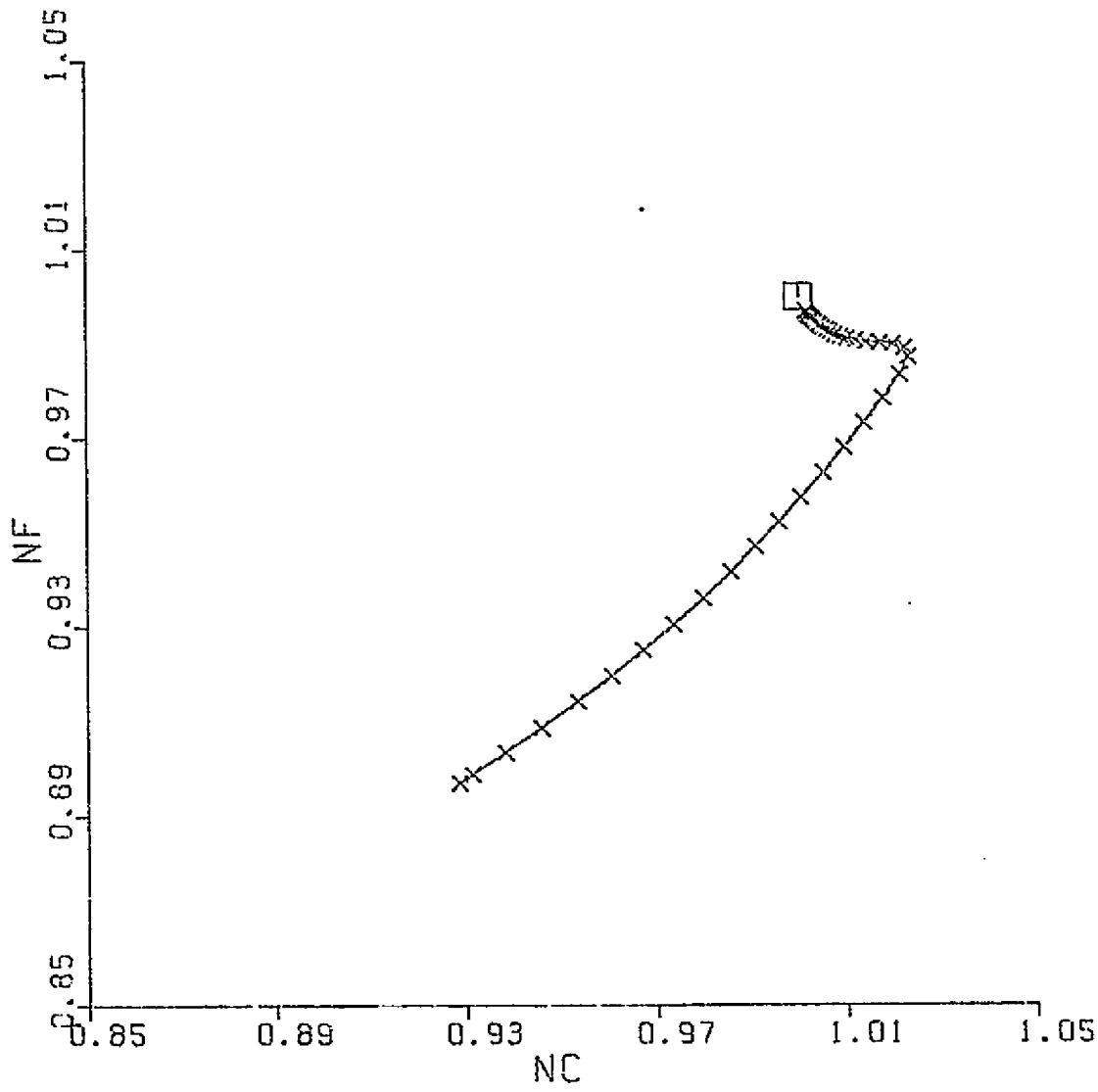

FIGURE 6.12. Model 2 Simulation Utilizing Model 2 (Constrained) Control Law; Δx (Quantization) = .02; marks indicate .01 second intervals

deficiencies, the cost is in good agreement with the Dynamic Programming results.

6.5 Model 1 Simulation Utilizing Model 2 (Constrained) Control Law

In view of all the evidence accumulated in Chapters 2 and 5 which show the differences between Model 1 and Model 2, non-optimal results are expected when applying on Model 1 a control law which was derived from Model 2. Indeed, this is clearly the case, as demonstrated by Figures 6.13 through 6.16. The starting state corresponds to an off-design point of (WFB = 2.2, A8 = 2.95) on the DYNGEN simulator, and is the same starting point as was used in Section 6.4. While the constraint variables are within acceptable limits, the state-time trajectories resemble very slow ramp functions. It takes 0.34 seconds to reach the target area and, while Model 1 is known to react more slowly than Model 2, it is not expected that the cost be that high. Clearly the control law is not satisfactory for use on Model 1.

6.6 Model 1 Simulation Utilizing Model 1L2 (Constrained) Control Law

Application of the Model 1L2 (constrained) control law produces the best results for Model 1. This is established by Figures 6.17 through 6.20, using the same starting state as the previous two simulations (approximately 74% of design thrust). After 0.23 seconds, both rotor speeds are within 1.0% of their respective design values, a significantly better performance than is provided by the Model 2 control law. It is somewhat slower, however, than the cost predicted by the Dynamic Programming results of Section 5.5 (.205 seconds). This is not disturbing, and perhaps quite satisfactory, when considering that Model 1 is a 16th order nonlinear simulation. It must be expected that the use of a second order linear approximation in obtaining a control law cannot

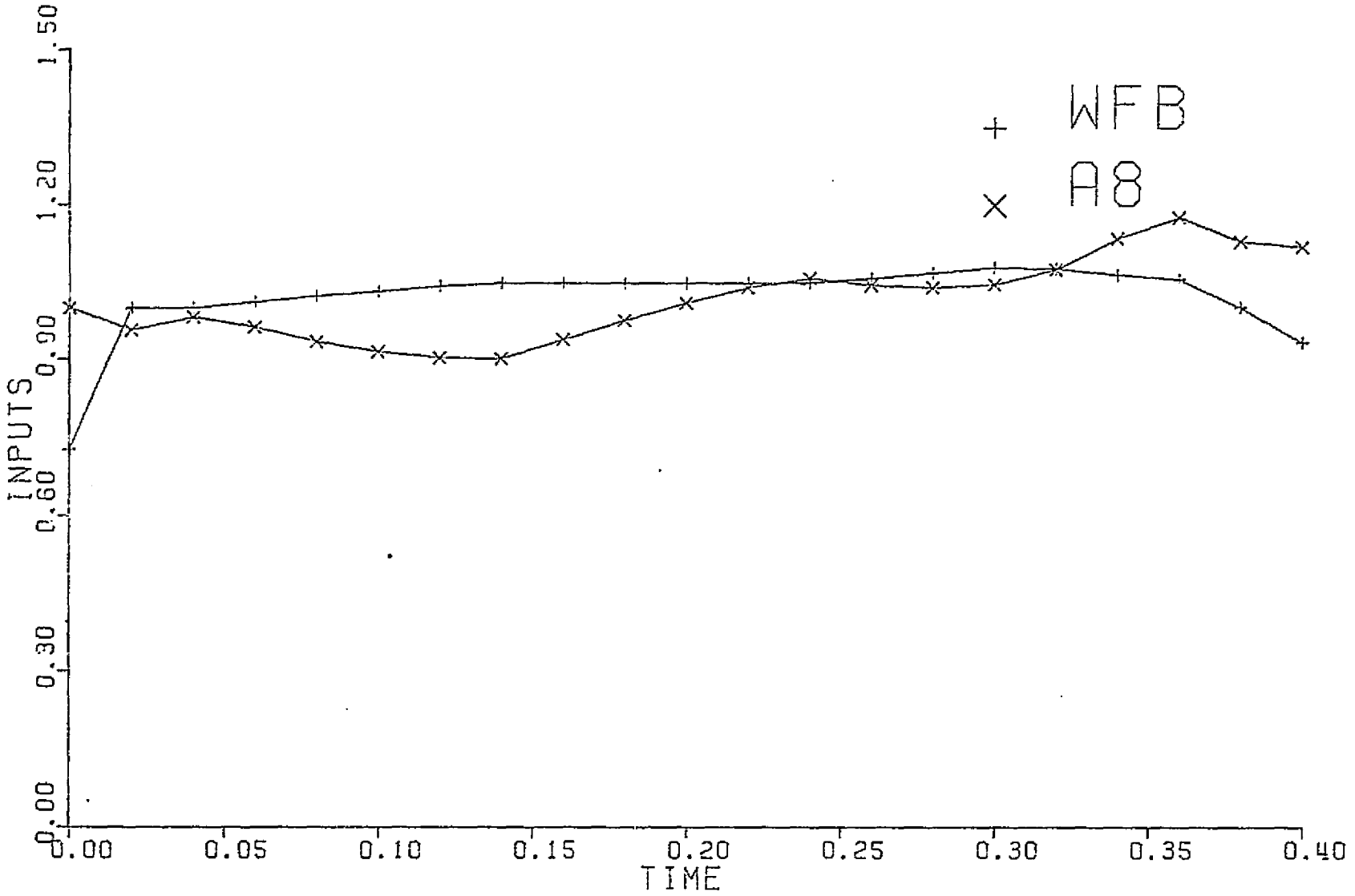

FIGURE 6.13. Model 1 Simulation Utilizing Model 2 (Constrained) Control Law;
Δx (Quantization) = .02

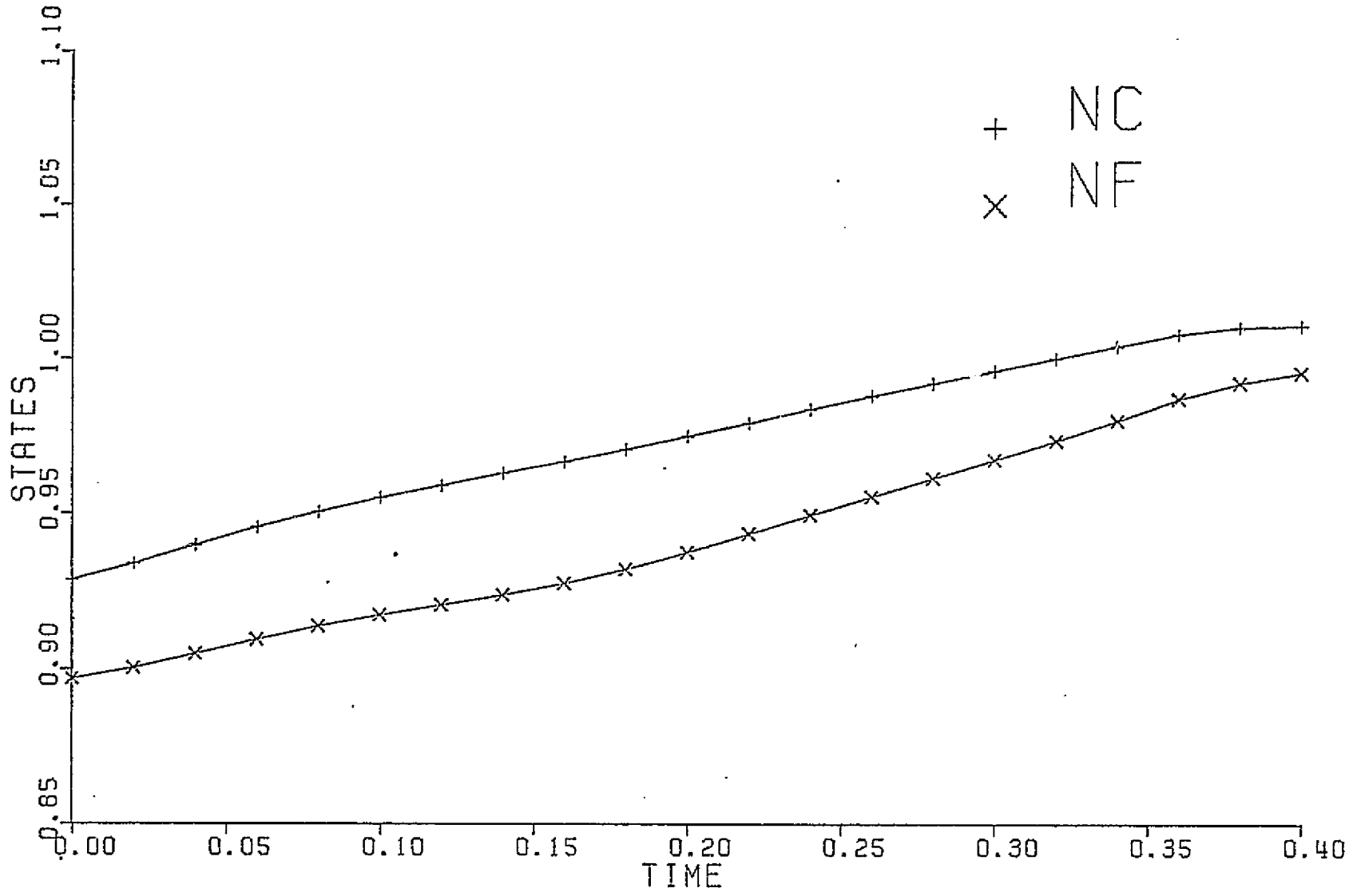

FIGURE 6.14. Model 1 Simulation Utilizing Model 2 (Constrained) Control Law; Δx (Quantization) = .02

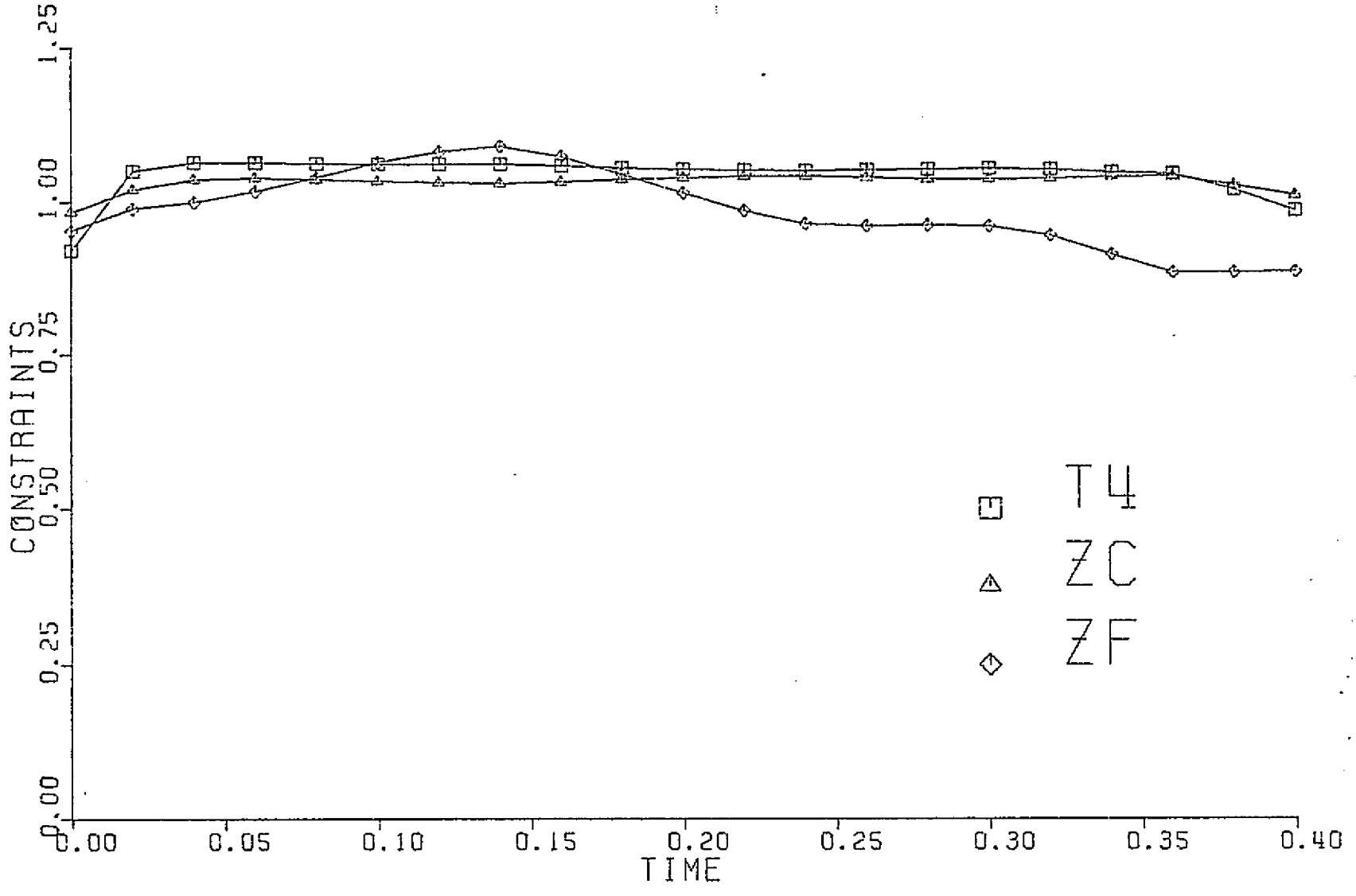

FIGURE 6.15. Model 1 Simulation Utilizing Model 2 (Constrained) Control Law; Δx (Quantization) = .02

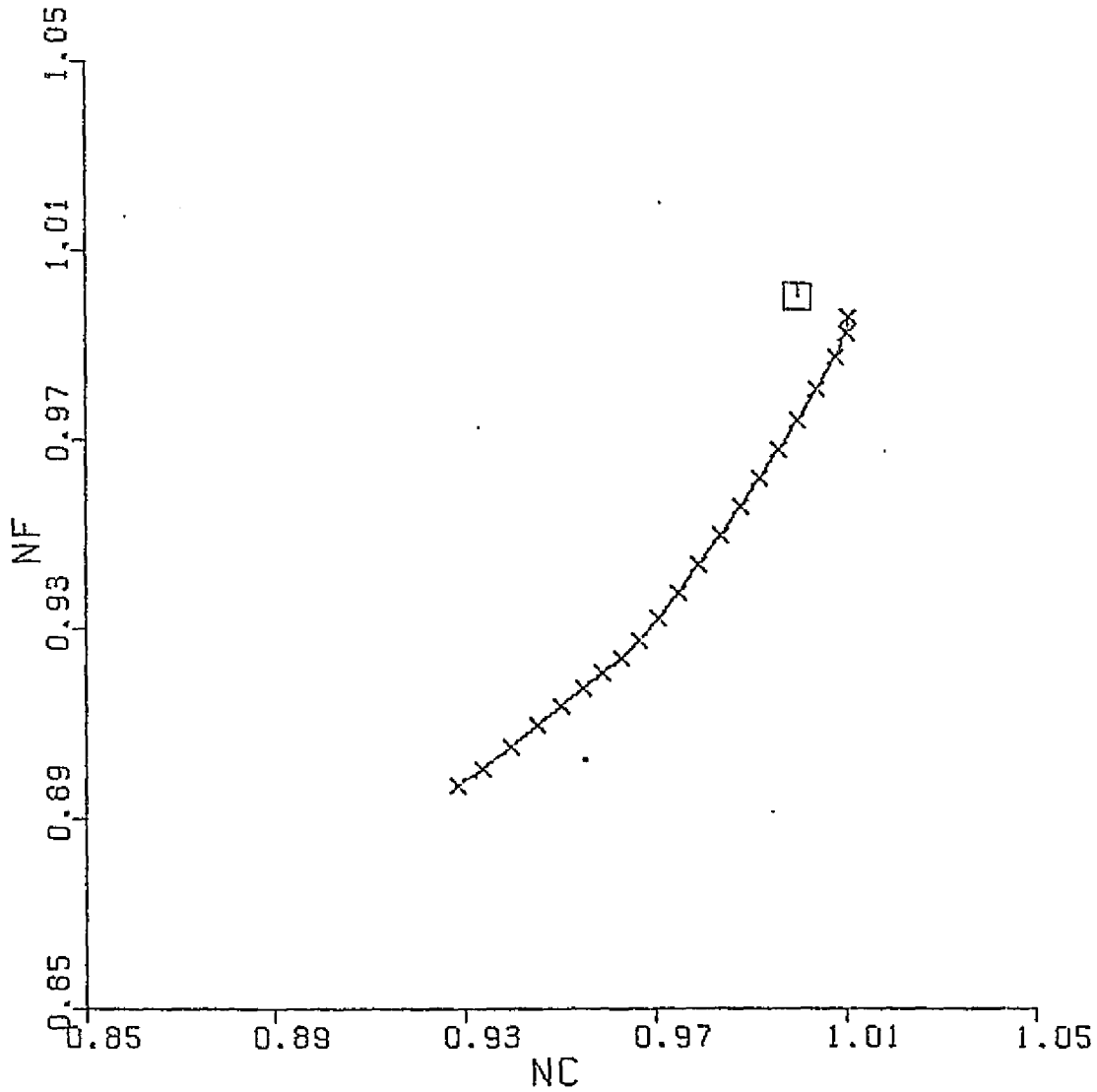

FIGURE 6.16. Model 1 Simulation Utilizing Model 2 (Constrained) Control Law; Δx (Quantization) = .02; marks indicate .02 second intervals

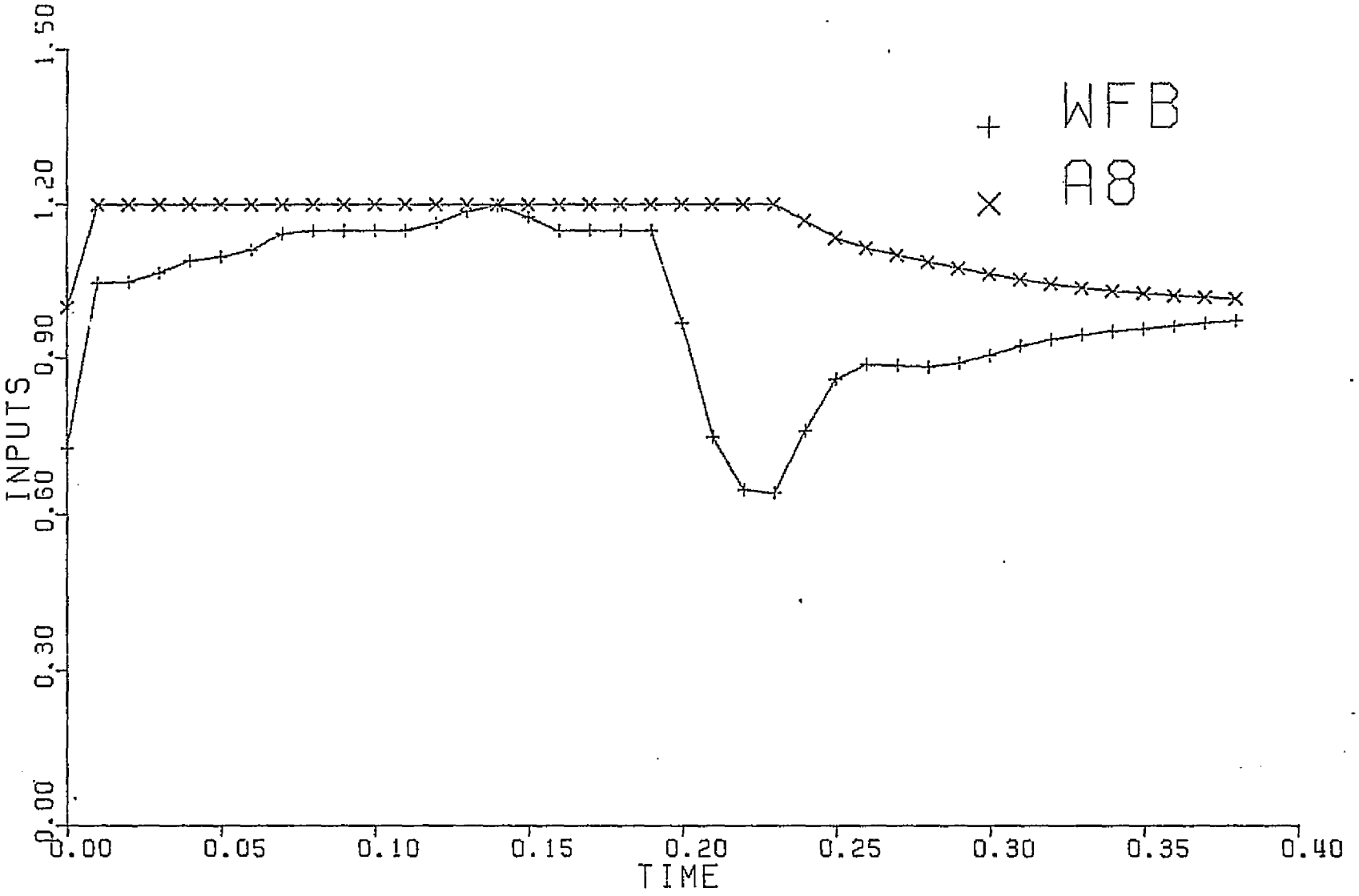

FIGURE 6.17. Model 1 Simulation Utilizing Model 1L2 (Constrained) Control Law; Δx (Quantization) = .01

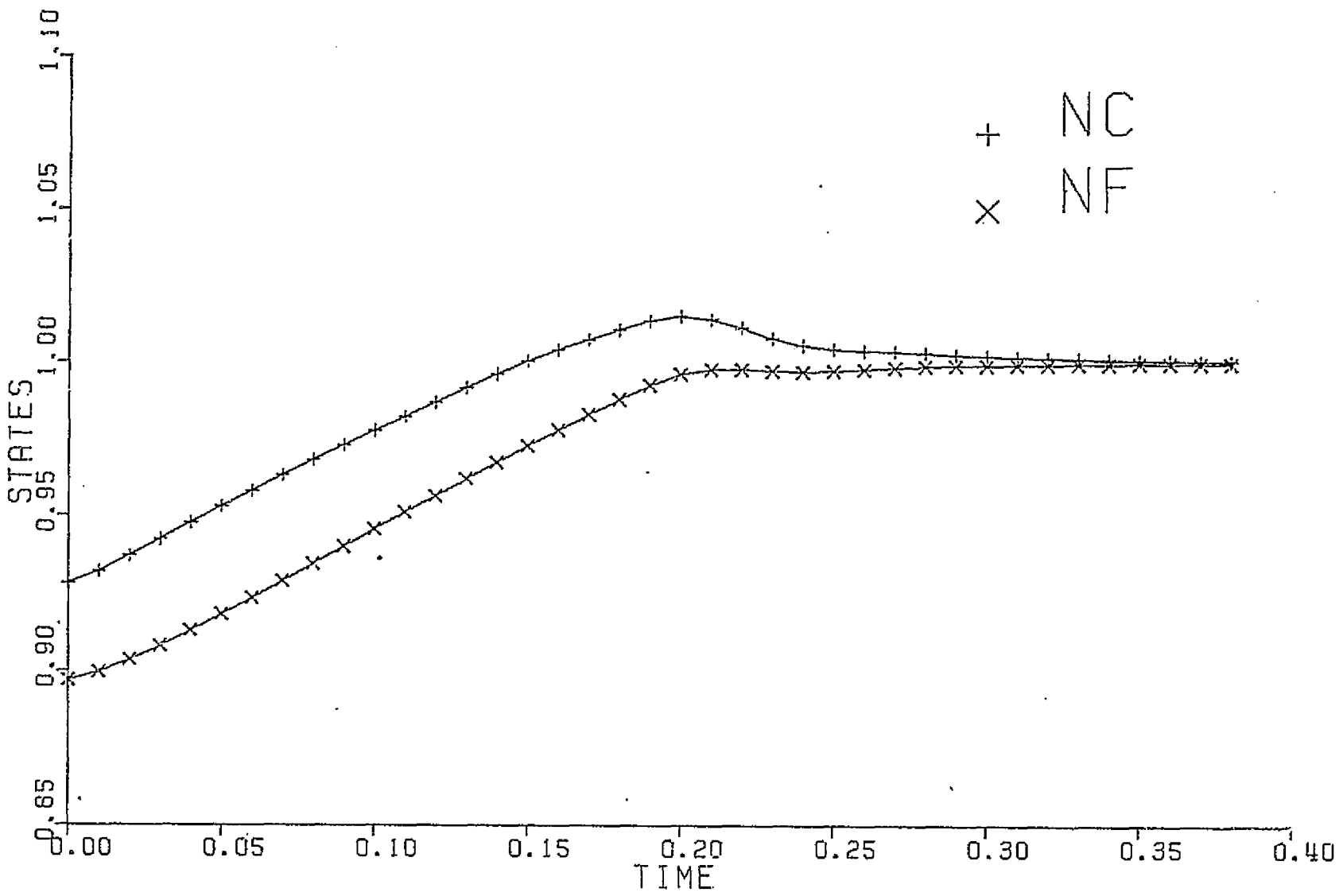

FIGURE 6.18. Model 1 Simulation Utilizing Model 1L2 (Constrained) Control Law; Δx (Quantization) = .01

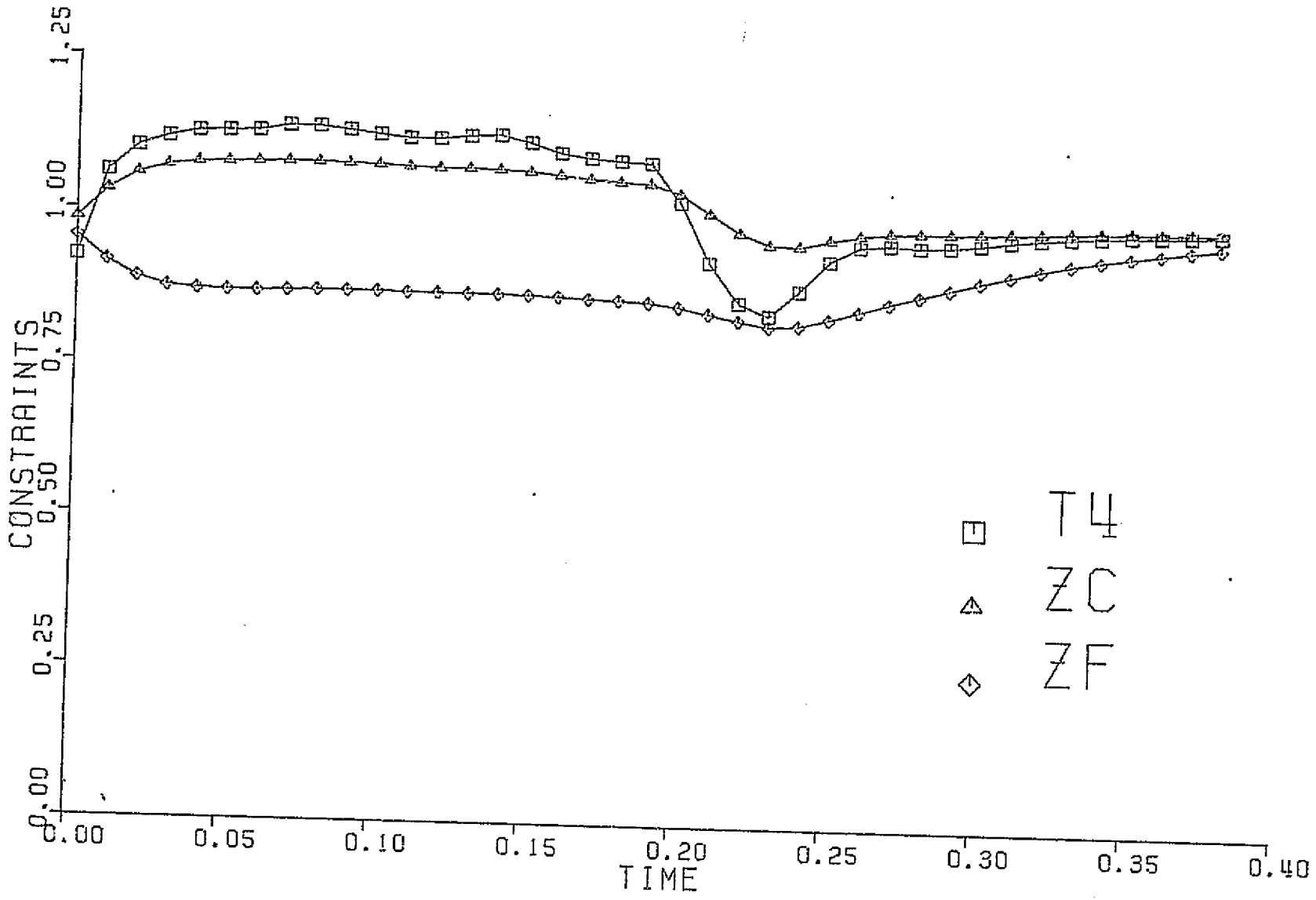

FIGURE 6.19. Model 1 Simulation Utilizing Model 1L2 (Constrained) Control Law; Δx (Quantization) = .01

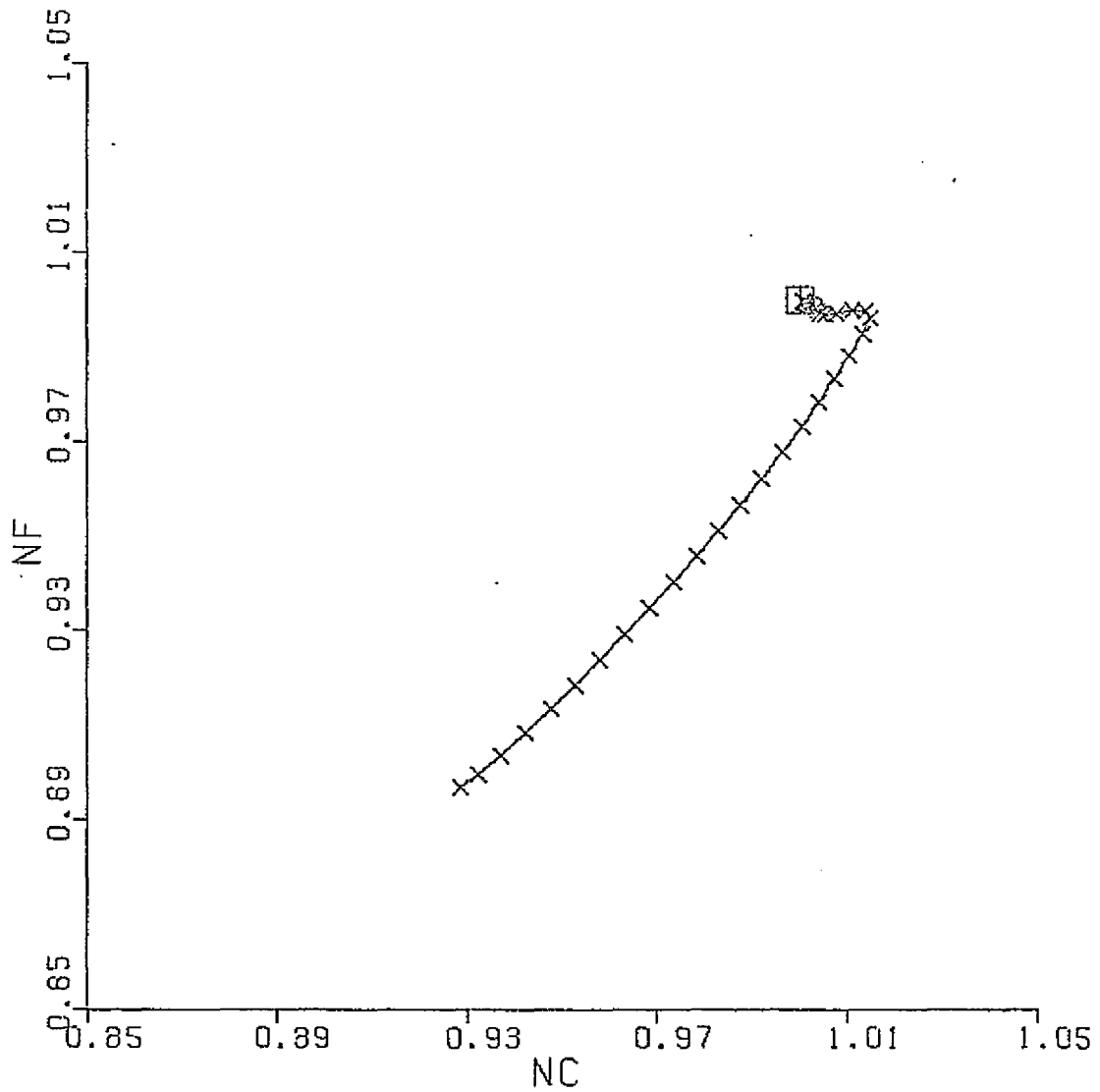

FIGURE 6.20. Model 1 Simulation Utilizing Model 1L2 (Constrained) Control Law; Δx (Quantization) = .01; marks indicate .01 second intervals

possibly result in the exact prediction of the minimum time it takes the trajectory to reach the target. The control quite clearly rides the turbine inlet temperature and compressor surge margin constraints over most of the trajectory, in agreement with the constraint analysis of Figure 5.18.

CHAPTER VII

SUMMARY

The goal of this work was to obtain a global nonlinear optimal control for a two spool turbofan jet engine. Various models were developed, pursuant to this goal. Most important of these models was the nonlinear analytically-expressed Model 2, which correctly models most of the qualitative behavior of the jet engine, but which fails to achieve strong numerical agreement with the non-analytical Model 1 simulator. The time optimal control program was then expressed in detail, and various constraints were added to the problem. Dynamic Programming theory and the Successive Approximations technique were explored, and applied to the problem of interest, while several improvements in the numerical programming were introduced. Analytical and numerical results were obtained for several models, both constrained and unconstrained. Finally, these results were tested on the two principal simulators, Model 1 and Model 2.

Indeed, this study has successfully achieved time optimal feedback control laws for various models of the two-spool turbofan jet engine. Furthermore, valuable insight into the nature of the problem has been obtained, and much useful computer software has been developed. Unfortunately, all enthusiasm for the results achieved in this study must be tempered by the realization that an optimal control law obtained from any model can only be as good as the model itself. For this reason, more work is needed to develop a better nonlinear analytical model, similar to Model 2 as presented in this study.

As the accuracy of these models is further improved, more consideration should also be given to the details which so greatly influence the time optimal feedback control law: the determination of the

allowable controls, U; and the limits placed on the selected constraint variables. As the entire analytical problem formulation (model, constraints, etc.) becomes closer and closer to the actual physical problem, more detailed solutions can then be obtained in the numerical analysis.

In conclusion, this study should be viewed as one more step in the efforts to achieve global optimal control laws for two-spool turbofan jet engines. It has accomplished much of its original goal, but leaves much more work remaining.

Appendix G

"DIRECT METHOD FOR OBTAINING NONLINEAR ANALYTICAL MODELS OF A JET ENGINE"

R. J. Leake
J. G. Comiskey

NATIONAL
ELECTRONICS
CONFERENCE

Oak Brook Executive Plaza #2 • 1211 W. 22nd St. • Oak Brook, Ill. 60521 • AC 312 325-5700

INTERNATIONAL FORUM
ON
ALTERNATIVES FOR LINEAR MULTIVARIABLE CONTROL

Hyatt Regency O'Hare Hotel
Chicago, Illinois, USA
October 13-14, 1977

A DIRECT METHOD FOR OBTAINING NONLINEAR ANALYTICAL MODELS OF A JET ENGINE

R. J. Leake and J. G. Comiskey

Department of Electrical Engineering
University of Notre Dame
Notre Dame, Indiana 46556

ABSTRACT

This paper describes an algorithm for obtaining a nonlinear analytical model of a jet engine from measurements of two equilibrium point values and the linearized A and B matrices at those points. The method is compared with more conventional procedures of interconnecting individual component approximations.

A DIRECT METHOD FOR OBTAINING NONLINEAR ANALYTICAL MODELS OF A JET ENGINE*

R. J. Leake and J. G. Comiskey

Department of Electrical Engineering
University of Notre Dame
Notre Dame, Indiana 46556

ABSTRACT

This paper describes an algorithm for obtaining a nonlinear analytical model of a jet engine from measurements of two equilibrium point values and the linearized A and B matrices at those points. The method is compared with more conventional procedures of interconnecting individual component approximations.

1. INTRODUCTION

In this work we continue the study of nonlinear analytical models for a two spool turbofan jet engine first reported in [1]. The model given in [1] is refined here and compared with an entirely new model which is the main subject of this paper. In order to distinguish the various models, we make the following designations.

Model 1. A large, flexible generalized engine simulator called DYNGEN which has been developed at NASA Lewis Research Center [2,3] and coded for a particular hypothetical two spool turbofan engine.

Model 2. An analytically expressed set of 5 nonlinear differential equations plus about 20 nonlinear static equations approximating the relationship between various engine variables.

Model 3. A relatively simple two-input, five-state model which can be generated automatically for any engine from data of two equilibrium points plus A and B matrices by the algorithm to be presented below.

2. DESCRIPTION OF MODEL 2

A refined and updated version of the two-input, five-state, two-output nonlinear analytical model presented in [1] is given in this section. The variable designations are:

U_1 = fuel flow (WFB)
U_2 = nozzle area (A_8)
X_1 = compressor rotor speed (N_C)
X_2 = fan rotor speed (N_F)
X_3 = burner exit pressure (P_4)
X_4 = after burner exit pressure (P_7)
X_5 = high inlet energy (U_4)
Y_1 = thrust (FG)
Y_2 = high turbine inlet temperature (T_4)

The system is completely specified as follows.

Constants

$J = AJ = 778.26$

$G = 32.174049$

$R = RA = .0252$

$\gamma^* = 1.4$

$P_2 = 518.668$

$I_C = PMIHP = 3.8$

$I_F = PMILP = 4.5$

$V_{COMB} = 1.65$

$V_{AFBN} = 49.77$

$CVMNOZ = .9494$

$CAPSF = 2116.217$

N_C DESIGN = XNHPDS = 10070

N_F DESIGN = XNLPDS = 9651

$\eta = 20.71175$

$C_{PC} = .24$

$C_{PF} = .24$

$C_{VB} = .20279$

$C_{PHT} = .22589$

$C_{PLT} = .27938$

$\phi = \frac{BLC}{WAC} = PCBLC = .16$

$\alpha = PCBLDU = .208$

$\beta = PCBLHP = .726$

$\gamma = PCBLLP = .066$

Design Equilibrium Point (Sea Level Static)

WFB = 2.75	$N_C = 11899.1$	FG = 13431.02
$A_8 = 2.9482558$	$N_F = 9873.95$	$T_4 = 2892.04$
	$P_4 = 23.9299$	
	$U_4 = 586.467$	
	$P_7 = 2.55142$	
CNF = 1.02310	$P_3 = 25.3522$	WG50 = 134.364
T21 = 742.957	$P_{21} = 2.9960$	WG4 = 118.375
CNC = .98730	WFMAX = 203.123	WG55 = 135.818
$T_3 = 1467.47$	PCMAX = 10.270	PFMAX = 3.3624
$T_{50} = 2103.47$	WG7 = 224.323	WAF = 221.573
$T_{55} = 1789.15$	WAC = 137.649	WCMAX = 54.4151
ZC = .81430	ZF = .8333	ΔWMAX = 1.5805
SFC = .737071	BYPASS = .609694	WG24 = 88.5047

State Equations

(1) $\frac{dN_C}{dt} = (\frac{30}{\pi})^2 \frac{J}{I_C N_C} [C_{PC} WAC(T_{21}-T_3) + C_{PHT} WG50(T_4-T_{50})]$

(2) $\frac{dN_F}{dt} = (\frac{30}{\pi})^2 \frac{J}{I_F N_F} [C_{PF} WAF(T_2-T_{21}) + C_{PLT} WG55(T_{50}-T55)]$

(3) $\frac{dP_4}{dt} = \frac{R\gamma^*}{V_{COMB}} [T_4 WA3 + WFB - WG4]$

(4) $\frac{dP_7}{dt} = \frac{R\gamma^* T_7}{V_{AFBN}} [WG4 - WFB - WA3]$

(5) $\frac{dU_4}{dt} = \frac{C_{VB} R T_4}{V_{COMB} P_4} [T_4(WG4 - WFB - WA3) + \gamma^*(T_3 WA3 - T_4 WG4 + T_4(1+n)WFB)]$

Nonlinear Functions Required for State Equations

(1) $CNF = \frac{N_F}{N_F DESIGN} = \frac{N_F}{9651}$

(2) $T_{21} = T_2 + 214.2732\ CNF^2 - 48(A_8 - 2.948255)$

(3) $CNC = \frac{N_C}{N_C DESIGN \sqrt{T_{21}/T_2}} = \frac{N_C}{10070\sqrt{T_{21}/518.668}}$

(4) $T_3 = T_{21} + 743.2722\ CNC^2 - 68(A_8 - 2.948255)$

(5) $T_4 = U_4/C_{VB}$

(6) $T_{50} = .727\ T_4$

(7) $P_3 = 1.05944\ P_4$

(8) $P_{21} = -6.20568 + .0129774\ T_{21} - .0185376\ P_3$

(9) $W_{FMAX} + 261.01\ CNF - 63.196$

(10) $P_{FMAX} = 3.516739\ CNF - .23561$

(11) $WAF = W_{FMAX} + 28.502\left[1 - e^{-2.313268(P_{FMAX} - P_{21})}\right]$

(12) $W_{CMAX} = 137.54 - 457.987\ CNC + 564.325\ CNC^2 - 188.113\ CNC^3$

(13) $\Delta W_{CMAX} = 6.492 - 4.9749\ CNC$

(14) $P_{CMAX} = 26.43184 - 89.0484\ CNC + 109.7243\ CNC^2 - 36.5756\ CNC^3$

(15) $WAC = \frac{P_{21}}{\sqrt{T_{21}/518.668}} \left\{ W_{CMAX} + \Delta W_{CMAX}\left(1 - e^{-.3662\left(P_{CMAX} - \frac{P_3}{P_{21}}\right)}\right) \right\}$

(16) $WA3 = (1-\phi)WAC = .84\ WAC$

(17) $WG50 = 301.957\ P4/\sqrt{T_4}$

(18) $WG4 = WG50 - \beta\phi WAC = WG50 - .11616\ WAC$

(19) $WG55 = WG50 + \gamma\phi WAC = WG50 + .01056\ WAC$

(20) $T_{55} = 106.002 - .86154\ T_{50} - .10458\ CNC\sqrt{T_{21} T_{50}}$

(21) $T_7 = .49661\ T_{55} + 205.886\ P_7$

(22) $WG7 = \frac{1121.786\ P_7 A_8}{\sqrt{T_7}}$

Nonlinear Equations for Outputs

(1) $FG = .02951\ WG7\sqrt{1934.415\ T_7 + 68558.365} + 2116.217\ A_8(.53978\ P_7 - 1)$

(2) $ZC = \dfrac{(P_3/P_{21}) - 1}{P_{CMAX} - 1}$

(3) $ZF = \dfrac{P_{21} - 1}{P_{FMAX} - 1}$

3. DIRECT METHOD

We now consider a direct computer method for obtaining nonlinear models. Let

$$\dot{x} = f(x,u) \tag{1}$$

with x an n vector and u an m vector denoting a dynamical system such as a jet engine, in which the state variables and parameters u remain positive throughout the system operation and there is a function g(u) such that for each equilibrium point

$$f(x,u) = 0 \longleftrightarrow x = g(u) \tag{2}$$

The steady state system analysis involves the study of the function g(u).

We propose to approximate the system (1) by

$$\dot{x} = A(x)[x - g(u)] \tag{3}$$

where A(x) is a square matrix which varies as a function of x. Notice that if x_D is an equilibrium point of (1), $x_D = g(u_D)$, then a linearization about this equilibrium point results in the linear system

$$\delta\dot{x} = A_D\delta x + B_D\delta u \tag{4}$$

and a linearization of the approximating system (2) at $x_D = g(u_D)$ results in

$$\delta\dot{x} = A(x_D)\delta x + \left[-A(x_D)\frac{\partial g}{\partial u}(u_D)\right]\delta u \tag{5}$$

Hence, the linearization of (2) will match the linearization of (1) if and only if

$$A(x_D) = A_D, \qquad -A_D\frac{\partial g}{\partial u}(u_D) = B_D \tag{6}$$

Also, if A_D is invertible, as is often the case for jet engine models, equation (6) yields

$$\frac{\partial g}{\partial u}(u_D) = -A_D^{-1}B_D \tag{7}$$

The basic idea of the proposed direct method is to use the above developments together with function approximations for A(x) and g(u) to arrive at a nonlinear model. Since equilibrium points and linearized models at those points can be obtained by known algorithms, we shall use this fact. Our initial approach is to use just two equilibrium points, say x_D and x_W. The input information is thus

$$x_D,\ x_W,\ u_D,\ u_W,\ A_D,\ A_W,\ B_D,\ B_W \tag{8}$$

where x_D and x_W are design and off-design equilibrium points. A_D and A_W are the system A-matrices at these points and u_D, u_W, B_D, B_W, are the associated parameter and input matrices. Mathematically,

$$A_D = \frac{\partial f(x_D,u_D)}{\partial x} \qquad B_D = \frac{\partial f(x_D,u_D)}{\partial u} \tag{9}$$

We shall employ a linear approximation for $A(x)$, given by

$$A(x) = A_W \operatorname{diag} \frac{x_{D_j} - x_j}{x_{D_j} - x_{W_j}} + A_D \operatorname{diag} \frac{x_j - x_{W_j}}{x_{D_j} - x_{W_j}} \tag{10}$$

in which diag $(\cdot)$ is a diagonal matrix which causes the jth column of $A(x)$ to be interpolated linearly between the jth columns of A_W and A_D with x_j as the interpolation variable.

The parameter vector u is presumed to be made up of physical control variables, and parameters such as altitude and Mach number. The equilibrium function is to be approximated in a manner such that both the equilibrium values and the linearizations of the approximating system (3) match those of system (1) at both x_D and x_W. This requires then that

$$g(u_D) = x_D \qquad g(u_W) = x_W \tag{11}$$

and also

$$\frac{\partial g}{\partial u}(u_D) = -A_D^{-1}B_D, \qquad \frac{\partial g}{\partial u}(u_W) = -A_W^{-1}B_W . \tag{12}$$

The method we propose here is to approximate each scalar component $g_i(u)$ of $g(u)$ by a <u>linear affine power law</u> form

$$g_i(u) = c_1 u_1 + \ldots + c_m u_m + c_{2m+1} u_1^{c_{m+1}} u_2^{c_{m+2}} \cdots u_m^{c_{m+m}} + c_{2m+2} \tag{13}$$

for which the jth partial derivative is

$$\frac{\partial g_i}{\partial u_j} = c_j + c_{2m+1} c_{m+j} \frac{u_1^{c_{m+1}} \cdots u_m^{c_{m+m}}}{u_j} \tag{14}$$

Now, if the variables are normalized and scaled such that

$$u_D = (1,1,\ldots,1) = \underline{1} \qquad u_W = (a,a,\ldots,a) = \underline{a} \tag{15}$$

then, the conditions of (11) and (12) can be put in the form

$$\begin{aligned}
k_j &= \frac{\partial g_i}{\partial u_j}(1) = c_j + c_{2m+1} c_{m+j} \\
k_{m+j} &= \frac{\partial g_i}{\partial u_j}(a) = c_j + c_{2m+1} c_{m+j} a^{\Sigma c_{m+j} - 1} \\
k_{2m+1} &= g_i(1) = \Sigma c_j + c_{2m+1} + c_{2m+2} \\
k_{2m+2} &= g_i(a) = a \Sigma c_j + c_{2m+1} a^{\Sigma c_{m+j}} + c_{2m+2}
\end{aligned} \tag{16}$$

and summing the first two of these over j yields

$$\begin{aligned}
\Sigma k_j &= \Sigma c_j + c_{2m+1} \Sigma c_{m+j} \\
\Sigma k_{m+j} &= \Sigma c_j + c_{2m+1} a^{\Sigma c_{m+j} - 1} \Sigma c_{m+j} \\
k_{2m+1} &= \Sigma c_j + c_{2m+1} + c_{2m+2}
\end{aligned} \tag{17}$$

$$k_{2m+2} = a\Sigma c_j + c_{2m+1} a^{\Sigma c_{m+j}} + c_{2m+2}$$

which is of the form

$$\begin{aligned} s_1 &= r_1 + r_3 r_2 \\ s_2 &= r_1 + r_3 r_2 a^{r_2 - 1} \\ s_3 &= r_1 + r_3 + r_4 \\ s_4 &= a r_1 + r_3 a^{r_2} + r_4 \end{aligned} \tag{18}$$

which, incidentally, is the m=1 condition also. This set of transcendental equations is solved numerically for r_1, r_2, r_3, r_4 and (16) is then used to solve for each c_j. In the event that (18) has no solution, a best fit is made on the second equation by varying r_2 while the other conditions are satisfied exactly.

4. ALGORITHM OF THE DIRECT METHOD

In this section, we present an algorithm which serves to automate the process of finding a nonlinear model for a system

$$\dot{x} = f(x,u) \tag{1}$$

to be approximated from $x_D, u_D, x_W, u_W, A_D, B_D, A_W, B_W$, by a normalized system. The algorithm will automatically perform the normalization and, hence, actually approximate the system

$$\dot{\hat{x}} = \hat{f}(\hat{x},\hat{u}) \tag{2}$$

where $\hat{x}_i = x_i/x_{D_i}$, $\hat{u}_j = u_j/u_{D_j}$. The approximating system is of the form

$$\dot{\hat{x}} = \hat{A}(\hat{x})[\hat{x} - \hat{g}(\hat{u})] \tag{3}$$

where

$$\hat{A}(\hat{x}) = \hat{A}_W \operatorname{diag} \frac{\hat{x}_{D_i} - \hat{x}_i}{\hat{x}_{D_i} - \hat{x}_{W_i}} + \hat{A}_D \operatorname{diag} \frac{\hat{x}_i - \hat{x}_{W_i}}{\hat{x}_{D_i} - \hat{x}_{W_i}} \tag{4}$$

and

$$\hat{g}_i = \sum_j c^i_j u^*_j + c^i_{2m+1} \prod_j u^{*\,c^i_{m+j}}_j + c^i_{2m+2} \tag{5}$$

where $u^*_j = \alpha_j \hat{u}_j + \beta_j$.

Algorithm I.

1. Input: $x_D, u_D, A_D, B_D, m, n, a, \varepsilon, x_W, u_W, A_W, B_W$
2. Calculate:

$$\hat{A}_D = \operatorname{diag}(1/x_{D_i})\, A_D \operatorname{diag}(x_{D_i})$$

$$\hat{A}_W = \operatorname{diag}(1/x_{D_i})\, A_W \operatorname{diag}(x_{D_i})$$

$$\hat{B}_D = \operatorname{diag}(1/x_{D_i})\, B_D \operatorname{diag}(u_{D_i})$$

$$\hat{B}_W = \mathrm{diag}(1/x_{D_i})\ B_W\ \mathrm{diag}(u_{D_i})$$

3. Calculate

$$\alpha_j = (1-a)u_{D_i}/(u_{D_j} - u_{W_j}) \qquad j = 1,\ldots,m$$

$$\beta_j = (au_{D_j} - u_{W_j})/(u_{D_j} - u_{W_j})$$

4. Calculate:

$$k^i_j = (-\hat{A}_D^{-1}\hat{B}_D)_{ij} \qquad k^i_{2m+1} = 1 = \hat{x}_{D_i} \qquad j = 1,\ldots,m$$

$$k^i_{m+j} = (-\hat{A}_W^{-1}\hat{B}_W)_{ij} \qquad k^i_{2m+2} = x_{W_i}/x_{D_i} = \hat{x}_{W_i} \qquad i = 1,\ldots,n$$

5. Calculate

$$s^i_1 = \sum_{j=1}^{m} k^i_j \qquad s^i_2 = \sum_{j=1}^{m} k^i_{m+j} \qquad i = 1,\ldots,n$$

$$s^i_2 = k^i_{2m+1} \qquad s^i_4 = k^i_{2m+2}$$

6. Go to Algorithm II.

Send: $s^i_1, s^i_2, s^i_3, s^i_4, a, \varepsilon$ $\qquad i = 1,\ldots,n$

Receive: $r^i_1, r^i_2, r^i_3, r^i_4, \gamma$

7. Calculate:

$$c^i_{2m+1} = r^i_3 \qquad c^i_{2m+2} = r^i_4 \qquad j = 1,\ldots,m$$

$$c^i_{m+j} = \frac{k^i_{m+j} - k^i_j + \gamma}{r^i_j(a^{r^i_2 - 1} - 1)} \qquad c^i_j = k^i_j - r^i_3\, c^i_{m+j} \qquad i = 1,\ldots,n$$

8. Output

$$c^i_1,\ldots, c^i_{2m+2}$$

$$\alpha_i,\ \beta_j \qquad j = 1,\ldots,m$$

$$\hat{x}_{D_i},\ \hat{x}_{W_i} \qquad i = 1,\ldots,n$$

$$\hat{A}_D,\ \hat{A}_W$$

Algorithm II

1. Input: $s_1, s_2, s_3, s_4, \varepsilon, a$

2. Calculate:

$$p_1 = s_1 - \frac{s_3 - s_4}{1-a}$$

$$p_2 = s_2 - \frac{s_3 - s_4}{1-a}$$

3. Minimize by line search:

$$\left| P_2 - P_1 \frac{ax^{x-1} - \frac{a^x-1}{a-1}}{x - \frac{a^x-1}{a-1}} \right|$$

for $-10 \leq x \leq 10$, $x \neq 0$, $x \neq 1$

4. Calculate:

$$r_2 = x \qquad r_3 = \frac{P_1}{r_2 - \frac{a^{r_2}-1}{a-1}}$$

$$r_1 = \frac{s_3 - s_4 + r_3(a^{r_2}-a)}{1-a} \qquad \gamma = \frac{1}{m}\left(s_1 - s_2 + r_2 r_3 \left(a^{r_2 - 1} - 1\right)\right)$$

$$r_2 = \frac{s_4 - as_3 - r_3(a^{r_2}-a)}{1-a}$$

5. Return to Algorithm I.6

5. NUMERICAL RESULTS

The algorithm of the previous section was applied to data obtained using DYNGEN with x_D and u_D specified as in Section 2. An off-design point was obtained using u_W = (.72727, .72727), with the resulting normalized state $\hat{x}_W$ = (.9000, .7897, .7381, .9401, .9454). The normalized A and B matrices are

$$\hat{A}_D = \begin{bmatrix} -3.8 & -1.277 & 2.067 & -1.152 & 1.448 \\ 2.748 & -5.39 & 1.585 & -1.991 & 1.071 \\ 377.9 & 49.51 & -264.9 & 86.807 & 78.91 \\ 31.26 & 139.39 & -6.269 & -88.69 & 27.83 \\ -176.5 & 23.91 & -10.27 & -37.4 & -246.7 \end{bmatrix} \qquad \hat{B}_W = \begin{bmatrix} -.00259 & .3553 \\ .2116 & -.31618 \\ 12.54 & -13.774 \\ -.6201 & -99.3 \\ 157.78 & 6.84 \end{bmatrix} \quad (1)$$

$$\hat{A}_W = \begin{bmatrix} -4.744 & -1.3888 & 3.2468 & -1.4591 & 1.1969 \\ .82186 & -26.726 & 2.5585 & -1.8609 & .45548 \\ 475.73 & 137.55 & -328.91 & 27.791 & 91.495 \\ -50.103 & 110.91 & 63.188 & -116.69 & 8.2883 \\ -186.77 & -67.682 & -41.681 & 24.586 & -243.23 \end{bmatrix} \qquad \hat{B}_W = \begin{bmatrix} -.04546 & .0013 \\ .0086 & -.0121 \\ 2.434 & -.613 \\ .67865 & -97.467 \\ 203.44 & .64755 \end{bmatrix} \quad (2)$$

Using the parameter value a = .7, the c_j^i coefficient which specify the equilibrium function $\hat{g}(\hat{u})$ as in Section 4 are given by the matrix

$$C = \begin{bmatrix} .24267 & -.00218 & 1.90082 & 8.09916 & .02864 & .73088 \\ 1.01593 & .85407 & .89872 & .66919 & -.81879 & -.05121 \\ .73445 & .10133 & 6.90586 & 3.09409 & .011495 & .15272 \\ .77234 & -.35905 & 2.49867 & 2.87415 & -075198 & .66191 \\ .39503 & -.27262 & -3.44682 & 13.4468 & .01838 & .85921 \end{bmatrix} \quad (3)$$

This matrix together with the values $\alpha = 1.1$ and $\beta = 0.1$ and the matrices $\hat{A}_D$ and $\hat{A}_W$ completely specify Model 3A.

Another model which we will call Model 3B is easily obtained by using a linear affine approximation to $\hat{g}(\hat{u})$ such that $\hat{g}(\hat{u}_D) = \hat{x}_D$, $\hat{g}(\hat{u}_W) = \hat{x}_W$. Model 3B is specified

by $a = e^{-1}$, $\alpha = 2.31778$, $\beta = -1.31778$ and the coefficient matrix

$$C = \begin{bmatrix} .1553 & .0028 & 1.0 & 1.0 & 0. & .8418 \\ .1619 & .1707 & 1.0 & 1.0 & 0. & .6674 \\ .5351 & -.1208 & 1.0 & 1.0 & 0. & .5857 \\ .5878 & -.49313 & 1.0 & 1.0 & 0. & .9053 \\ .2962 & -.2099 & 1.0 & 1.0 & 0. & .9137 \end{bmatrix} \quad (4)$$

In order to compare the four models, a test point x_T far removed from x_W was chosen by setting $\hat{u}_T = (.8,1)$, and calculating the equilibrium $\hat{x}_T$. A step change to $\hat{u} = (1,1)$ then causes an acceleration transient back to $\hat{x}_D$. The results of this comparison for the rotor speeds are shown in Table 1. More detailed information is shown for Models 1 and 2 in Figure 1.

	Model 1		Model 2		Model 3A		Model 3B	
t	N_c	N_F	N_c	N_F	N_c	N_F	N_c	N_F
0	.948	.929	.934	.901	.936	.940	.928	.925
.1	.968	.946	.985	.943	.958	.955	.954	.945
.3	.990	.977	1.004	.986	.984	.978	.983	.975
.5	.998	.993	1.004	.998	.994	.991	.995	.990
.7	1.000	.998	1.003	1.002	.998	.997	.998	.997

Table 1. Comparison of $\hat{x}_T$ Equilibrium and Acceleration Transients

6. DISCUSSION

A numerical algorithm for obtaining nonlinear analytical models for jet engines is presented. The method is to separate the transient A(x) and equilibrium g(u) parts of the system dynamics and approximate these using easily accessible data. The components of g(u) are approximated by a linear affine power law form. The principal numerical difficulty is that all boundary conditions may be impossible to meet. The algorithm then satisfies all but the second of the equations (18) in Section 3 and fits the second as closely as possible. The variable γ is zero when an exact fit occurs; but, otherwise, it causes a least squares fit on the derivative conditions at x_W of equations (16), Section 3, while matching the other conditions exactly. The free parameter in the linear affine approximation of Model 3B are handled similarly.

7. ACKNOWLEDGMENT

This research was supported by the National Aeronautics and Space Administration under Grant NASA NSG-3048.

8. REFERENCES

[1] W. E. Longenbaker, R. J. Leake, "Hierarchy of Simulation Models for a Turbofan Gas Engine," Proc. 8th Annual Pittsburgh Conference on Modeling and Simulation, April, 1977

[2] J. F. Sellers, C. J. Daniele, "DYNGEN - A Program for Calculating Steady State and Transient Performance of Turbojet and Turbofan Engines," NASA TN D-7901, April, 1975.

[3] L. Geyser, "DYGABCD - A Program for Calculating LInear A,B,C, and D Matrices from a Nonlinear Dynamic Engine Simulator," Tech. Report in Preparation at NASA Lewis Research Center, Cleveland, Ohio.

[4] W. E. Longenbaker, "Time Optimal Control of a Two-Spool Turbofan Jet Engine," MSEE Thesis, University of Notre Dame, 134 pages, September, 1977.

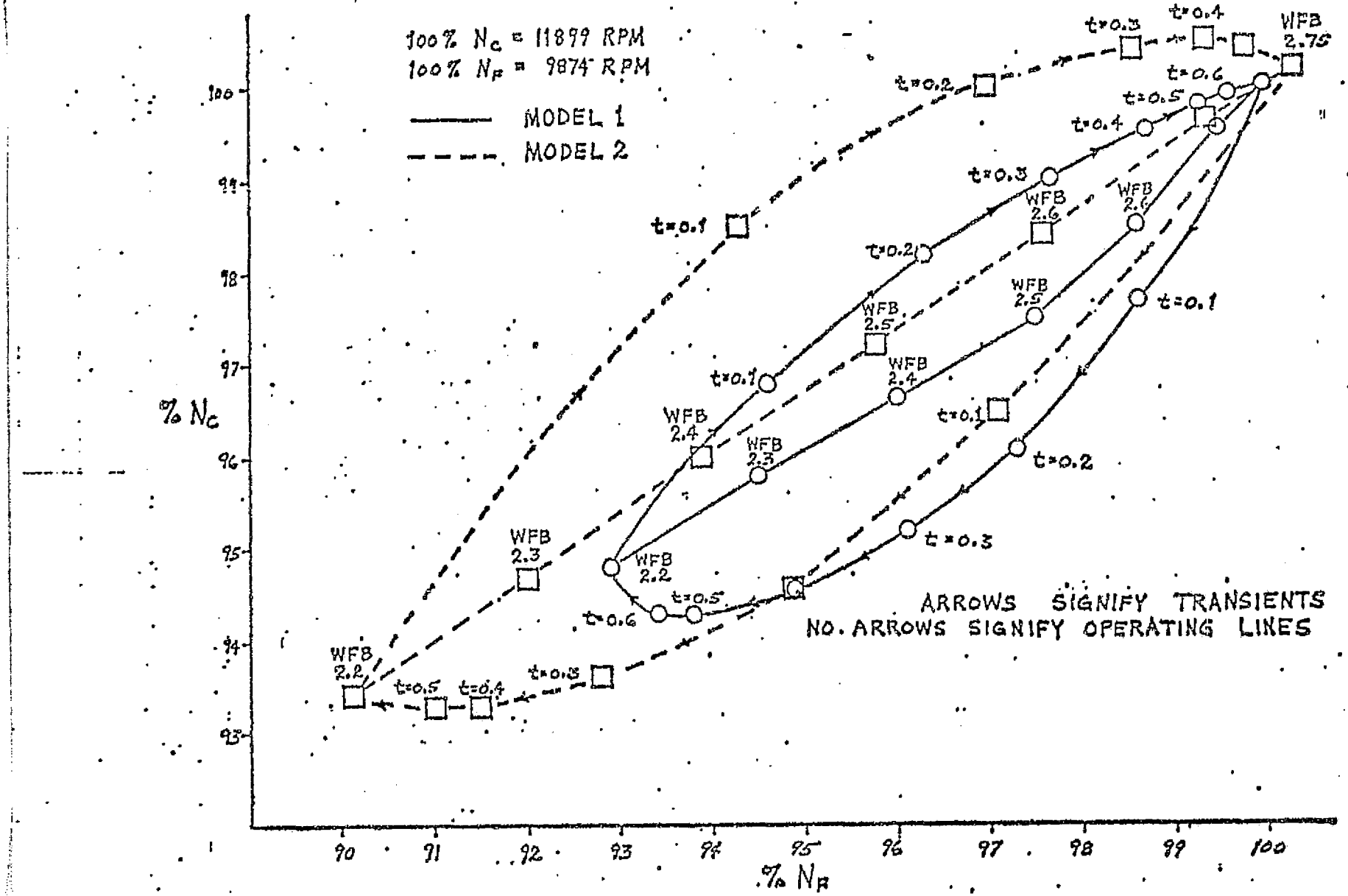

FIGURE 1. State Space Trajectories - Model 1 vs. Model 2

Appendix H

"SOME FEATURES OF CARDIAD PLOTS FOR SYSTEM DOMINANCE"

R. M. Schafer
M. K. Sain

SOME FEATURES OF CARDIAD PLOTS FOR SYSTEM DOMINANCE*

R. Michael Schafer
Department of Electrical Engineering
University of Notre Dame
Notre Dame, Indiana 46556

Michael K. Sain
Department of Electrical Engineering
University of Notre Dame
Notre Dame, Indiana 46556

Abstract

Recently, the CARDIAD (Complex Acceptability Region for DIAgonal Dominance) plot has been introduced and applied to the problem of designing dynamical precompensation to achieve column dominance. This paper illustrates several basic features of the method while using it to design a single, low-order dynamical compensator which achieves dominance at five operating points of a realistic two-spool turbofan digital simulation.

1. Introduction

The CARDIAD (Complex Acceptability Region for DIAgonal Dominance) plot is a graphical technique for choosing dynamical compensators to achieve diagonal row or column dominance, as defined by Rosenbrock [1]. Without essential loss of generality, the compensator is assumed to have its diagonal elements equal to unity, and a typical CARDIAD plot describes the acceptable range of the real and imaginary parts of the off-diagonal elements such that dominance is achieved. The basic graphical building block is the circle. Each circle represents the acceptable range at a specific frequency. Solid circles are drawn if acceptable real and imaginary pairs correspond to points inside the circle, and dashed circles are drawn if acceptable pairs correspond to points outside the circle. Plotted as a function of frequency, these circles describe the acceptable range of the compensator element in question, considered as a complex function of frequency.

Recently, CARDIAD plots have been shown to be an effective design tool in dynamical precompensation of multivariable plants to achieve dominance [2, 3, 4, 5]. This paper focuses upon another aspect of the CARDIAD plot, namely its ability to assist with the classification of various operating points of a nonlinear system with regard to their dominance possibilities and to help with the design of compensators which achieve dominance of multiple operating points.

*This work was supported in part by the National Aeronautics and Space Administration under Grant NSG 3048 and in part by the National Science Foundation under Grant ENG 75-22322.

2. Specific Assumptions

Plant models used to construct the plots in the sequel have been generated from the general purpose digital jet engine simulator DYNGEN [6] under a load which provides behavior similar to that of the F-100 two-spool turbofan engine at sea level static conditions. The models have two inputs, five states, and two outputs. They are linearizations of DYNGEN obtained with the aid of the DYGABCD package [7] under development at NASA Lewis Research Center. Physical description of the states can be found in the references [3]. The inputs are fuel flow and exhaust area; the outputs are thrust and high turbine inlet temperature. Parameterization is accomplished through the nominal value of the fuel flow WFB, which takes the five values 2.145, 2.31, 2.475, 2.64, and 2.75 LBM/SEC, ranging from a low thrust condition to high thrust without augmentation. All the models have been normalized.

Thus the plant transfer function matrix has two rows and two columns, and exhibits transfer functions of degree five in both numerator and denominator. Space limitations preclude their presence in this manuscript.

Denote the plant by G(s). Then the issue is to select a precompensator K(s) in such a way that G(s) K(s) is column dominant [1]. In particular, it is desired to select one K(s) so that column dominance is maintained over all five nominal fuel flow conditions.

3. General CARDIAD Features

If the origin of the CARDIAD plot for a given column is included by all solid circles and excluded by all dashed circles, that column of the system is dominant without further compensation, in as much as the origin represents unity compensation. Thus, the eventual goal of compensation using the CARDIAD plot method is to arrive at a system where all the CARDIAD plots have this feature. If there exists a point on the real axis such that the point is included by all solid circles and excluded by all dashed circles in the CARDIAD plot for a given column, then the choice of the value of this point in the off-diagonal

entry which the CARDIAD plot represents will make the column dominant at all frequencies. If there is no such point the CARDIAD plot describes the range of a frequency dependent off-diagonal entry which will make the column dominant.

CARDIAD plots for two input, two output systems have some interesting features. A circle at a specific frequency in the CARDIAD plot for one column will be solid if and only if the other column is dominant at that frequency. Thus, when a system is dominant at all frequencies, all the circles in the CARDIAD plots will be solid and all will contain the origin. Another interesting feature is the effect of a column switch, that is, multiplication by a matrix with the only non zero elements being ones on the off-diagonal. The effects of such a switching of the inputs are that all the solid circles become dashed, all the dashed circles become solid, and the shapes of the column one and two plots are switched. This fact will be used in the next section to achieve dominance in the various set point models.

4. Design Example

The CARDIAD plots of the five uncompensated models are all very similar in shape. This great similarity suggests that one compensator might be found that will make all of the models column dominant. The uncompensated plots also show that a column switch would make the first column of each of the models dominant at all frequencies without further compensation. Thus, K_1 was chosen to be

$$\begin{matrix} 0 & 1 \\ 1 & 0 \end{matrix}.$$

Figures 1 - 10 are the CARDIAD plots of $G(s)K_1$ for the five models. The repetition of the general shapes of the plots, which is unaffected by the column switch, is very apparent. The plots also show that the first column of each of the models is now dominant. This can be ascertained either by the fact that the origins of the column one plots are included by all solid circles and excluded by all dashed circles or by noting that all of the circles in the column two plots are solid.

To achieve dominance in the second columns of the models, it is clear that some sort of frequency dependent compensation will be necessary because there exist no points on the real axes of the plots which lie inside all of the solid circles. A first choice of a function to fit the paths of the circles could be a simple first order function which traces a semicircle through the complex plane as the frequency varies. However, it is desired that one such function be found that will work on all five of the models; so, a second order compensator will be used to fit better the shape of the circles at the hihger frequencies. Two things that should be noted about the shapes of the circles in the column two plots are that the circles tend to be larger for the lower values of fuel flow and that in general, the center of the lowest frequency (largest) circles moves toward the origin as the nominal value of the fuel flow increases. Since there is more margin for error in the lower nominal value of fuel flow models, a compensator which is fit to a rough average of the five plots and which tends to be closer to the higher nominal value of fuel flow models, might achieve dominance in all five models.

The average value of the center of the lowest frequency circle of the five plots is -9.81. This suggests that designing a compensator to fit the nominal fuel flow of 2.75 model which has as the center of the lowest frequency circle the value of -9.59 might achieve dominance in all of the models. The second order funtion that was chosen is

$$\frac{-.742s - 9.59}{.014s^2 - .998s + 1.}$$

and the next compensator, $K_2(s)$, is

$$K(s) = \begin{matrix} 1 & \dfrac{-.742s - 9.59}{.014s^2 - .998s + 1} \\ 0 & 1 \end{matrix}.$$

Thus, the overall compensation is K(s) given by

$$K(s) = \begin{matrix} 0 & 1 \\ 1 & \dfrac{-.742s - 9.59}{.014s^2 - .998s + 1.} \end{matrix}.$$

Figures 11 - 20 are the CARDIAD plots of G(s)K(s) for the five models. It is clear that they are all dominant at all frequencies since all of the circles are solid and all include the origin. Thus, one compensator has been found which will make all five of the models considered in this paper dominant.

5. Conclusions

Through the use of CARDIAD plots, it has been possible to achieve dominance over a range of operating points of a jet engine simulation. The compensator given above also achieves dominance at all but a very narrow range of frequencies in the model of another operating point. The results suggest two things. First, using the CARDIAD plots as a guide, it could be possible to design a compensator which varies with the nominal value of the fuel flow and achieves global dominance over a wide range of operating points. This is currently being studied. Second, the repetitive shape of the CARDIAD plots over the range of operating points suggests that the CARDIAD plot might be a useful tool in the classification of operating points with regard to interaction. Such a feature could be quite helpful in analysis of which models to use over flight envelopes varying from sea level to high altitude and from low through high thrust.

entry which the CARDIAD plot represents will make the column dominant at all frequencies. If there is no such point the CARDIAD plot describes the range of a frequency dependent off-diagonal entry which will make the column dominant.

CARDIAD plots for two input, two output systems have some interesting features. A circle at a specific frequency in the CARDIAD plot for one column will be solid if and only if the other column is dominant at that frequency. Thus, when a system is dominant at all frequencies, all the circles in the CARDIAD plots will be solid and all will contain the origin. Another interesting feature is the effect of a column switch, that is, multiplication by a matrix with the only non zero elements being ones on the off-diagonal. The effects of such a switching of the inputs are that all the solid circles become dashed, all the dashed circles become solid, and the shapes of the column one and two plots are switched. This fact will be used in the next section to achieve dominance in the various set point models.

4. Design Example

The CARDIAD plots of the five uncompensated models are all very similar in shape. This great similarity suggests that one compensator might be found that will make all of the models column dominant. The uncompensated plots also show that a column switch would make the first column of each of the models dominant at all frequencies without further compensation. Thus, K_1 was chosen to be

$$\begin{matrix} 0 & 1 \\ 1 & 0 \end{matrix}.$$

Figures 1 - 10 are the CARDIAD plots of $G(s)K_1$ for the five models. The repetition of the general shapes of the plots, which is unaffected by the column switch, is very apparent. The plots also show that the first column of each of the models is now dominant. This can be ascertained either by the fact that the origins of the column one plots are included by all solid circles and excluded by all dashed circles or by noting that all of the circles in the column two plots are solid.

To achieve dominance in the second columns of the models, it is clear that some sort of frequency dependent compensation will be necessary because there exist no points on the real axes of the plots which lie inside all of the solid circles. A first choice of a function to fit the paths of the circles could be a simple first order function which traces a semicircle through the complex plane as the frequency varies. However, it is desired that one such function be found that will work on all five of the models; so, a second order compensator will be used to fit better the shape of the circles at the hihger frequencies. Two things that should be noted about the shapes of the circles in the column two plots are that the circles tend to be larger for the lower values of fuel flow and that in general, the center of the lowest frequency (largest) circles moves toward the origin as the nominal value of the fuel flow increases. Since there is more margin for error in the lower nominal value of fuel flow models, a compensator which is fit to a rough average of the five plots and which tends to be closer to the higher nominal value of fuel flow models, might achieve dominance in all five models.

The average value of the center of the lowest frequency circle of the five plots is -9.81. This suggests that designing a compensator to fit the nominal fuel flow of 2.75 model which has as the center of the lowest frequency circle the value of -9.59 might achieve dominance in all of the models. The second order funtion that was chosen is

$$\frac{-.742s - 9.59}{.014s^2 - .998s + 1.}$$

and the next compensator, $K_2(s)$, is

$$K(s) = \begin{matrix} 1 & \dfrac{-.742s - 9.59}{.014s^2 - .998s + 1} \\ 0 & 1 \end{matrix}.$$

Thus, the overall compensation is K(s) given by

$$K(s) = \begin{matrix} 0 & 1 \\ 1 & \dfrac{-.742s - 9.59}{.014s^2 - .998s + 1.} \end{matrix}.$$

Figures 11 - 20 are the CARDIAD plots of G(s)K(s) for the five models. It is clear that they are all dominant at all frequencies since all of the circles are solid and all include the origin. Thus, one compensator has been found which will make all five of the models considered in this paper dominant.

5. Conclusions

Through the use of CARDIAD plots, it has been possible to achieve dominance over a range of operating points of a jet engine simulation. The compensator given above also achieves dominance at all but a very narrow range of frequencies in the model of another operating point. The results suggest two things. First, using the CARDIAD plots as a guide, it could be possible to design a compensator which varies with the nominal value of the fuel flow and achieves global dominance over a wide range of operating points. This is currently being studied. Second, the repetitive shape of the CARDIAD plots over the range of operating points suggests that the CARDIAD plot might be a useful tool in the classification of operating points with regard to interaction. Such a feature could be quite helpful in analysis of which models to use over flight envelopes varying from sea level to high altitude and from low through high thrust.

Acknowledgment

The authors thank R. R. Gejji for his assitance in obtaining the linear models used for these plots.

References

1. H. H. Rosenbrock, Computer Aided Control System Design. London: Academic Press, 1974.

2. R. Michael Schafer, "A Graphical Approach to System Dominance," Technical Report No. 778, Department of Electrical Engineering, University of Notre Dame, March 26, 1977.

3. R. M. Schafer, R. R. Gejji, P. W. Hoppner, W. E. Longenbaker, and M. K. Sain, "Frequency Domain Compensation of a DYNGEN Turbofan Engine Model," Preprints 1977 Joint Automatic Control Conference, Volume Two, pp. 1013-1018.

4. R. Gejji, R. M. Schafer, M. K. Sain, and P. Hoppner, "A Comparison of Frequency Doman Techniques for Jet Engine Control System Design," Proc. 20th Midwest Symposium on Circuits and Systems, Part 2, pp. 680-685, August 1977.

5. R. M. Schafer and M. K. Sain, "A Dynamical Approach to Diagonal Dominance, with Illustrations for a Turbofan Engine Model," Proc. 1977 NEC International Forum on Alternatives for Linear Multivariable Control, October 1977.

6. J. F. Sellers and C. J. Daniele, "DYNGEN - A Program for calculating Steady State and Transient Performance of Turbojet and Turbofan Engines," NASA TN D-7901, April 1975.

7. L. Geyser, "DYGABCD - A Program for Calculating Linear A, B, C, and D Matrices from a Nonlinear Dynamic Engine Simulator," private Communication.

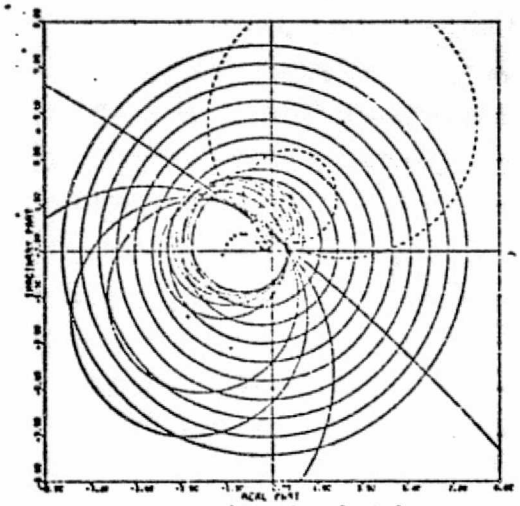

Fig. 1. WFB=2.145, $G(s)K_1$, Column 1.

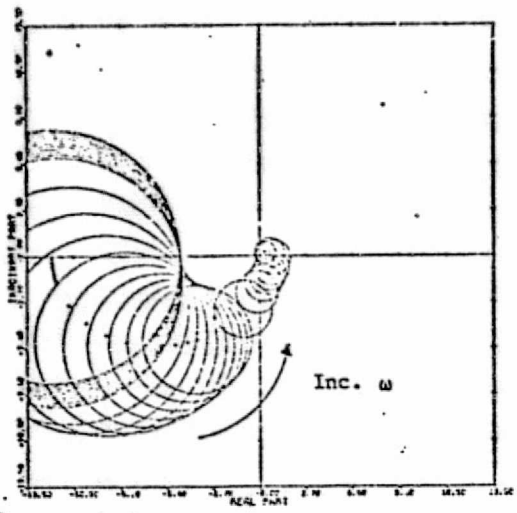

Fig. 2. WFB=2.145, $G(s)K_1$. Column 2.

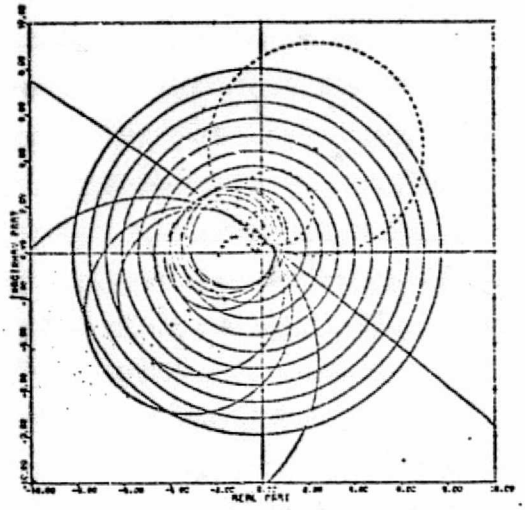

Fig. 3. WFB=2.31, $G(s)K_1$, Column 1.

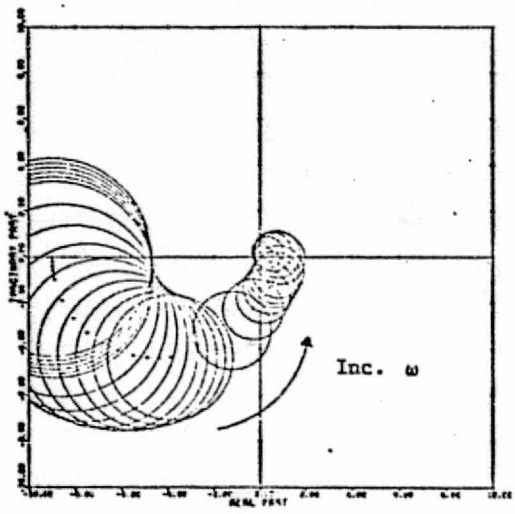

Fig. 4. WFB=2.31, $G(s)K_1$, Column 2.

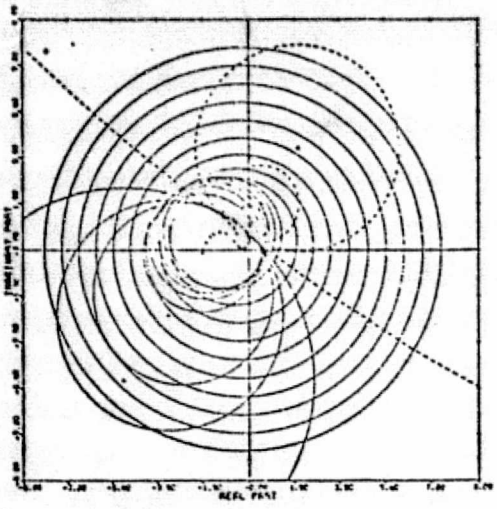

Fig. 5. WFB=2.475, $G(s)K_1$, Column 1.

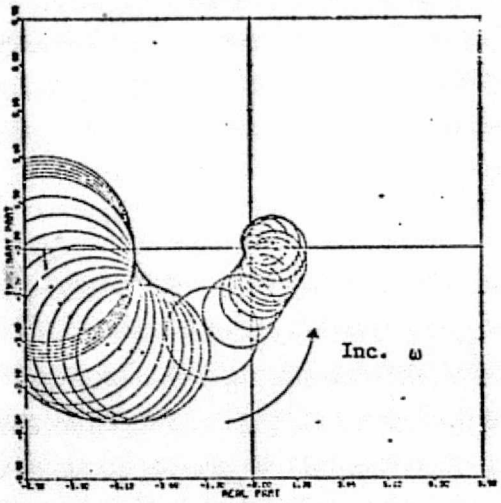

Fig. 6. WFB=2.475, $G(s)K_1$, Column 2.

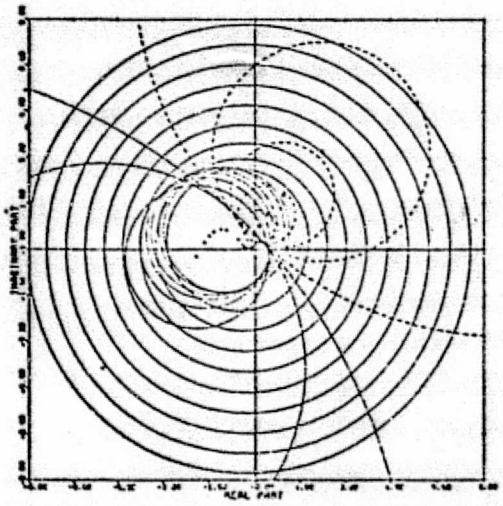

Fig. 7. WFB=2.64, $G(s)K_1$, Column 1.

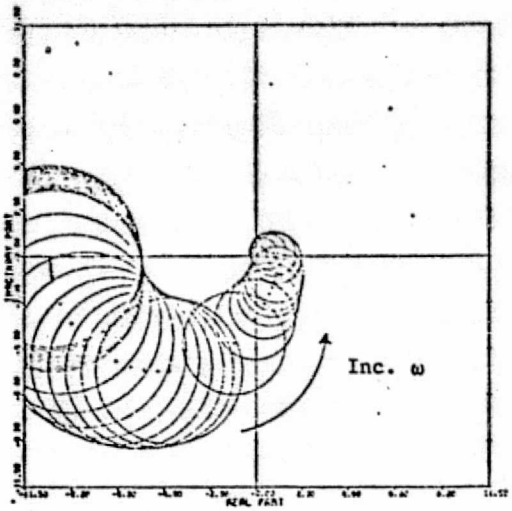

Fig. 8. WFB=2.64, $G(s)K_1$, Column 2.

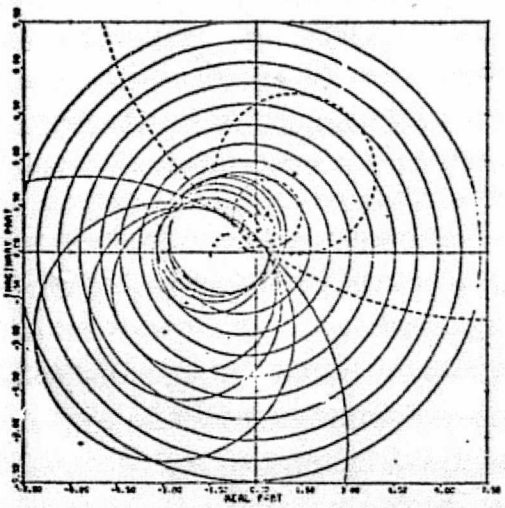

Fig. 9. WFB=2.75, $G(s)K_1$, Column 1.

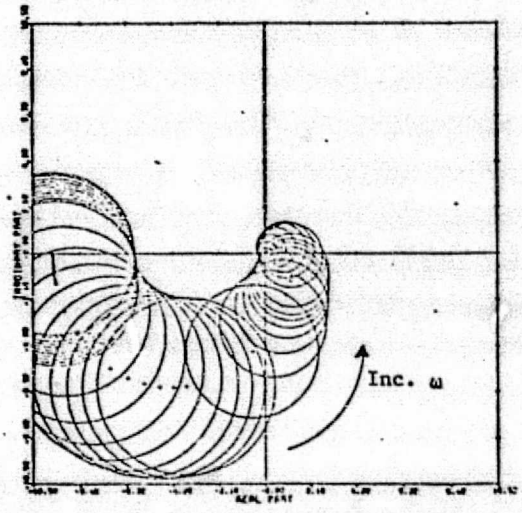

Fig. 10. WFB=2.75, $G(s)K_1$, Column 2.

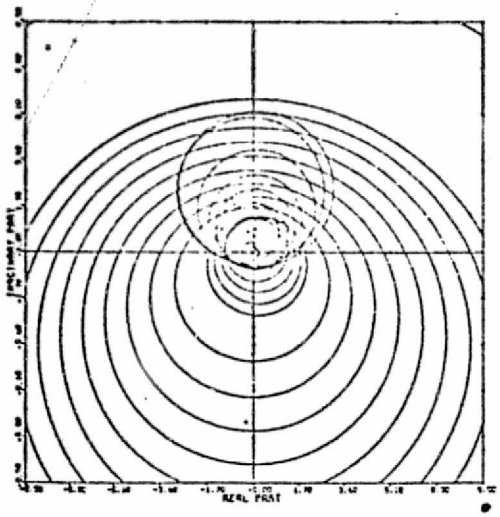

Fig. 11. WFB=2.145, G(s)K(s), Column 1.

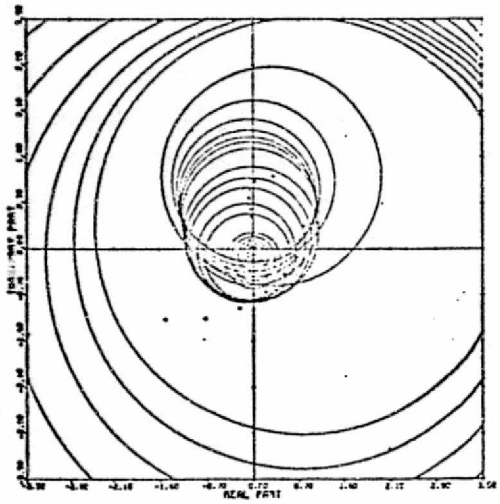

Fig. 12. WFB=2.145, G(s)K(s), Column 2.

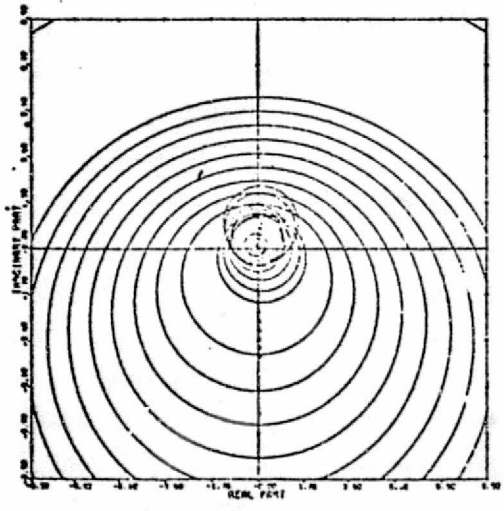

Fig. 13. WFB=2.31, G(s)K(s), Colugn 1.

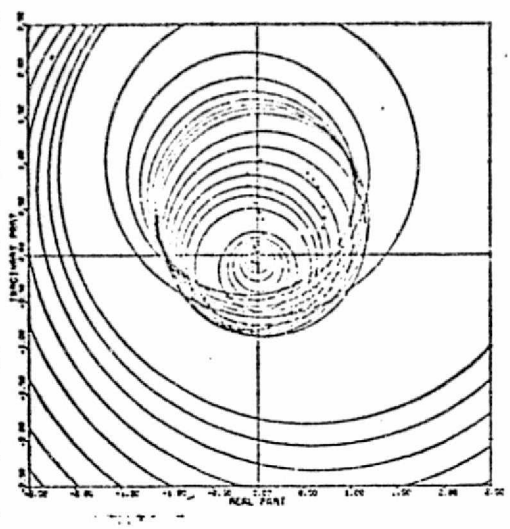

Fig. 14. WFB=2.31, G(s)K(s), Column 2.

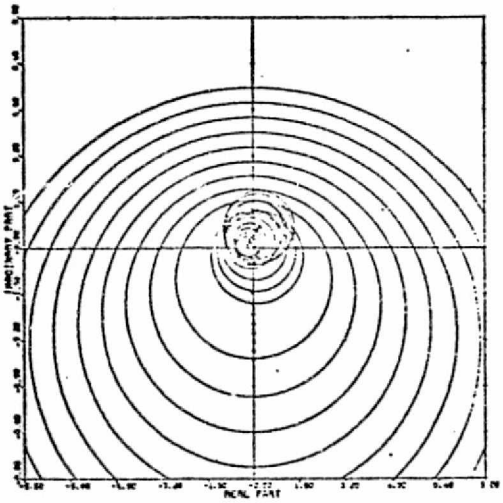

Fig. 15. WFB=2.475, G(s)K(s), Column 1.

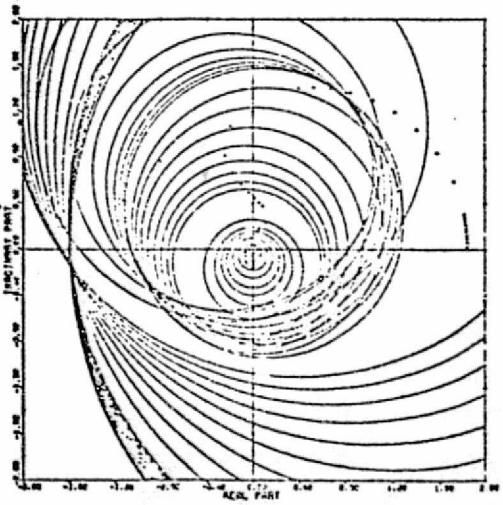

Fig. 16. WFB=2.475, G(s)K(s), Column 2.

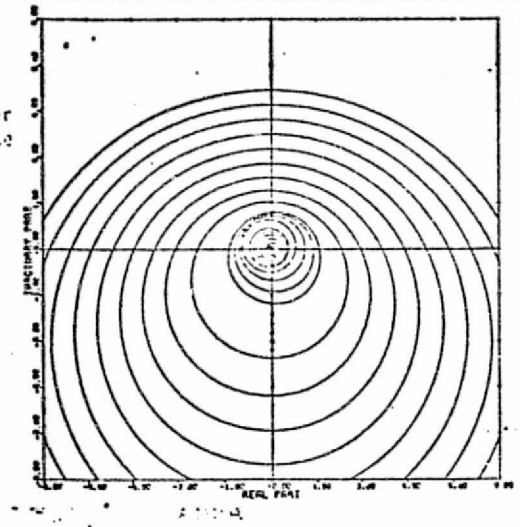

Fig. 17. WFB=2.64, G(s)K(s), Column 1.

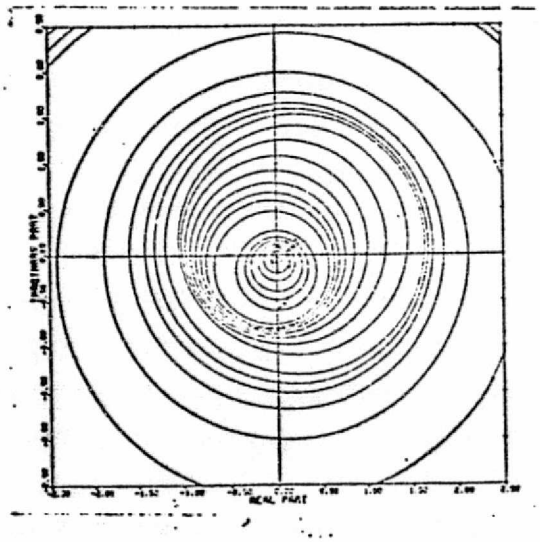

Fig. 18. WFB=2.64, G(s)K(s), Column 2.

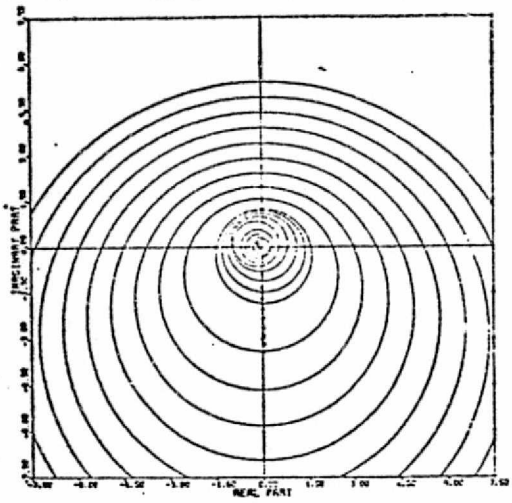

Fig. 19. WFB=2.75, G(s)K(s), Column 1.

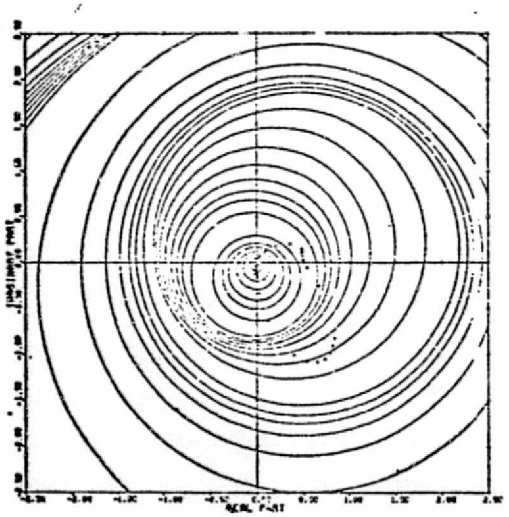

Fig. 20. WFB=2.75, G(s)K(s), Column 2.

Appendix I

THE THEME PROBLEM

M. K. Sain

THE THEME PROBLEM

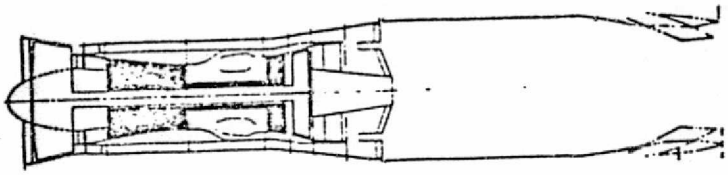

Foreword

From the outset, the use of a Theme Problem has posed certain challenges. Authors from academic backgrounds tend to be in need of highly detailed information about plant and specifications, while workers in industry and laboratories must often be satisfied with indirect information and sometimes with none at all. We have tried to arrange a reasonable compromise somewhere on middle ground. Our decision to select a problem related to a realistic modern turbofan engine had special ramifications of its own, not the least of which was the fact that certain types of additional data were precluded for proprietary or other reasons. We believed all along that the advantages of data realism outweigh the disadvantages of incomplete information.

The chronology of the Theme Problem begins in late summer, 1976, during discussions with J. L. Melsa. Subsequent contacts with several potential Forum participants led to the drafting of a Tentative Theme Problem Description, which was sent out to various workers for critique in early 1977. When evaluations were in hand, a Theme Problem Description was prepared on March 1, 1977 and became the working document for authors preparing papers for the meeting. Communications with several additional researchers established the need for minor modifications and clarifications, which were decided at a committee meeting held during the Joint Automatic Control Conference at San Francisco in June, 1977. These decisions formed the basis for an addition Theme Problem Memorandum mailed to all participants on July 18, 1977.

All these adjustments are included in the Final Theme Problem Description, which is included here.

Any clarity which may be present in this final problem description is due in large part to the valued advice of many colleagues, among whom I must especially mention R. L. DeHoff, R. D. Hackney, B. Lehtinen, W. C. Merrill, J. L. Peczkowski, C. A. Skira, and H. A. Spang, III. Credit for any and all obscurities must, of necessity, accrue to the author.

M. K. Sain
Notre Dame, Indiana
September, 1977

ABSTRACT

The theme design problem should serve the Forum goals in at least three ways. First, it should help to unify the presentations and, thus, make them more useful for group study after publication. Second, it should help to make the Forum relevant to the present-day design world by focusing upon a real system of considerable current interest. Third, it should help to delineate the state of computational readiness of the various design viewpoints, and so help to point out where additional numerical researches would be useful.

Caveat: It is important to recognize the generally positive intent involved with the use of this problem. It is not intended that the theme problem usage degenerate into a computational contest.

1. INTRODUCTION

A very important developing area for linear multivariable control has arisen because of recent increases in the complexity of aircraft turbine engines. Engines in use today have, essentially, the one control variable of fuel flow, though some make use of a variable nozzle area which is not unlike the iris diaphragm that controls aperture settings in a camera. Engines in the not-so-distant future can be expected to permit control of vanes in the stator portions of the various compressor stages. Further down the development line are engines with enough variable geometry to receive the informal designation of "rubber engines" by research engineers in the industry.

It is widely accepted that the older, workhorse, hydromechanical control methods are not equal to these new tasks and that they will, therefore, give way to electronic digital control. The entrance of the digital computer opens up vast numbers of new design possibilities, which are now beginning to receive increased attention in the industry. The central role played by the aircraft turbine engines in civil and military aviation makes clear the economic import of these trends. It would be hard to select a more timely theme design example for comparison of linear control alternatives than the jet engine.

In the United States, a joint study is now underway on the Pratt & Whitney F100-PW-100 afterburning turbofan, a low-bypass-ratio, twin-spool, axial-flow engine. Sponsored by the Air Force and by the National Aeronautics and Space Administration, this study focuses on the linear quadratic regulator theory, applied at multiple operating points in the control regime.

One effect of the theme usage of such a plant in the NEC Forum should be a broadening of the design discussion to include other design viewpoints as well.

2. PLANT

The numerical model of the jet engine is supplied in (A,B,C,D) form on Attachment 1. For the A and C matrices, note that columns 9-16 are listed below columns 1-8. This model is for zero altitude and for a power lever angle (PLA) of 83 degrees, which is near maximum non-afterburning power. The motivation for choosing this operating point comes from the fact that every engine has to pass through this condition, as, for example, on takeoff. Also supplied is a list of the input, state, and output variables associated with this model. These two pages are taken from the report

R. J. Miller and R. D. Hackney, "F100 Multivariable Control System Models/ Design Criteria," Pratt and Whitney Aircraft Group, United Technologies Corporation, West Palm Beach, Florida, November 1976.

Because a number of the techniques which will be discussed at the Forum have graphical aspects, it is planned to facilitate the inclusion of curves in the publication by limiting the plant to three control inputs. In consultation with numbers of our Theme Problem Advisory Committee, we have selected U_1, U_2, and U_3 as these inputs. Workers who feel an absolute necessity to use all five inputs are welcome to do so; however, we would ask that in such a case they provide a comparison of the effect of using five inputs over and above that of using only three. This request is designed to increase the comparability of the various design results.

Actuator information for the three control inputs is given in Attachment 2. Also provided is information associated with the actuation of U_4, if that input is used in addition to U_1, U_2, and U_3. Finally, should U_5 be used in addition to U_1, U_2, and U_3, a servo time constant of 0.02 sec. can be assumed for actuation. Various rate limits on the actuators can be noted, as in Table A.

Table A
Actuator Rate Limits

U_1	15,800	(lb/hr)/sec.
U_2	3.6	Ft^2/sec.
U_3	48	Deg/sec.
U_4	40	Deg/sec.

The actuators have some limits, also, which will be mentioned here. On U_3, it may be assumed that the limit is $\pm$ 6°. On U_2, a limit arises because the nozzle area is pretty well down to its minimum at this operating point; the limit is assumed to be about 1 square feet in that direction.

The Theme Problem models are in absolute, unnormalized form, without any mention of the set point values. This makes it difficult to size inputs. The committee worked out a proposal to supply "ballpark" set point values so that the model could be normalized. Unfortunately, it was not possible to obtain even such approximate information.

A consequence of this fact is that the absolute rate limits of Table A have meaning only in relationship to the size of reference commands assumed. Because we are unable to supply the suggested reference command, the effect of actuator rate limits can be treated only hypothetically; and we have to leave the issue of whether to do this, and how to do this, in the hands of the authors.

Turning now to the sensed variables, we have available X_1, X_2, X_3, X_5, and (X_{12} + X_{13}), the last of which is denoted FTIT for "fan turbine inlet temperature." Sensor time constants in seconds are listed in Table B.

Table B

Sensor Time Constants

X_1	0.03
X_2	0.05
X_3	0.05
X_5	0.05

Sensing of FTIT is a bit more elaborate and is indicated on Attachment 3.

3. ENVIRONMENT

Measurement noise is on the order of 1%; and state noise is negligible. Therefore it is not planned to supply any noise data. Authors wishing to make noise studies must make their own assumptions. This is not unrealistic for the present stage of discussion. Though some techniques may well make use of observers or dynamical output feedback, no formal stress on filters is anticipated. The Forum, then, is visualized primarily as a control meeting, although contributed papers in the stochastic area will be accepted if they contribute to the Forum theme.

Practice in the industry involves the use of multiple linear models at various operating points from sea level to high altitude and from low to high thrust. As operation transitions from the neighborhood of one operating point to the neighborhood of another, these models change in consonance with some physical variable. Parameter variation is, therefore, an aspect of design.

But publicly available neighboring linear models are not near enough to the Theme Problem model to provide meaningful data on parametric variation. This fact, combined with lack of set point information, led the committee to suggest a 5% change in eigenvalues as one, hopefully useful, measure of such variation. Because normalization of the model is a similarity transformation, this characterization is independent of set point.

4. REDUCED ORDER MODELS

Approximate eigenvalues of the Theme Problem plant are -577, -176, -59.2, -50.7, -47.1, -38.7, $-21.3 \pm i.822$, $-17.3 \pm i4.78$, -19.0, $-6.71 \pm i1.31$, -2.62, -1.91, -.648. It is the nature of the jet engine control problem that these can usually be well identified with physical variables. For example, -.648 associates with X_{10}, -1.91 associates with X_{13}, -2.62 associates with X_2, and so forth. X_1 is related to the eigenvalue pair $-6.71 \pm i1.31$. This type of information can be deduced from a study of the eigenvectors corresponding to a particular eigenvalue. It can be expected that actuator modes, such as that involved with fuel flow, will enter into this list. Some discussion on this point can be found in R. L. DeHoff and W. E. Hall, Jr., "Design of a Multivariable Controller for an Advanced Turbofan Engine," Proceedings 1976 IEEE Conference on Decision and Control, page 1002.

In the interest of offering some assistance to authors who might be having computational difficulty with the full size problem, the following reduced model has been made available by Dr. DeHoff of Systems Control, Inc. (Vt.). It is a model which neglects sensor dynamics, augments the plant by the dominant actuator dynamics, and then reduces to fifth order. The resulting five states are

$\hat{X}_1$ = Fan Speed (rpm)

$\hat{X}_2$ = Compressor Speed (rpm)

$\hat{X}_3$ = "Augmentor" Pressure (psia)

$\hat{X}_4$ = Fuel Flow (lb./hr.)

$\hat{X}_5$ = Burner Pressure (psia)

Note that the "Augmentor" Pressure $\hat{X}_3$ is not to be identified with X_5; the quantities are not defined at the same physical location. Note also that $\hat{X}_5$ was not one of the original states.

Remark: The U_3 Actuator diagram shows a Servo System gain of 2.4. It has come to our attention that a more realistic number for this gain would be about 12.0. The effect of this gain change is to take the dominant CIVV position actuator eignevalue from a location of high dominance in the overall plant-actuator system to a location of considerably less dominance. It is not necessary for authors to make this change if they have already completed their calculations, inasmuch as the 2.4 gain apparently is one of those "glitches" which crept in an uninvited manner. Some authors may choose to compare the effect of the gain 12.0 with the gain 2.4, if time and space permits. We have included this remark here so that the reduced order model, which has the same controls and outputs as the full size system, may be more understandable.

A (5 x 5)

-.3245E+01	-.2158E+01	-.9155E+03	.5731E+00	.1342E+03
.1642E+01	-.5941E+01	-.2816E+03	.1897E+00	.5705E+02
.1685E-01	-.2554E-01	-.1003E+02	.7994E-02	.5807E+00
.0000	.0000	.0000	-.1000E+02	.0000
-.2163E+01	.6862E+01	.7405E+03	.1195E+01	-.1715E+03

B (5 x 5)

.1432E-01	-.3553E+03	-.9906E+02	-.1549E+02	.2220E+05
.2871E+00	.7286E+03	.2514E+02	-.6487E+02	.8122E+04
-.2469E-02	-.1030E+03	.6333E+00	-.3213E+00	-.7418E+02
.1000E+02	.0000	.0000	.0000	.0000
-.1311E+00	.3295E+03	-.2500E+02	.6257E+02	-.6445E+05

C (5 x 5)

.1662E+01	-.1768E+01	.7999E+02	-.1890E+00	.3771E+02
.1383E-01	.3142E-05	-.1060E-01	.1289E-03	-.1839E-06
.1694E+00	-.1129E+00	-.4959E+01	.7386E-01	-.1835E+00
.7590E-04	.3269E-05	-.1477E-01	.2284E-05	.4315E-04
-.4859E-04	.1381E-03	.1140E-01	.1951E-04	-.2688E-02

D (5 x 5)

.1302E+00	.1992E+03	.4802E+02	-.1503E+02	.1083E+05
.1449E-06	.3395E+00	.6806E+00	.2812E-03	.3204E-03
.2967E-01	.7927E+02	.2567E+01	-.7631E+00	.2066E+04
.1046E-05	-.7720E-02	-.5814E-02	.1157E-03	.6605E-01
-.8395E-05	-.7897E-02	-.6841E-03	-.9643E-03	-.2815E+00

5. SPECIFICATIONS

The overall viewpoint of the controller is quite simple. The pilot has one lever, which we might intuitively call the throttle and which sets what is called in the industry the "power lever angle." Basically, the pilot increases the lever angle to obtain more thrust. All the other variables must be controlled so as to achieve the new thrust quickly, but without overshoot and without violating some important physical considerations. An example of one of these is the temperature at the inlet to the "high" turbine just aft of the burner. This temperature is ordinarily scheduled very near its maximum safe value, and temperature increases are not welcome because the turbine elements are thin, respond very fast, and can be permanently damaged or create a need for more frequent engine overhauls. Another example of a constraint is the various undesirable stall conditions in the compressor.

This problem comes down to us in the following form. Assuming a step change in power lever angle, we want to move the engine to a slightly different operating point in the above described acceptable dynamic fashion. The power lever angle change is converted by a master engine scheduler into a reference input for our linearized feedback model. The nature of this reference input is not highly specific. Step inputs are commonly studied. It is not likely that highly detailed information about these references will be available, but we can try to firm up any particular issues which may be crucial to one paper or another. The exact nature of these references gets one into the exact nature of the schedulers. It does not seem too productive in a linear meeting to go very far into such "global" issues. If greater reference variety is needed, it can probably be safely assumed. It would be good, however, if each paper tried to discuss at least the reference step.

For purposes of design, we can group the variables into two families. Y_1, Y_3, X_1, and X_2 are desired to respond fast without overshoot. Y_4 should not decrease more than .05; Y_5 should not decrease more than .15.

Remark: The decrease limits on Y_4 and Y_5 are to be regarded in the same spirit as the U_3 actuator gain change in the preceding section. If calculations are complete, there is no requirement to incorporate it. Some authors may wish to study its effect, however.

6. VIEWPOINT

We believe that the theme problem should appear in each presentation as the major, and probably the only, illustration of the particular design methodology being described. We visualize each paper as an exposition of design viewpoint, with jet engine illustration. We do not visualize the paper as an exposition of jet engine design. In other words, the theme problem will be an apparent thread through the fabric of the Forum, but the pattern of the fabric will be set by the various linear control alternatives as entities in themselves. Put in yet another way, the Forum is on "Alternatives for Linear Multivariable Control" and is not upon "Various Approaches to Jet Engine Control."

ORIGINAL
OF POOR QUALITY

F100 MODEL ALT=0.0 PLA=83

THE A MATRIX

-4.328	.1714	5.376	401.6	-724.6	-1.933	1.020	-.9820
-.4402	-5.643	127.5	-233.5	-434.3	20.59	2.040	-2.592
1.038	6.073	-165.0	-4.483	1049.	-82.45	-5.314	5.097
.5304	-.1086	131.3	-578.3	102.0	-9.240	-1.146	-2.408
.8476E-02	-.1563E-01	.5602E-01	1.573	-10.05	.1952	-.8804E-02	-.2110E-01
.8350	-.1249E-01	-.3567E-01	-.6074	37.65	-19.79	-.1813	-.2962E-01
.6768	-.1264E-01	-.9683E-01	-.3567	80.24	-.8239E-01	-20.47	-.3928E-01
-.9696E-01	.8666	16.87	1.051	-102.3	29.66	.5943	-19.97
-.8785E-02	-.1636E-01	.1847	.2169	-8.420	.7003	.5666E-01	6.623
-.1298E-03	-.2430E-03	.2718E-02	.3214E-02	-.1246	.1039E-01	.8395E-03	.9812E-01
-1.207	-6.717	26.26	12.49	-1269.	103.0	7.480	36.84
-.2730E-01	-.4539	-52.72	198.8	-28.09	2.243	.1794	9.750
-.1206E-02	-.2017E-01	-2.343	8.835	-1.248	.9975E-01	.8059E-02	.4333
-.1613	-.2469	-24.05	23.38	146.3	1.638	.1385	4.486
-.1244E-01	.3020E-01	-.1198	-.4821E-01	5.675	-.4525	19.81	.1249
-1.653	1.831	-3.822	113.4	341.4	-27.34	-2.040	-.6166
.9990	1.521	-4.062	9.567	10.08	-.6017	-.1312	.9602E-01
11.32	10.90	-4.071	-.5739E-01	-.6063	-.7488E-01	-.5936	-.9602E-01
-.9389E-02	.1352	5.638	.2246E-01	.1797	.2407E-01	1.100	.2743E-01
-3.081	-4.529	5.707	-.2346	-2.111	-.2460	-.4686	-.3223
.2090E-02	-.5256E-01	-.4077E-01	-.9182E-02	-.8178E-01	.3428E-01	.4995E-02	-.1256E-01
-.1953E-01	-.1622	-.6439E-02	-.2346E-01	-.2201	-.2514E-01	-.3749E-02	-.3361E-01
.1878E-01	-.2129	-.9337E-02	-.3144E-01	-.2919	-.3370E-01	.8873E-01	-.4458E-01
.2253E-01	.1791	.8371E-02	.2645E-01	.2560	.2835E-01	-.3749E-01	.3635E-01
-49.99	.6760E-01	39.46	.4991E-02	.8983E-01	.5349E-02	.0	.1372E-01
-.6666	-.6657	.5847	.6654E-04	.1347E-02	.7131E-04	.0	.2057E-03
.2854	2.332	-47.65	.3406	3.065	.3624	-.4343	.4681
-9.627	-9.557	38.48	-50.01	.1011	.1203E-01	-.4686E-01	.1715E-01
-.4278	-.4245	1.710	-2.000	-1.996	.5349E-03	-.1999E-02	.7544E-03
-4.414	-4.354	17.66	-3.113	-3.018	-19.77	-.4999E-01	.1509E-01
-.1127E-02	-.6760E-02	.1835E-01	-.9981E-03	-.1347E-01	-.1070E-02	-20.00	-.2057E-02
.5004	-.1437	-2.416	-.1073	-1.078	30.63	19.89	-50.16

THE B MATRIX

-.4570E-01	-451.6	-105.8	-1.506	851.5
.1114	-546.1	-6.575	-107.8	3526.
.2153	1362.	13.46	20.14	-.6777E+05
.3262	208.0	-2.888	-1.653	-269.1
.9948E-02	-98.39	.5069	-.1940	-94.70
.2728E-01	71.62	9.608	-.3160	-184.1
.1716E-01	71.71	8.571	.7989	-515.2
-.7741E-01	-141.2	-.8215	39.74	1376.
.3855E-01	-7.710	-.4371E-01	-.1024	-6684.
.5707E-03	-.1144	-.6359E-03	-.1432E-02	-99.02
5.727	-1745.	-8.940	-17.96	.8898E+05
.1392	-24.30	-.2736	-.3403	-6931.
.6172E-02	-1.082	-.1183E-01	-.1452E-01	-307.7
.6777E-01	16.60	.3980	.2311E-01	-2588.
.1880E-02	9.147	-.8241	.8984E-01	-32.31
.1677	435.8	-89.94	4.900	-295.5

THE C MATRIX

.4866	-.6741	5.392	95.42	24.03	10.52	.8190	-.4492
.1383E-01	.2789E-05	.0	.0	-.1081E-01	-.5545E-04	.4722E-04	.0
.0	.0	.0	.0	.0	.0	.0	.0
.7418E-04	.5496E-05	.4790E-05	.1478E-03	-.1504E-01	-.6503E-04	.8820E-04	.4999E-05
.1538E-04	.1201E-03	-.2579E-02	-.1609E-03	.1618E-01	-.1071E-02	-.9561E-04	-.5503E-05
.5195	.8437	-1.863	.5709E-01	.4815	3.428	2.161	.7681E-01
.0	.0	.0	.0	.0	.0	.0	.0
.0	.0	1.000	.0	.0	.0	.0	.0
.3434E-05	.2727E-04	.1128E-05	.4002E-05	.3673E-04	.4290E-05	-.4958E-05	.5609E-05
-.3732E-05	-.2996E-04	-.1234E-05	-.4380E-05	-.4024E-04	-.4721E-05	.5324E-05	-.6103E-05

THE D MATRIX

-.6777E-01	-420.5	32.97	-1.824	1245.
.1282E-03	.3353	.6804	-.5605E-04	-.1199E-01
.0	.0	.0	.0	.0
.1030E-05	-.1193E-01	-.5806E-02	.6015E-04	.4463E-01
.8109E-05	.2328E-01	.1178E-03	-.5538E-02	-.1039

1. Engine State Variables

X_1 = Fan Speed, SNFAN (N_1) - rpm

X_2 = Compressor Speed, SNCOM (N_2) - rpm

X_3 = Compressor Discharge Pressure, P_{t3} - psia

X_4 = Interturbine Volume Pressure, $P_{t4.5}$ - psia

X_5 = Augmentor Pressure, P_{t7m} - psia

X_6 = Fan Inside Diameter Discharge Temperature, $T_{t2.5h}$ - °R

X_7 = Duct Temperature, $T_{t2.5c}$ - °R

X_8 = Compressor Discharge Temperature, T_{t3} - °R

X_9 = Burner Exit Fast Response Temperature, T_{t4hi} - °R

X_{10} = Burner Exit Slow Response Temperature, T_{t4lo} - °R

X_{11} = Burner Exit Total Temperature, T_{t4} - °R

X_{12} = Fan Turbine Inlet Fast Response Temperature, $T_{t4.5hi}$ - °R

X_{13} = Fan Turbine Inlet Slow Response Temperature, $T_{t4.5lo}$ - °R

X_{14} = Fan Turbine Exit Temperature, T_{t5} - °R

X_{15} = Duct Exit Temperature, T_{t6c} - °R

X_{16} = Duct Exit Temperature, T_{t7m} - °R

2. Engine Inputs

U_1 = Main Burner Fuel Flow, WFMB - lb/hr

U_2 = Nozzle Jet Area, A_j - ft^2

U_3 = Inlet Guide Vane Position, CIVV - deg

U_4 = High Variable Stator Position, RCVV - deg

U_5 = Customer Compressor Bleed Flow, BLC - %

3. Engine Outputs

Y_1 = Engine Net Thrust Level, FN - lb

Y_2 = Total Engine Airflow, WFAN - lb/sec

Y_3 = Turbine Inlet Temperature, T_{t4} - °R

Y_4 = Fan Stall Margin, SMAF

Y_5 = Compressor Stall Margin, SMHC

ATTACHMENT 2

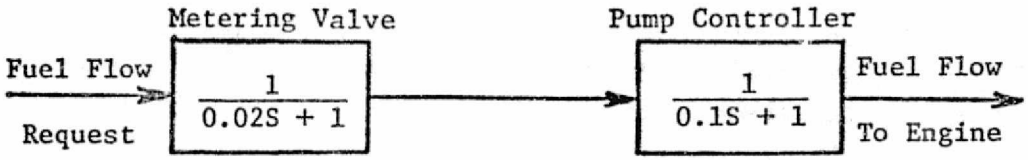

U_1 Actuator

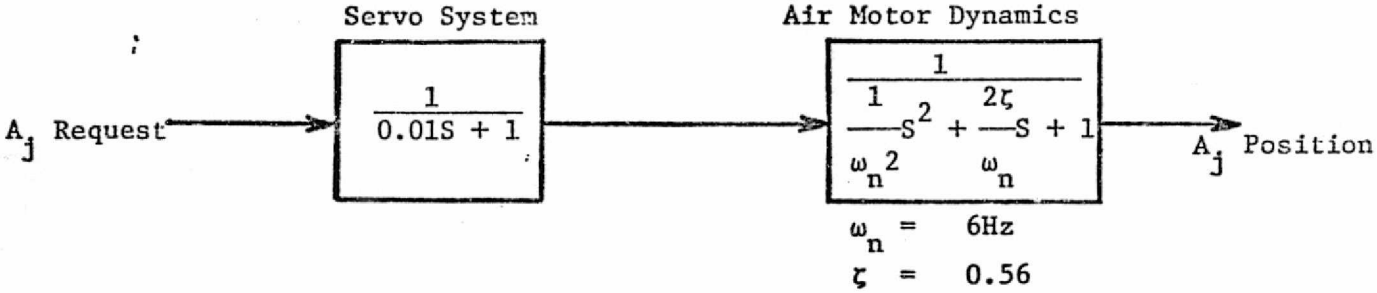

U_2 Actuator

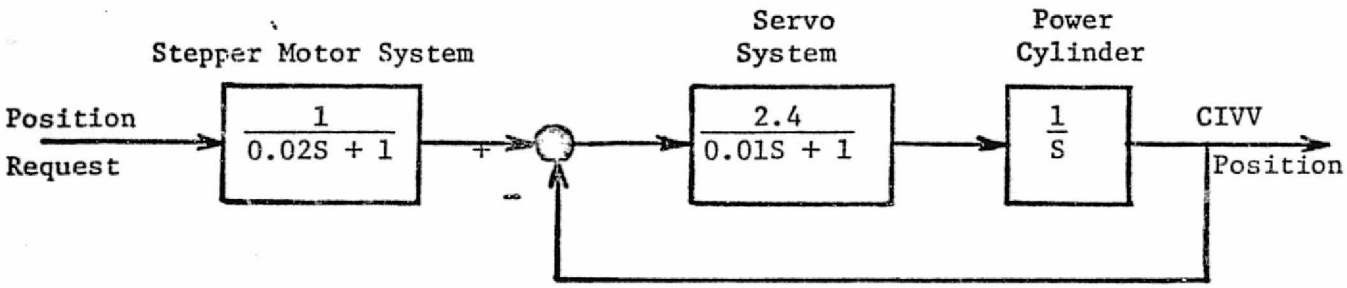

U_3 Actuator

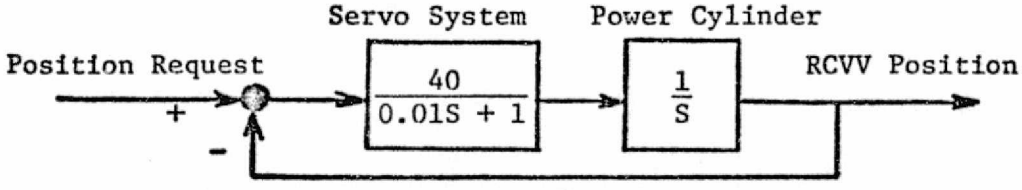

U_4 Actuator

FTIT Sensor

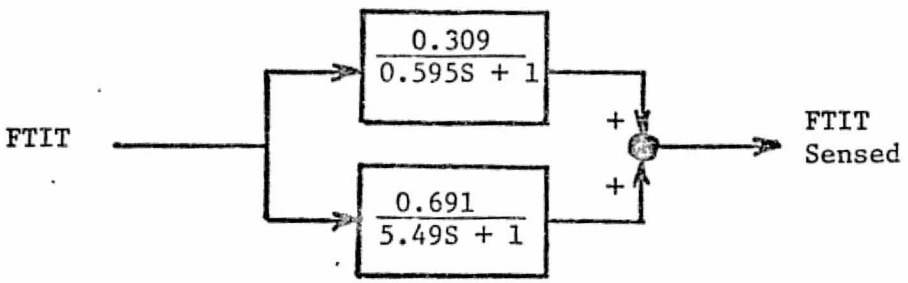

Appendix J

"INPUT COMPENSATION FOR DOMINANCE OF TURBOFAN MODELS"

R. M. Schafer
M. K. Sain

INPUT COMPENSATION FOR DOMINANCE OF TURBOFAN MODELS

R. M. Schafer and M. K. Sain

Department of Electrical Engineering
University of Notre Dame
Notre Dame, Indiana 46556
U.S.A.

ABSTRACT

The determinant of return difference establishes a crucial link between open and closed loop characteristic polynomials in multivariable feedback control systems. As a result, Nyquist constructions on this determinant carry important design information. One way to extract this information is by achieving diagonal dominance. This paper presents a method which uses dynamical input compensation to achieve column dominance. Application to the Theme Problem is included.

INPUT COMPENSATION FOR DO[illegible]NCE OF TURBOFAN MODELS

R. M. Schafer and M. K. Sain

Department of Electrical Engineering
University of Notre Dame
Notre Dame, Indiana 46556
U.S.A.

ABSTRACT

The determinant of return difference establishes a crucial link between open and closed loop characteristic polynomials in multivariable feedback control systems. As a result, Nyquist constructions on this determinant carry important design information. One way to extract this information is by achieving diagonal dominance. This paper presents a method which uses dynamical input compensation to achieve column dominance. Application to the Theme Problem is included.

1. INTRODUCTION

Recent advances in the generalized Nyquist theory for linear multivariable feedback control systems have brought about very substantial new opportunities for research in the area of frequency domain control design. Most of these advances are predicated upon the relationship between closed loop and open loop characteristic polynomials--as embodied in the determinant of return difference. Features of the Nyquist diagram of this determinant are important aids to control system design.

It is apparent that a diagonal return difference will decompose the return difference determinant into a product of its diagonal elements, thus reducing a multivariable problem to classical single-input, single-output form. Less apparent, but of much greater practical significance is the fact that an approximately diagonal return difference can have essentially the same reducing effect on a multivariable problem, when regarded from a generalized Nyquist viewpoint. The best known of these approximately diagonal conditions has come to be described as diagonal dominance. A productive design strategy can be mounted, therefore, in two steps. First, achieve diagonal dominance; second, apply classical single-input, single-output techniques [1].

Unfortunately, methods to attain diagonal dominance have been rather slow to advance. For the most part, they have been restricted to the selection of constant real compensators, the entries of which are typically obtained by procedures of optimization that do little to preserve some of the classical advantages, such as insight, afforded by the frequency domain approach. Much work needs yet to be done on the theory of attaining diagonal dominance by use of frequency dependent, dynamical compensation.

This paper considers the application to the Theme Problem of a useful new design aid called the CARDIAD Plot. In its present form, this method deals with the design of a dynamic precompensator for the plant, in such a way that column dominance is achieved. An important feature of the approach is the enhancement of designer insight toward the coupling present in a plant.

Section 2 introduces the CARDIAD method for two-input, two-output plants, and Section 3 provides an illustration of certain basic features of the method, in the context of a jet engine plant related to the Theme Problem. Section 4 gives a generalization of the idea to three inputs and three outputs, and Section 5 applies these results to the Theme Problem. Conclusions appear in Section 6.

2. GRAPHICAL APPROACH

The i^{th} column of a matrix $Z(s)$ is said to be dominant if

$$\left|z_{ii}(s)\right| - \sum_{\substack{j=1 \\ j\neq i}}^{n} \left|z_{ji}(s)\right| > 0 \tag{1}$$

for all s on a Nyquist contour D. A similar definition can be made for row dominance.

For a two-input, two-output system, Eq. (1) can be equivalently written

$$\left|z_{ii}(s)\right|^2 - \left|z_{ji}(s)\right|^2 > 0 \quad i \neq j \tag{2}$$

for all s on D.

Consider a two-input, two-output system having only precompensation. The open loop transfer function of the system is

$$Q(s) = G(s)K(s). \tag{3}$$

Let K(s) be restricted to the form

$$K(s) = \begin{bmatrix} 1 & \alpha_2(s) \\ \alpha_1(s) & 1 \end{bmatrix}. \tag{4}$$

Since any matrix having nonzero entries on its main diagonal may be put into this form by multiplication with a diagonal matrix, and since multiplication by a diagonal matrix does not affect dominance, this can be done without essential loss of generality.

Let G(s) be evaluated at a specific frequency ω. Then

$$Q(j\omega) = \begin{bmatrix} r_{11} + i_{11}j & r_{12} + i_{12}j \\ r_{21} + i_{21}j & r_{22} + i_{22}j \end{bmatrix} \begin{bmatrix} 1 & x_2 + y_2 j \\ x_1 + y_1 j & 1 \end{bmatrix}. \tag{5}$$

Performing the indicated matrix multiplication, the four entries in the matrix $Q(s)\Big|_{s=j\omega}$ are

$$q_{11} = r_{11} + i_{11}j + (r_{12} + i_{12}j)(x_1 + y_1 j), \tag{6}$$

$$q_{12} = r_{12} + i_{12}j + (r_{11} + i_{11}j)(x_2 + y_2 j), \tag{7}$$

$$q_{21} = r_{21} + i_{21}j + (r_{22} + i_{22}j)(x_1 + y_1 j), \tag{8}$$

$$q_{22} = r_{22} + i_{22}j + (r_{21} + i_{21}j)(x_2 + y_2 j). \tag{9}$$

From Eq. (2), the first column of $Q(s)\Big|_{s=j\omega}$ will be dominant if

$$\left|q_{11}\right|^2 - \left|q_{21}\right|^2 > 0. \tag{10}$$

Performing the indicated subtraction results in what will be referred to as the dominance inequality for column 1. The form of this inequality is

$$f_1(x_1, y_1) = ax_1^2 + ay_1^2 + 2bx_1 + 2cy_1 + d \quad 0,$$

where the constants are defined as

$$a = r_{12}^2 + i_{12}^2 - r_{22}^2 - i_{22}^2 \tag{11}$$

$$b = r_{11}r_{12} + i_{11}i_{12} - r_{21}r_{22} - i_{21}i_{22}, \tag{12}$$

$$c = r_{12}i_{11} + r_{21}i_{22} - r_{11}i_{12} - r_{22}i_{21}, \tag{13}$$

$$d = r_{11}^2 + i_{11}^2 - r_{21}^2 - i_{21}^2. \tag{14}$$

Note that each constant is composed of complex field elements which come from evaluation of G(s) at a specific frequency ω.

The function $f_1(x_1,y_1)$ is a paraboloid in three-space and is normal to the x_1-y_1 plane. If this paraboloid intersects the x_1-y_1 plane, the intersection will be a circle. Standard maximum-minimum analysis gives that the maximum or minimum of the dominance function occurs at

$$x_1 = -b/a \qquad y_1 = -c/a \tag{15}$$

To determine if the point that was found is a minimum or a maximum, the hessian is formed. If the hessian is negative definite, the point found is a maximum. If the hessian is positive definite, the point found is a minimum. The hessian of the dominance equation for column one is

$$\begin{bmatrix} 2a & 0 \\ 0 & 2a \end{bmatrix} \tag{16}$$

so that the second derivative test reduces to a test on the sign of a.

Proceeding from this analysis, there are four possible cases. The point that was found was a positive maximum, positive minimum, negative maximum, or negative minimum. The two cases that are of interest are the positive maximum and the negative minimum since it has been shown [2] that the other two cases cannot occur. In each of the cases of interest, the positive maximum and the negative minimum, there is an intersection of the x_1-y_1 plane. Recalling that the column will be dominant if $f_1(x_1,y_1)$ is positive, the analysis of the two cases is as follows. In the positive maximum case, the values of x_1 and y_1 which will result in solution of the dominance inequality are those points which lie inside the intersection of $f_1(x_1,y_1)$ and the x_1-y_1 plane, that is the circle which is the solution of $f_1(x_1,y_1) = 0$. In the negative minimum case, the choices of x_1 and y_1 which result in solution of the dominance inequality are those points which lie outside the circle of intersection. Thus, the intersection of the dominance function $f_1(x_1,y_1)$ for column one and the x_1-y_1 plane defines the acceptable range of x_1 and y_1 such that the system will be dominant in the first column at the specific frequency at which the analysis was performed. In like fashion, the second column of the system may be analyzed, and the acceptable choices of x_2 and y_2 may be determined.

If this dominance analysis is repeated over a range of frequencies, and the resulting circles of intersection plotted, a CARDIAD (Complex Acceptability Region for DIAgonal Dominance) Plot is produced. A solid circle is drawn if the acceptable choice of x and y lie inside the circle, and a dashed circle is drawn if the acceptable region is outside the circle of intersection. Associated with each CARDIAD plot is a locus of centers plot, which indicates the centers and labels the frequency of each. Space limitations do not allow the locus of centers plots to be included with the CARDIAD plots in this paper, but they will be mentioned and referenced as necessary.

3. ILLUSTRATION

Figs. 1 and 2 are CARDIAD Plots of a two-input, five-state, two-output model of a jet engine. The model is derived from a jet engine simulator called DYNGEN [3,4] and represents an F-100 turbofan jet engine with a fuel flow of 2.75 Lbm/sec. (full

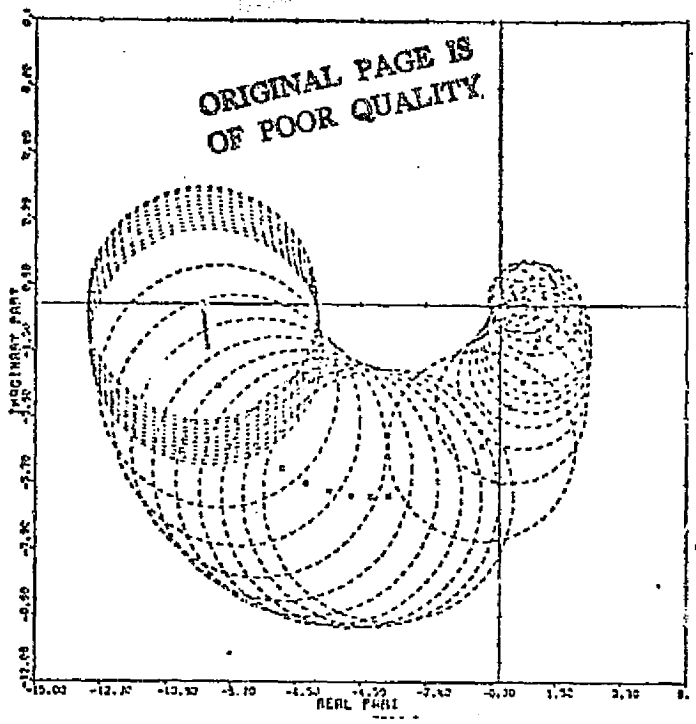

Fig. 1. Column 1, Uncompensated

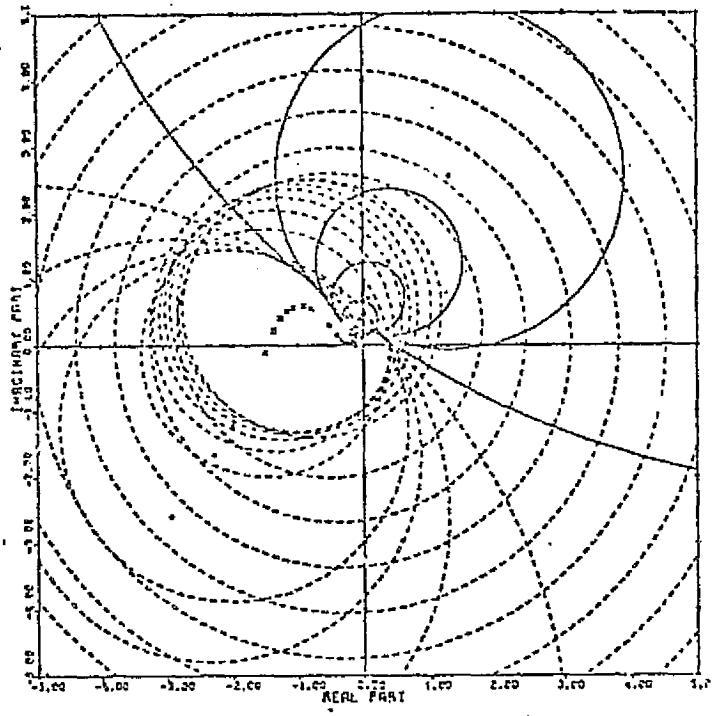

Fig. 2. Column 2, Uncompensated

throttle without afterburners). The inputs are fuel flow and exhaust area and the outputs are thrust and high turbine inlet temperature. This model is one of a series of such models presently being used in a set point study of an F-100 like jet engine.

The analysis of CARDIAD plots proceeds as follows. Recall that, at any given frequency, the acceptable region is outside the circle if the circle is dashed or inside if the circle is solid. The first question of interest is whether the columns of the system are dominant uncompensated. For this to be the case, the origin of the CARDIAD plot must be included in all solid circles and excluded by all dashed circles, since the origin represents identity compensation of the column. This is not the case for either of the two CARDIAD plots of this system. The next question is whether the system can be made dominant by constant real precompensation. If this is the case, there will exist a point on the real axis which lies inside all solid circles and outside all dashed circles. Fig. 1 shows that the first column of the system can be made dominant at all frequencies by the choice of any constant x_1 which lies outside all the dashed circles of the CARDIAD plot. Fig. 2 shows that there exists no constant value that will make the second column of the system dominant at all frequencies. Thus, some form of frequency dependent precompensation will be necessary.

Before proceeding with dominating this system, some of the features of CARDIAD plots should be mentioned. One property is that a circle at a specific frequency in the plot for one column will be solid if the other column is dominant at that frequency and will be dashed if the other column is not dominant. From this fact it follows that the transition from one type of circle to the other in the CARDIAD plot for one column occurs when there is a change in dominance in the other column. Once again considering Figs. 1 and 2, these facts indicate that the second column is not dominant at any frequency since all of the circles in the CARDIAD plot for the first column are dashed and that the first column is dominant at low frequencies (until $\omega=7$) because the circles in the CARDIAD plot for the second column are solid for this and all lower frequencies.

A second feature of the CARDIAD Plot is the effects of a column switch on the plots,

that is, premultiplication by a matrix with the only nonzero entries being off-diagonal 1's. The effects of such a switching of the inputs are that all solid circles become dashed circles, all dashed circles become solid, and the shapes of the column one and two plots are switched. The CARDIAD plots of the system with this type of compensation are given in Figs. 3 and 4. Note that the first column is now dominant at all frequencies without further compensation. This fact can be ascertained

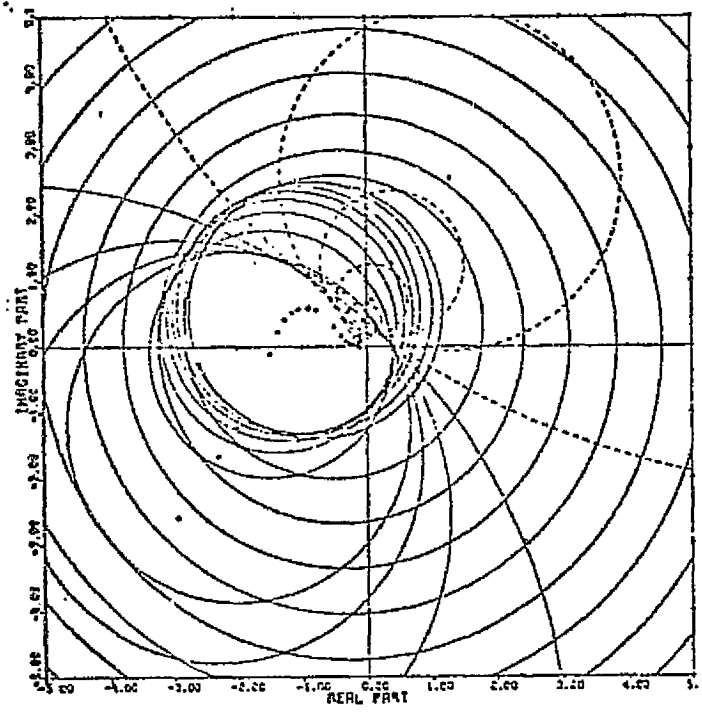

Fig. 3. Column 1, $G(s)*K_1$

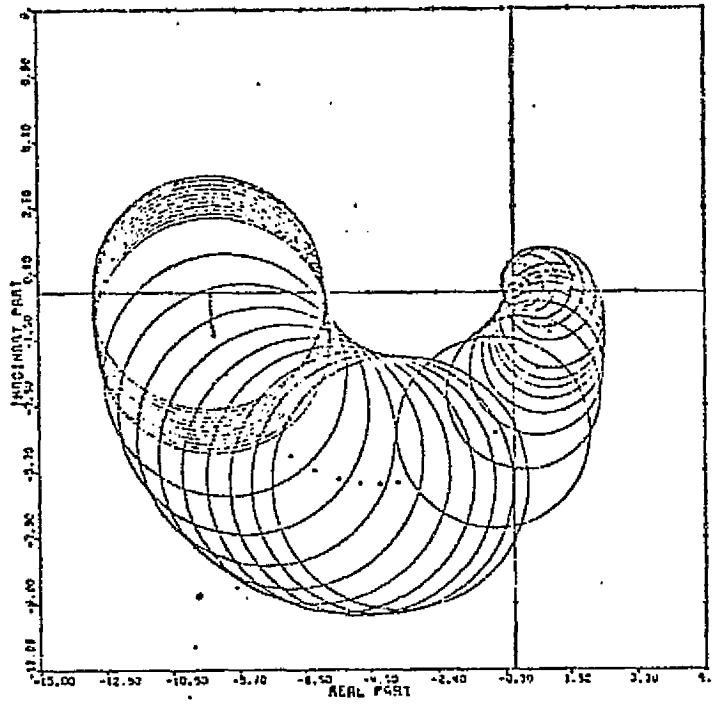

Fig. 4. Column 2, $G(s)*K_1$

either from the fact that the origin in the CARDIAD plot for column one is included by all solid circles and excluded by all dashed circles, or from the fact that all of the circles in the CARDIAD plot for the second column are solid.

Since switching the inputs makes one column dominant uncompensated, it seems a logical first step in compensating for dominance at all frequencies. Thus, K_1 is chosen to be

$$K_1 = \begin{bmatrix} 0 & 1 \\ 1 & 0 \end{bmatrix}. \qquad (17)$$

It is still necessary to make the second column of the system dominant. From the CARDIAD plot for this column (Fig. 4), it is apparent that frequency dependent compensation will be necessary since there exists no point in the real axis which is included in all the solid circles of this plot. To design such a compensator, a function of s is fitted to the shape of the CARDIAD plot so that, at any given frequency, the compensator lies inside the solid circle associated with the same frequency in the CARDIAD plot. While it is possible to find a first order compensator that will make this column dominant, a second order compensator has been used because this same compensator could also achieve dominance at four other set points of the model. $K_2(s)$ is the compensator that achieves dominance in the second column of $G(s)*K_1$.

$$K_2(s) = \begin{bmatrix} 1 & \dfrac{-.742s - 9.59}{.014s^2 - .998s + 1.} \\ 0 & 1 \end{bmatrix} \qquad (18)$$

The overall compensation is $K_1 * K_2(s) = K(s)$ given below.

$$K(s) = \begin{bmatrix} 0 & 1 \\ 1 & \dfrac{-0.742s - 9.59}{.014s^2 - .998s + 1.} \end{bmatrix} \tag{19}$$

The CARDIAD plots of the system with this compensator are given in Figs. 5 and 6. It is obvious either from the fact that only solid circles appear in the plots or from the fact that all the solid circles include the origin that each column of the system is now dominant at all frequencies.

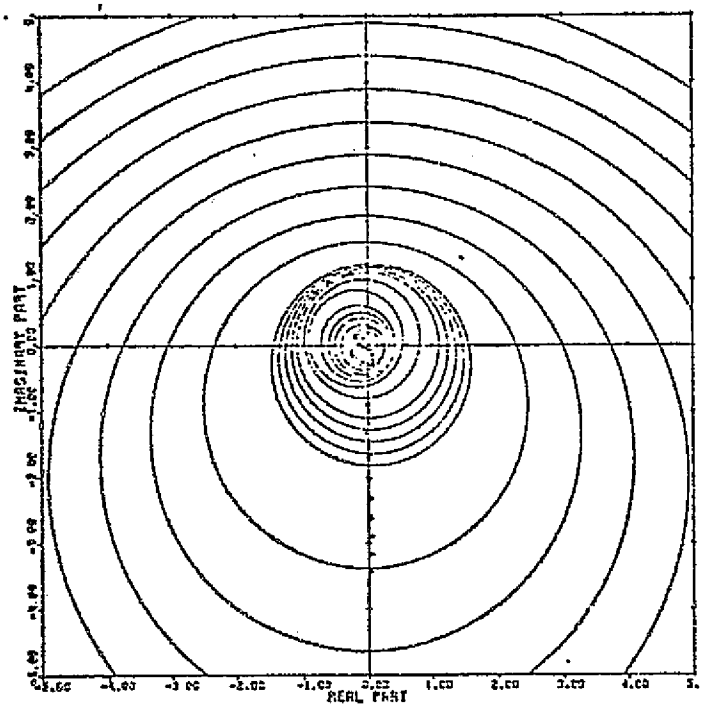

Fig. 5. Column 1, G(s)*K(s)

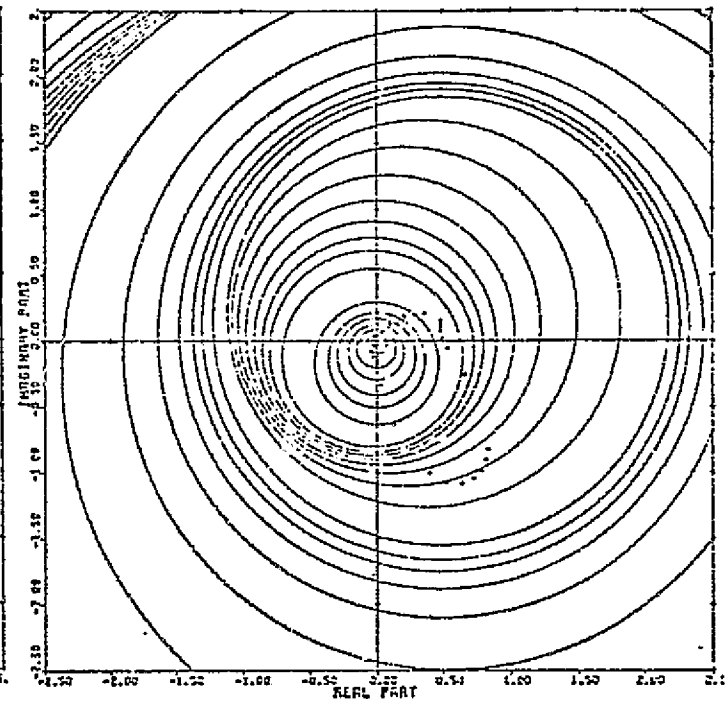

Fig. 6. Column 2, G(s)*K(s)

4. GENERALIZATION

The CARDIAD Plot approach to system dominance in the three-input, three-output case is similar to the approach in the two-input, two-output case.

The actual condition for dominance in the 3 x 3 case is the i^{th} column of a matrix Z(s) will be dominant if

$$|z_{ii}(s)| > \sum_{\substack{j=1 \\ j \neq i}}^{3} |z_{ji}(s)| \tag{20}$$

for all s on D. If both sides of this inequality are squared as in the 2 x 2 case, then an equivalent condition is

$$|z_{ii}(s)|^2 > \left[\sum_{\substack{j=1 \\ j \neq i}}^{3} |z_{ji}(s)| \right]^2. \tag{21}$$

Using inequality (21), the condition for dominance in, say, the first column is

$$|z_{11}(s)|^2 > |z_{21}(s)|^2 + |z_{31}(s)|^2 + 2|z_{21}(s)||z_{31}(s)|. \tag{22}$$

The cross term produced by squaring adds non-integral power terms to the dominance

inequality for the 3 x 3 system. To circumvent this problem, the last term of inequality (22) is replaced by an upper bound. Since

$$|z_{21}(s)|^2 + |z_{31}(s)|^2 \geq 2|z_{21}(s)||z_{31}(s)| \tag{23}$$

with equality when $|z_{21}(s)| = |z_{31}(s)|$, it is convenient to replace the last term of inequality (22) with the left member of inequality (23). This yields a sufficient condition for dominance. For column 1, the condition is

$$|z_{11}(s)|^2 - 2|z_{21}(s)|^2 - 2|z_{31}(s)|^2 > 0; \tag{24}$$

and the general form is

$$|z_{ii}(s)|^2 - 2\sum_{\substack{j=1 \\ j\neq i}}^{3} |z_{ji}(s)|^2 > 0, \quad i = 1,2,3. \tag{25}$$

From inequality (24), the derivation of the dominance equation for the 3 x 3 case proceeds analogously to the 2 x 2 derivation. The general form of the compensator used in the analysis is

$$K(s) = \begin{bmatrix} 1 & \alpha_{12}(s) & \alpha_{13}(s) \\ \alpha_{21}(s) & 1 & \alpha_{23}(s) \\ \alpha_{31}(s) & \alpha_{32}(s) & 1 \end{bmatrix} \tag{26}$$

where $\alpha_{ij}\Big|_{s=j\omega} = x_{ij} + y_{ij}j$.

Once again, the open loop transfer function matrix G(s) and the general form (26) of the compensator are evaluated at a specific frequency and multiplied to form Q(jω). Then, using inequality (25), a dominance inequality for each of the three columns of Q(jω) can be formed. For example, the first column of Q(jω) will be dominant at the frequency ω if

$$|q_{11}|^2 - 2|q_{21}|^2 - 2|q_{31}|^2 > 0 \tag{27}$$

and the dominance function for column 1 is

$$\begin{aligned} f_1(x_{21},y_{21},x_{31},y_{31}) &= c_1 + x_{21}^2 c_2 + y_{21}^2 c_2 + x_{31}^2 c_3 + y_{31}^2 c_3 \\ &+ 2x_{21}c_4 + 2y_{21}c_5 + 2x_{31}c_6 + 2y_{31}c_7 + 2x_{21}x_{31}c_8 \\ &+ 2y_{21}y_{31}c_8 + 2x_{21}y_{31}c_9 - 2x_{31}y_{21}c_9 > 0 \end{aligned} \tag{28}$$

where the constants c_1-c_9 are functions of G(s) evaluated at the frequency ω. Similar dominance functions can be derived for the other two columns.

The maximum-minimum analysis is performed in two different ways. In the first approach, which will be referred to as the standard analysis, the variables of the dominance inequality are first paired by the entry in the compensator which they represent; and the maximum-minimum analysis is performed on each pair assuming that the other pair is zero. The resulting maximums or minimums are

$$x_{21} = -c_4/c_2; \quad y_{21} = -c_5/c_2,$$

$$x_{31} = -c_6/c_3; \quad y_{31} = -c_7/c_3.$$

The hessian for each pair of variables is diagonal and the second derivative test once again reduces to a sign test.

The dominance analysis is repeated over a range of frequencies and CARDIAD plots result. There is one plot for each off-diagonal entry in the compensator and each entry is plotted assuming that the other off-diagonal entry in the column is zero. Using CARDIAD plots generated by the standard analysis, dominance is achieved by setting one of the off-diagonal entries to zero while the other is chosen as was the case in the 2 x 2 design.

There does not always exist a value in one off-diagonal entry of a column of the compensator that will make the column of the system dominant when the other off-diagonal entry in that column of the compensator is zero. When this occurs, the maximum-minimum analysis is performed by finding the full gradient of the dominance function. The hessian is no longer diagonal but the eigenvalues of the hessian are all negative in Section 5, so the point that is found is a maximum. Design which is performed on plots generated by the full gradient analysis involves both of the off-diagonal entries of a column of the compensator, and functions must be fit to each to achieve dominance.

A new symbol appears in the plots. At any given frequency, unless dominance can be achieved at that frequency with the other entry zero, a small triangle is drawn which shows the best that can be done towards achieving dominance. It should be noted that the triangle can appear in plots generated by either analysis. In the standard analysis CARDIAD plots, if triangles appear in one plot for a column but not the other, dominance can be achieved by keeping the entry in which the triangles appeared zero and using the other entry to achieve dominance. In the full gradient analysis plots, triangles appearing in both plots do not mean that dominance cannot be achieved. Given that one entry in the compensator is chosen exactly on the triangle at a certain frequency, there is a radius of points around the triangle in the other plot that will achieve dominance; but since the size of the circle is a function of how well the other entry is fit to the triangles, such a circle could easily be misleading. Both of these points will be illustrated in the next section.

5. THEME PROBLEM ANALYSIS

The following design is performed on the reduced order model of the theme problem with state feedback. The states being fed back are the two turbine speeds and the pressure P_b. Dominance will be achieved using only precompensation.

The plots for the uncompensated system using the standard dominance analysis showed that the first two columns of the system could be made dominant with one off-diagonal entry in each of the first two columns of the compensator zero. The third column, however, could not be made dominant at any frequency with either one of the off-diagonal entries in the third column zero. Physically, this indicates that the principal effects of all three inputs (fuel flow, exhaust area, and guide vanes) are on the two speed states. To facilitate achieving dominance, a column switch was done by choosing the first compensator to be

$$K_1 = \begin{bmatrix} 0 & 1 & 0 \\ 0 & 0 & 1 \\ 1 & 0 & 0 \end{bmatrix}.$$

Figs. 7-12 are the CARDIAD plots of the system with this compensator and use the standard dominance analysis. The plots for the entries in the first column, Figs. 7 and 8, show that the first column is dominant without further compensation, since the origin of each plot is included inside all solid circles and excluded by all dashed circles. Figs. 9 and 10 are the CARDIAD plots for the second column. Fig. 10, the plot for the 3,2 entry, has several triangles in it, indicating that, at

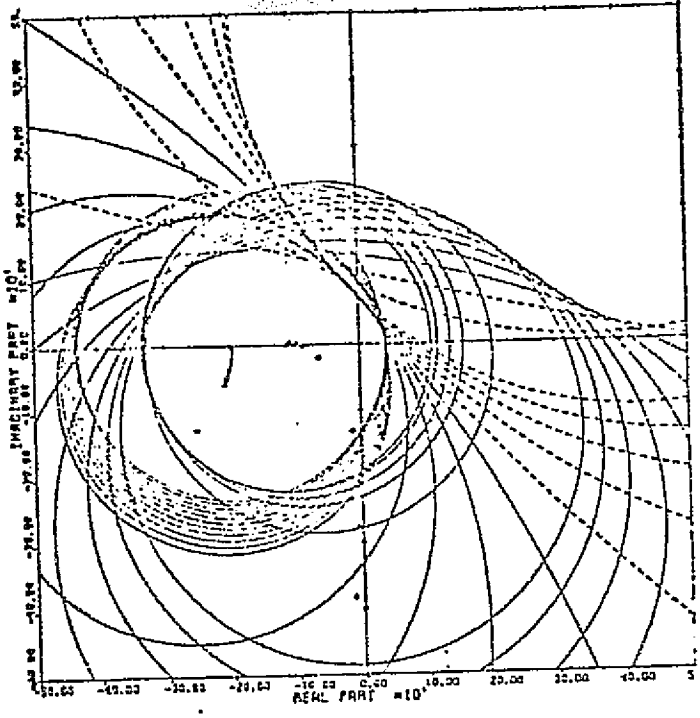

Fig. 7. $G(s)*K_1$, 2,1 Entry

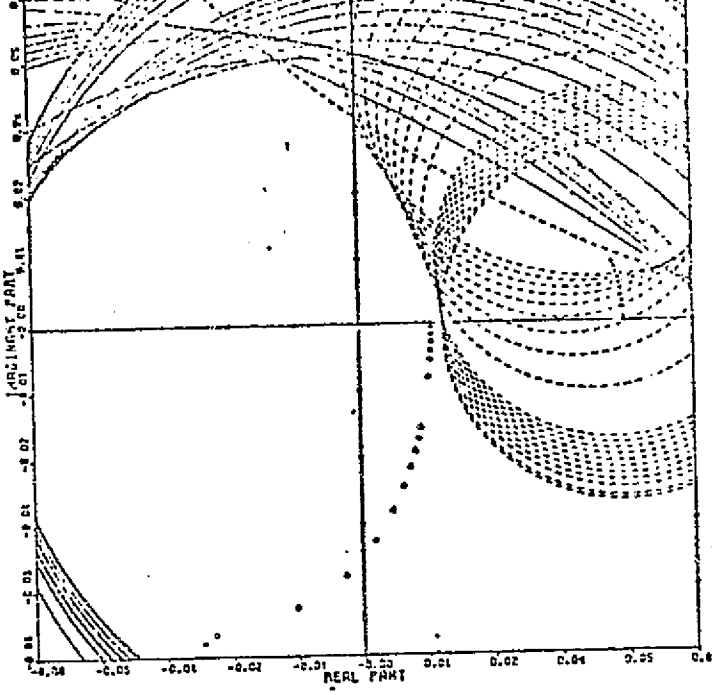

Fig. 8. $G(s)*K_1$, 3,1 Entry

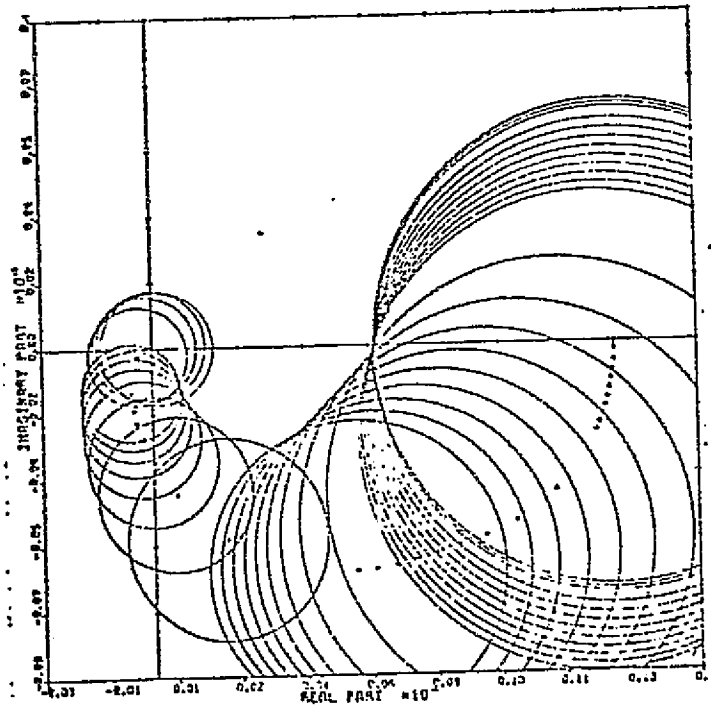

Fig. 9. $G(s)*K_1$, 1,2 Entry

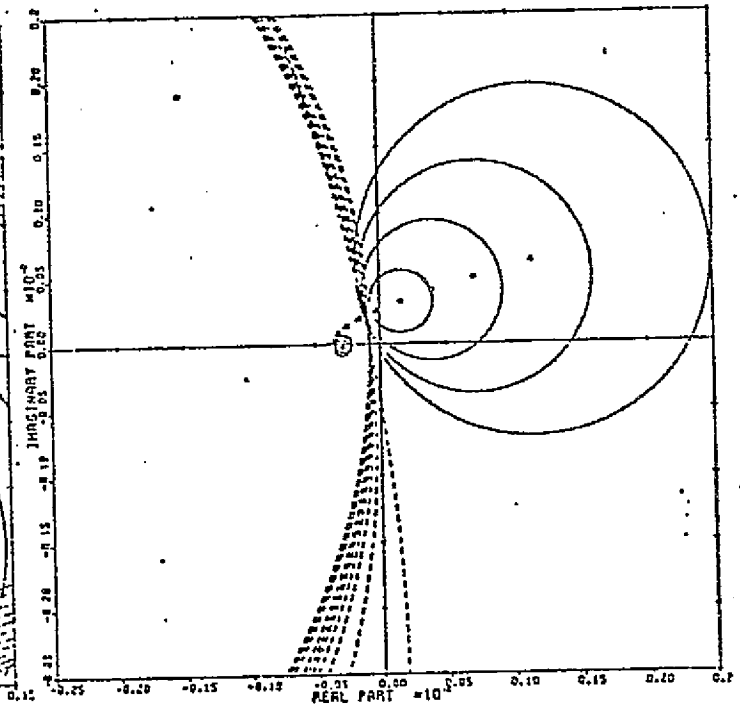

Fig. 10. $G(s)*K_1$, 3,2 Entry

the frequencies where they occur, there is no value in the 3,2 entry that will make the column dominant with the 1,2 element zero. However, Fig. 9 shows that there are no such triangles in the 1,2 entry; so, if a function is fit to the shape of the solid circles of this plot and if the 3,2 entry is kept at zero, dominance can be achieved. Figs. 11 and 12 are the CARDIAD plots for the third column. The 1,3 entry is all triangles and the 2,3 entry has triangles at lower frequencies. Thus, there is no way to make this column of the system dominant with one of the off-

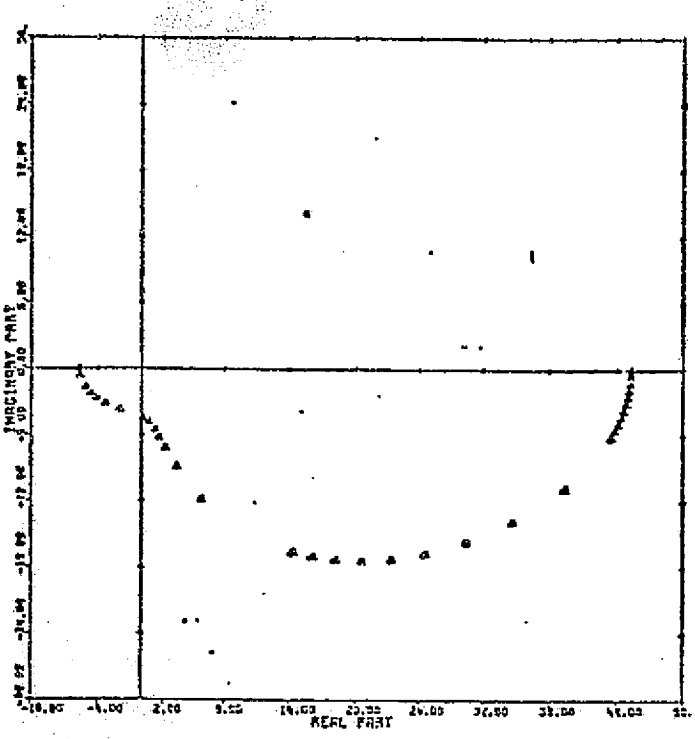

Fig. 11. $G(s)*K_1$, 1,3 Entry

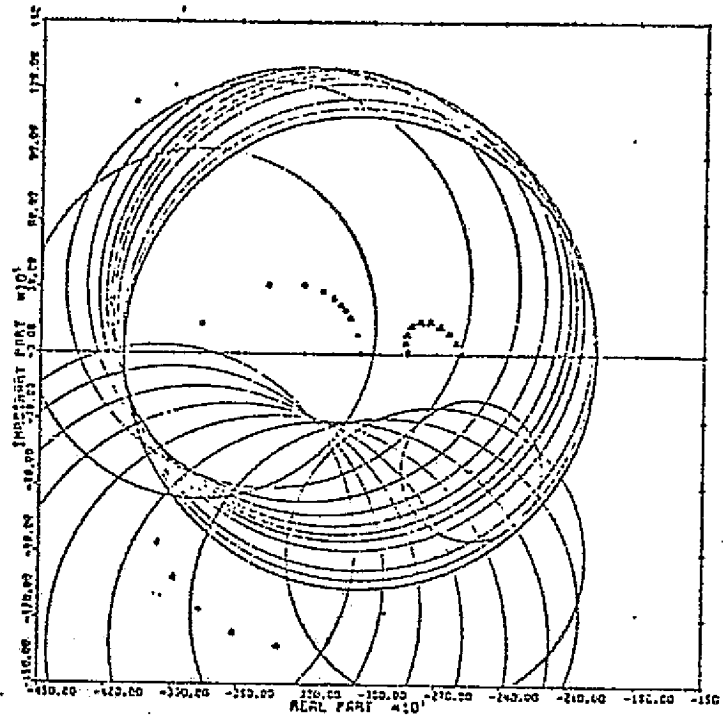

Fig. 12. $G(s)*K_1$, 2,3 Entry

diagonal entries in the compensator zero.

Figs. 13 and 14 are the plots for the third column using the full gradient rather than the standard analysis. The solid circles which appear at high frequencies in Fig. 14 are very important. Recall that the circle will only be drawn if dominance can be achieved while the other entry is zero. This means that by staying inside these solid circles, dominance can be achieved at the frequencies at which they occur while the 1,3 entry in the compensator is zero. Thus, in designing the 2,3

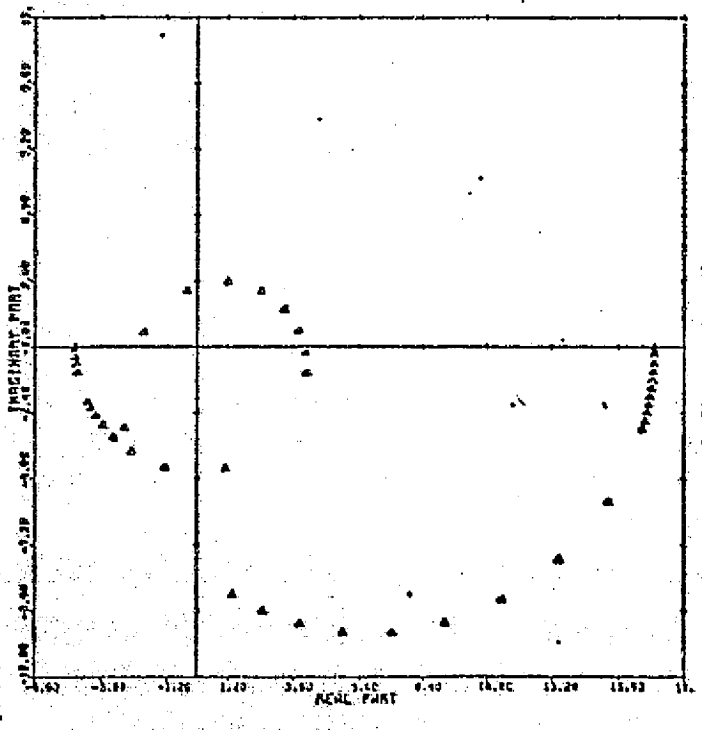

Fig. 13. $G(s)*K_1$, 1,3 Entry (Gradient)

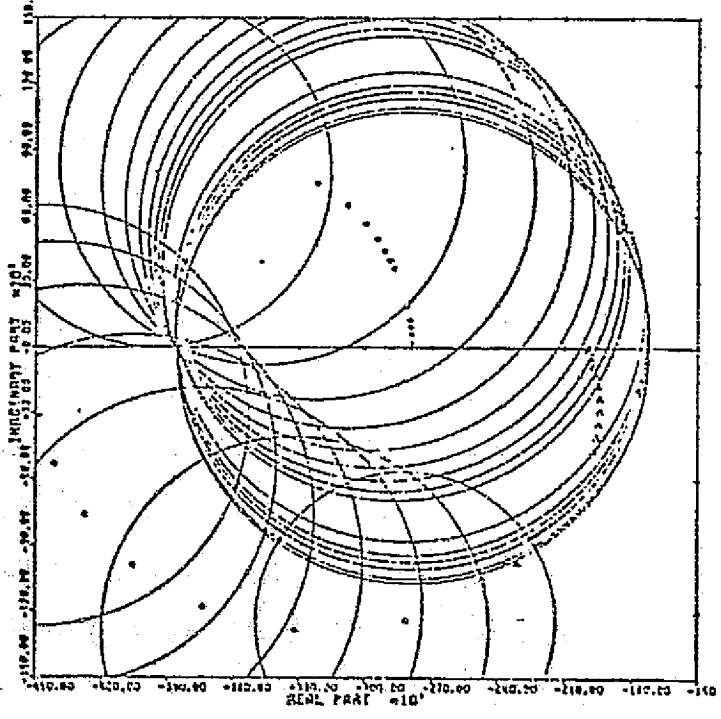

Fig. 14. $G(s)*K_1$, 2,3 Entry (Gradient)

entry, the strategy that is employed is to follow the triangles at low frequencies and stay inside the solid circles at the higher frequencies. If this is done, the design of the 1,[illegible]ntry will be simplified because it will only be necessary to fit the entry to the low frequency triangles and have the function go to zero at higher frequencies.

Using this strategy, a lag compensator was designed to fit the 2,3 entry as described previously. The compensator entry that was chosen is

$$k_{23}(s) = \frac{-129.4s - 1940.2}{.0365s + 1.} .$$

At the same time, another lag compensator is fit to the solid circles in Fig. 9, the CARDIAD plot for the 1,2 entry. This was chosen to be

$$k_{12}(s) = \frac{.0127}{.1162s + 1.} .$$

Defining this compensator as $K_2(s)$ with all the other off-diagonal entries zero, the overall compensation thus far is $K_3(s) = K_1K_2(s)$.

$$K_3(s) = \begin{bmatrix} 0 & 1 & \frac{-129.4s - 1940.2}{.0365s + 1} \\ 0 & 0 & 1 \\ 1 & \frac{.0127}{.1162s + 1.} & 0 \end{bmatrix}$$

Figs. 15-20 are the CARDIAD plots of $G(s)K_3(s)$ using the standard dominance analysis. The plots show that the first two columns of the system are dominant at all frequencies since in Figs. 15-18 the origin of each plot is contained by all solid circles and excluded by all dashed circles. Fig. 19 shows that the strategy applied in the design for the 2,3 entry was successful. To make the third column dominant, it is now only necessary to fit a compensator to the shape of the solid circles in Fig. 19

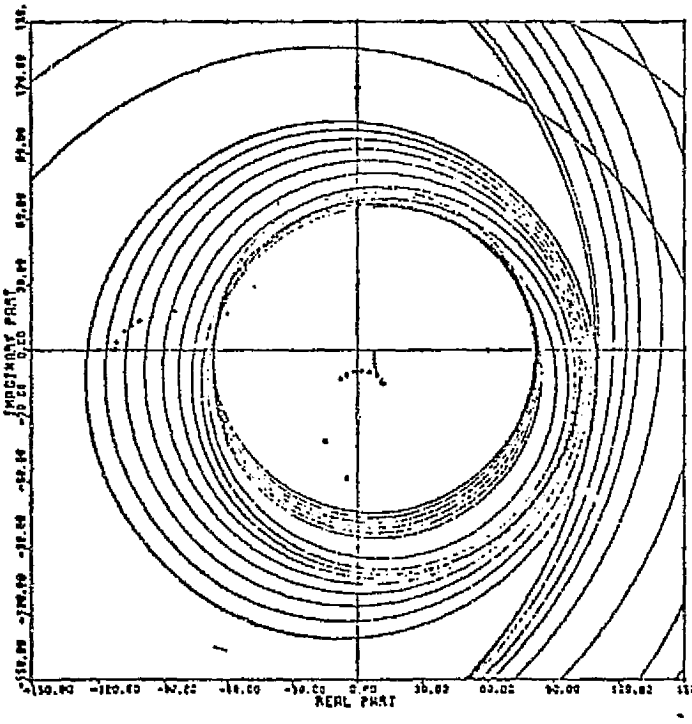

Fig. 15. $G(s)*K_3(s)$, 2,1 Entry

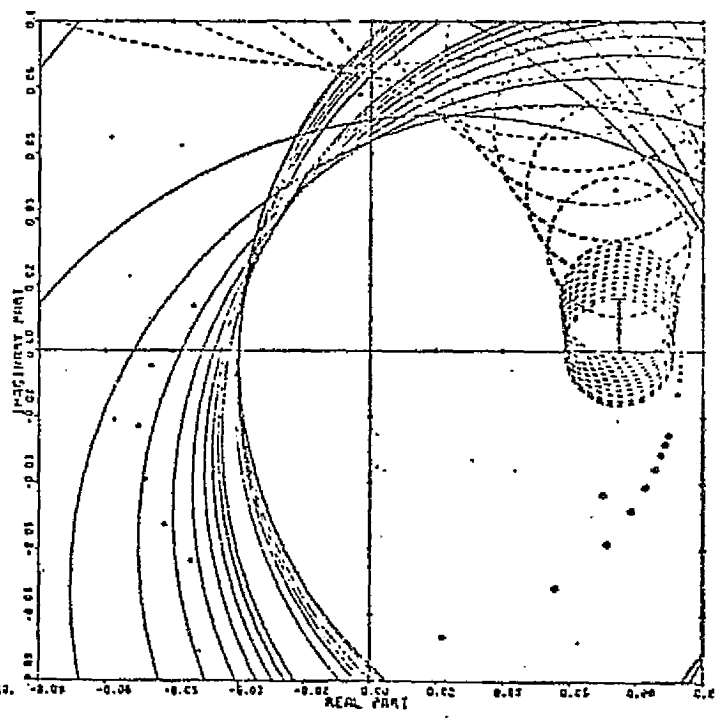

Fig. 16. $G(s)*K_3(S)$, 3,1 Entry

and have it go to zero at higher frequencies. The function that was chosen is

$$k_{13}(s) = \frac{.532s + 16.917}{.0127s^2 + .1986s + 1.}$$

The only change this has on the overall compensator is that the zero in the 3,3 entry is replaced by this function. When the third column is replotted using this compensator and standard dominance analysis, Figs. 21 and 22, the CARDIAD plots show that the third column is now dominant at all frequencies. Thus, the system is now dominant at all frequencies.

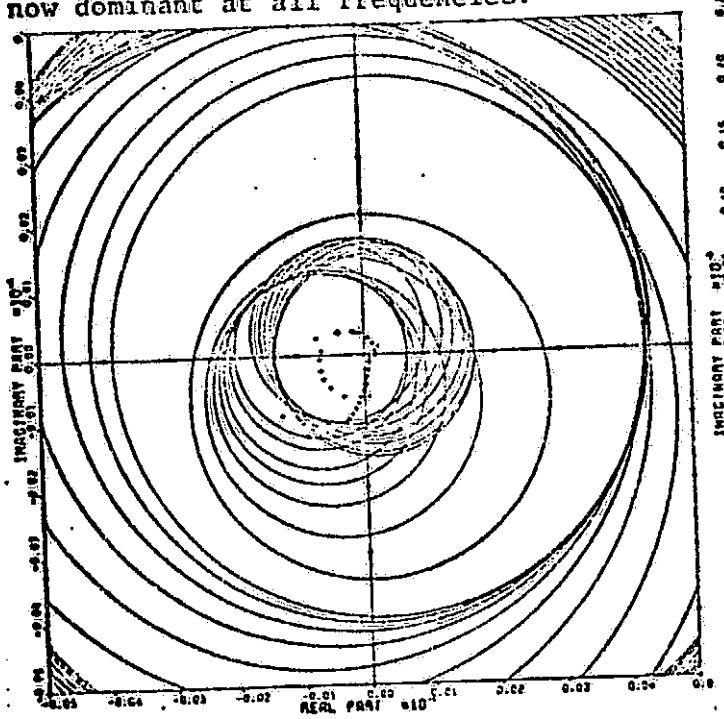

Fig. 17. $G(s)*K_3(s)$, 1,2 Entry

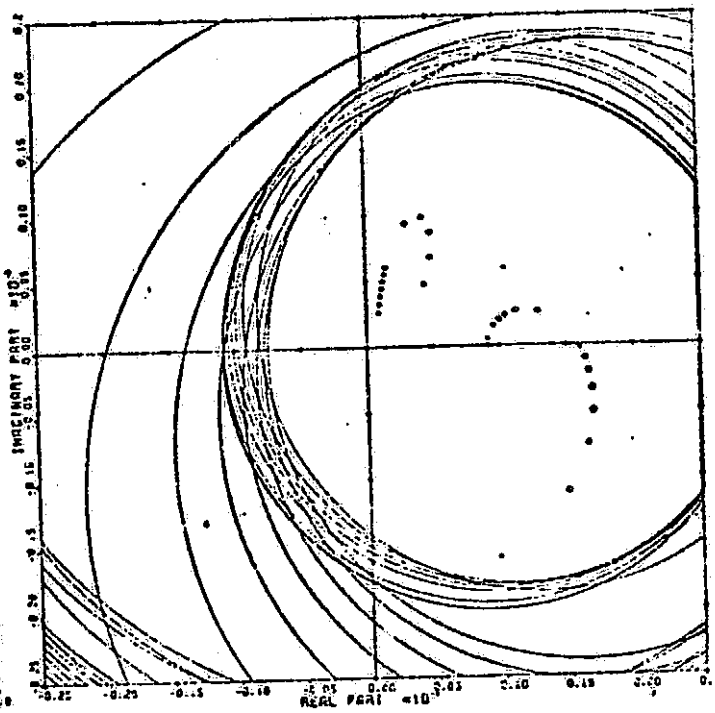

Fig. 18. $G(s)*K_3(s)$, 3,2 Entry

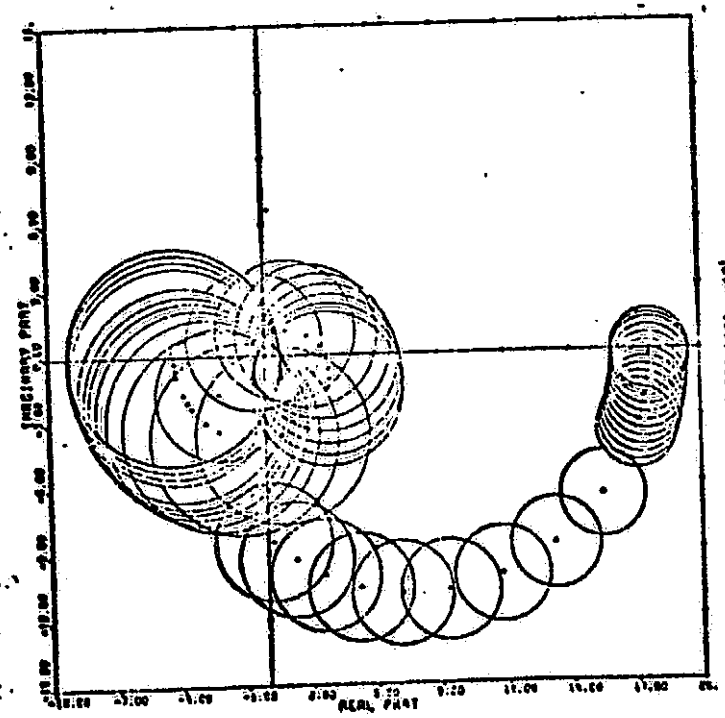

Fig. 19. $G(s)*K_3(s)$, 1,3 Entry

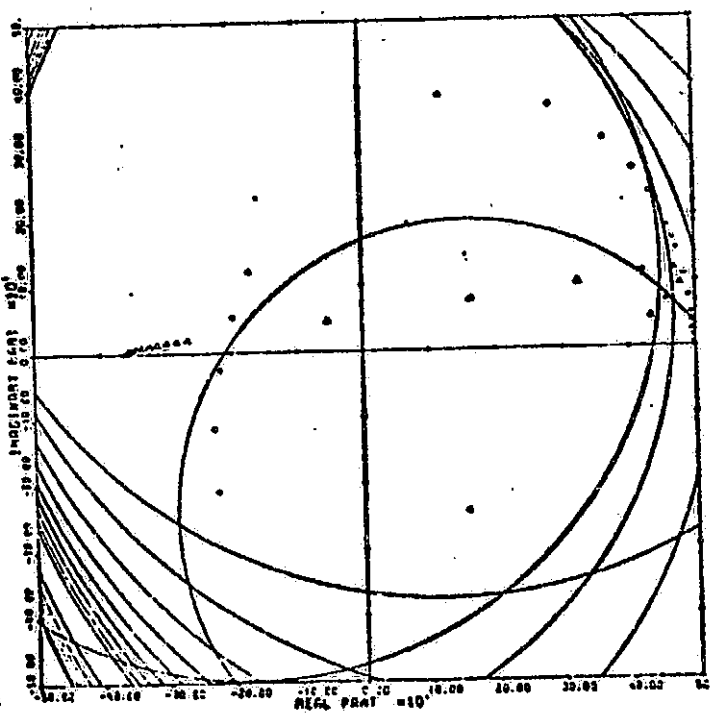

Fig. 20. $G(s)*K_3(s)$, 2,3 Entry

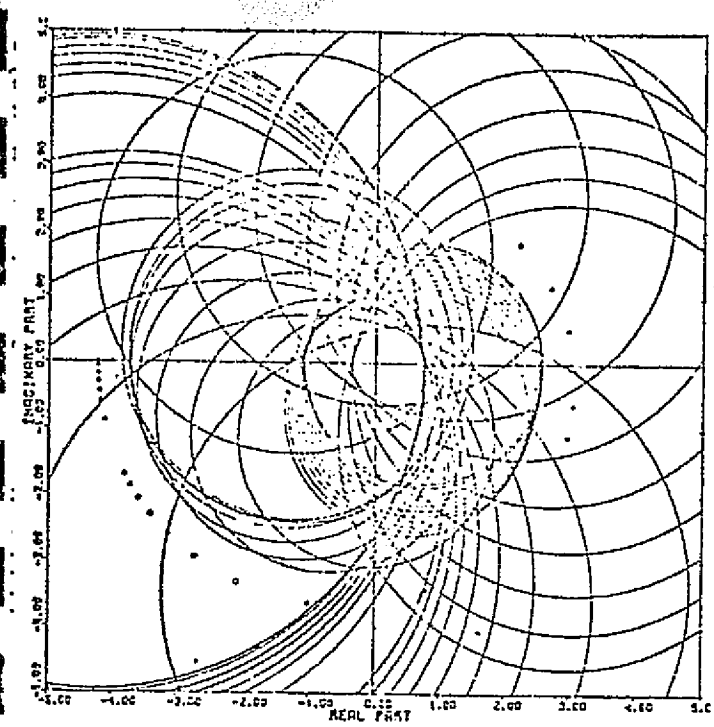

Fig. 21. G(s)*K(s), 1,3 Entry

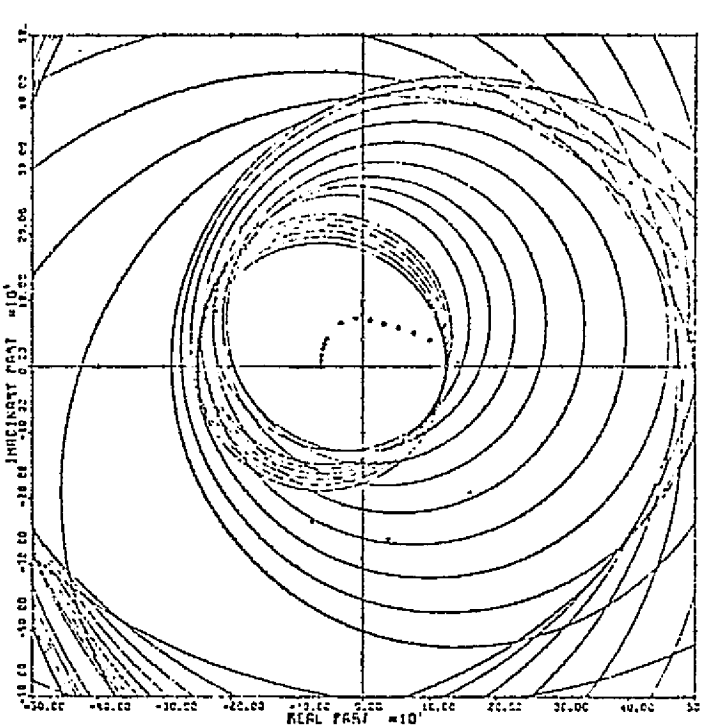

Fig. 22. G(s)*K(s), 2,3 Entry

6. CONCLUSIONS

The graphical CARDIAD method described in this paper has been effective on the Theme Problem. The authors' experience indicates that it is an easily learned design aid which can be quite helpful in achieving dominance for realistic plants. A special advantage of the CARDIAD approach lies in the way in which it provides insight to the designer. The plots indicate whether or not it will be possible to achieve dominance with simple, lead-lag compensators. Examples up to this time suggest that, over the useful bandwidth, simple compensators are often successful in this regard.

It should be noted that this paper illustrates only compensator selection for dominance. Completion of the design is by classical means. For an example, see [5]. Of particular note is the fact that compensator denominators having right half plane zeros do not necessarily lead to unstable controllers. This may also be seen in [5].

Continued research on this class of graphical, interactive methods is in progress.

7. ACKNOWLEDGMENT

This work was supported in part by the National Science Foundation under Grant ENG 75-22322 and in part by the National Aeronautics and Space Administration under Grant NSG 3048.

8. REFERENCES

1. H. H. Rosenbrock, Computer Aided Control System Design. New York: Academic Press, 1974.

2. R. M. Schafer, "A Graphical Approach to System Dominance," M.S. Thesis, Department of Electrical Engineering, University of Notre Dame, Notre Dame, Indiana, May 1977.

3. J. F. Sellers and C. J. Daniele, "DYNGEN--A Program for Calculating Steady-State

and Transient Performance of Turbojet and Turbofan Engines," NASA Technical Notes, NASA TN D-7901, Washington, D.C., April 1975.

4. W. C. Geyser, "NASA Preliminary Report on DYGABCD," April 1976.

5. R. M. Schafer, R. R. Gejji, P. W. Hoppner, W. E. Longenbaker, and M. K. Sain, "Frequency Domain Compensation of DYNGEN Turbofan Engine Model," Proc. Joint Automatic Control Conference, pp. 1013-1018, June 1977.